

Aus der Experimentellen und Klinischen Pharmakologie und Toxikologie (FR. 2.4)
Bereich Theoretische Medizin und Biowissenschaften
der Medizinischen Fakultät
der Universität des Saarlandes, Homburg

TRPC6 Channel Complex: Identification of Novel Regulatory Subunits in Human Platelets

Dissertation zur Erlangung des Grades eines Doktors
der Naturwissenschaften der Medizinischen Fakultät
der UNIVERSITÄT DES SAARLANDES
2020

Vorgelegt von

Teqiyya Bentrcia

geb. am 20. Dezember 1989 in Algerien

Day of oral examination: June 7th, 2021

Dean of the Faculty: Prof. Dr. med. Michael D. Menger

Examinants: Prof. Dr. med. Veit Flockerzi

Prof. Dr. Dieter Bruns

Dedicated to my family

Acknowledgement

I wish to express my deep sense of gratitude to my supervisor, Prof. Dr. med. Veit Flockerzi for giving me the opportunity to work in his laboratory and for his deep and continues support, guidance and advices throughout my doctoral research.

I am very thankful to all friends and colleagues in the lab and to all members of the department of Pharmacology and Toxicology in Homburg. My special thanks to Stefanie Buchholz for her help in the cloning of many cDNA constructs. Many thanks go to Martin Simon-Thomas, Heidi Löhr, Ute Soltek, Karin Wolske, Christine Wesely and Sandra Plant for their expert technical assistance and support. I would like to thank Claudia Ecker for her great administrative help.

Special thanks to Dr. Claudia Fecher-Trost for her help in mass spectrometry measurements and analysis. I would like to thank Dr. Petra Weissgerber and the team of the SPF Animal Facility of the Fakultät Medizin, for taking care of the mice described in my study. Many thanks as well to Dr. Ulrich Wissenbach for translating the abstract, Dr. Andreas beck and Dr. Stephan Philipp for their scientific advices and fruitful discussion.

I thank the Institute of Clinical Hemostaseology and Transfusion Medicine at the Saarland University Medical Center (Director: Univ.-Prof. Dr. med. Hermann Eichler) and his deputy director Professor Dr. med. Joachim Schenk for providing expired „Leukozyten-depletierte Thrombozytapheresekonzentrate“.

My sincere thanks go to Gabriele Amoroso for her kind help and support and for the great organization of the international research training group IRTG1830.

My acknowledgement could never adequately express obligation to my family, especially my parents, sisters and brothers for their love, encouragement and prayers for my success.

Finally, but most importantly, many thanks to the very special person in my life, my husband Anouar for his unfailing love and unconditional support all the time, also to my little daughter(s) for their patience and for giving me unlimited happiness.

Table of Content

Table of Content	I
List of Abbreviations	III
List of Figures	V
List of Tables	VII
Abstract	VIII
Zusammenfassung	X
1 Introduction	12
1.1 Transient Receptor Potential TRP channels	12
1.1.1 TRPC6 channel	15
1.2 Platelets function in mice and human	23
1.2.1 Activation and aggregation of platelets	24
1.2.2 Signaling pathways downstream platelet activation	25
1.3 Aim	27
2 Materials and Methods	28
2.1 Buffers and solutions	28
2.2 Methods.....	39
2.2.1 Preparation of human platelets sample	39
2.2.2 Antibody-based affinity purification of TRPC6	39
2.2.3 Cell lines and transfections	40
2.2.4 Western blot analysis	42
2.2.5 Blue Native PAGE (BN-PAGE)	43
2.2.6 Two-dimensional Blue Native/SDS PAGE	43
2.2.7 Gel digestion for mass spectrometry analysis	44
2.2.8 Mass spectrometry analysis	44
2.2.9 Calcium imaging	45
2.2.10 Electrophysiological recordings	46
2.2.11 Pull-down assay using ³⁵ S-labeled proteins	47
2.2.12 Cell surface biotinylation assay	48
2.2.13 <i>In vitro</i> scratch migration assay	49
2.2.14 Live cell imaging	50

TABLE OF CONTENT

2.2.15	Immunofluorescence staining of human platelets	50
2.2.16	Platelet adhesion assay	51
2.2.17	Mice	52
2.2.18	Statistical analysis	52
3	Results	53
3.1	Identification of the transient receptor potential canonical 6 (TRPC6) protein in human platelets	53
3.2	Identification of TRPC6 associated proteins in human platelets by mass spectrometry analysis	56
3.3	Density gradient fractionation of the TRPC6 protein complex solubilized from human platelets and the HEK-TRPC6 cell line	59
3.4	TRPC6 channel expression, localization and function in HEK293 cells stably expressing <i>Trpc6</i> cDNA	62
3.5	GIT1 protein is expressed endogenously and after overexpression in the HEK-TRPC6 cells as well as in the human platelets	65
3.6	GIT1 protein constrains TRPC6-mediated calcium influx and current in the HEK-TRPC6 cell line	67
3.7	GIT1 protein acts negatively on cell migration in HEK-TRPC6 cells	69
3.8	The IP3R type 2 does not interfere with the inhibitory effect of GIT1 on the TRPC6 channel	71
3.9	GIT1 protein binds TRPC6 channel via its ankyrin repeat domain	73
3.10	The TRPC6 N-terminus is critical for the TRPC6-GIT1 binding	74
3.11	The first 249 amino acid residues of the TRPC6 channel are essential for its binding to GIT1 protein	77
3.12	GIT1 depletion in HEK293 cells stably expressing <i>Trpc6</i> cDNA increases the TRPC6 channel function	79
3.13	GIT1 protein does not affect TRPC6 channel membrane localization	81
3.14	TRPC6 plays an important role in <i>in vitro</i> platelet adhesion	83
3.15	Collagen and OAG stimulate proteins phosphorylation in human platelets	87
4	Discussion	91
5	Conclusion and outlook	108
6	References	110
7	Curriculum vitae	124
8	Publications	126
9	Supplementary data	128

List of Abbreviations

µg	Microgram
µM	Micromolar
µL	Microliter
v/v	Volume per volume
w/v	Weight per volume
Aa	Amino acid
AM (Ester)	Acetoxymethyl ester
ATP	Adenosine triphosphate
BCA	Bicinchoninic acid
BN	Blue native
BSA	Bovine-Serum-Albumin
°C	Degree Celsius
Ca ²⁺	Calcium ions
cpm	Counts per minute
cDNA	Complementary deoxyribonucleic acid
CPA	Cyclopiazonic acid
Cryo-EM	Cryogenic Electron Microscopy
DAG	Diacylglycerol
ERK1	Extracellular signal-regulated kinase
FCS	Fetal calf serum
FSGS	Focal segmental glomerulosclerosis
g	Gram
GFP	Green fluorescent protein
GIT1	G-protein-coupled receptor kinase interacting protein 1
h	Hour
HEK	Human embryonic kidney
IP3	Inositol trisphosphate
KDa	Kilodalton
L	Liter
M	Molar
MAPK	Mitogen-activated protein kinase

LIST OF ABBREVIATIONS

mg	Milligram
Mg ²⁺	Magnesium ions
min	Minute
mL	Milliliter
mm	Millimeter
mM	Millimolar
mRNA	Messenger ribonucleic acid
ms	Millisecond
MS	Mass spectrometry
mV	Millivolt
m/z	Mass to charge ratio
MΩ	Megaohms
nm	Nanometer
nM	Nanomolar
OAG	1-oleoyl-2-acetyl-sn-glycerol
PAGE	Polyacrylamide gel electrophoresis
PAK2	p21 activated kinases
PBS	Phosphate-Buffered Saline
P _{Ca}	Permeability for calcium
PIP ₂	Phosphatidylinositol-4,5-bisphosphate
PLC	Phospholipase C
pmol	Picomole
P _{Na}	Permeability for sodium
Rb IgG	Rabbit immunoglobulin
SDS	Sodium dodecyl sulfate
S.E.M	Standard error of the mean
SERCA	Sarco/endoplasmic reticulum Ca ²⁺ -ATPase
TRP	Transient receptor channel
TRPC	Transient receptor potential canonical
× g	Times Earth's gravitational force

List of Figures

Figure 1-1. Phylogenetic tree of the TRP channel family and TRPC6 topology domains	14
Figure 1-2. Amino acid sequence alignment of the mouse and human TRPC6	16
Figure 2-1. Antibody-based affinity purification method	41
Figure 3-1. TRPC6 protein enrichment from human platelets and mass spectrometry data .	55
Figure 3-2. Potential TRPC6 associated proteins detected by mass spectrometry from human platelets	58
Figure 3-3. Density gradient separation of the TRPC6 protein complex in human platelets and HEK-TRPC6 cell line	61
Figure 3-4. TRPC6 protein localization and function in HEK-TRPC6 cells	64
Figure 3-5. GIT1 protein expression and localization	66
Figure 3-6. GIT1 protein inhibits OAG-induced calcium entry and current in HEK-TRPC6 cells	68
Figure 3-7. GIT1 modulates TRPC6-dependent cell migration	70
Figure 3-8. Impact of IP3RII on the inhibitory effect exerted by GIT1 protein on the TRPC6 activity in HEK-TRPC6 cells	72
Figure 3-9. GIT1 protein binds TRPC6 channel <i>via</i> its ankyrin repeat domain	74
Figure 3-10. The N- terminus of TRPC6 is essential for TRPC6 channel and GIT1 protein binding.....	76
Figure 3-11. The ankyrin repeats containing domain of TRPC6 is required for GIT1 protein binding.....	78
Figure 3-12. Co-expression of the TRPC6 N- terminus (1-249 aa) cDNA in HEK293 cells stably expressing the full length <i>Trpc6</i> cDNA frees TRPC6 function from GIT1 inhibition	80

LIST OF FIGURES

Figure 3-13. GIT1 protein did not alter TRPC6 localization at the plasma membrane.....	82
Figure 3-14. Signaling pathway of TRPC6 associated proteins in human platelets.....	85
Figure 3-15. The TRPC6 channel contributes to platelet adhesion.....	86
Figure 3-16. Platelet treatment with the collagen or OAG stimulates PAK2 and ERK1/2 phosphorylation.....	89
Figure 4-1. Graphical abstract summarizing the TRPC6 associated proteins signaling pathways in the platelet hemostasis.....	106

List of Tables

Table 2-1. Composition of buffers and solutions28

Table 2-2. Primary and Secondary antibodies33

Table 2-3. Compounds and Reagents35

Table 2-4. Devices and Instruments.....37

Table 3-1. Proteins potentially associated with the TRPC6 protein59

Abstract

The canonical transient receptor potential channel 6 (TRPC6) is a Ca²⁺ permeable cation channel. To identify the TRPC6 protein containing complex in human platelets, I used antibodies against the human TRPC6, which recognized TRPC6 in platelets homogenates by Western blots. Next, I established an antibody-based affinity purification procedure to enrich the solubilized TRPC6 protein from human platelets. Under non-denaturing condition, the TRPC6 protein was eluted from the beads, run on blue native gels and analysed by mass spectrometry. By the latter approach, the G-protein-coupled receptor kinase interacting protein-1 (GIT1) and proteins of the phospholipase C γ pathway including ARHGEF, MAPK, PAK2 and IP3R were found to be associated with the TRPC6 protein. In contrast, none of these proteins were retained by non-specific immunoglobulins used as a control. TRP channels comprise four subunits, but no other TRP protein was found to be associated with TRPC6 in the human platelets indicating that TRPC6 is a homotetrameric channel. The physical interaction between TRPC6 and both GIT1 and IP3R was confirmed by coimmunoprecipitation by antibodies against all three proteins and *in vitro* pull-down assays. By mapping the interaction, I could show that GIT1 protein binds to the TRPC6 protein *via* its ankyrin repeat domain. Similarly, coimmunoprecipitation showed that the N- terminus of TRPC6 is essential for the TRPC6-GIT1 interaction. TRPC6-mediated calcium entry and currents were measured by calcium imaging and whole cell patch clamp recordings, respectively and were activated by either diacylglycerol or its membrane permeable derivative 1-oleoyl-2-acetyl-sn-glycerol (OAG). The OAG induced calcium entry and current in HEK293 cells stably expressing the *Trpc6* cDNA were reduced in the presence of GIT1 protein, indicating an inhibitory effect of GIT1 on the TRPC6-mediated calcium entry and current. In addition, in an *in vitro* scratch migration assay, I could show that the migration of HEK293 cells stably expressing the *Trpc6* cDNA is negatively affected by GIT1 protein. Furthermore, depletion of the GIT1 protein, endogenously expressed in HEK293 cells, by the overexpressed

ABSTRACT

TRPC6 N- terminus abolished the inhibitory effect of GIT1 on TRPC6 function and results in larger currents and faster cell migration. To investigate the role of TRPC6 protein in the early stages of blood haemostasis I performed platelet adhesion assays using primary human and mouse platelets. Human platelets treated with the TRPC6 agonist OAG showed an increase in platelet adhesion and this effect was significantly reduced in the presence of the TRPC6 antagonist SAR7334. Moreover, mouse platelets isolated from *Trpc6* gene-deficient mice showed a significant reduction in platelet adhesion compared with platelets from wild-type controls. Taken together, this study identifies the phospholipase C γ 2 pathway to be associated with TRPC6 in platelets and especially GIT1 a novel TRPC6 channel regulatory subunit, which inhibits TRPC6 channel function. The results showing an increase of platelet adhesion after directly stimulating TRPC6 places TRPC6 downstream of receptor mediated processes initiated by fibrinogen and collagen.

Zusammenfassung

TRPC6 ist ein Ca^{2+} permeabler Ionenkanal, der zur Familie der kanonischen transient receptor potential (TRP)-Kanäle zählt. Ich habe Antikörper, die gegen das TRPC6 Protein von Mensch gerichtet sind, benutzt um solubilisiertes TRPC6 Protein aus humanen Blutblättchen anzureichern. Das an Antikörper gebundene TRPC6 Protein wurde unter nicht-denaturierenden Bedingungen eluiert, auf nativen Gelen aufgetrennt und mittels Massenspektrometrie analysiert. Durch den letzteren Versuch konnten das Adenosyl-Ribosylierungs-Faktor (ARF)-GTPase-aktivierende Protein 1 (GIT1) als auch Proteine aus der Phospholipase $\text{C}\gamma$ Signalkaskade wie ARHGEF, MAPK, PAK2 und IP3R als Komponenten des TRPC6 Kanalkomplexes identifiziert werden. Keines dieser Proteine wurde mittels unspezifischer Immunglobuline, die als Kontrolle benutzt wurden, identifiziert. TRP Kanäle bestehen aus 4 Untereinheiten, aber kein anderes TRP-Kanalprotein wurde gefunden, das an TRPC6 bindet. Das Ergebnis impliziert, das TRPC6 Kanäle in Blutblättchen als Homotetramere vorliegen. Die Interaktionen von TRPC6 jeweils mit GIT1 und IP3R wurden mittels Co-Immunopräzipitationen und Pulldown Verfahren bestätigt. Ich konnte zeigen, dass die „Ankyrin repeat“ Domäne des TRPC6 Proteins an das GIT1 Protein bindet und dass der N-terminus des TRPC6 Proteins essentiell für die Interaktion mit GIT1 ist. Die Kanalaktivität von TRPC6 wurde mittels Calcium-Imaging und Patch Clamp Strommessungen bestimmt. Die TRPC6 vermittelte Calciumaufnahme konnte durch Diacylglycerol als auch durch ein Membran-gängiges Derivat, 1-Oleoyl-2-Acetyl-sn-glycerol (OAG), aktiviert werden. In HEK293 Zellen, die stabil TRPC6 exprimieren, konnte der durch TRPC6 vermittelte Calciumeinstrom nach Expression der GIT1 cDNA vermindert werden. Die Ergebnisse zeigen, dass GIT1 einen inhibitorischen Effekt auf TRPC6 Ströme und die TRPC6-vermittelte Calciumaufnahme hat. Mittels eines Migrationversuchs, der in vitro durchgeführt wurde konnte ich zeigen das HEK293 Zellen, die stabil TRPC6 exprimieren, in Gegenwart von GIT1 langsamer migrieren. HEK293 Zellen bilden bereits endogen GIT1. Die zusätzliche Überexpression des N-terminus von

ABSTRACT

TRPC6 fängt das endogen gebildete GIT1 ab und hebt die Hemmung auf: Der TRPC6 vermittelte Calciumeinstrom ist erhöht und die Migration der TRPC6-HEK293 Zellen ist verstärkt. Um die Rolle von TRPC6 Kanälen in der Frühphase der Hämostase zu untersuchen habe ich einen Adhäsionstest mit humanen und murinen Blutplättchen ausgeführt. Humane Blutplättchen, die bereits mit OAG inkubiert wurden, zeigten eine verstärkte Adhäsionsneigung in vitro. Dieser Effekt war in Gegenwart des TRPC6 Antagonisten SAR7334 deutlich vermindert. Zusätzlich zeigten murine Blutplättchen, die aus TRPC6 defizienten Mäusen isoliert worden waren, eine deutlich geringere Adhäsionsneigung als Blutplättchen aus Wildtyp Mäusen. Die Arbeit zeigt, dass in Blutplättchen die Phospholipase C γ 2 Signalkaskade mit dem TRPC6 Protein assoziiert ist. Das GIT1 Protein, welches die Funktion des TRPC6 Kanals inhibiert, wurde als neue regulatorische Untereinheit identifiziert. Die Ergebnisse deuten darauf hin, dass TRPC6 in der Rezeptor-vermittelten Signalkaskade, die durch Fibrinogen und Kollagen angestoßen wird „downstream“ liegt und dass TRPC6 eine Rolle bei der Adhäsion der Blutplättchen zukommt.

1 Introduction

1.1 Transient Receptor Potential TRP channels

The TRP channel journey began in the year 1969, when Cosens and Manning observed that mutant fruit flies *Drosophila melanogaster*, subjected to a prolonged light stimulation showed a defect in the visual transduction. Unlike wild-type flies, these mutants failed to sustain a steady-state response in the electroretinogram recording, thus exhibiting a transient receptor potential and therefore the mutant was named Transient Receptor Potential (Cosens and Manning, 1969). Twenty years after the first identification of the TRP mutant, Montell and Rubin identified the *Trp* gene and proposed from its primary structure that the protein might be an ion channel (Montell and Rubin, 1989). Few years later, (Hardie and Minke, 1992) show by whole-cell patch clamp recordings from *Drosophila* photoreceptors that the TRP protein form calcium-permeable cation channels. Since the cloning of the first mammalian TRP channel in 1995 (Wes et al., 1995; Zhu et al., 1995), this family of proteins has been extensively investigated and the complementary DNAs of 28 mammalian members were cloned (Venkatachalam and Montell, 2007). Most of the TRP channels are localized at the plasma membrane, but also in several intracellular organelles (Zhang et al., 2018), playing an important role in the regulation and fine tuning of intracellular divalent cation homeostasis (Caterina et al., 1997). Calcium selectivity for most of TRP channels is poor and calcium permeability ranges from 0.3 to 10 relative to sodium ions (P_{Ca}/P_{Na}). However, some channels are unique in their permeability properties, for example TRPM4 and TRPM5 are calcium impermeable (Hofmann et al., 2003; Nilius et al., 2003), whereas, both TRPV5 and TRPV6 show a high calcium selectivity ($P_{Ca}/P_{Na} > 100$) in comparison with other TRP channels (Hirnet et al., 2003).

TRP channels are widely expressed and can be detected in almost every cell type and tissue suggesting an important role of these channels in the regulation of many cellular processes ranging from taste (Philippaert et al., 2017) and pain sensation (Caterina et al., 1997) to inflammatory response (Meseguer et al., 2014) and cancer (Wissenbach et al., 2001). TRP channels are also believed to be sensitive to different physical stimuli, including, temperature (Voets et al., 2004), osmotic pressure and stretch (Liu and Montell, 2015). Pharmacologically, TRP channels can be activated by a wide range of chemical and botanical compounds. For example, TRPV1 is activated by active component of chili peppers capsaicin (8-methyl-N-vanillyl-6-nonenamide) (Caterina et al., 1997). TRPA1 responds to allicin, a component of fresh garlic (Macpherson et al., 2005). TRPM8 activation is triggered by menthol (Bautista et al., 2007). TRPV2 (Qin et al., 2008) and TRPA1 (Jordt et al., 2004) channels are shown to respond to Δ^9 -Tetrahydrocannabinol and TRPV1, TRPV2, TRPV3, TRPM8 channels to cannabidiol (Muller et al., 2018), both extracts of the *Cannabis Sativa* plant.

TRP channels share similar general structure and consist of four subunits assembled as homo- or heterooligomer (Madej and Ziegler, 2018). Each subunit includes six hydrophobic transmembrane spanning domains, a pore forming region between the fifth and sixth transmembrane domains and intracellular amino and carboxy termini (Phelps et al., 2008). Based on TRP channel amino acid sequence similarity, mammalian TRP channels were classified into six subfamilies (Figure 1-1) (Wu et al., 2010): TRPC (Canonical), TRPM (Melastatin), TRPV (Vanilloid), TRPA (Ankyrin), TRPML (Mucolipin), TRPP (PKD) (Polycystin) (Clapham et al., 2005).

Cryo-electron microscopy (Cryo-EM) structures of almost all TRP channels have been solved in the last seven years and helped in elucidate structure, function and gating properties. The first solved TRP cryo-EM structure was the TRPV1 channel in the year 2013 (Cao et al., 2013; Liao et al., 2013).

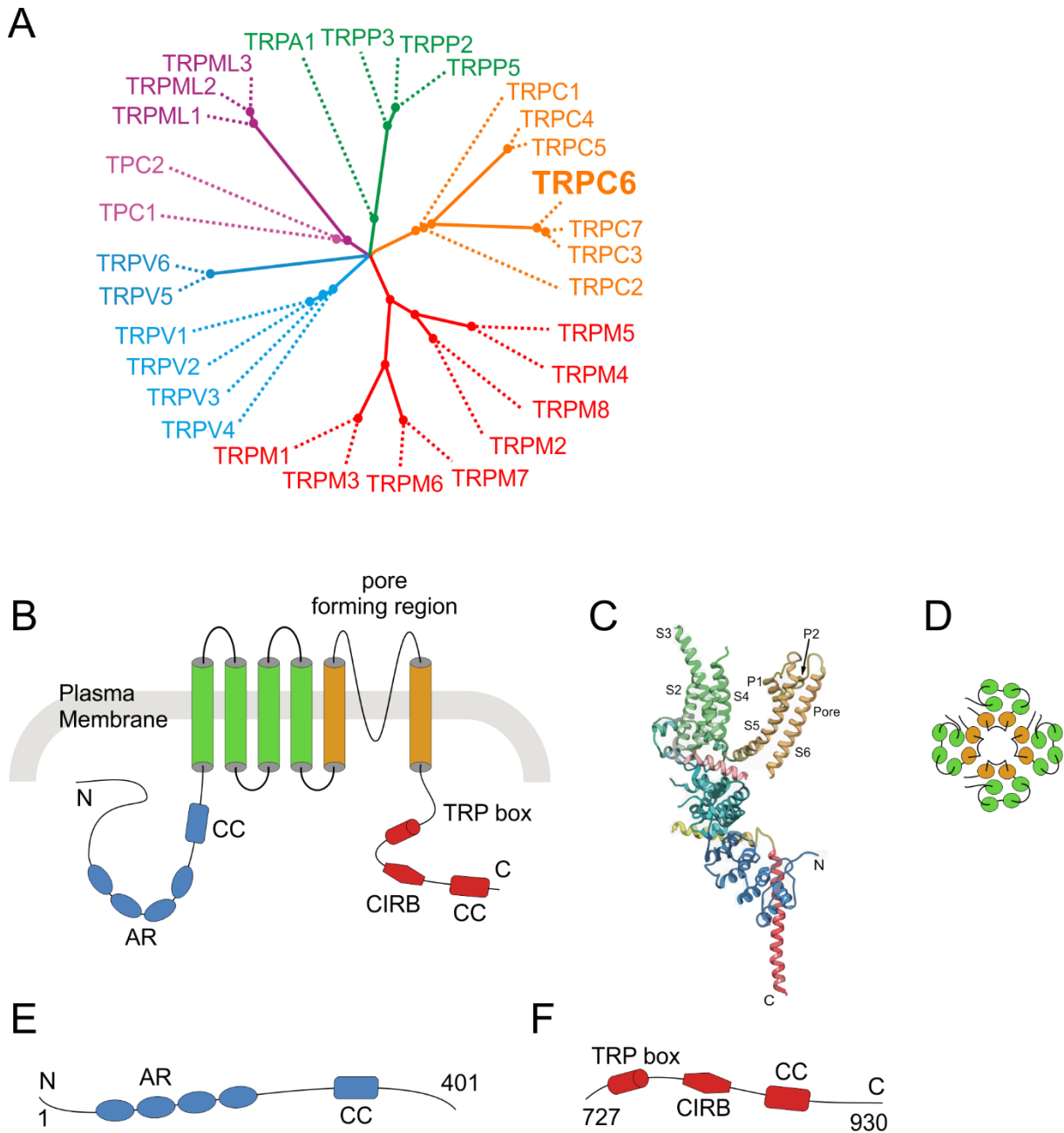


Figure 1-1. Phylogenetic tree of the TRP channel family and TRPC6 topology domains

(A) Phylogenetic tree of transient receptor potential channels showing the six subfamilies represented in different colors. (B) Structure of the TRPC6 monomer illustrating the six transmembrane domains crossing the plasma membrane, the pore forming region including the fifth and sixth transmembrane domains and the S5-S6 linker and an intracellular N- and C- termini. (C) Cryo-electron microscopy structure of one monomer subunit of TRPC6 channel (Tang et al., 2018) showing the TRPC6 domains represented in the different colors used in B (Permission from Springer Nature, Cell Research, Tang et al., 2018). (D) Top view of TRPC6 tetramer formed by four subunits to constitute a functional channel. (E, F) The TRPC6 N- terminus containing four ankyrin repeats and coiled coil (CC) domain (E) and the

C- terminus of TRPC6 containing the TRP box, the calmodulin/IP3R binding domain (CIRB) and coiled coil (CC) domain (F).

1.1.1 TRPC6 channel

1.1.1.1 TRPC6 structure, expression and associated proteins

The human TRPC6 cDNA was firstly cloned from placenta (Hofmann et al., 1999) while the mouse was cloned from the brain (Boulay et al., 1997). TRPC6 human gene is localized on chromosome 11q21-q22, whereas the mouse *Trpc6* gene is localized on chromosome 9 (D'Esposito et al., 1998). Human and mouse TRPC6 protein consists of 931 and 930 amino acid residues, respectively. The human and mouse proteins share more than 94% amino acid sequence identity (Figure 1-2).

The cryo-electron microscopy (Cryo-EM) structure of TRPC6 has been recently solved, and this could show many new structural properties of this ion channel in apo and bound states (Bai et al., 2020; Tang et al., 2018).

Like other transient receptor potential (TRP) channels, the TRPC6 channel is organized in four subunits, circling the ion-permeation pathway (Figure 1-1). Each subunit has a conserved structure of transmembrane domain composed of six alpha-helices (S1-S6) where the pore forming loop is located between the fifth and sixth (S5 and S6) transmembrane helices with S6 lining the ion permeation pore (Bai et al., 2020; Tang et al., 2018). The N- and C- termini are cytoplasmic and contain different domains, which are involved in regulating the channel function by serving as putative binding domains for other regulatory proteins (Engelke et al., 2002; Erlen et al., 2004). The long N- terminus of TRPC6 includes four ankyrin repeats and adjacent linker helices, whereas the C- terminus contains a conserved TRP box, a calmodulin/IP3R binding domain and a coiled-coil motif as demonstrated in the cryo-EM structure (Bai et al., 2020; Tang et al., 2018). Two glycosylation sites were identified in the

TRPC6 sequence and have shown to be located within the S1-S2 and S3-S4 extracellular linkers and are believed to control the TRPC6 channel activity (Dietrich et al., 2003).

<i>m</i> TRPC6	MSQSPRFVTRRGGSLKAAPGAGTRRNESQDYLLMD-ELGDDGYPQLPLPPYGYYSFRGN	59
<i>h</i> TRPC6	MSQSPAFGPRRGSSPRGAAGAAARRNESQDYLLMDSSELGEDGCPQAPLPCYGYYPCFRGS	60
<i>m</i> TRPC6	ENRLTHRRQTIILREKGRRLANRGPAYMFDHSTSLSEIEERFLDAAEYGNIPVVRKMLEE	119
<i>h</i> TRPC6	DNRLAHRRQTVLREKGRRLANRGPAYMFSDRSTSLSEIEERFLDAAEYGNIPVVRKMLEE	120
<i>m</i> TRPC6	CHSLNVNCVDYMGQNALQLAVANEHLEITELLKKNENLSRVGDALLLAISKGYVRIVEAI	179
<i>h</i> TRPC6	CHSLNVNCVDYMGQNALQLAVANEHLEITELLKKNENLSRVGDALLLAISKGYVRIVEAI	180
<i>m</i> TRPC6	LNHPAFAEGKRLATSPSQSELQODDFYAYDEDGTRFSDVTPPIILAAHCQEYEVHTLLR	239
<i>h</i> TRPC6	LSHPAFAEGKRLATSPSQSELQODDFYAYDEDGTRFSDVTPPIILAAHCQEYEVHTLLR	240
<i>m</i> TRPC6	KGARIERPHDYFCKCTECSQKQKHDSFHSRSRINAYKGLASPAYLSLSSDPVMTALEL	299
<i>h</i> TRPC6	KGARIERPHDYFCKCNDCKNQKQKHDSFHSRSRINAYKGLASPAYLSLSSDPVMTALEL	300
<i>m</i> TRPC6	SNELAVLANIEKEFKNDYRKLMSQCKDFVVGLLDLCRNTEEVEAILNGDAETROPDGFGR	359
<i>h</i> TRPC6	SNELAVLANIEKEFKNDYKKLMSQCKDFVVGLLDLCRNTEEVEAILNGDVEETLQSGDHGR	360
<i>m</i> TRPC6	PNLSRLKLAIKYEVKKFVAHPNCQQQLLSIWYENLSGLRQQTMAVKFLVVLAVAIIGLPFL	419
<i>h</i> TRPC6	PNLSRLKLAIKYEVKKFVAHPNCQQQLLSIWYENLSGLRQQTMAVKFLVVLAVAIIGLPFL	420
<i>m</i> TRPC6	ALIYWCAPCSKMGKILRGPFMKFVAHAASFTIFLGLLMNAADRFEFGTKLLPNETSTDNA	479
<i>h</i> TRPC6	ALIYWFAPCSKMGKIMRGPFMKFVAHAASFTIFLGLLMNAADRFEFGTKLLPNETSTDNA	480
<i>m</i> TRPC6	RQLFRMKTSCFSWMEMLIISWVIGMIWAECKEIWTOGPKEYLFELWNMLDFGMLAIFAAS	539
<i>h</i> TRPC6	KQLFRMKTSCFSWMEMLIISWVIGMIWAECKEIWTOGPKEYLFELWNMLDFGMLAIFAAS	540
<i>m</i> TRPC6	FIARFMAFWHASKAQSIIDANDTLKDLTKVTLGDNVKYYNLARIKWDPIDPQIISEGLYA	599
<i>h</i> TRPC6	FIARFMAFWHASKAQSIIDANDTLKDLTKVTLGDNVKYYNLARIKWDPIDPQIISEGLYA	600
<i>m</i> TRPC6	IAVVLSFSRIAYILPANESFGPLQISLGRVTVKDIFKFMVIFIMVFVAFMIGMFNLYSYYI	659
<i>h</i> TRPC6	IAVVLSFSRIAYILPANESFGPLQISLGRVTVKDIFKFMVIFIMVFVAFMIGMFNLYSYYI	660
<i>m</i> TRPC6	GAKQNEAFTTVEESFKTLFWAIFGLSEVKSVVINYNHKFIENIGYVLYGVYNVTMIVLL	719
<i>h</i> TRPC6	GAKQNEAFTTVEESFKTLFWAIFGLSEVKSVVINYNHKFIENIGYVLYGVYNVTMIVLL	720
<i>m</i> TRPC6	NMLIAMINSSFQEIEDDADVEWKFARAKLWFSYFEEGRTPVPFNLVPSPKSLFYLLLLKF	779
<i>h</i> TRPC6	NMLIAMINSSFQEIEDDADVEWKFARAKLWFSYFEEGRTPVPFNLVPSPKSLFYLLLLKL	780
<i>m</i> TRPC6	KKWMCELIQGGKQGFQEDAEMNKRNNEEKKFGISGSHEDLSKFLSLDKNQLAHNKQSSSTRSS	839
<i>h</i> TRPC6	KKWISSELFQGHKKGFQEDAEMNKINNEEKKLGIILGSHEDLSKFLSLDKKQVGHNKQPSSTRSS	840
<i>m</i> TRPC6	EDYHLNSFSNPPRQYQKIMKRLIKRYVLAQAIDKESDEVNEGELKEIKQDISSLRYELLE	899
<i>h</i> TRPC6	EDFHLNSFNPPRQYQKIMKRLIKRYVLAQAIDKESDEVNEGELKEIKQDISSLRYELLE	900
<i>m</i> TRPC6	EKSQNTEDLAELIRKLGERSLEPKLEESRR	930
<i>h</i> TRPC6	EKSQNTEDLAELIRELGEKLSMEPNQEEENR	931

Figure 1-2. Amino acid sequence alignment of the mouse and human TRPC6

Sequence identity of the TRPC6 proteins from mouse and human showing the conserved amino acids on black background.

The TRPC6 protein is abundantly present in smooth muscle cells where it contributes to the vascular muscle cell contractility (Dietrich et al., 2005). In the lung, it has been suggested that

the TRPC6 channel is responsible for enhancing the pulmonary vascular permeability (Weissmann et al., 2012) and maybe involved in pulmonary fibrosis (Dietrich and Gudermann, 2014). In the glomerulus and the collecting duct of the kidney, TRPC6 protein was identified (Hsu et al., 2007) and several TRPC6 point mutations were shown to cause kidney diseases (Reiser et al., 2005; Winn et al., 2005). Furthermore, TRPC6 protein was shown by immunocytochemistry to be present in the cardiac myocytes from wild-type mouse heart and was suggested to be involved in the pathologic cardiac hypertrophy (Kuwahara et al., 2006). In immune cells, TRPC6 was shown to be functionally expressed and to modulate immune responses. In addition, TRPC6 mRNA and protein were shown to be expressed in the human alveolar macrophages and lung tissue macrophages. Moreover, compared with controls, TRPC6 mRNA was increased in alveolar macrophages from chronic obstructive pulmonary disease (COPD) patients (Finney-Hayward et al., 2010). It has been also demonstrated that the TRPC3 and TRPC6 proteins may form a heteromeric functional channel in human T cells (Carrillo et al., 2012). Furthermore, TRPC6 proteins were identified by Western blot in mice erythrocytes (Foller et al., 2008). In addition, several studies have shown the presence of TRPC6 in platelets (Hassock et al., 2002; Mahaut-Smith, 2012). In the brain, TRPC6 transcripts were detected but the level of expression was lower compared with some other TRPCs (Hartmann et al., 2008).

So far, TRPC6 has been shown to hetero-multimerizes with other members of the TRPC family *in vitro*, after heterologous expression of the cDNAs like TRPC1 (Storch et al., 2012), TRPC3 and TRPC7 (Hofmann et al., 2002) to form hetero-tetrameric channels. Nevertheless, properties of channels formed by TRPC3/6/7 proteins including gating and permeation pathways are still enigmatic.

Some studies suggested that TRPC6 can be modulated by interacting with the IP3Rs (Boulay et al., 1999) and calmodulin (CaM) (Zhang et al., 2001) through the calmodulin/IP3R binding

domain located on the TRPC6 C- terminus. The latter binding domain has been shown to be also a binding site for phosphoinositides (PIs), which disrupt the TRPC6/CaM interaction (Kwon et al., 2007). At the N- terminus of TRPC6, the four ankyrin repeats represent potential binding sites for other proteins. For example MxA, an interferon-induced 76-kDa GTPase, which belongs to the dynamin superfamily can bind to the second ankyrin repeat of TRPC6 at the N- terminus part and play an important role in regulating the TRPC6 channel activity (Lussier et al., 2005). Fyn, a member of the Src family protein tyrosine kinases, was identified as an interaction partner of the TRPC6 by co-immunoprecipitation from rat brains as well as in heterologous overexpression systems. Fyn was binding to the N- terminus of the TRPC6 channel and single channel recordings show that it modulates the channel function in a tyrosine phosphorylation-dependent manner (Hisatsune et al., 2004). Moreover, in a proteomic study using lysates extracted from rat brain or kidney, the Na⁺/K⁺ ATPase pump was among proteins associated with the TRPC6 protein complex and this was confirmed by further biochemical assays (Goel et al., 2005). In the glomerular podocyte, the TRPC6 protein was identified and its binding to nephrin and podocin was demonstrated by coimmunoprecipitation and immunohistochemistry studies (Reiser et al., 2005). Furthermore, a recent study has reported a proteomics list of TRPC6 binding partners in human podocytes including the phospholipase C gamma 2 (PLC γ 2) (Farmer et al., 2019). Other TRPC6 binding partners identified by the latter study are Calpain, Caldesmon-1 and extracellular signal-regulated kinases (Erk1/2).

1.1.1.2 Biophysical and pharmacological properties of the TRPC6 channel

Transient receptor potential channel 6 (TRPC6) belongs to the TRPC subfamily and is closely related to the TRPC3 and TRPC7 (Pedersen et al., 2005). Based on the amino acid sequence alignment and pharmacological properties, the three channels form together the Diacylglycerol (DAG)-sensitive family (Hofmann et al., 1999; Pedersen et al., 2005). The TRPC6 channel is a calcium permeable non-selective cation channel with a poor selectivity for calcium (Gees et al., 2010). In patch clamp recordings, it displays a characteristic current-voltage curve with a

double-rectifying current. The TRPC6 channel activity can be modulated by calcium and this regulation varies and depends on the calcium concentration. Another factor involved in mediating TRPC6 channel activity is its phosphorylation by calmodulin-dependent kinase II (Shi et al., 2013). In A7r5 smooth muscle cells, the vasopressin induced TRPC6 currents were dependent on the extracellular calcium concentration levels. At physiological extracellular calcium concentration of around 2 mM, TRPC6 channels are partially inhibited. In contrast, when the extracellular calcium concentration is decreased, below the physiological level (50-200 μ M), the TRPC6 current is potentiated in comparison with physiological calcium concentrations (2 mM) (Jung et al., 2002).

Endogenously, the TRPC6 channel can be activated by the lipid Diacylglycerol (DAG), a product generated upon cleavage of the phosphatidylinositol 4,5-bisphosphate (PIP₂) in response to the activation of G_{q/11}-coupled receptor signaling pathways. TRPC6 can also be activated by the soluble membrane permeable, analog of DAG, the 1-oleoyl-2-acetyl-sn-glycerol (OAG) and it leads to the activation of TRPC6 channel independently of the protein kinase C (PKC) (Hofmann et al., 1999). The mechanism by which OAG induces TRPC6 channel activation is still not completely solved and needs further investigation. Lichtenegger and colleagues suggested that the Gly709 of the human TRPC6 protein (a conserved amino acid residue among TRPCs) and located at the sixth transmembrane domain (S6) of TRPC6, is a crucial element for DAG recognition (Lichtenegger et al., 2018). This year, Bai et al., propose that the human TRPC6 amino acid residues Glu672 (pore helix), Asn702 and Tyr705 (sixth transmembrane domain, S6), which are conserved among TRPC3/6/7, composing most probably the DAG binding region (Bai et al., 2020). Flufenamic acid, a member of the class of nonsteroidal anti-inflammatory drugs, was shown to activate the TRPC6 channel in HEK293 cells and in acutely isolated lung endothelial cells (Weissmann et al., 2012). It has been claimed that hyperforin, a natural phytochemical compound produced and extracted from *Hypericum perforatum* (St. John's wort), which has an anti-depressive effect, could activate

TRPC6 channels at 10 μM concentration in heterologous systems (Leuner et al., 2007). However, hyperforin has a protonophore activity (Sell et al., 2014), which has been interpreted as TRPC6 activity by Leuner et al. Recently, Bai et al reported a novel specific TRPC6 small molecule agonist AM-0883 with an EC_{50} of 45.5 nM (Bai et al., 2020).

Several TRPC6 inhibitors have been described. Similar to other TRPs, TRPC6 channels are inhibited by the trivalent ions La^{3+} and Gd^{3+} (Inoue et al., 2001). On one hand, 2-Aminoethoxydiphenyl borate (2-APB) showed an inhibitory effect on the TRPC6 channel activity (Tsfai et al., 2001). On the other hand, 2-APB activates the TRPV1, TRPV2 and TRPV3 channels at higher concentrations (Hu et al., 2004). Clotrimazole discovered in 1969 and used as an antifungal medicament turned out to block TRPC6 and other members of the TRP channel family (Harteneck et al., 2011). SKF-96365, is another nonspecific transient receptor potential 6 (TRPC6) blocker, which was found to suppress TRPC6 channel activity in human podocytes (Zhang et al., 2017). Moreover, it has been shown that TRPC6 activation by mechanical stretch or by application of diacylglycerol was blocked by tarantula peptide, GsMTx-4 (Spasova et al., 2006). But again, GsMTx-4 is a blocker of mechanosensitive channels like Piezo and TACAN (TMEM120A), which had not been identified in the year 2006. Taken together, the previously described TRPC6 channel activators and blockers appear to be non-specific and have less selectivity towards the TRPC6 channel, which argue against their use and the accuracy of the obtained results.

During the last couple of years, a lot of efforts have been made to identify new compounds with higher selectivity and specificity towards TRPC6 channel. The synthetic gestagen norgestimate, initially discovered and used in birth control pills and as a treatment for some hormonal disorders, was found to inhibit TRPC3 and TRPC6 with IC_{50} values of 3-5 μM (Miehe et al., 2012). Furthermore, the SAR7334 inhibitor showed a potent and specific inhibition of the TRPC6 channel activity in the range of nanomolar concentration, IC_{50} of 9.5 nM (Maier et al., 2015). The last identified compound was reported this year, the AM-1473, a small molecule

antagonist with an IC_{50} of 0.22 nM (Bai et al., 2020). The cryo-EM structure of TRPC6 and the discovery of novel TRPC6 activators and blockers open new opportunities to further investigate and target the TRPC6 channel in healthy and diseased organisms.

1.1.1.3 TRPC6 channel related diseases

Accumulating evidence showed that calcium influx through ion channels including TRPC6 plays a critical role in maintaining the integrity of cellular function. TRPC6 is widely expressed in the cardiovascular system and Kuwahara and colleagues showed that the TRPC6 gene expression is increased in animal models of cardiac hypertrophy and heart failure. The mice overexpressing *Trpc6* cDNA under the cardiac-specific α -MHC promoter develop a severe cardiac hypertrophy in early stages of life (Kuwahara et al., 2006). However, it is still an open issue whether *Trpc6* is expressed at all in cardiac myocytes (Camacho Londono et al., 2015).

In lung tissues and pulmonary artery smooth muscle cells from idiopathic pulmonary arterial hypertension patients, the mRNA and protein expression of the TRPC3 and TRPC6 were much higher than in those from normotensive individuals (Yu et al., 2004). TRPC6 was also described to play a role in the depolarization and constriction of small arteries and arterioles induced by elevated intravascular pressure in the vascular smooth muscle cells (Welsh et al., 2002). However, *Trpc6* gene-deficient mice display an elevated systemic blood pressure and increased agonist-induced muscle contractility of aortic rings and in the cerebral arteries as well. This observed effect was interpreted by the compensatory effect induced by the high expression levels of TRPC3 in these cells (Dietrich et al., 2005). The TRPC6 was demonstrated as a key regulator of hypoxic pulmonary vasoconstriction and this control mechanism was abrogated in mice lacking the *Trpc6* gene (Weissmann et al., 2006). In addition, lung endothelial calcium and permeability response to platelets-activating factor was shown to be mediated by Acid sphingomyelinase and TRPC (Samapati et al., 2012).

In the central nervous system, TRPC6 mRNA was less abundant compared with the mRNA of other TRPCs and the levels of detection were variable (Riccio et al., 2002). The TRPC6-evoked calcium entry was altered by presenilin 2, a protein which was linked to the development of early onset of Alzheimer's disease (Lessard et al., 2005). TRPC6 was identified in the kidney along the glomerulus and the collecting duct (Hsu et al., 2007). Mutations in the gene located on chromosome 11q encoding the cation permeable channel TRPC6 were found in patients with glomerular dysfunction and kidney failure. These mutations are linked hereditary to the development of the autosomal dominant form of focal segmental glomerulosclerosis (FSGS), which is characterized by a loss of the integrity and alteration of the glomerular filter (Reiser et al., 2005). So far, more than twenty TRPC6 mutations were identified in patients with focal segmental glomerulosclerosis (P112Q, N143S, S270T, K874*, R895C, E897K, P15S, N110H, G109S, N125S, L780P, M132T, R175Q, R360H, L395A, A404V, Q889K, 85_88dupAYMF, G757D, H218L and R895L), and the majority of these mutations appeared to be gain of function mutations (Reiser et al., 2005; Riehle et al., 2016; Winn et al., 2005). Functional studies showed that the expression of the TRPC6 mutant cDNAs in heterologous expression systems lead to an increase in the TRPC6 channel activity and results in higher calcium influx compared with the wild-type controls (Reiser et al., 2005). Subsequently, it is believed that increased calcium load is responsible for podocytes apoptosis and therefore focal segmental glomerulosclerosis (FSGS). Nonetheless, five human TRPC6 gene mutations (N125S, L395A, G757D, L780P, and R895L) were described to cause a loss of function and were also identified in patients with FSGS. These studies show that both the gain of function as well as the loss of function mutations of TRPC6 channel are causing related and similar kidney diseases (Riehle et al., 2016), pointing to the importance of maintaining and fine tuning of the intracellular calcium concentration in order to sustain healthy physiological kidney functions. In human and mouse platelets, the TRPC6 channel was suggested to modulate the thromboxane receptor-dependent calcium entry and therefore regulate the platelet function (Paez Espinosa et al., 2019; Vemana et al., 2015).

1.2 Platelets function in mice and human

Already in 2002, the TRPC6 protein has been identified in platelets, but its function in platelets is enigmatic (Chen et al., 2014; Harper et al., 2013; Ramanathan et al., 2012). My doctoral thesis deals with the function of TRPC6 in platelets and in the following I want to give a start introduction into platelets function.

Platelets are small (2-5 μm) non-nucleated cells in the blood. They play a crucial role in the blood hemostasis by cell adhesion and initiating blood clots following vessel damage. They were first described in the 1880s by Bizzozero, to be the major components participating in both hemostasis and thrombosis using intravascular microscopy and *in vitro* flow chamber studies (Coller, 2011). Once the platelets are released from their precursor, megakaryocytes, through a regulated process, suggested to occur mainly in the bone marrow or in the lung (Lefrancais et al., 2017), they circulate in the cardiovascular system for 7-10 days. The 7-10 days old platelets undergo phagocytosis and are destroyed in the liver and spleen (Brown et al., 2000). In the healthy human individuals, platelets count ranges from 140 to 440 $\times 10^9/\text{L}$. Although platelets were known for long time as the main components and regulators of the blood hemostasis and thrombosis, it has been shown in the last years that platelets are involved also in other pathophysiological processes including inflammation (Lindemann et al., 2007), innate immunity (Engelmann and Massberg, 2013), and tumor growth and metastasis (Gay and Felding-Habermann, 2011).

Structurally, the non-activated platelets are not round but having a biconvex discoid shape, which changes upon activation. Based on organization and function, platelet regions can be divided into different zones: i) A peripheral zone containing glycoproteins responsible initially for platelets activation, adhesion and aggregation. ii) A sol-gel zone consisting of microtubules suggested to be involved in maintaining platelets shape. iii) An organelle zone, which includes different secretory organelles such as: α -granules, dense granules and lysosomes besides to

the presence of simple mitochondria. Finally, iv) membrane systems are also present in the platelets surrounding the intracellular zones (Geraldo et al., 2014).

1.2.1 Activation and aggregation of platelets

Platelets maintain blood hemostasis within the circulation and any dysfunction of the platelets can lead to various complications (Huebsch and Harker, 1981). Thrombocytopenia and thrombocytosis can result from low or elevated platelets concentration, respectively. Under healthy condition, platelets circulate within the blood vasculature in a proximity to the vessel walls without any interaction. This behavior is regulated in a part by the release of inhibitory factors such as nitric oxide, prostaglandins and the expression of CD39, which is a cell surface enzyme hydrolyzing γ - and β -phosphate residues of extracellular phosphonucleosides (Bye et al., 2016; Gayle et al., 1998). Once the endothelial layer is disrupted, the platelets bind through their receptors to the collagen and von Willebrand factor, which are in the exposed matrix, further platelets are recruited from the circulation to induce platelets clot formation (Golebiewska and Poole, 2015). Binding of the platelets to fibrinogen results in platelets spreading and adhesion, which is induced by fibrinogen receptor clustering followed by activation of the glycoprotein IIb/IIIa (α IIb β 3-integrin) on the platelets surface. The release of the content of alpha- and dense granules including adenosine diphosphate (ADP), which is cleaved to AMP by CD39, as well as the generation of thrombin by the coagulation cascade, strongly enhances platelets activation particularly through integrin receptor pathways (Jurk and Kehrel, 2005). Upon activation and a subsequent binding to the collagen, fibrinogen and others, platelets undergo a signal cascade, which activates other signaling pathways inside the platelets to control their function (Li et al., 2010). Platelets gathering to the injury site are promoted by different factors and result in linking activated platelets through fibrinogen bridges to form aggregates. Thrombin conversion from prothrombin amplifies platelets activation and converts fibrinogen to fibrin, which stabilizes the blood clot formation (Clemetson, 2012). Blood hemostasis requires a tight regulation and any defect can lead to severe consequences.

Abnormal or insufficient blood coagulation can be caused by inherited genetic disorders like hemophilia or autoimmune diseases like immune thrombocytopenia, which both result in a high risk of bleeding. Contrary, abnormal hyperactivity of the platelets or blood coagulation under certain conditions can lead to increased blood clot formation, which in turn results in thrombosis. The arterial thrombosis is the cause of myocardial infarction and stroke whereas the venous thrombosis is the reason of pulmonary embolism (Koupenova et al., 2017).

1.2.2 Signaling pathways downstream platelet activation

Different receptors are expressed on the platelets surface and play a role in the hemostatic platelets function. Among these receptors are glycoproteins, which serve as binding sites for other molecules. Glycoprotein (GP) Ib-IX-V complex consists of the association of four subunits, GPIb α , GPIb β , GPV and GPIX, and serves as a receptor for von Willebrand factor (vWF) (Huang et al., 2019). Initially, platelet adhesion at the damaged vessel site is enabled by different interactions. These bindings associate with conformational changes within the membrane receptor glycoproteins IIb/IIIa (integrin α IIb β 3) and thereafter their activation. Glycoproteins IIb/IIIa or (integrin α IIb β 3) are the most abundant receptors in the outer membranes of the platelets and by their binding to fibrinogen they initiate adhesion and activation of platelets, leading to clot formation (Floyd and Ferro, 2012). Activation of platelets by collagen binding to glycoprotein VI triggers the activation of the γ chain of the Fc receptor, which binds to the intracellular domain of the glycoprotein VI. By consequence, the stimulation of tyrosine kinases such as Src kinase FYN/LYN leads to phospholipase C γ activation (Senis et al., 2014). Platelet stimulation associates also with PLC γ activation, which triggers tyrosine kinases to phosphorylate the downstream substrates (Huang et al., 2019). G protein-coupled receptors (GPCRs) are also expressed on platelet surface and are suggested to be targets for several diffusible mediators such as ADP, thromboxane A₂, and thrombin (Offermanns, 2006). Adenosine diphosphate (ADP) is stored in the dense granules. Upon release, it binds to the

P2Y1 and P2Y12 receptors, which in turn play a role in the platelet activation process in an autocrine and paracrine manner (Offermanns, 2006). Nowadays, the adenosine diphosphate (ADP) receptors especially P2Y12, are used as drug targets to inhibit platelet aggregation. These adenosine P2Y12 receptor antagonists include Ticlopidine, Clopidogrel, Prasugrel and Ticagrelor, each of which is combined with low-dose acetylsalicylic acid in patients with coronary heart disease. The binding of thrombin, which converts fibrinogen to fibrin, to its receptor protease-activated receptors PAR1 and PAR4 results in activation by specific cleavage of the extracellular amino terminal PAR domain. Thrombin binding to the PAR receptors on the platelets promotes platelet activation and aggregation (Coughlin, 2005). The produced thromboxane A2 by the activated platelets can interact thereafter with thromboxane A2 receptors, which in turn stimulates activation of other platelets and their aggregation (Offermanns, 2006). Signaling through the G protein-coupled receptors, induces activation of phospholipase C β but not of phospholipase C γ (Ozaki et al., 2005). Nonetheless, activation of both phospholipase C isoforms, C β /C γ hydrolyses of membrane phosphatidylinositol (4,5)-bisphosphate (PIP2) into diacylglycerol (DAG) and inositol (1,4,5)-triphosphate (IP3). PIP2 and DAG contribute to many signaling pathways, which in turn result in regulation of cellular functions. IP3 is bound by the IP3 receptor channels in the endoplasmic reticulum (ER), initiating calcium release and causing an increase in the cytoplasmic calcium concentration in the cells (Streb et al., 1983). Diacylglycerol (DAG) remaining at the cell membrane is involved in the activation of the protein kinase C (PKC), which acts on other proteins in the cell (Nishizuka, 1995). Diacylglycerol (DAG) is also known to activate many cation channels including TRPC6, which triggers calcium influx and may regulate different cellular processes (Varga-Szabo et al., 2009). However, while the TRPC6 protein has been reliably detected in platelets (Hassock et al., 2002), the detection of other TRPCs is far less reliable.

1.3 Aim

The aims of my study are:

1. Identification of the TRPC6 protein in human platelets.
2. Investigation of the TRPC6 channel function in human platelet adhesion using TRPC6 agonists and antagonists, and in murine platelet adhesion, using platelets acutely isolated from wild-type mice and from *Trpc6* gene-deficient mice as controls.
3. Establishment of an antibody-based protocol to purify the undenatured TRPC6 channel containing protein complex from human platelets.
4. Analysis and identification of the TRPC6-associated proteins in human platelets using quantitative label-free mass spectrometry.
5. Characterization of TRPC6 function by the identified TRPC6-associated proteins, especially GIT1.

2 Materials and Methods

2.1 Buffers and solutions

Table 2-1. Composition of buffers and solutions

Buffers/Solutions	Components
Mass spectrometry	
Coomassie staining solution	0.12% (w/v) Coomassie Brilliant Blue G 250 10% (w/v) (NH ₄) ₂ SO ₄ 10% (v/v) H ₃ PO ₄ 20% (v/v) Methanol
Extraction solution	2.5% (v/v) Formic acid 50% (v/v) Acetonitrile
Fixation solution	40% (v/v) Ethanol 10% (v/v) Acetic acid
Solution A	50 mM NH ₄ HCO ₃
Solution B	25 mM NH ₄ HCO ₃ 50% (v/v) Acetonitrile
Reduction solution	50 mM NH ₄ HCO ₃ 10 mM Dithiothreitol
Alkylation solution	50 mM NH ₄ HCO ₃ 5 mM Iodoacetamid
Trypsin solution	50 mM NH ₄ HCO ₃ 10 ng/μL Trypsin
2D-BN/SDS PAGE	
Equilibrating buffer A	12.5 mM Tris 4% (w/v) SDS 20% (v/v) Glycerol 9% (v/v) β-Mercaptoethanol pH 6.8 (HCl)

MATERIALS AND METHODS

Buffers/Solutions	Components
Equilibrating buffer B	12.5 mM Tris 4% (w/v) SDS 20% (v/v) Glycerol 2.5% (w/v) Iodoacetamid pH 6.8 (HCl)
SDS-PAGE and Western blot	
2X SDS denaturing buffer	120 mM Tris 8% (w/v) SDS 20% (v/v) Glycerin 10% (v/v) β -Mercaptoethanol 0.01% (v/v) Bromophenol blue pH 6.8 (HCl)
10X TBS buffer	0.5 M Tris 1.5 M NaCl pH 8.0 (HCl)
TBST buffer	1X TBS buffer 0.05% (v/v) Tween 20
4X Stacking gel buffer	0.5 M Tris 0.4% (w/v) SDS pH 6.8 (HCl)
4X Separating gel buffer	1.5 M Tris 0.4% (w/v) SDS pH 8.8 (HCl)
10X SDS Electrophoresis buffer	0.25 M Tris 1.92 M Glycine 1% (w/v) SDS pH 8.3 (HCl)
Stripping buffer	62.5 mM Tris 2% (w/v) SDS 0.7% (v/v) β -Mercaptoethanol pH 6.8 (HCl)
Running buffer	1X SDS buffer
Immunoprecipitation	
PBS buffer	137 mM NaCl 2.7 mM KCl 1.5 mM KH_2PO_4 8.1 mM Na_2HPO_4 pH 7.4

MATERIALS AND METHODS

Buffers/Solutions	Components
Buffer B	0.1 M NaH ₂ PO ₄ and Na ₂ HPO ₄ pH 7.4 (NaOH)
Buffer C	Buffer B 3 M (NH ₄) ₂ SO ₄ pH 7.4 (NaOH)
Buffer E	PBS 0.1% (w/v) BSA pH 7.4
Solubilization buffer	150 mM NaCl 1 mM CaCl ₂ 100 mM HEPES 1% (w/v) digitonin pH 7.4
Calcium imaging	
Calcium imaging buffer	140 mM NaCl 4 mM KCl 1 mM MgCl ₂ 10 mM HEPES 10 mM Glucose 2 mM CaCl ₂ pH 7.35
Radioactive assay	
Binding buffer	20 mM Tris 100 mM NaCl 0.1% (w/v) Triton x-100 pH 7.5
Fractionation assay	
Homogenization buffer	20 mM Tris 250 mM Sucrose 1 mM EDTA 1 mM EGTA pH 7.4 (HCl)
Electrophysiological recordings	
Patch pipette solution	8 mM NaCl 1 mM MgCl ₂ 120 mM Cs-glutamate 10 mM HEPES 10 mM Cs-BAPTA

MATERIALS AND METHODS

Buffers/Solutions	Components
	3.1 mM CaCl ₂ (100 nM free Ca ²⁺) pH 7.2 (CsOH)
Bath solution	140 mM NaCl 2.8 mM KCl 2 mM MgCl ₂ 1 mM CaCl ₂ 10 mM HEPES 10 mM Glucose pH 7.2 (NaOH)
<i>In vitro</i> binding	
Binding buffer	PBS 0.1% (v/v) NP40 50 µg/mL BSA pH 7.4
Pull-down	
Lysis buffer	PBS 1% (w/v) Triton x-100 1 mM EDTA pH 7.4
Washing buffer	PBS 1% (w/v) Triton x-100 1 mM EDTA 0.25 M NaCl pH 7.4
Cell surface biotinylation	
Biotinylation buffer	PBS 1 mM MgCl ₂ 0.5 mM CaCl ₂ pH 8.0
Platelet adhesion	
1X Tyrode's buffer	12 mM NaHCO ₃ 10 mM HEPES 137 mM NaCl 2.7 mM KCl 2 mM CaCl ₂ 1 mM MgCl ₂ 5.5 mM D-Glucose 0.1% (w/v) BSA pH 7.4

MATERIALS AND METHODS

Buffers/Solutions	Components
Fixation buffer	PBS 2% (w/v) Paraformaldehyde
Permeabilization buffer	PBS 0.2% (w/v) Triton x-100
Blocking buffer	PBS 2% (w/v) BSA
Platelet immunostaining	
Modified Tyrode's buffer	1X Tyrode's buffer 1 mM CaCl ₂ pH 7.4
Fixation buffer	PBS 1% (w/v) Paraformaldehyde
Permeabilization buffer	PBS 0.3% (w/v) Triton x-100
Blocking buffer	PBS 1% (w/v) BSA
Washing buffer	PBS 0.3% (w/v) Triton x-100 0.1% (v/v) Tween 20

MATERIALS AND METHODS

Table 2-2. Primary and Secondary antibodies

Primary/Secondary antibodies	Dilution	Company	Reference
Primary antibodies			
Human TRPC6 1263 (rabbit polyclonal)	1:100	HOM-MADE	This study
Mouse TRPC6 861 (rabbit polyclonal)	1:100	HOM-MADE	(Foller et al., 2008)
TRPC6 2F2-D10 (1:100) (rat monoclonal)	1:100	HOM-MADE	This study
HA (mouse monoclonal)	1:500	Thermo-pierce	26183
GIT1 (rabbit polyclonal)	1:200	Santa Cruz Biotechnology	sc-13961
IP3RI (mouse monoclonal)	1:1000	NeuroMab	75-035
IP3RII (goat polyclonal)	1:200	Santa Cruz Biotechnology	sc-7278
α 1-subunit of the Na ⁺ /K ⁺ ATPase (mouse monoclonal)	1:250	Abcam	7671
Calnexin (rabbit polyclonal)	1:500	Enzo Life Sciences	ADI-SPA-860-F
MBP (mouse monoclonal)	1:100	Santa Cruz Biotechnology	sc-13564
GST (goat polyclonal)	1:100	Sigma-Aldrich	GE27-4577-01
phospho-p44/42 MAPK (rabbit polyclonal)	1:100	Cell signaling	9101
p44/42 MAPK (rabbit polyclonal)	1:500	Cell signaling	9102

MATERIALS AND METHODS

Primary/Secondary antibodies	Dilution	Company	Reference
phospho-PAK2 (S20) (rabbit polyclonal)	1:500	Cell signaling	2607
PAK2 (S20) (rabbit polyclonal)	1:500	Cell signaling	2608
Secondary antibodies			
ECL™ anti-rabbit IgG HRP linked F(ab') ₂ fragment (donkey)	1:50 000	GE Healthcare Lifescience	NA9340V
ECL™ anti-mouse IgG HRP linked F(ab') ₂ fragment (sheep)	1:20 000	GE Healthcare Lifescience	LNA9310V/AF
ECL™ anti-rat IgG HRP linked whole antibody (goat)	1:10 000	GE Healthcare Lifescience	LNA935V/AG
IgG (H+L) rabbit anti-goat, HRP, superclonal™	1:5000	Invitrogen	A27014
Cy3™-secondary goat polyclonal anti-rabbit	1:1000	Invitrogen	A10520
Alexa Fluor® 488 affiniPure donkey anti-mouse	1:1000	Jackson ImmunoResearch	715-545-150

Table 2-3. Compounds and Reagents

Reagents	Company	Reference
Peptide 1445	HOM-MADE	IRELGEKLSMEPNQEETNR
Serva blue G solution	SERVA Electrophoresis GmbH	42538.01
Cathode buffer	SERVA Electrophoresis GmbH	42536.01
Anode buffer	SERVA Electrophoresis GmbH	42535.01
Trypsin	Promega	V5111
Digitonin	AppliChem	A1905
Phosphatase inhibitor tablets	Roche	04906845001
BSA	Applichem	A1391,0100
Opti prep	Axis-Shield PoC AS	
EZ-link™ Sulfo-NHS-LC-Biotin	Thermo Scientific	21335
Triton x-100	CARL ROTH	3051.2
Tween 20	CARL ROTH	9127.1
Paraformaldehyde	Sigma-Aldrich	P6148
Western lightning plus	PerkinElmer	NEL 105001EA
BCA reagent A and B	Pierce™ BCA Protein Assay Kit	23225

MATERIALS AND METHODS

Reagents	Company	Reference
L- [³⁵ S] Methionine	Hartmann Analytic	SRM-01
Fura-2 AM	Invitrogen	F1221
DMSO	Sigma-Aldrich	D-2650
OAG	Cayman Chemical Company	62600
SAR7334	Tocris	5831
Collagen Reagans HORM	Takeda	1130630
Fibrinogen	Sigma-Aldrich	F4883
Alexa Fluor™ 488 Phalloidin	Thermo Scientific	A12379
Poly-L-lysine	Sigma-Aldrich	P1274
FCS	Life Technologies	10270106
MEM	Life Technologies	31095-029
DMEM	Life Technologies	41966-029
FuGENE HD	Promega	E2312
Opti-MEM	Life Technologies	51985-026
Fluoromount-G	SouthernBiotech	0100-01

Table 2-4. Devices and Instruments

Instrument	Company	Reference
Ultimate 3000 RSLCnano system	ThermoFisher Scientific	
LTD Orbitrap Velos Pro	ThermoFisher Scientific	
Ultimate 3000 RS autosampler	ThermoFisher Scientific	
OPTIMA XPN - 90 ultracentrifuge	Beckman Coulter	A94468
Jouan multifunction centrifuge	Thermo Scientific	cr3i
Microcentrifuge	Eppendorf	5418R
Vacuum centrifuge	Savant	Speed Vac Sc 110
Luminescent image analyzer	Fujifilm	LAS-3000
Western blot shaker	Desaga Sarstead-Gruppe	DE 24
Cold room roller	Assistant	RM5
Fluorescence microscope for calcium imaging	Carl Zeiss	Axiovert S100
Confocal microscopy	Carl Zeiss	LSM 780
Fluorescence microscope for patch clamp	Carl Zeiss	Axiovert 135 M
Light microscope	Carl Zeiss	Axiovert 25
Fluorescence microscope	Carl Zeiss	Observer, Z1

MATERIALS AND METHODS

Instrument	Company	Reference
Cooled Charged-Coupled Device (CCD) camera	TILL Photonics	Imago
Monochromator	TILL Photonics	Polychrome V
Patch clamp amplifier	HEKA Electronics	EPC-9 patch clamp
Vertical Puller	Narishige	PC-10
Phosphor-imaging plate	Fujifilm	BAS-SR 2040
Phosphor-imager reader	Fujifilm	BAS-2500
Liquid scintillation counter	Wallac	1409
Plate reader	Tecan	Infinite M200
Objectif 5X	Carl Zeiss	A-Plan 5X/0.25
Objectif 10X	Carl Zeiss	A-Plan 10X/0.25 ph1var1
Objectif 20X	Carl Zeiss	Fluar 20X/0.75
Objectif 63X	Carl Zeiss	63X/1.4 oil DIC/M27
Objectif 100X	Carl Zeiss	EC plan- Noefluar 100X/ 1.3 oil
Camera	Carl Zeiss	Axiocam color 412/312
Camera	Carl Zeiss	Axiocam MRm
Cell culture incubator	Binder	CB-150

2.2 Methods

2.2.1 Preparation of human platelets sample

Human platelets were obtained from the Blood Bank (Institute of Clinical Hemostaseology and Transfusion Medicine) at the Saarland University Medical Center (Director: Univ.-Prof. Dr. med. Hermann Eichler) and his deputy director Professor Dr. med. Joachim Schenk with approval by the ethics commission at the Ärztekammer des Saarlandes (approval number 203/13). To obtain the platelet-rich plasma (PRP), platelets were centrifuged at $1730 \times g$ (Jouan cr3i multifunction centrifuge, Thermo Scientific) for 15 min at 4°C (Table 2-4). The sedimented platelets were either used immediately for experiments e.g. for immunoprecipitation, platelet adhesion assay or stored at -80°C until use.

2.2.2 Antibody-based affinity purification of TRPC6

To purify the TRPC6 protein from human platelets, first 100 μg of the specific anti-TRPC6 antibody and non-specific immunoglobulins as a control (Table 2-2) were covalently coupled to 5 mg beads (corresponding to 165 μL beads suspension) (Dynabeads® M-280 Tosylactivated) in the presence of 50 μL buffer B and 100 μL buffer C (Table 2-1) for 12-16 h at 21°C under rotation. Next day, the free binding sites on the beads were blocked by incubating the beads in 1 mL of buffer D (Table 2-1) for 1 h at 21°C . Beads were then washed thoroughly 3 times with 1 mL buffer E (Table 2-1) and used either immediately or stored in the same buffer at 4°C until further use. To prepare the lysate of human platelets, 30 mL of PRP (platelets-rich plasma) was centrifuged at $1730 \times g$ for 15 min at 4°C . The sedimented platelets were resuspended in 20 mL buffer containing 1X solubilization buffer (Table 2-1), supplemented with protease inhibitors (0.3 μM aprotinin, 10 μM leupeptin, 1 μM pepstatin, 1 μM phenylmethanesulfonyl fluoride, 90 mM iodoacetamid and 1 μM benzamidine) and phosphatase inhibitor (1 tablet per 10 mL), transferred into a glass Teflon potter and

homogenized 10 times using up and down shaking at 4°C. Thereafter, the homogenate was incubated for 60 min at 4°C on a tube rotator, followed by centrifugation at 100.000 × *g* for 45 min at 4°C to eliminate cellular debris (OPTIMA XPN-90 ultracentrifuge, type 50.2 Ti rotor). The resulting supernatant was then incubated with antibodies coupled to magnetic beads (see above) at 4°C for 3 h under gentle rotation. The beads were then washed 5 times with 5 mL buffer containing 1X solubilization buffer (Table 2-1) supplemented with the protease and phosphatase inhibitors indicated above, but only with 0.1% (w/v) digitonin using a magnetic rack.

In order to elute the TRPC6 channel complex without disrupting any interactions, the beads were incubated with the antigenic 1445 peptide (4 mg/mL in solubilization buffer) (Table 2-1), which corresponds to the epitope recognized by the anti-TRPC6 (1263) antibody, under vortexing using a vortex mixer shaker and this elution was performed 5 times (Figure 2-1). The first two elution steps were conducted for 20 min at 4°C whereas the last three ones were performed for 10 min at 21°C. The eluted proteins were concentrated by filtration through a molecular weight cut-off filter of 100 kDa to separate TRPC6 complex and centrifuged at 3000 × *g* for 40 min at 4°C until around 500 µL is left on the top of the filter. The eluate was further analyzed by blue native PAGE, SDS-PAGE and mass spectrometry.

2.2.3 Cell lines and transfections

HEK293 and Cos-7 cells (ATCC CRL-1573 and CRL-1651) were purchased from the American Type Culture Collection (ATCC, Manassas, VA) and the HEK293 cell line stably expressing the mouse *Trpc6* cDNA (Boulay et al., 1997) tagged with the HA epitope at the C- terminus was kindly provided by Dr. M.X. Zhu (University of Texas Health Science Center, Houston). HEK293 and Cos-7 cells were grown in MEM and DMEM medium (Table 2-3), respectively and supplemented with 10% fetal bovine serum (FBS) and 1% GlutaMAX (Cos-7). HEK293 cells stably expressing the mouse *Trpc6* cDNA (HEK-TRPC6) were cultured in DMEM

supplemented with 10% FBS. All cells were maintained in an incubator at 37°C and 5% CO₂, and the medium was changed every third day. For transient transfection, cells were cultured in 3.5 mm petri dishes until their confluency reaches 70%. A mixture containing 2 µg cDNA, 5 µL FuGENE HD reagent and 100 µL Opti-MEM medium (Table 2-3) was incubated for 15 min at 21°C and then was added to the cells and incubated for 48 h at 37°C and 5% CO₂. Cells were either used directly or plated on coated coverslips for further experiments (e.g. patch clamp).

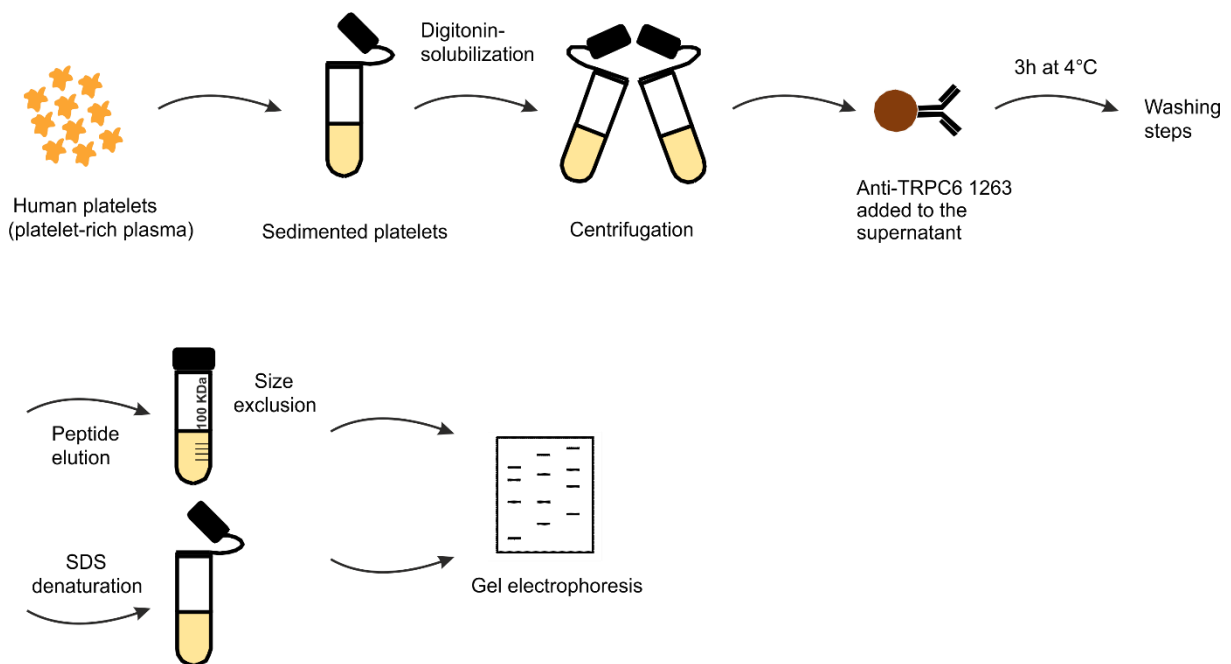


Figure 2-1. Antibody-based affinity purification method

Sedimented platelets were prepared from human platelet-rich plasma (PRP). The solubilization was performed in the presence of 1% (w/v) digitonin. Centrifugation step at 100.000 × g was applied to separate cell debris. The supernatant was incubated for 3 h at 4°C with the anti-TRPC6 antibody (1263) coupled to beads. After 5 times washing, protein complexes were eluted either by using an antigenic peptide or 2X SDS denaturing buffer. Filter tubes were used to concentrate protein complexes which can be used in further experiments. Eluted proteins were separated by gel electrophoresis.

2.2.4 Western blot analysis

Before Western blot was performed, protein concentration in the cell lysate was determined using the bicinchoninic acid assay (BCA). BCA exhibits a purple color that is measured using a colorimetric technique. Increasing concentrations of BSA standards as well as different dilutions of the sample were incubated with BCA reagent A and B (Pierce™ BCA Protein Assay Kit) for 30 min at 60°C. Finally, 300 µL from each sample was loaded into a 96 well-plate, then the absorbance at 562 nm was recorded.

For Western blot analysis, lysates of HEK293, Cos-7 or platelets, or eluates from immunoprecipitations were incubated with equal volumes of 2X SDS denaturing buffer (Table 2-1) for 20 min at 61°C to fully denature proteins and remove all higher order structures. For correct interpretation of the Western blot, a negative and a positive control as well as a marker have been included while running the gel.

After denaturing, the samples were applied to sodium dodecyl sulfate polyacrylamide gels along with a molecular weight marker and separated by size by electrophoresis. Proteins were allowed to migrate through the gel at 80 V for 20 min and then 200 V until the dye front reaches the end of the gel at 21°C. Separated proteins were transferred to a nitrocellulose membrane (Nitrocellulose membranes, 0.2 µm, BIO-RAD), followed by blocking free sites left on the membrane by incubation in a blocking buffer (Table 2-1) for 1 h at 21°C. The membrane was then incubated at 4°C overnight under gentle shaking with the primary antibody solution directed against the protein of interest. The final concentration of the anti-TRPC6 antibody solution was 10 µg/mL. The next day, the antibody solution was collected and kept at 4°C for further use. The membrane was washed 3 times for 10 min at 21°C with 1X TBS buffer (Table 2-1). The membrane was then incubated for 1 h at 21°C with the blocking buffer (Table 2-1) containing the specific secondary antibody coupled with horseradish peroxidase directed to the bound primary antibody (Table 2-2). After the membrane was washed 3 times for 10 min at 21°C with 1X TBS buffer (Table 2-1), the labeled antibodies were detected after addition of

the Western lightning chemiluminescence reagent plus (Table 2-3) by using the LAS 3000 (Table 2-4). The resulting images showing the target protein were saved as TIFF files and then transferred to CorelDraw X17 for labeling.

2.2.5 Blue Native PAGE (BN-PAGE)

To study protein-protein interactions, blue native PAGE (BN-PAGE) was used (Schagger and von Jagow, 1991; Wittig et al., 2006). Undenatured protein complexes eluted natively from the magnetic beads by the competing antigenic peptide were diluted by mixing with the sample buffer for blue native PAGE (SERVA) at a 1:1 ratio. The dye in the SERVA sample buffer contains SERVA Blue G (Table 2-3), which builds with the proteins a negatively charged complex without any denaturing. The prepared probes were loaded to the dry wells of the gel (SERVA Gel TM N3-12, vertical native gel 3-12%) at 4°C. For gel electrophoresis, the inner and the outer chambers were filled with cold cathode buffer and anode buffer, respectively supplemented with 1% SERVA blue G solution. Protein complexes were allowed to migrate through the gel at 50 V for 10 min and then 200 V until the dye front reaches the end of the gel at 4°C. The size of protein complexes was estimated by running SERVA native size markers in parallel with the samples. The resulting gel was either stained with coomassie for further mass spectrometric analysis or excised for SDS PAGE in the second dimension.

2.2.6 Two-dimensional Blue Native/SDS PAGE

After blue native PAGE was performed, a lane correspond to the target protein complex was excised and processed for further denaturing steps. The excised lane was incubated first in the equilibrating buffer A (Table 2-1) for 30 min at 21°C, thereafter transferred to an equilibrating buffer B (Table 2-1) for 15 min at 21°C. The denatured lane was placed horizontally on the top of a SDS gel and the free space was filled by 2X SDS denaturing buffer. The SDS-PAGE and Western blot were performed as described above (see section 2.2.4).

2.2.7 Gel digestion for mass spectrometry analysis

Separated proteins on the BN-PAGE were fixed using a fixation solution (40% (v/v) ethanol, 10% (v/v) acetic acid) for 1 h. After 3 times washing with distilled water, proteins were stained with the coomassie staining solution (Table 2-1) for 1 h at 21°C. After gel staining, several washing steps with Milli-Q water were performed to remove the background staining. The stained area in the gel, which contained protein complexes, was cut into seven slices and collected using the lane picker (biostep®, lane picker for 34 bands, each 2x9 mm, 1 lane). Gel pieces were washed two times for 5 min each with solution A (50 mM NH₄HCO₃) and B (50 mM NH₄HCO₃ and 50% (v/v) acetonitrile), alternatively (Table 2-1). To reduce the disulfide bonds, the gel pieces were incubated in the presence of a reducing solution (Table 2-1) for 30 min at 56°C. Next, gel pieces were incubated with an alkylation solution (Table 2-1) for 30 min in the dark at 21°C. The gel pieces were washed twice with solution A and B, respectively then dried by a vacuum centrifuge (Table 2-4). Dried gel pieces were incubated with trypsin over night at 37°C (porcine trypsin 10 ng/μL, Promega) for in gel-digestion (Table 2-3). The resulting peptides were then extracted with the extraction buffer (Table 2-1). Acetonitrile was evaporated and peptides were concentrated using a vacuum centrifuge. Peptides were rehydrated by adding 0.1% (v/v) formic acid as a final step before mass spectrometry analysis.

2.2.8 Mass spectrometry analysis

As previously described by (Fecher-Trost et al., 2013a), an aliquot (20 μL) of the extracted tryptic peptide for each antibody-based affinity purification (anti-hTRPC6, non-specific immunoglobulins) was analyzed and processed by a high-resolution nanoflow LC-HR-MS/MS (Ultimate 3000 RSLC nano system equipped with an Ultimate 3000 RS autosampler coupled to an LTQOrbitrap Velos Pro, all ThermoFisher Scientific, Dreieich, Germany) (Table 2-4). The trypsin digested proteins and thereafter the fragmented peptides were loaded to a C18 trap column (75 μm × 2 cm, Acclaim PepMap100C18, 3 μm) where they got separated by reversed

phase column (nano viper Acclaim PepMap capillary column, C18; 2 μm ; 75 μm \times 50 cm, ThermoFisher) with a flow rate of 200 nL/min. Two buffers were used to initiate a gradient, buffer A containing 0.1% (v/v) formic acid in water and buffer B containing 90% (v/v) acetonitrile and 0.1% (v/v) formic acid. After ionization, the eluent was transferred from LC into the MS with the help of a coated silica electrospray emitter (PicoTipEmitter, 30 m, New Objective, Woburn, MA) using a spray voltage of 2.2 kV. In this measurement, the collision-induced dissociation MS/MS top 10 method was used where the 10 most intense peptide ions with charge states equal or higher than 2 were selected and fragmented in the high-pressure linear ion trap. The resulted peptides were then identified by MASCOT algorithm and ThermoFisher Scientific Proteome Discoverer 1.4 software. The identified peptides were matched to tandem mass spectra by running a search in a SwissProt database (version2012_03, April 14th, 2012, number of protein sequences 535.251).

2.2.9 Calcium imaging

Differences in the calcium concentration can be monitored by fluorescent calcium binding dyes. Calcium binding by Fura-2, a chemical ratiometric calcium indicator, changes its fluorescence properties (Poenie and Tsien, 1986). Initially, a stock solution of Fura-2 (50 μg) (Table 2-3) was dissolved in dimethyl sulfoxide (DMSO) (Table 2-3) to yield a 1 mM stock solution. Addition of 5 μL of the stock solution to 1 mL cell media results in a 5 μM final concentration. HEK293 cells stably expressing *Trpc6* cDNA plated on Poly-L-Lysine coated glass coverslips were loaded with 5 μM Fura-2 AM in medium for 45 min at 37°C in the dark. Coverslips containing cells were washed with calcium imaging buffer (containing in mM: 140 NaCl, 4 KCl, 2 CaCl₂, 2 MgCl₂, 10 HEPES and 10 glucose; pH 7.2; 300 mOsmol/kg) (Table 2-1) and placed into an open bottom chamber where 300 μL of the calcium imaging buffer was added. Calcium changes were monitored and recorded before and after application of different agonists and antagonists. Changes in intracellular calcium concentration were detected using an inverted microscope (Axiovert S100, Zeiss) equipped with a Polychrome V, cooled charge-

coupled device (CCD) camera (TILL Imago)-based imaging system from TILL Photonics (Martinsried, Germany) and 20X Fluar objective (Table 2-4). Every 2 seconds, cells loaded with Fura-2 AM were excited alternatively at wavelength of 340 nm and 380 nm for 20 ms each and the emitted fluorescence was recorded (> 440 nm, Fura Filter chroma, Olching, Germany). Data acquisition and analysis were monitored with the imaging software TILLvision (TILL Photonics). After the background was subtracted, the F340/F380 ratios as measure for the calcium concentration, were calculated from the corresponding images. Single cells were selected as regions of interest (ROIs) and calcium imaging traces were presented as F340/F380 ratio, which were plotted versus time.

2.2.10 Electrophysiological recordings

To measure currents through TRPC6 channels, I applied whole-cell patch clamp recordings using an EPC-9 amplifier (HEKA Electronics, Lambrecht, Germany) (Table 2-4) and the PatchMaster software (HEKA). All patch clamp experiments were performed at 21°C on transfected HEK293 cells stably expressing *Trpc6* cDNA and attached to circular glass coverslips pre-coated with Poly-L-lysine. Patch pipette resistance ranged from 2 to 4 M Ω when filled with the „internal solution” (containing in mM: 120 Cs-glutamate, 8 NaCl, 1 MgCl₂, 10 HEPES, 10 Cs-BAPTA (1,2-bis (2-aminophenoxy) ethane-N,N,N',N'-tetraacetic acid), 3.1 CaCl₂ (100 nM free Ca²⁺, calculated with *WebMaxC*), pH 7.2) (Table 2-1). Patch pipettes were pulled from glass capillaries GB150T-8P (Science Products, Hofheim, Germany) at a vertical PC-10 micropipette Puller (Table 2-4). TRPC6 currents were activated by adding directly 100 μ M 1-oleoyl-2-acetyl-sn-glycerol (OAG) to the patch-clamped cell in the external solution containing (in mM: 140 NaCl, 2.8 KCl, 2 MgCl₂, 1 CaCl₂, 10 HEPES, 10 glucose, pH 7.2, see Table 2-1). To measure TRPC6 currents, voltage ramps ranging from -100 to +100 mV with a duration of 400 ms were applied from a holding potential (V_h) of 0 mV every 2 seconds. Currents were filtered at 2.9 kHz, digitized at 100 μ s intervals and voltages were adjusted for a 10 mV liquid junction potential. Inward and outward current amplitudes at -80 and +80 mV

were extracted from each individual ramp recording and plotted versus time where n represents the number of measured cells. All currents were normalized to the cell capacitance to obtain the current densities (pA/pF). Current-voltage relationships (IVs) were extracted at each indicated time points.

2.2.11 Pull-down assay using ^{35}S -labeled proteins

2.2.11.1 *In vitro* translation and ^{35}S -Methionine labeling

In order to generate the TRPC6 N- terminus fragments labeled with ^{35}S -Methionine (Table 2-3), the corresponding cDNAs were transcribed and translated *in vitro* using the TNT T7 coupled reticulocyte lysate system (Promega). To incorporate ^{35}S -Methionine (L- [^{35}S] Methionine SRM-01, Hartman Analytic), 25 μL of TNT T7 reticulocyte lysate was mixed with, 1 μL of ^{35}S -Methionine (1000 Ci/mmol), 1,5 μg plasmid cDNA and nuclease-free water to obtain a total volume of 30 μL , and incubated for 90 min at 30°C. The resulting ^{35}S -Methionine labeled TRPC6 N- terminus fragments were separated from the free- ^{35}S -Methionine, which was not incorporated by size exclusion chromatography (ilustra™ Nick™ Column Sephadex™ G-50 DNA Grade-GE Healthcare Life Sciences) and eluted with 4 mL binding buffer containing (20 mM Tris-HCl, 100 mM NaCl and 0.1% (w/v) Triton-x 100, pH 7.5). Ten fractions containing 400 μL each were collected and aliquots from each fraction were mixed with the scintillation liquid and the radioactivity was monitored in a scintillation counter (Table 2-4). Before starting with the pull-down assay, the integrity of the *in vitro* translated fragments of the TRPC6 N- terminus was controlled by SDS-PAGE. The samples were mixed with the SDS denaturing buffer (Table 2-1) in a 1:1 ratio, incubated for 20 min at 60°C and then samples corresponding to 50 000 counts per minute (cpm) were applied into SDS-PAGE. The gels were dried under vacuum overnight, exposed to phosphor imaging screen for 3 or 24 h and then the ^{35}S -labeled proteins were visualized using a phosphor-imager reader (BAS-2500, Fujifilm) (Table 2-4) and software

BAS-reader 3.14 version. Images were saved as Tiff files and transferred to CorelDraw 17X for labeling.

2.2.11.2 Pull-down assay

GIT1 fragment (130-244 aa) fused to GST tag or GST tag alone as a control (500 pmol) were immobilized on glutathione sepharose beads at 4°C overnight under end-over-end rotation. To map the TRPC6 binding domain, different fragments of TRPC6 N- terminus (300 000 cpm for each fragment) resulted from the *in vitro* translation were incubated with the GIT1 ankyrin repeat fragment 130-244 aa or GST as a control pre-coupled to glutathione beads for 3 h or overnight at 4°C under gentle shaking. Thereafter, beads were washed 3 times with the binding buffer (Table 2-1), followed by the addition of the 2X SDS denaturing buffer (Table 2-1) in ratio 1:1 and the incubation for 20 min at 60°C. Eluted proteins (containing the protein fragments retained and the GIT1-GST) were separated by SDS-PAGE. GST-tagged proteins were visualized by staining the gel with the coomassie brilliant blue. The stained gels were then dried under vacuum overnight at room temperature, exposed to phosphor imaging screen for 3 or 48 h. The ³⁵S-labeled proteins were visualized using a phosphor-imager reader (BAS-2500, Fujifilm) (Table 2-4) and software BAS-reader 3.14 version. Images were saved as Tiff files and transferred to CorelDraw 17X for labeling.

2.2.12 Cell surface biotinylation assay

To control targeting of TRPC6 to the plasma membrane in the absence and presence of interacting proteins, biotinylation assays were performed. HEK293 cells stably expressing the *Trpc6* cDNA were transiently transfected with *Git1* or GFP cDNAs, incubated thereafter with 2 mL cold Biotin-solution (EZ-link™ Sulfo-NHS-LC-Biotin) (10 mM stock) diluted in 8 mL biotinylation buffer (containing PBS pH 8, 1 mM MgCl₂ and 0.5 mM CaCl₂) for 30 min at 4°C under shaking. Then, cells were washed twice with cold biotinylation buffer (Table 2-1) followed by one washing step by the biotinylation buffer supplemented with 0.1% (v/v) BSA. Thereafter,

cells were detached from the cell culture flask by trypsin, collected in a 15 mL falcon tube, washed twice with PBS and centrifugation for 5 min at $200 \times g$ at 4°C . The cell pellet was resuspended in a lysis buffer (containing PBS, 1% (w/v) Triton x-100, 1 mM EDTA, pH 7.4) (Table 2-1), and the cell suspension was passed through a 27-Gauge needle, followed by incubation for 15 min at 4°C on a tube rotator. The solubilized proteins were centrifuges at $10000 \times g$ for 15 min at 4°C to remove cell debris, and the protein concentration in the supernatant was determined by BCA (see section 2.2.4). Protein lysates (900 μg) were incubated with 200 μL avidin-agarose beads overnight at 4°C under gentle shaking to enrich the biotinylated proteins. The next day, avidin-agarose beads were washed 5 times with a washing buffer (Table 2-1) and then the bound biotinylated proteins were denatured by incubation in 120 μL of 2X SDS denaturing buffer (Table 2-1) for 30 min at 37°C . Denatured protein samples were loaded to SDS-PAGE, and the biotinylated proteins were detected by Western blot (see section 2.2.4). Antibodies against calnexin (which should not be biotinylated) and Na^+/K^+ ATPase (which should be biotinylated) (Table 2-2), were used to control the cell surface biotinylation assay.

2.2.13 *In vitro* scratch migration assay

HEK293 cells stably expressing the *Trpc6* cDNA were plated into a six well-plate and transfected with either *Git1*-IGFP or IGFP cDNAs as a control. When cells reach 100% confluency, culture medium was discarded and a scratch was applied using a 200 μL pipette tip, followed by two times washing with phosphate buffered saline (PBS) (Table 2-1) to remove detached cells. Fresh medium, containing either 10% or 1% FCS (Table 2-3) was added to the cells. Bright field microscopic images (Table 2-4) of the scratched areas were taken immediately after applying the scratch and then after 6, 9 and 24 h. The scratched areas repopulated by migrating cells were calculated and normalized to the initial scratch area at time zero.

2.2.14 Live cell imaging

HEK293 cells were cultured on glass coverslips pre-coated with Poly-L-lysine. Twenty-four hours after plating, cells were co-transfected with the *Trpc6*-GFP and *Tmem16a*-RFP cDNAs or *Git1*-GFP and *Tmem16a*-RFP cDNAs in order to study the localization of the TRPC6 and GIT1 proteins. TMEM16A was used as a plasma membrane marker. Twenty-four to forty-eight hours after transfection, cells were washed with calcium imaging buffer (Table 2-1) and placed into a circular open-bottom chamber in the presence of the same buffer and placed under a confocal laser scanning microscope (LSM 780) equipped with a Plan-Apochromat 63x/1.4 oil DIC M27 objective (Carl Zeiss, Göttingen, Germany) (Table 2-4). Zen software (Zeiss) was used for the acquisition of confocal images with the excitation laser set at 488 nm and 561 nm for GFP and RFP, respectively by a multi-band beam splitter and images were exported as Tiff files after setting a scale bar and the labeling was accomplished in CorelDraw X7 Version 17.0.

2.2.15 Immunofluorescence staining of human platelets

For staining, platelets collected by centrifugation at $900 \times g$ for 10 min at 4°C were resuspended in modified Tyrode's buffer (Table 2-1) at a concentration of 5×10^7 platelets/mL. The suspension was incubated in the presence of 1% paraformaldehyde (PFA) for 30 min at 21°C, followed by 3 times washing with PBS (Table 2-1). The platelets were then applied into coverslips pre-coated with Poly-L-lysine and allowed to attach for 1-2 h at 37°C. After attachment, the cells were permeabilized with 0.3% (w/v) Triton x-100 for 30 min at 21°C. After 2 times washing with PBS, non-specific binding sites were blocked by incubation in a blocking buffer (Table 2-1) containing 1% (w/v) BSA in PBS for 1 h at 21°C. The platelets were incubated with the primary anti-TRPC6 and anti-GIT1 antibodies (Table 2-2) diluted in a blocking buffer containing 1% (w/v) BSA in PBS at 1:1000 and 1:500 ratio, respectively overnight at 4°C. After overnight incubation with primary antibodies, platelets were washed 3 times with PBS supplemented with (0.3% (w/v) Triton x-100 and 0.1% Tween-20) (Table 2-1) and incubated

successively with the conjugated secondary antibodies (Cy3™-secondary goat polyclonal anti-rabbit and Alexa Fluor® 488 AffiniPure Donkey Anti-Mouse) (Table 2-2) diluted at 1:1000 in a blocking buffer (Table 2-1) for 2 h at 21°C. After three washing steps with PBS, coverslips were mounted with the mounting medium (Fluoromount-G, 0100-01 SouthernBiotech), and the cells were visualized under the confocal microscopy (Table 2-4).

2.2.16 Platelet adhesion assay

For the platelet adhesion assay (Mountford et al., 2015), glass coverslips were placed into a 24 well-plate and coated either with 100 µg/mL fibrinogen (Table 2-3) or with 25 µg/mL collagen (Table 2-3) for ≥ 3 hours at 4°C. Thereafter, non-immobilized fibrinogen/collagen were removed by washing with Tyrode's buffer (Table 2-1) followed by incubation for 60 min at 21°C in a blocking buffer (Table 2-1) to block the free binding sites. To study platelet function, an *in vitro* adhesion assay was performed on fibrinogen/collagen immobilized on coverslips surface. Platelet-rich plasma was centrifuged at $900 \times g$ (Jouan cr3i multifunction centrifuge) (Table 2-4) for 10 min at 4°C to obtain the sedimented platelets. After washing once with Tyrode's buffer (Table 2-1), 5×10^7 platelets were plated into glass coverslips pre-coated with fibrinogen/collagen and were allowed to spread for 15, 30 and 60 min at 37°C directly after treating them with 100 µM 1-Oleoyl-2-acetyl-sn-glycerol (OAG, TRPC6 activator), 20 nM SAR7334 (TRPC6 inhibitor) or DMSO (control solvent) (Table 2-3). At each time point, the non-adherent cells were washed twice with Tyrode's buffer and the attached cells were fixed with a fixation buffer (Table 2-1) for 30 min. The cells were permeabilize with 0.2% (w/v) Triton x-100 in PBS for 20 min at 21°C, followed by two times washing with PBS. Permeabilized platelets were then incubated with Alexa Fluor™ 350 Phalloidin (1:40 dilution, A22281 Molecular Probes by Life Technologies, USA) for 20 min at 21°C in the dark. After 5 times washing with PBS, the coverslips were mounted with Fluoromount-G and then imaged using a fluorescence microscope equipped with EC Plan-Neofluar 100X/1.3 oil objective (Table 2-

4). Ten to fifteen images per each coverslip were randomly taken and the attached platelets were counted and analyzed by ImageJ program (Schindelin et al., 2012).

2.2.17 Mice

Trpc6^{-/-} mice (Dietrich et al., 2005; Tsvilovsky et al., 2009) on a pure C57BL/6 background (backcrossed 15 times with the C57BL/6 mice) and the wild-type C57BL/6 were kept under standard light/dark cycle with free access to food and water. All animal care and experiments procedure involving animals were carried out in accordance to ethic regulations and approved with the guidelines determined by the animal welfare committee of the Saarland state and the University of Saarland.

2.2.18 Statistical analysis

Data analysis were carried out using GraphPad Prism version 6.07 (GraphPad Software, La Jolla, CA), Microsoft Excel, Igor Pro 5.1 (WaveMetrics), TILLvision (TILL Photonics), PatchMaster (HEKA), AxioVision Rel. 4.7 (Zeiss), AIDA Image Analyzer version 4.14 and ImageJ (NIH). First, data were tested for normality using Kolmogorov–Smirnov test (KS test), D’Agostino-Pearson omnibus or Shapiro-Wilk normality tests. Significance difference was estimated as following: to compare between two groups, unpaired two-tailed Student’s t test or a Mann-Whitney test were used as indicated. For comparisons between three or more groups, one-way ANOVA followed by Bonferroni’s multiple-comparisons test was used, as indicated in the corresponding figure legend. Data are presented as mean ± standard error of the mean (SEM) with n represents the number of cells for calcium imaging, patch clamp recording and number of scratches for migration assay performed in each experiment. Data were considered statistically significant when the p value was < 0.05.

3 Results

3.1 Identification of the transient receptor potential canonical 6 (TRPC6) protein in human platelets

Almost twenty years ago, the TRPC6 protein was identified in human platelets (Hassock et al., 2002). In my project, antibodies directed against the C- and N- terminus of human or mouse sequence were used to detect the TRPC6 protein in the transfected cells (Figure 3-1 A, B, C) as well as in the human platelets (Figure 3-1 E). First, I established a protocol to isolate the TRPC6 protein together with associated proteins (Figure 3-1 D). Human platelets were lysed in the presence of the nonionic detergent digitonin (1%) to solubilize membrane proteins. HOM-made specific anti-TRPC6 antibody (1263), which is directed against the C- terminus of the human TRPC6 protein or as a control, non-specific immunoglobulins (IgG) were immobilized on beads and used for immunoprecipitation (Figure 3-1 E). In order to elute the TRPC6 protein complex bound to the antibody without disrupting the binding of any associated proteins, I used a peptide representing the antigenic epitope of the 1263 antibody. This peptide at a 4 mg/mL concentration was incubated with proteins bound by the beads after immunoprecipitation. The eluate was collected and denatured by addition of the SDS buffer (Table 2-1) and the proteins were separated by sodium dodecyl sulfate polyacrylamide gel electrophoresis. The gel was divided into two parts, a and b. The part (a) was blotted to the nitrocellulose membrane and incubated with the antibody against human TRPC6 protein (Figure 3-1 E). The TRPC6 protein band of around 106 kDa molecular weight, was visible in the fraction enriched by the anti-TRPC6 antibody, but not detectable in the control fraction using non-specific immunoglobulins (Figure 3-1 E). The second part of the gel (b) was stained with coomassie, and both lanes of TRPC6 and IgG enriched fractions were cut into seven pieces (Figure 3-1 F), trypsin digested and the peptides were extracted and thereafter analyzed by mass spectrometry. TRPC6 was

RESULTS

not detectable in the control fraction obtained by the non-specific immunoglobulins. In contrast, peptides of the TRPC6 protein were identified when the specific anti-TRPC6 antibody (1263) was used for immuno-purification (Figure 3-1 G). 48% of the amino acid sequence of human TRPC6 protein was covered by the sequence obtained from the peptides by mass spectrometry (Figure 3-1 I). Moreover, the TRPC6 protein was mostly detected by mass spectrometry in the third gel piece of the stained gel, which is located between 75 and 120 kDa corresponding to the apparent molecular weight of human TRPC6 of 106.565 Da. Thereafter, I performed blue native PAGE followed by SDS-PAGE in the second dimension. The TRPC6 protein complex run at 110 kDa in the SDS-PAGE, corresponding to a size > 242 kDa in the blue native gel (Figure 3-1 H). The Western blot and mass spectrometry data demonstrate that the TRPC6 protein is present in the human platelets.

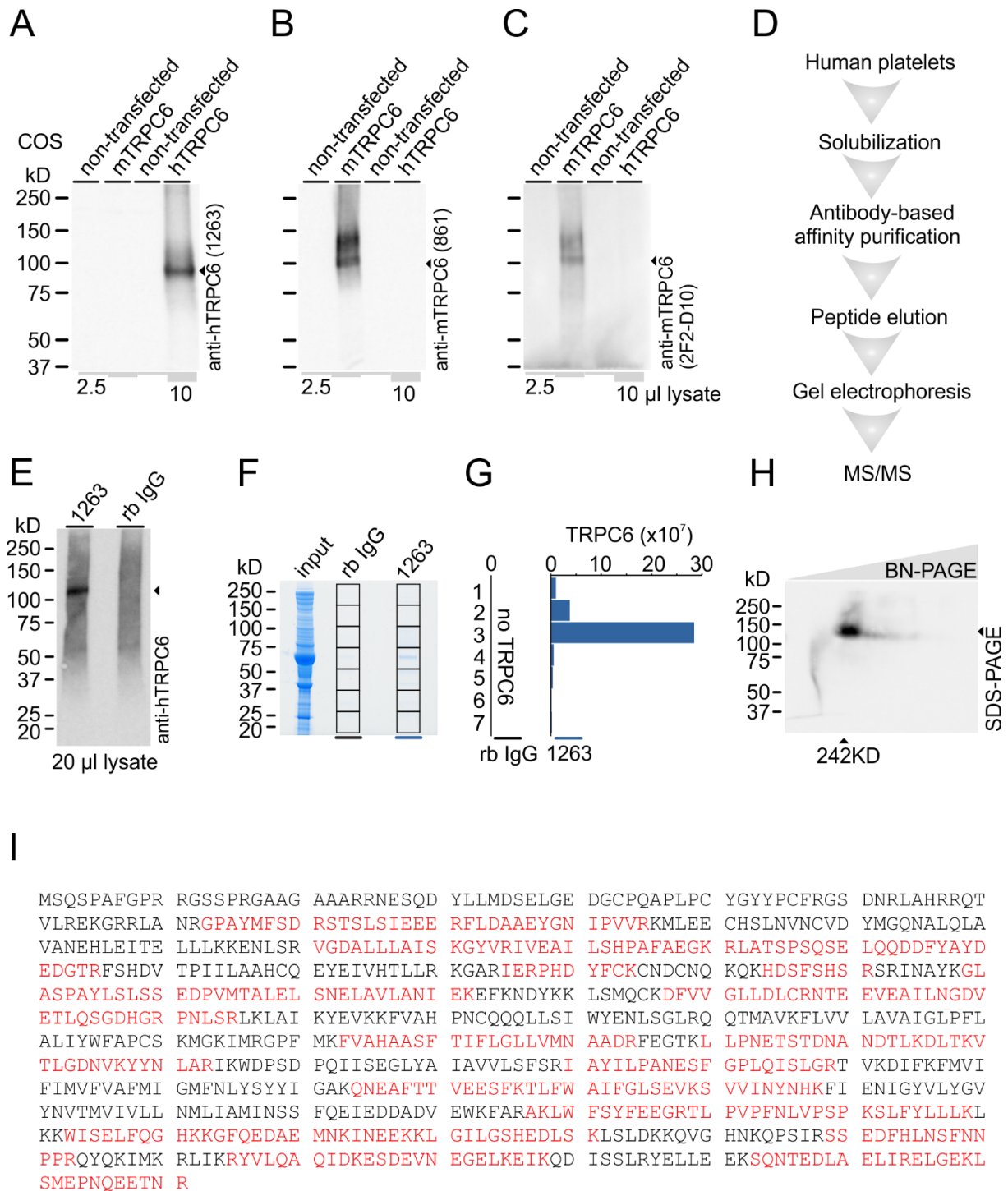


Figure 3-1. TRPC6 protein enrichment from human platelets and mass spectrometry data

(A, B, C) Western blots showing the TRPC6 protein in Cos-7 cells transfected either with the mouse or human TRPC6 cDNA or left non-transfected. (A) The human anti-TRPC6 antibody directed against the C-terminus of TRPC6 (1263) was used to detect the human TRPC6 protein in the Cos cells. (B) The mouse TRPC6 was detectable using the mouse anti-TRPC6 antibody directed against the C-terminus

of TRPC6 (861). **(C)** The anti-TRPC6 antibody, directed against the N- terminus of the mouse TRPC6, was used to detect the TRPC6 protein in cells transfected with the mouse but not with the human TRPC6 or the non-transfected cells. **(D)** Workflow of TRPC6 protein enrichment from human platelets. Human platelets lysates were prepared in the presence of digitonin and the human anti-TRPC6 antibody (1263) directed against the C- terminus of TRPC6, or non-specific immunoglobulins were used for binding. The TRPC6 protein bound to the antibodies was eluted under non-denaturing condition by the TRPC6 antigenic peptide. After electrophoresis, proteins were stained, and the gel was cut into pieces. Gel pieces were incubated with trypsin and the resulting peptides were analysed by mass spectrometry. **(E)** Western blot: TRPC6 protein enriched by the 1263 antibody-based purification from human platelets was detectable in the fraction enriched by the specific anti-hTRPC6 against the C- terminus (left lane) but not in the lane where proteins bound to the non-specific immunoglobulins were applied (right lane). **(F)** Coomassie-stained gel showing the input (platelets lysate) and the fractions enriched by rabbit IgG (rb IgG) and by the 1263 antibody (right). Each fraction/lane was cut into seven gel pieces as indicated, incubated with trypsin for in-gel tryptic digestion and the resulting peptides were analyzed by mass spectrometry. **(G)** Bar graph summarizing the relative abundance of TRPC6 detected by mass spectrometry (the most 10 intense peptides) in each fraction and gel piece, indicating that the TRPC6 protein is mainly identified within the third gel piece (right) but completely absent in the control fraction (left). **(H)** TRPC6 protein complex detected by Western blot after two dimensional BN/SDS PAGE using the 1263 antibody. **(I)** The human TRPC6 amino acid sequence, with the peptides identified by the nano-LC MS/MS highlighted in red.

3.2 Identification of TRPC6 associated proteins in human platelets by mass spectrometry analysis

After identification of the TRPC6 protein by Western blot and mass spectrometry in human platelets, I wanted to further understand TRPC6 functions in these cells to identify associated proteins, which might regulate TRPC6 channel activity. I followed the protocol for immunoprecipitation as described above (Figure 3-1 D) and used the antigenic peptide to competitively displace the TRPC6 protein and associated proteins from the antibody. In the first part of the gel, which was blotted to nitrocellulose membrane and incubated with the anti-hTRPC6 antibody, the TRPC6 protein band was observed in the input as well as in the eluate where increasing amounts of protein were applied to the gel (Figure 3-2 A). The other part of the gel was stained with coomassie (Figure 3-2 B) and processed for LC MS/MS analysis after

tryptic digestion, in order to identify the TRPC6 protein and other proteins associated with this channel. The results obtained by mass spectrometry were plotted as a two-dimensional abundance ratio plot of two independent experiments. In this plot, the abundance of TRPC6 and of each protein associated with the TRPC6 immunoprecipitated by the antibody is divided by the abundance of the same protein identified in the control fraction precipitated by the non-specific immunoglobulins (Figure 3-2 C). The TRPC6 protein appears in the upper right corner of the plot (Figure 3-2 C, red dot), indicating that the TRPC6 protein is identified in both experiments, only among those proteins immunoprecipitated by the anti-hTRPC6 antibody. TRPC6 protein was not detectable in the control fraction. The dots within the circled region in the upper right quadrant adjacent to the TRPC6 dot represent candidate proteins associated with the TRPC6 protein. These proteins are summarized in (Table 3-1). Some of these potential associated proteins, have already been described and shown to interact with the TRPC6 protein or with other proteins in the complex, for example the inositol 1,4,5-trisphosphate receptor (IP3R) (Boulay et al., 1999) and PLC γ 2 (Farmer et al., 2019). Among the potential associated proteins, the IP3 receptor type 1, IP3 receptor type 2 and GIT1 proteins were the most abundant. To confirm the association of TRPC6 and these three proteins, I performed co-immunoprecipitation and Western blot with platelet lysates. Proteins precipitated with anti-hTRPC6 antibody were separated by SDS-PAGE, blotted to nitrocellulose membranes. The membranes were incubated with anti-IP3RI, anti-IP3RII and anti-GIT1 antibodies. All three proteins are among the proteins associated with the TRPC6 protein confirming the results obtained by mass spectrometry (Figure 3-2 D, E and F). These data represent a list of novel proteins specifically interacting with the TRPC6 channel and might modulate its function in human platelets.

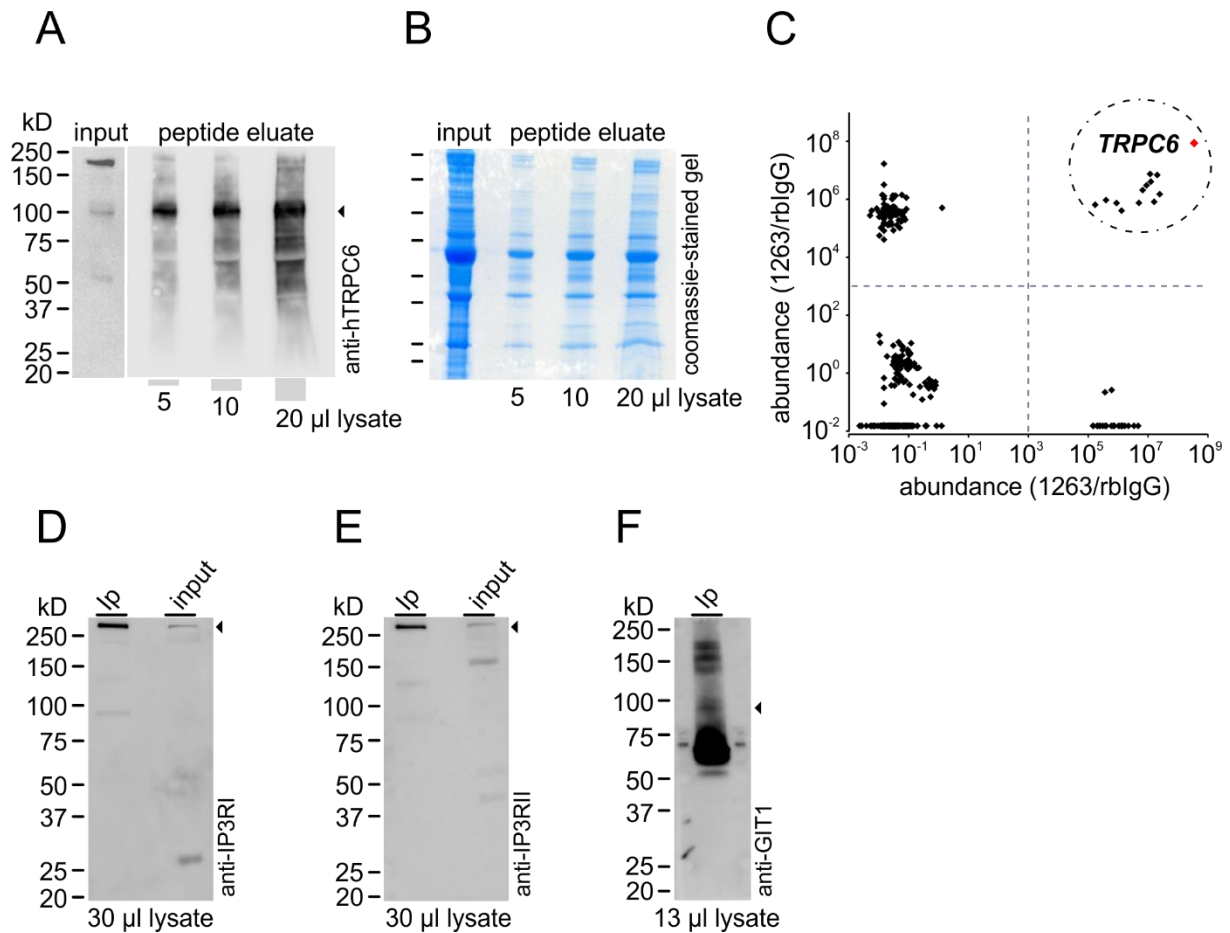


Figure 3-2. Potential TRPC6 associated proteins detected by mass spectrometry from human platelets

(A) Representative immunoblot image showing specific bands at ~106 kDa corresponding to the human TRPC6 protein in human platelets using anti-hTRPC6 antibody 1263. Membrane proteins were solubilized in the presence of digitonin (1%) and immunoprecipitation was performed using the anti-hTRPC6 antibody. An antigenic peptide was added to elute natively the TRPC6 complex from the immobilized antibody. Increasing amounts of the eluate were separated by SDS-PAGE and analyzed by Western blot or stained with coomassie for mass spectrometry analysis. Using the anti-hTRPC6 antibody in the Western blot, the TRPC6 protein was detected in the human platelets input as well as after immunoprecipitation. **(B)** A coomassie-stained gel for mass spectrometry showing input and increasing cell lysate amounts of the peptide eluate. **(C)** Two-dimensional logarithmic abundance ratio plot from two independent experiments (experiment 1, abundance of proteins specifically eluted from the antibody 1263/ abundance of proteins eluted from the non-specific immunoglobulins. Experiment 2, as in experiment 1 but with independently prepared platelet lysates from another sample of platelets obtained from the blood bank). Logarithmic ratios of experiment 1 are plotted versus ratios of experiment 2. The red dot represents TRPC6 protein and the circulated dots near to the TRPC6 represent proteins which are potentially associated with the TRPC6 protein. They are detected only in the fraction enriched

by the specific anti-hTRPC6 antibody. **(D, E, F)** The three most abundant proteins identified in B and C, GIT1, IP3RI and IP3RII were among the proteins associated with the TRPC6, which was immunoprecipitated from human platelet lysates by the anti-hTRPC6 antibody 1263. In independent coimmunoprecipitation experiments, the three proteins were detected by Western blot by anti-GIT1 antibody at ~85 kDa, anti-IP3RI and anti-IP3RII antibodies at ~300 kDa, respectively.

Table 3-1. Proteins potentially associated with the TRPC6 protein

Accession	Potential associated proteins in trpc6 complex	Gene name
Q14643	Inositol 1,4,5-Trisphosphate Receptor Type 1	ITPR1
Q14571	Inositol 1,4,5-Trisphosphate Receptor Type 2	ITPR2
Q9Y2X7	ARF GTPase-activating protein GIT1 (G-Protein-Coupled Receptor Kinase Interacting Protein 1)	GIT1
P16885	1-phosphatidylinositol 4,5-bisphosphate phosphodiesterase gamma-2	PLCG2
Q14155	Rho guanine nucleotide exchange factor 7	(Beta-Pix) ARHGEF7
Q99683	Mitogen-activated protein kinase kinase kinase 5	MAP3K5
Q13177	Serine/threonine-protein kinase PAK 2	PAK2
Q92614	Unconventional myosin-XVIIIa	MYO18A
Q9NVI7	ATPase family AAA domain-containing protein 3A	ATAD3A
O95831	Apoptosis-inducing factor 1, mitochondrial	AIFM1
Q8NG06	E3 ubiquitin-protein ligase TRIM58	TRIM58
P55884	Eukaryotic translation initiation factor 3 subunit B	EIF3B

3.3 Density gradient fractionation of the TRPC6 protein complex solubilized from human platelets and the HEK-TRPC6 cell line

To investigate the TRPC6 containing protein complexes by an additional method, density gradient fractionation was performed using Opti Prep solution (Axis Shield), which contains

RESULTS

60% iodixanol in water with a density of 1.32 g/mL (Sadler et al., 2016). The sedimented platelets obtained from 20 mL platelet-rich plasma were mixed with 2 mL of the homogenization buffer (Table 2-1) supplemented with protease inhibitors. The post nuclear supernatant was generated by centrifuging the obtained cell lysates for 3 min at 3000 × *g* at 4°C. After protein estimation, different percentage of the gradient were generated by diluting the 60% iodixanol, with homogenization buffer, to obtain 10%, 20% and 30%. Only the 30% gradient (containing 2 mg protein) was placed on the bottom of the tube whereas the 20% and the 10% contain only the 60% iodixanol mixed with the homogenization buffer and placed gently on the top of the 30%, respectively. Upon centrifugation for 446 mins at 252.406 × *g* (55 000 rpm) using NVT65 rotor, proteins were distributed according to their density within the gradient. To achieve the best results, I avoided mixing the different percentages (10%, 20% and 30%) of Opti Prep solutions when pipetting the gradient, by letting the solution run down the tube wall while holding the pipette tip just on the top of the solution in the tube. Fractionation was done by a peristaltic pump linked to a fraction collector to continuously collect the samples from the bottom (400 µL per fraction). After denaturing the collected fractions with 2X SDS denaturing buffer, they were separated by SDS-PAGE, blotted to nitrocellulose membrane and the membrane was incubated with specific antibodies for TRPC6, GIT1 and IP3RII proteins. The antibody stain intensities of each lane/fraction were quantified and plotted according the density gradient fraction (Figure 3-3). The TRPC6 and IP3RII proteins are in the same protein complex in the human platelets after density fractionation (Figure 3-3 A, C). In the HEK-TRPC6 cell line, GIT1 partially localized with the TRPC6 protein (Figure 3-3 B, D). These data support the previous data obtained by mass spectrometry and co-immunoprecipitation, that IP3RII, GIT1 and TRPC6 are components of a complex.

RESULTS

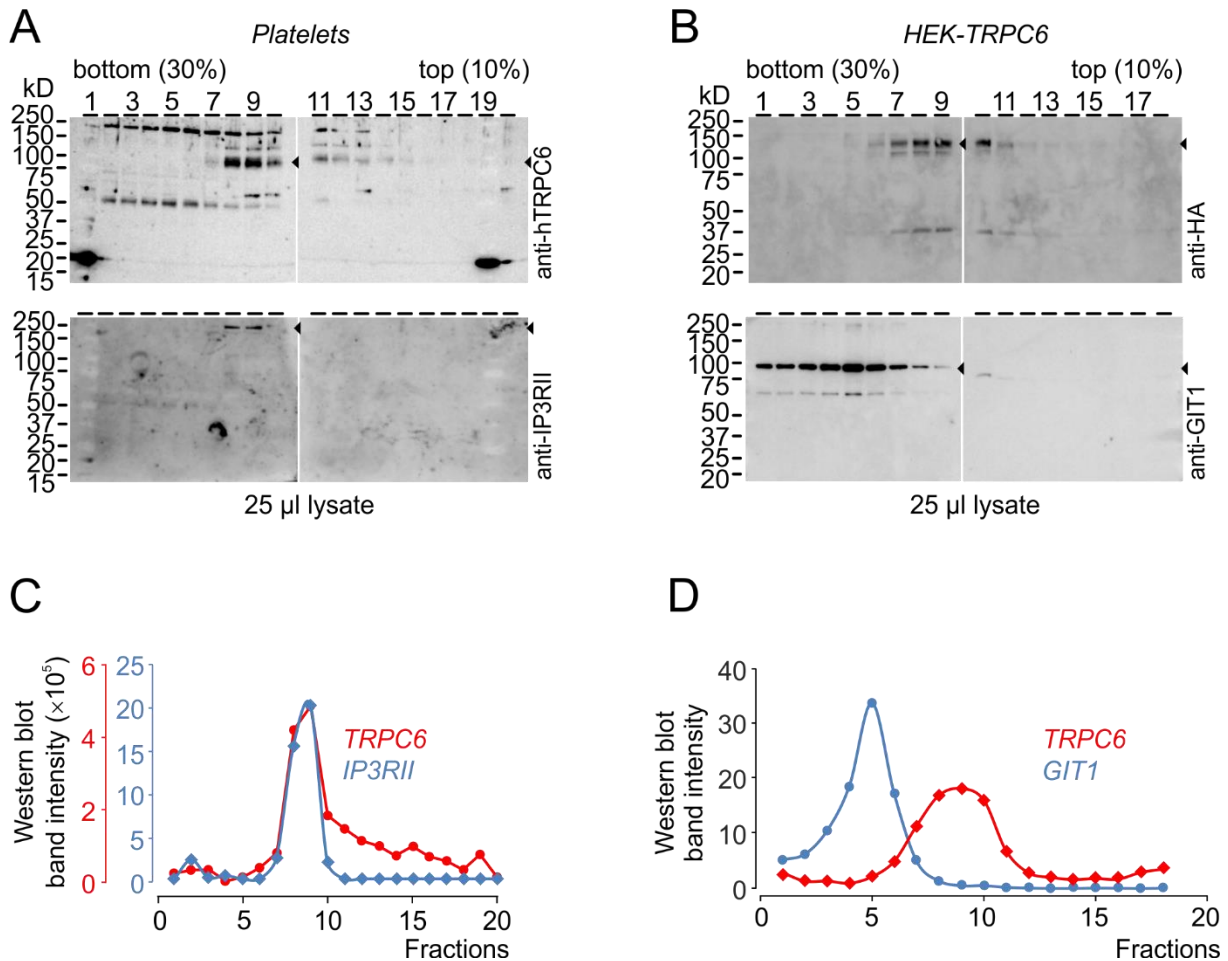


Figure 3-3. Density gradient separation of the TRPC6 protein complex in human platelets and HEK-TRPC6 cell line

Density gradient fractionation was used to separate proteins based on their densities. Protein lysates were separated after centrifugation for 446 mins at $252.406 \times g$ (55 000 rpm) using NVT65 rotor and the resulting proteins were collected into twenty fractions (400 μ L/fraction). After denaturing the samples with 2X SDS denaturing buffer, 25 μ L from each fraction was applied and proteins were separated by SDS-PAGE, blotted to nitrocellulose membrane and incubated with specific antibodies against TRPC6, GIT1 and IP3RII proteins. **(A)** Immunoblots of different fractions from human platelet lysates using anti-hTRPC6 (top) and anti-IP3RII (bottom) antibodies. **(B)** As in A, TRPC6 (top) and GIT1 (bottom) proteins were detected in the HEK-TRPC6 cells by the corresponding antibodies after loading 25 μ L of the cell lysate to the gel starting from the bottom of the tube, which represent the denser molecules. **(C, D)** Antibody stain intensities from the Western blots in A and B plotted versus the corresponding fractions. The peak of the human TRPC6 protein localizes with the peak of the IP3RII protein in fractions from platelets whereas the mouse TRPC6 and GIT1 proteins only partially overlap. HEK293 cells express endogenous GIT1 but only very low amounts of IP3R.

3.4 TRPC6 channel expression, localization and function in HEK293 cells stably expressing *Trpc6* cDNA

In the following I concentrate on the interaction of TRPC6 and GIT1 proteins. I used the HEK293 cells stably expressing the mouse *Trpc6* cDNA tagged with the HA sequence (HEK-TRPC6) and kindly provided by Dr. M.X. Zhu, University of Texas Health Science Center, Houston. Before starting experiments using this stable cell line, I confirmed the presence of the mouse TRPC6 protein by Western blot. In non-transfected HEK293 cells, TRPC6 protein is not detectable by Western blot, indicating that the protein is absent. In the HEK293 cell line stably expressing the *Trpc6* cDNA (HEK-TRPC6), the TRPC6 protein is visible in the Western blot at a molecular weight of 106 kDa (Figure 3-4 A). TRPC6 protein has been reported to locate at the plasma membrane (Cayouette et al., 2004). Using HEK293 cells transiently expressing the GFP-tagged *Trpc6* cDNA we could confirm this data. As a control for plasma membrane localization, I used TMEM16A (Ca²⁺ activated Cl⁻ channel) (Fecher-Trost et al., 2013b; Tian et al., 2012). Confocal images and the intensity profile analysis across the cell show that the TRPC6 fused to the green fluorescent protein (GFP) colocalizes with the TMEM16A fused to the red fluorescent protein (RFP) at the plasma membrane (Figure 3-4 B). To verify that the TRPC6 channel present in HEK-TRPC6 cells is functional, I used two methods: i) calcium-imaging and ii) patch clamp recordings. For calcium imaging, the cells were loaded with the membrane-permeant calcium indicator; Fura-2-acetoxymethyl ester (Fura-2 AM) and changes in the calcium signals were monitored in response to the application of the TRPC6 agonist OAG. The TRPC6 activator 1-oleoyl-2-acetyl-sn-glycerol (OAG) also induces calcium store depletion (Smani et al., 2008), thereby activating store-operated calcium entry, which could overrule the TRPC6 channel activity. Therefore, calcium store depletion was accomplished by cyclopiazonic acid (CPA) in the presence of extracellular calcium before applying OAG. Cyclopiazonic acid is a reversible inhibitor of the sarco/endoplasmic reticulum Ca²⁺-ATPase. Its addition induces an increase of the cytoplasmic calcium (Figure 3-4 C), most

probably by store depletion dependent calcium entry. After the Fura-2 F340/F380 ratio returned to the base line, OAG was added which now, with the intracellular stores being depleted by CPA, activates TRPC6-dependent calcium entry (Figure 3-4 C). For whole-cell patch clamp recordings, voltage ramps at 0.5 Hz frequency from a holding potential of 0 mV spanning a voltage range from -100 to 100 mV were applied for 400 ms duration over a period of 400 sec. Inward and outward current amplitudes at -80 and +80 mV were significantly increased upon application of OAG to the bath solution (Figure 3-4 D). The currents after OAG application were extracted and plotted versus the voltage to get the current-voltage (IV) relationship of the OAG-induced currents. The resulting IV curves with a doubly rectifying current-voltage show a typical feature of TRPC6 currents (Figure 3-4 E). These results demonstrate that the TRPC6 channel in HEK293 cells stably expressing the *Trpc6* cDNA is located at the plasma membrane and mediates calcium entry and current in response to the TRPC6 agonist OAG.

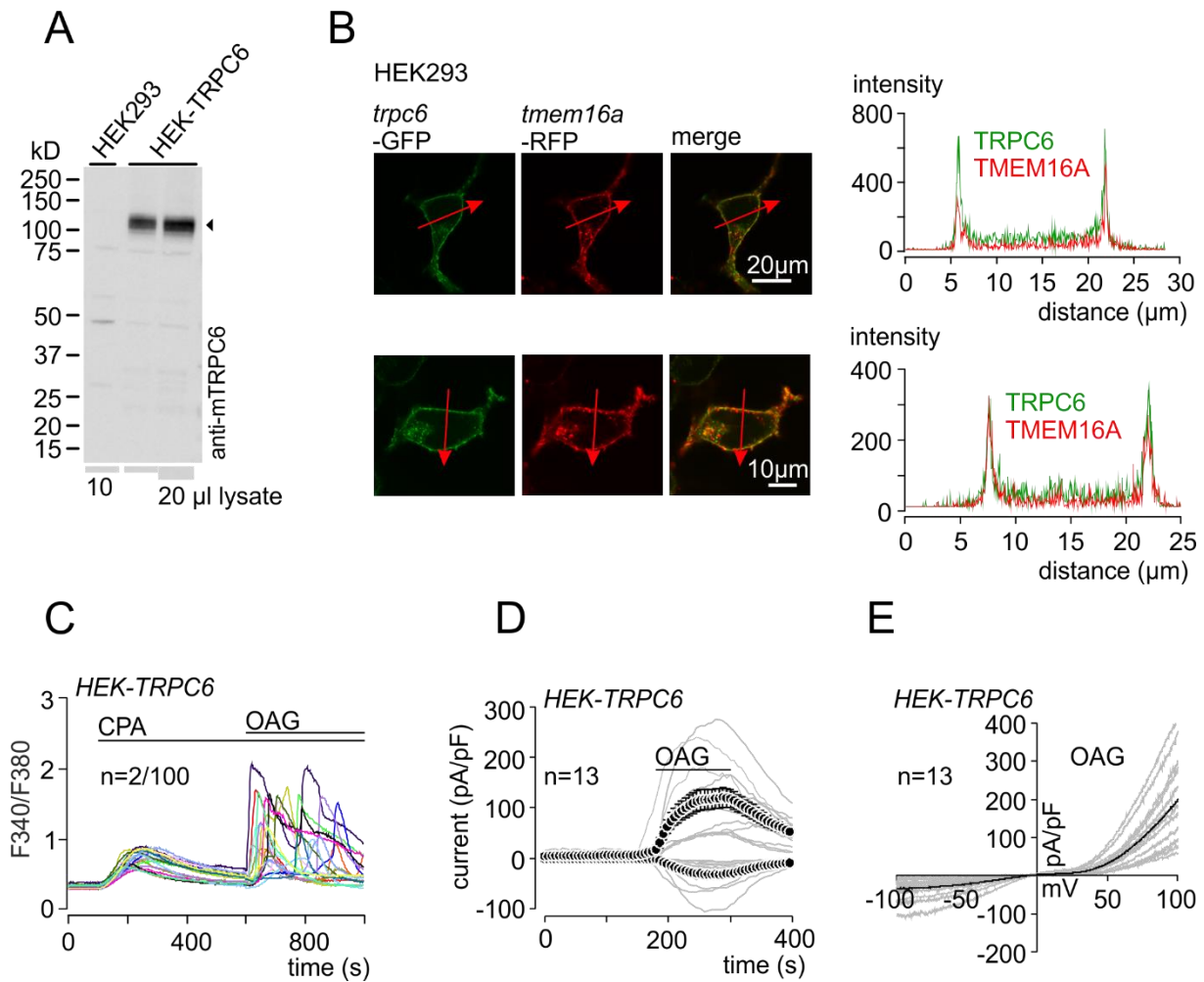


Figure 3-4. TRPC6 protein localization and function in HEK-TRPC6 cells

(A) Western blot of different amounts of the protein lysate from non-transfected HEK293 cells and HEK293 cells stably expressing the mouse *Trpc6* cDNA (HEK-TRPC6). The TRPC6 protein runs at ~106 kDa in SDS-PAGE and was detectable by the anti-mTRPC6 antibody (861). The TRPC6 protein was detectable in the HEK-TRPC6 cells but not in the non-transfected HEK293 cells. **(B)** Left: Confocal images showing the TRPC6 protein fused to GFP (green), the TMEM16A fused to RFP (red) and the merge, indicating that both proteins colocalize at the plasma membrane of HEK293 cells. Right: Intensity profiles of region of interest across the cell from the corresponding image (left) illustrating the overlapping of peak intensities of TRPC6 and TMEM16A indicating identical subcellular localization. **(C)** Single Fura-2 (F340/380) ratiometric example traces from HEK293 cells stably expressing *Trpc6* cDNA. After store depletion by 10 μ M cyclopiazonic acid (CPA) in the presence of 2 mM extracellular calcium, which activates the store operated calcium entry, TRPC6 channel activation was stimulated with 100 μ M OAG after Fura F340/F380 ratios returned to the baseline. **(D)** Single current traces and mean \pm SEM of TRPC6 current traces at -80 and +80 mV plotted over time upon external application of 100 μ M OAG. **(E)** The corresponding current-voltage relationship of the currents in D. Currents were normalized

to the cell size (given by cell capacitance) after subtraction of the initial currents before OAG application and n represents cell number used in the experiment.

3.5 GIT1 protein is expressed endogenously and after overexpression in the HEK-TRPC6 cells as well as in the human platelets

GIT1 protein is one of the TRPC6 associated proteins identified by mass spectrometry (Figure 3-2 C, Table 3-1) and co-immunoprecipitation assay (Figure 3-2 F). To look for GIT1 expression in HEK293 cells, cell lysates from non-transfected HEK293 cells and HEK293 cells stably expressing *Trpc6* cDNA, transiently transfected with the mouse *Git1* cDNA, were separated by SDS-PAGE. Western blot shows that GIT1 protein is endogenously present in the non-transfected HEK293 cells (Figure 3-5 A, left lane). After expressing the mouse *Git1* cDNA, GIT1 protein is readily detectable in the HEK-TRPC6 cells (Figure 3-5 A, right lanes). To investigate GIT1 protein localization, two approaches were applied. First, GIT1 was fused to GFP and expressed the resulting cDNA in HEK293 cells together with the TMEM16A cDNA fused to RFP. Based on fluorescent images and intensity profiles, GIT1 protein shows a diffuse cytoplasmic localization, in contrast to TMEM16A, which is located at the plasma membrane (Figure 3-5 B). In the second approach, antibodies against the TRPC6 and GIT1 proteins were used to stain these proteins in human platelets (Figure 3-5 C). Immunostaining of the human platelets demonstrates that the TRPC6 protein is mostly located at the plasma membrane, whereas GIT1 protein shows a cytoplasmic localization (Figure 3-5 C).

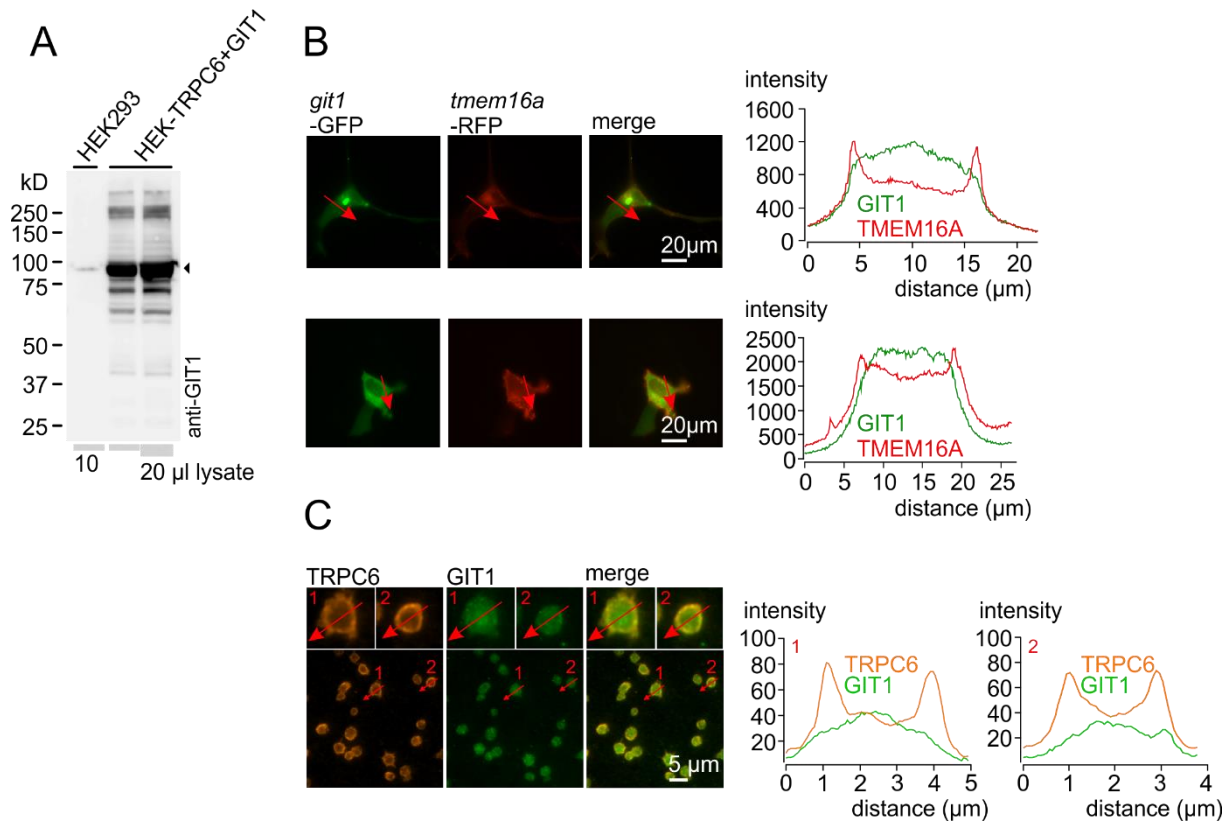


Figure 3-5. GIT1 protein expression and localization

(A) Western blot of two different amounts of protein lysates from non-transfected HEK293 cells and the HEK293 cells stably expressing the mouse *Trpc6* cDNA and transfected with the mouse *Git1* cDNA. After proteins were separated by SDS-PAGE and blotted to nitrocellulose membrane, GIT1 protein was detectable at ~85 kDa using anti-GIT1 antibody. GIT1 protein is already endogenously present in HEK293 cells (left lane) but at higher abundance in the transfected cells. **(B)** Left: Two fluorescent images showing the cytoplasmic localization of GIT1 protein fused to GFP (green) in the HEK293 cells. The TMEM16A fused to RFP (red) is localized at the plasma membrane and is used as a marker. Right: Intensity profiles of region of interest across the cell from the corresponding images (left) illustrating that the peak intensities of GIT1 and TMEM16A are different. **(C)** Immunostaining of human platelets. Left: Fluorescence microscope images of stained TRPC6 and GIT1 proteins, and the merge. Right: Intensity profiles of region of interest across two human platelets from the corresponding images (left).

3.6 GIT1 protein constrains TRPC6-mediated calcium influx and current in the HEK-TRPC6 cell line

To determine whether GIT1 protein modulates TRPC6 channel function, I measured calcium entry and current mediated through TRPC6 channel upon OAG application in HEK293 cells stably expressing the *Trpc6* cDNA either in the presence or absence of GIT1 protein. For recording TRPC6-dependent calcium entry, I applied the protocol described above (section 3.4, Figure 3-4 C). In cells co-expressing *Git1*-IGFP cDNA, the peak amplitude and area under the curve of the intracellular store depletion by CPA was reduced compared with the control transfected cells (Figure 3-6 A, B). Moreover, the OAG-induced calcium entry after store depletion by CPA, was significantly reduced compared with the control transfected cells (Figure 3-6 A, B). The TRPC6 expressing control cells were co-transfected with IGFP cDNA only. The OAG peak amplitude and area under the curve are both significantly reduced as well as the percentage of cells responding to OAG application (Figure 3-6 B). In whole-cell patch clamp recordings, application of OAG induces TRPC6 channel activation. The inward and outward currents at -80 and +80 mV are shown (Figure 3-6 C) and the corresponding current-voltage relationships (IVs) (Figure 3-6 D). The peak of the OAG-induced TRPC6 currents at -80 and +80 mV were quantified and in agreement with the calcium imaging results, the TRPC6 inward and outward currents were significantly reduced in *Git1*-IGFP cDNA co-expressing cells (Figure 3-6 E). Apparently, GIT1 protein constrains the TRPC6 channel activity.

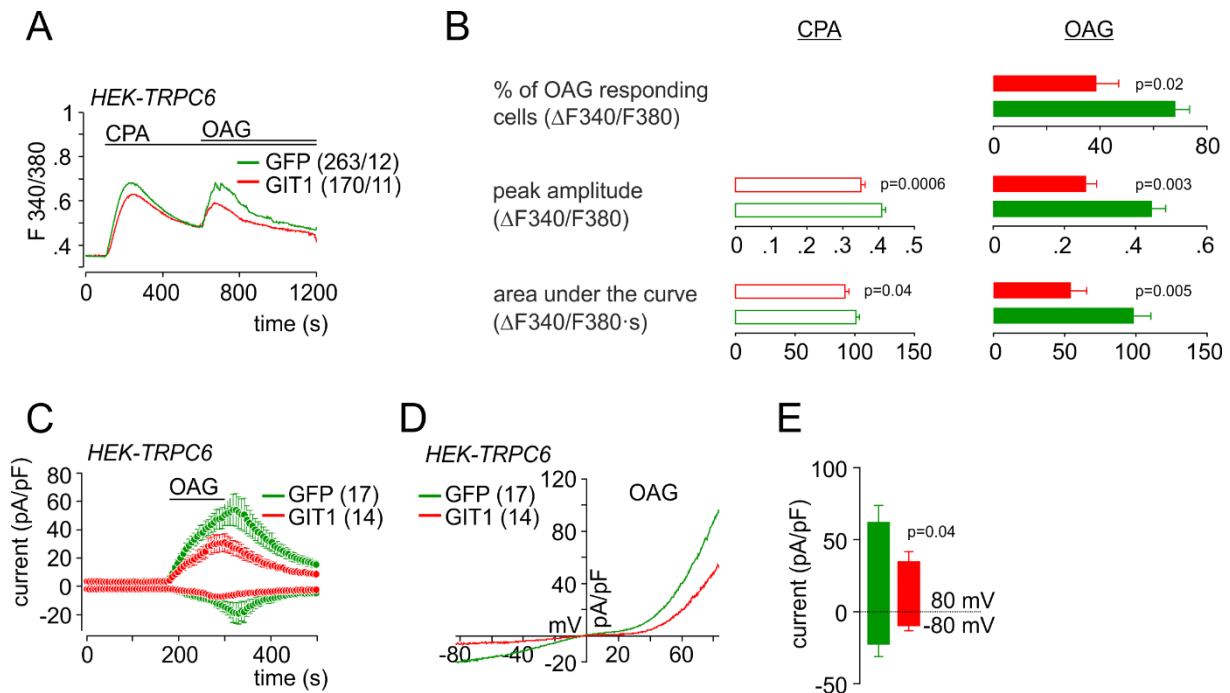


Figure 3-6. GIT1 protein inhibits OAG-induced calcium entry and current in HEK-TRPC6 cells

(A) Fura-2 ratio traces in HEK293 cells stably expressing the *Trpc6* cDNA and co-transfected either with *Git1*-IGFP cDNA (red) or IGFP (green) as a control. The ratiometric F340/F380 Fura-2 signals were recorded in the presence of 2 mM extracellular calcium and plotted versus time. Store depletion in the presence of 10 μ M cyclopiazonic acid (CPA), induces store operated calcium entry. After almost returning to the baseline, 100 μ M OAG was applied to the bath solution to activate the TRPC6 channel in the presence and absence of GIT1 protein. The OAG-induced calcium entry is reduced in cells expressing *Git1* cDNA compared with the control cells. **(B)** Bar graphs summarizing the percentage (%) of OAG responding cells, the peak amplitude and area under the curve of CPA-induced store operated calcium entry and OAG-induced calcium entry. Data are shown as mean \pm SEM with n = number of single cells/number of dishes. Normality was tested and p values were calculated using Mann-Whitney test. **(C)** TRPC6 inward and outward currents at -80 and +80 mV plotted versus time and recorded from HEK-TRPC6 cells transfected with IGFP (green) or *Git1*-IGFP (red) cDNAs. GIT1 protein inhibits TRPC6 currents activated by OAG. **(D)** Current-voltage relationships from the experiments in C. **(E)** Bar graphs summarizing the current amplitudes at -80 and +80 mV of the correspondent TRPC6 currents in C. Data are presented as means \pm SEM and n represents the number of cells. Normality was tested and p values were calculated using unpaired two-tailed Student's t test.

3.7 GIT1 protein acts negatively on cell migration in HEK-TRPC6 cells

GIT1 protein has been shown to play a role in cell migration (Manabe et al., 2002) and the effect of GIT1 on the TRPC6 channel function might also translate into an alteration of the cell motility. To investigate this, I performed an *in vitro* scratch migration assay. HEK-TRPC6 cells were plated into six well-plates and transfected with the IGFP cDNA as a control or with *Git1*-IGFP cDNAs. Twenty-four hours after transfection, a scratch was applied on the cell monolayer in each well using a 200 μ L pipette tip, an image of the scratched area at time point zero was taken and the cells were further incubated under normal cell culture conditions. Cell migration was monitored over time by taking images after 6, 9 and 24 hours. By quantifying the percentage of scratch area repopulated by the migrating HEK-TRPC6 cells over time, we observed that the migration rate of the HEK-TRPC6 cells co-transfected with *Git1*-IGFP cDNA was significantly slower compared with HEK-TRPC6 cells co-transfected with the IGFP only (Figure 3-7 A, B). In order to exclude the effect of cell proliferation, the same experiment was performed, but in the presence of 1% instead of 10% FCS, to minimize the contribution of cell proliferation. The overall migration rate was reduced in the presence of 1% FCS, but the inhibitory effect on the cell migration observed in the presence of GIT1 protein remained (Figure 3-7 C, D). To investigate whether GIT1 effect on the cell migration depends on the presence of TRPC6 channel, the scratch migration assay was repeated with HEK293 cells co-transfected with *Git1*-IGFP cDNA or IGFP as a control. In this experiment, GIT1 protein had no significant effect on cell migration in comparison with the migration of the control cells (Figure 3-7 E, F). Then the migration rate of the HEK-TRPC6 cells transfected with IGFP was compared with the control transfected HEK293 cells. TRPC6-expressing cells do migrate faster compared with the HEK293 cells (Figure 3-7 G). In conclusion, TRPC6-expressing cells migrate faster and GIT1 protein acts negatively on the TRPC6 cell migration.

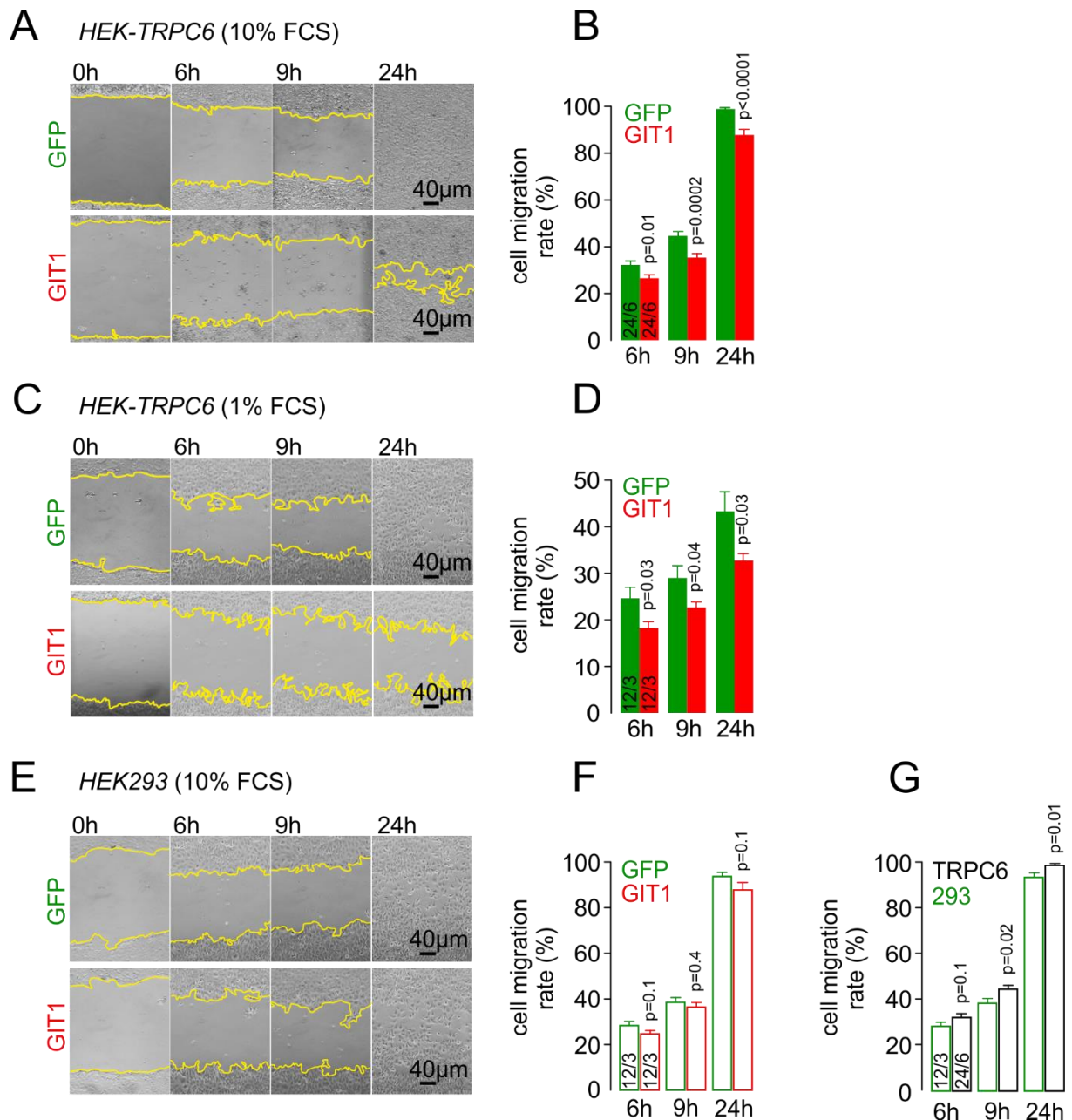


Figure 3-7. GIT1 modulates TRPC6-dependent cell migration

(A, C) Example bright field microscopic images taken with a 10x objective showing the scratch migration assay performed using HEK-TRPC6 cells co-transfected with the IGFP or *Git1*-IGFP cDNAs, cultured with 10% fetal calf serum (A) and with 1% FCS in the culture medium (C). After cells reached confluency, a scratch was applied in the confluent monolayer cells using a 200 µL pipette tip. Images were acquired directly after the scratch was performed (time zero), then after 6, 9 and 24 hours. The yellow lines define border of areas lacking cells. (B, D) Bar graphs summarizing the percentage of area occupied by the migrating cells over time and normalized to the scratch applied at the beginning of the assay (time zero). The presence of GIT1 protein in HEK-TRPC6 cells inhibits cell migration compared with the IGFP control transfected cells. (E) Bright field microscopic images of HEK293 cells transfected with IGFP or *Git1*-

IGFP cDNAs and cultured in the presence of 10% FCS as described in A. The scratch migration assay was performed with HEK293 cells (in the absence of TRPC6) transfected with IGFP or *Git1*-IGFP cDNAs. **(F)** Bar graphs show the cell migration rate over time from the corresponding image in E. In HEK293 cells lacking the TRPC6 protein, the negative effect of GIT1 protein on the cell migration was absent. **(G)** Bar graphs summarizing the migration rate of HEK-TRPC6 cells from A, B and HEK293 cells from E, F cultured in the presence of 10% FCS and transfected with the IGFP control. The migration rate was faster in the presence of TRPC6 compared with cells lacking the TRPC6 protein. Data are presented as mean \pm SEM and n = number of images/number of experiments and p values were calculated using unpaired two-tailed Student's t test.

3.8 The IP3R type 2 does not interfere with the inhibitory effect of GIT1 on the TRPC6 channel

GIT1 protein has been shown to interact with the IP3-receptor (Zhang et al., 2009) and the IP3R was shown itself to interact with the TRPC6 channel (Boulay et al., 1999; Zhang et al., 2001). In the present study, as described in (Figure 3-2), the three proteins are parts of a common protein complex. To answer the question whether the IP3R modulates the inhibitory effect of GIT1 on TRPC6 protein, I performed calcium imaging in HEK-TRPC6 cells transfected with *Git1*-IRFP cDNA in the presence or absence of the *ltp2*-IGFP cDNA. In the presence of extracellular calcium, cells were challenged with 100 μ M OAG after store depletion with 10 μ M CPA as in (Figure 3-4 C). In this experiment, the peak amplitude of the CPA-induced store depletion was significantly increased in HEK-TRPC6 expressing the *ltp2*-IGFP cDNA (Figure 3-8 A). There was no significant difference in the OAG-induced calcium entry between HEK293 cells expressing TRPC6 plus GIT1 and HEK293 cells expressing TRPC6 plus GIT1 plus IP3RII. Basic calcium levels, the peak amplitude and area under the curve of the OAG response were not different (Figure 3-8 A). Furthermore, the endogenous IP3 receptor protein levels present in non-transfected HEK293 cells and in HEK-TRPC6 cells were evaluated by Western blot. Increasing amounts of protein lysate from both cell lines were applied to the gel. After SDS-PAGE and blotting, the membrane was incubated with the anti-IP3 receptor antibody and after stripping the membrane, the anti-Na⁺/K⁺ ATPase antibody was used as a

RESULTS

control. Both proteins, IP3RIII and the α -subunit of the Na⁺/K⁺ ATPase appear to be strongly expressed in the HEK293 and HEK-TRPC6 cells, but normalized values indicate no difference in expression levels dependent on the presence of the TRPC6 protein (Figure 3-8 B). Taken together, the IP3 receptor does not interfere with the inhibitory effect of GIT1 protein on the TRPC6-dependent calcium entry.

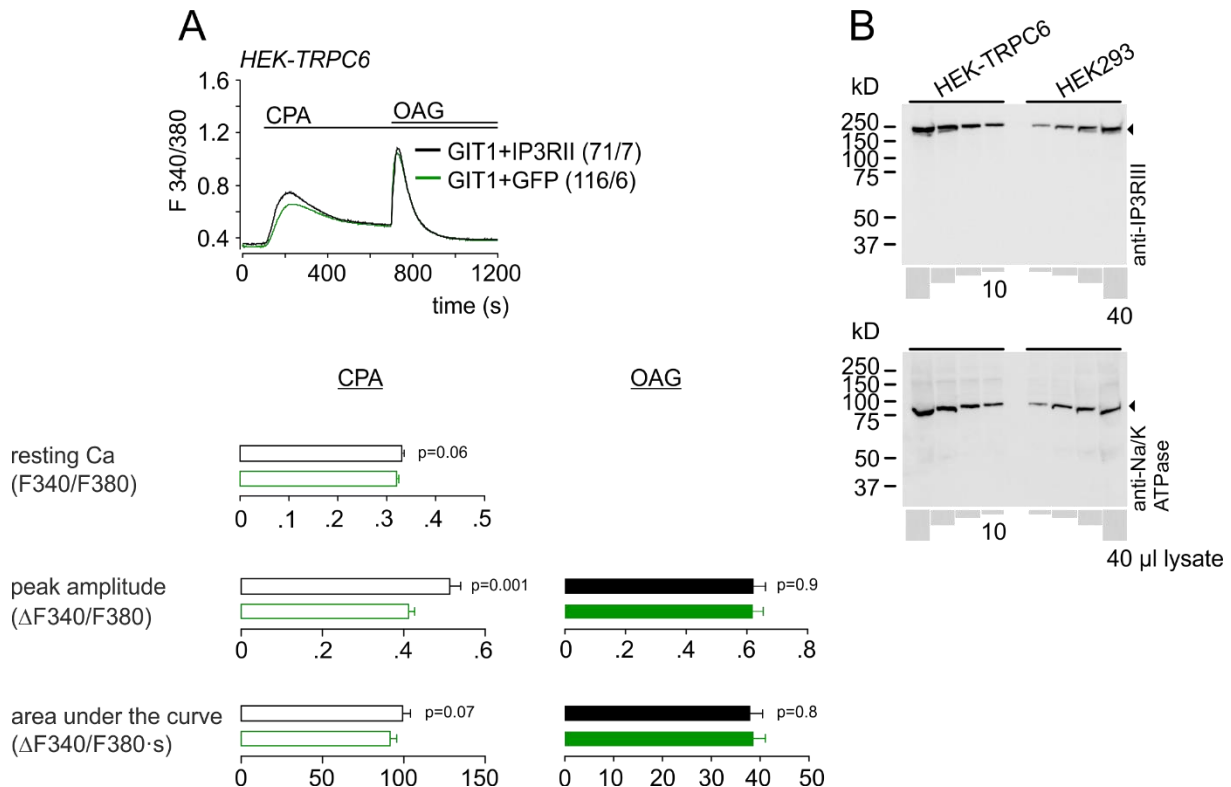


Figure 3-8. Impact of IP3RII on the inhibitory effect exerted by GIT1 protein on the TRPC6 activity in HEK-TRPC6 cells

(A) Top: Calcium imaging traces from HEK-TRPC6 cells expressing either the *Ip3rII*-IGFP cDNA (black) or IGFP (green) as a control in the presence of *Git1*-IRFP cDNA. Following the protocol described in (Figure 3-4 C), cells were loaded with the cell permeable Fura-2AM dye and the ratio F₃₄₀/F₃₈₀ was calculated and plotted versus time. After store depletion with 10 μ M cyclopiazonic acid (CPA), 100 μ M OAG was applied to activate TRPC6-dependent calcium entry. The OAG-induced calcium entry was not different in TRPC6/GIT1/IP3RII expressing cells compared with TRPC6/GIT1 expressing cells. Bottom: Bar graphs summarizing the resting calcium, peak amplitude and area under the curve of CPA (left) and OAG (right). **(B)** Western blots showing the endogenous IP3RIII protein level in the HEK-TRPC6 and HEK293 cells as indicated (top). Increasing amounts (10, 20, 30 and 40 μ L) of protein lysates from both cell lines were loaded to the gel. After SDS-PAGE and blotting to nitrocellulose membrane, the

membrane was incubated with the anti-IP3RIII antibody, followed by stripping the antibody and incubation of the membrane in the presence of an antibody directed to the α -subunit of the Na⁺/K⁺ ATPase as a control (bottom). Data are presented as mean \pm SEM and n = number of cells/number of dishes. Normality was tested and p values were calculated using unpaired two-tailed Student's t test.

3.9 GIT1 protein binds TRPC6 channel *via* its ankyrin repeat domain

Next, I started to map the domains responsible for TRPC6-GIT1 interaction. The Arf GTPase-activating protein or G-protein-coupled receptor kinase interacting protein 1, GIT1, is widely expressed and contains several structural domains (Figure 3-9 A). The full-length GIT1 includes an N-terminal ARF GTPase-activating protein (ARF-GAP) domain, three ankyrin repeats (ANK), a Spa2-homology domain (SHD), a coiled coil domain including a leucine zipper, and a paxillin-binding site (PBS) (Hoefen and Berk, 2006). To identify which domain of GIT1 protein is binding to the TRPC6 channel, I performed pull-down assays. First, different domains of GIT1 were subcloned into a pGEX-4T3 vector, expressed in *E. coli* and the GST tagged GIT1 recombinant fragments were purified (Figure 3-9 A, Figure 3-9 B lower panel). Thereafter, recombinant GST-GIT1 fusion proteins, bound to glutathione beads, were incubated together with the protein lysate from HEK-TRPC6 cells. After several washing steps, proteins bound to the glutathione beads were eluted with the denaturing buffer and separated by SDS-PAGE. The separated proteins were blotted to nitrocellulose membranes and incubated with the anti-TRPC6 antibody. The membrane was stripped and incubated with the anti-GST antibody to control GIT1 fragments ability to retain the TRPC6 protein (Figure 3-9 B lower panel). The fragments of the recombinant GIT1 protein able to retain the TRPC6 full length protein are the following amino acid residues of GIT1: 1-244 aa, 1-374 aa, 130-244 aa and 130-374 aa (* in Figure 3-9 A, B). All these fragments have in common the three ankyrin repeats (130-244 aa) domain of GIT1 protein, indicating that this domain is the minimal binding domain of TRPC6 protein in GIT1 (Figure 3-9 C). GST alone and the other GST-GIT1 fragments do not retain the TRPC6 protein.

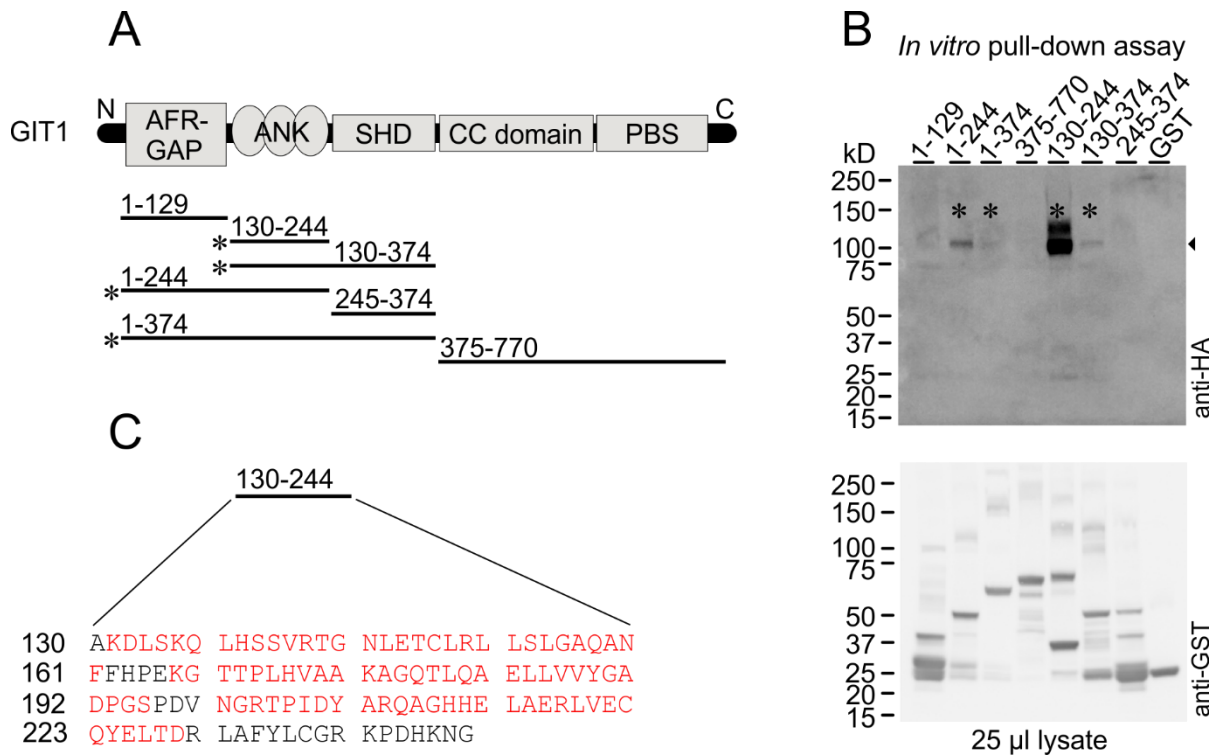


Figure 3-9. GIT1 protein binds TRPC6 channel *via* its ankyrin repeat domain

(A) Top: GIT1 protein domains showing the N- terminal (ARF-GAP) domain, three ankyrin repeats (ANK), a Spa2-homology domain (SHD), a coiled coil domain (CC) and a paxillin-binding site (PBS). Bottom: GST-GIT1 fusion constructs used in the pull-down assay in B. GIT1 fragments with stars represent the identified TRPC6 retaining fragments in B. **(B)** Pull-down assays were conducted using GST-GIT1 fusion constructs shown in A and protein lysates from HEK-TRPC6 cells. The GST-GIT1 constructs (500 pmol) were immobilized on glutathione sepharose beads and incubated with (500 μg) of the HEK-TRPC6 protein lysate. Western blots show the TRPC6 retained by GIT1 fragments 1-244 aa, 1-374 aa, 130-244 aa and 130-374 aa. The TRPC6 protein was visualized by the anti-HA antibody (top) and the GST-GIT1 fragments by the anti-GST antibody (bottom). **(C)** Amino acid sequence of GIT1 domain (130-244 aa) showing the three ankyrin repeats (red).

3.10 The TRPC6 N- terminus is critical for the TRPC6-GIT1 binding

The recently published cryo-EM structures of TRPC6 (Bai et al., 2020; Tang et al., 2018) confirm again that the TRPC6 channel intracellular domains including: the amino-terminus and the carboxyl-terminus of TRPC6, both containing different binding and regulatory domains. We have asked the question if GIT1 protein binds to the C- or N- terminus of the TRPC6 protein.

RESULTS

To answer this question, two cDNAs encoding the N- and C- terminus of the mouse TRPC6 protein were cloned (Figure 3-10 A, D), expressed in HEK293 and Cos-7 cells, respectively and performed Western blot to confirm the presence of the TRPC6 fragments. In Western blot, we could see the N- terminus with a molecular weight of around 44 kDa and the C- terminus with around 22 kDa, using anti-mTRPC6 antibodies against the N- (2F2-D10) and C- terminus (861), respectively (Figure 3-10 B, E). Thereafter, I co-expressed *Git1* cDNA with either the cDNA encoding the N- terminus (1-401 aa) or with the cDNA encoding the C- terminus (727-930 aa). To examine which TRPC6 fragment binds to GIT1 protein, a co-immunoprecipitation assay was performed in both directions using anti-mTRPC6 (against N- or C- terminus) and anti-GIT1 antibodies. Eluted proteins were subjected to Western blot analysis, which shows the TRPC6 N- terminus protein in the input (cell lysate before immunoprecipitation) and in the fraction immunoprecipitated with the anti-mTRPC6 antibody against the N- terminus (Figure 3-10 C). The TRPC6 N- terminus protein band was observed in the fraction immunoprecipitated with anti-GIT1 antibody, indicating that both the TRPC6 N- terminus and GIT1 protein are binding together (Figure 3-10 C). In contrast, the C- terminus of TRPC6 was not retained by GIT1 protein and vice versa (Figure 3-10 F). These results indicate that the cytosolic N- terminus of TRPC6 protein is a critical domain for GIT1 binding.

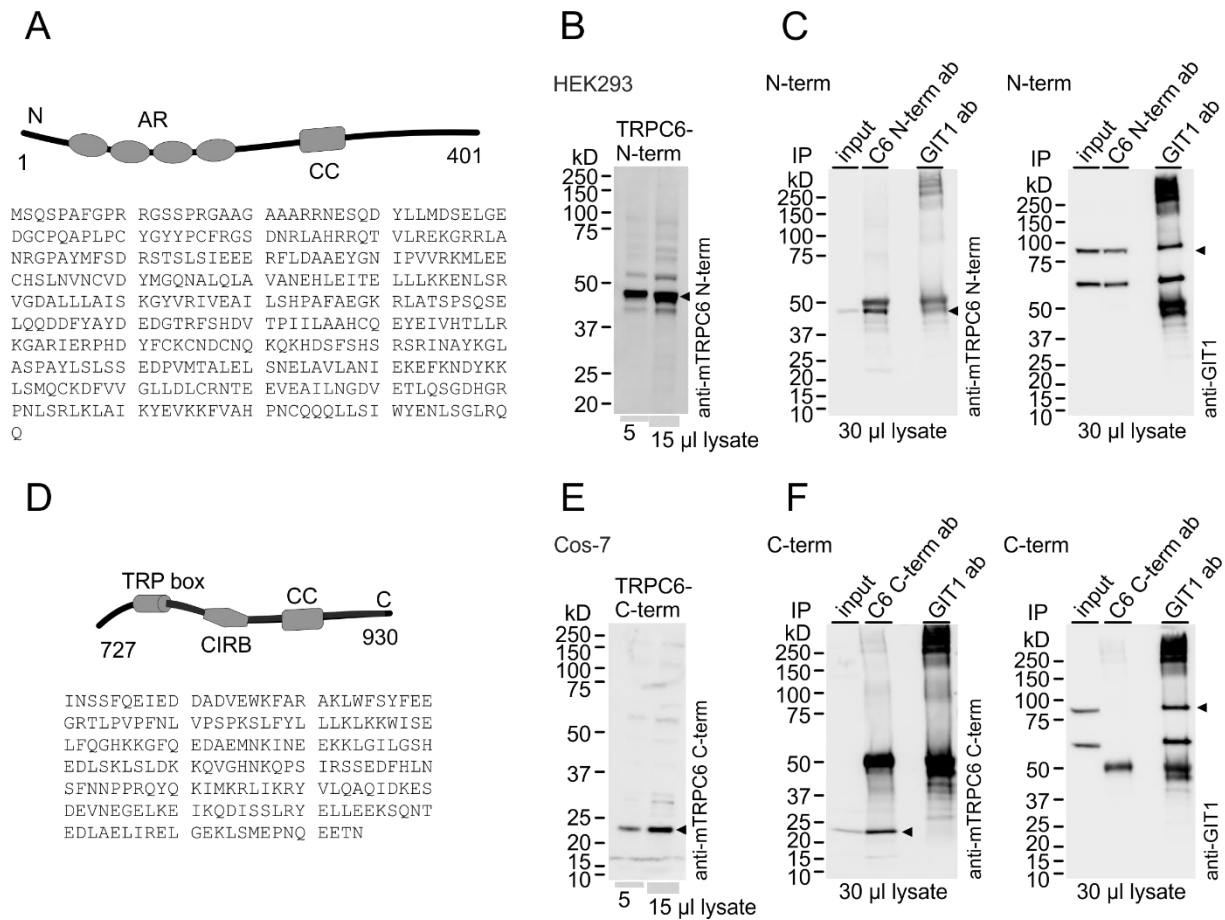


Figure 3-10. The N- terminus of TRPC6 is essential for TRPC6 channel and GIT1 protein binding

(A) Schematic illustration of the TRPC6 structure showing different domains of the N- terminus (top) and amino acid sequence of the N- terminus of TRPC6 protein (bottom). HEK293 and Cos-7 cells were co-transfected with the TRPC6 (N- or C-) terminus and the full length of *Git1* cDNA. **(B)** Western blot showing the TRPC6 N- terminal fragment at ~44 kDa after loading two different amounts of the cell lysate to the gel. Separated proteins were blotted to nitrocellulose membrane and the TRPC6 N-terminus was detectable using anti-mTRPC6 antibody against the N- terminus of TRPC6 protein (2F2-D10). **(C)** Co-immunoprecipitation assay conducted by two different antibodies; anti-mTRPC6 antibody against the N- terminus and anti-GIT1 antibody. After immunoprecipitation and denaturing, proteins were separated by SDS-PAGE and visualized by Western blot with the anti-mTRPC6 N- terminus (left) or anti-GIT1 (right) antibodies, respectively. **(D)** Top: Scheme of the domains within the C- terminus of the TRPC6 protein. Bottom: Amino acid sequence of the C- terminus of TRPC6 protein. **(E)** Immunoblot of the TRPC6 C- terminal fragment expressed in Cos-7 cells and visualized at ~22 kDa by the anti-mTRPC6 antibody directed against the C- terminus (861). **(F)** Co-immunoprecipitation as described in C. Anti-mTRPC6 antibody against the C- terminus and anti-GIT1 antibody were used in the immunoprecipitation assay. Left: Western blot showing that the TRPC6 C- terminus was detectable

using the anti-mTRPC6 C- terminus antibody. Right: GIT1 protein was shown at ~85 kDa using anti-GIT1 antibody. Western blots reveal that GIT1 does not bind to the C- terminus of TRPC6 protein.

3.11 The first 249 amino acid residues of the TRPC6 channel are essential for its binding to GIT1 protein

With the aim to narrow down the binding site of GIT1 on the TRPC6 protein, two N- terminal fragments of the TRPC6 were cloned, one fragment containing the four ankyrin repeats (1-249 aa) and a second fragment covered amino acids 247-401 aa (Figure 3-11 A). After *in vitro* translation in the presence of ³⁵S-Methionine, both TRPC6 N- terminal fragments (1-249 aa and 247-401 aa) were visible after SDS-PAGE and autoradiography (Figure 3-11 B). To evaluate which of the TRPC6 N- terminal fragments bind the ankyrin repeat domain (130-244 aa) of GIT1 protein, the GST-GIT1 fusion construct (130-244 aa) was tested for its ability to pull-down either TRPC6 fragment (1-249 aa or 247-401 aa). The TRPC6 fragment (1-249 aa) was retained by the GIT1 domain 130-244 aa as shown after exposure on a phosphor-imager screen. The TRPC6 fragment (247-401 aa) was not retained and was not detectable. Only a very faint band was detected when GST alone was used for the pull-down assay (Figure 3-11 C, D). Taken together, the data show that the first 249 aa of the TRPC6 protein containing ankyrin repeats are the essential binding domain for GIT1 protein and that binding is most probably by the ankyrin repeats within TRPC6 and GIT1 proteins.

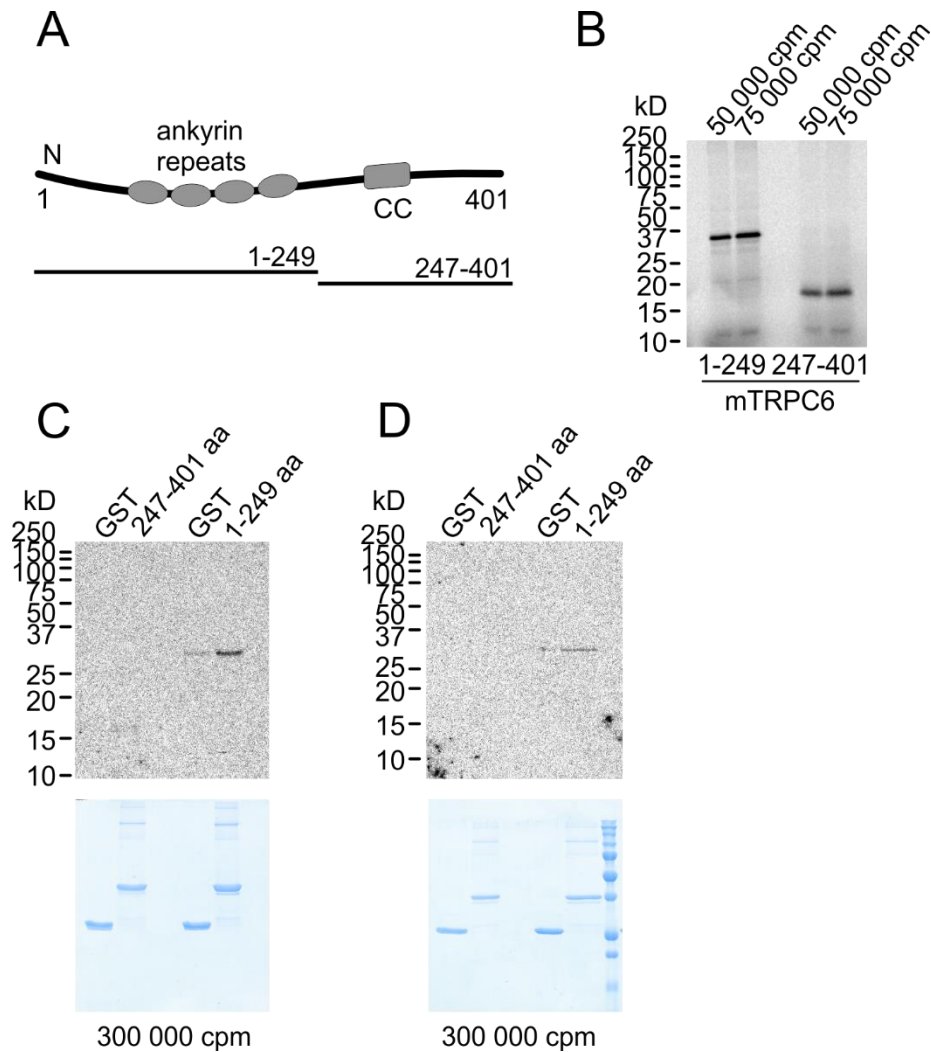


Figure 3-11. The ankyrin repeats containing domain of TRPC6 is required for GIT1 protein binding

(A) Top: Domain structures of the TRPC6 N- terminus (1-401 aa) indicating the four ankyrin repeats (AR) followed by the coiled coil domain (CC). The two fragments of TRPC6 were cloned for pull-down assays (bottom). **(B)** *In vitro* translation of N- terminal TRPC6 fragments, 1-249 aa and 247-401 aa in the presence of ^{35}S -methionine. Autoradiograph showing the intact ^{35}S -labeled fragments. **(C, D)** Top: Pull-down assays of GST-GIT1 fragment 130-244 aa and the ^{35}S -labeled TRPC6 fragments. The GST-GIT1 fragment (130-244 aa) was immobilized on glutathione sepharose beads and incubated with either the ^{35}S -labeled TRPC6 fragments 1-249 aa or 247-401 aa. After several washing steps, denatured proteins were separated by SDS-PAGE. Gels were dried and exposed to phosphor-imaging screens for 3 h **(C)** or 24 h **(D)**. The TRPC6 N- terminal fragment 1-249 aa was retained by GIT1 domain 133-244 aa. GST alone did not retain TRPC6 fragments. Bottom: Coomassie-stained GST and GST-GIT1 fragments.

3.12 GIT1 depletion in HEK293 cells stably expressing *Trpc6* cDNA increases the TRPC6 channel function

So far, our results show that GIT1 protein inhibits the TRPC6 channel activity, which results in a reduction of the TRPC6 current and decreased OAG-induced calcium entry. GIT1 protein also slows down the migration of TRPC6-expressing HEK293 cells. Furthermore, the minimal binding domain of TRPC6 required for GIT1 binding covers the first 249 amino acids of the TRPC6 N- terminus and the ankyrin repeat domain of GIT1 protein 130-244 aa. As shown in (Figure 3-5 A), GIT1 protein is endogenously present in HEK293 cells suggesting that there is already an endogenous GIT1 inhibitory levels on the TRPC6 channel function. In order to deplete the endogenous GIT1 protein and maybe increase the TRPC6 channel function, HEK-TRPC6 cells were transfected with the TRPC6 N- terminus cDNA to bind the endogenous GIT1 protein (Figure 3-12). In HEK-TRPC6 cells transfected with the TRPC6 N- terminus cDNA, larger inward and outward TRPC6 currents were recorded upon application of 100 μ M OAG (Figure 3-12 A, B, C). Most probably the expressed TRPC6 N- terminus competes with the TRPC6 protein for binding to the endogenous GIT1 protein. This assumption also explains the following results: Cells overexpressing the N- terminus of TRPC6 in addition to the full length TRPC6 migrate faster compared with cells only expressing the full length TRPC6 in the scratch migration assay (Figure 3-12 D). In addition, the OAG-induced TRPC6-dependent calcium entry was slightly enhanced in HEK-TRPC6 cells co-transfected with the TRPC6 N- terminus cDNA (Figure 3-12 E, F). The area under OAG-induced TRPC6-dependent calcium entry was significantly enhanced in the presence of TRPC6 N- terminus but the peak amplitude, the number of OAG responding cells and the number of peaks per OAG responding cells were not significantly changed (Figure 3-12 F).

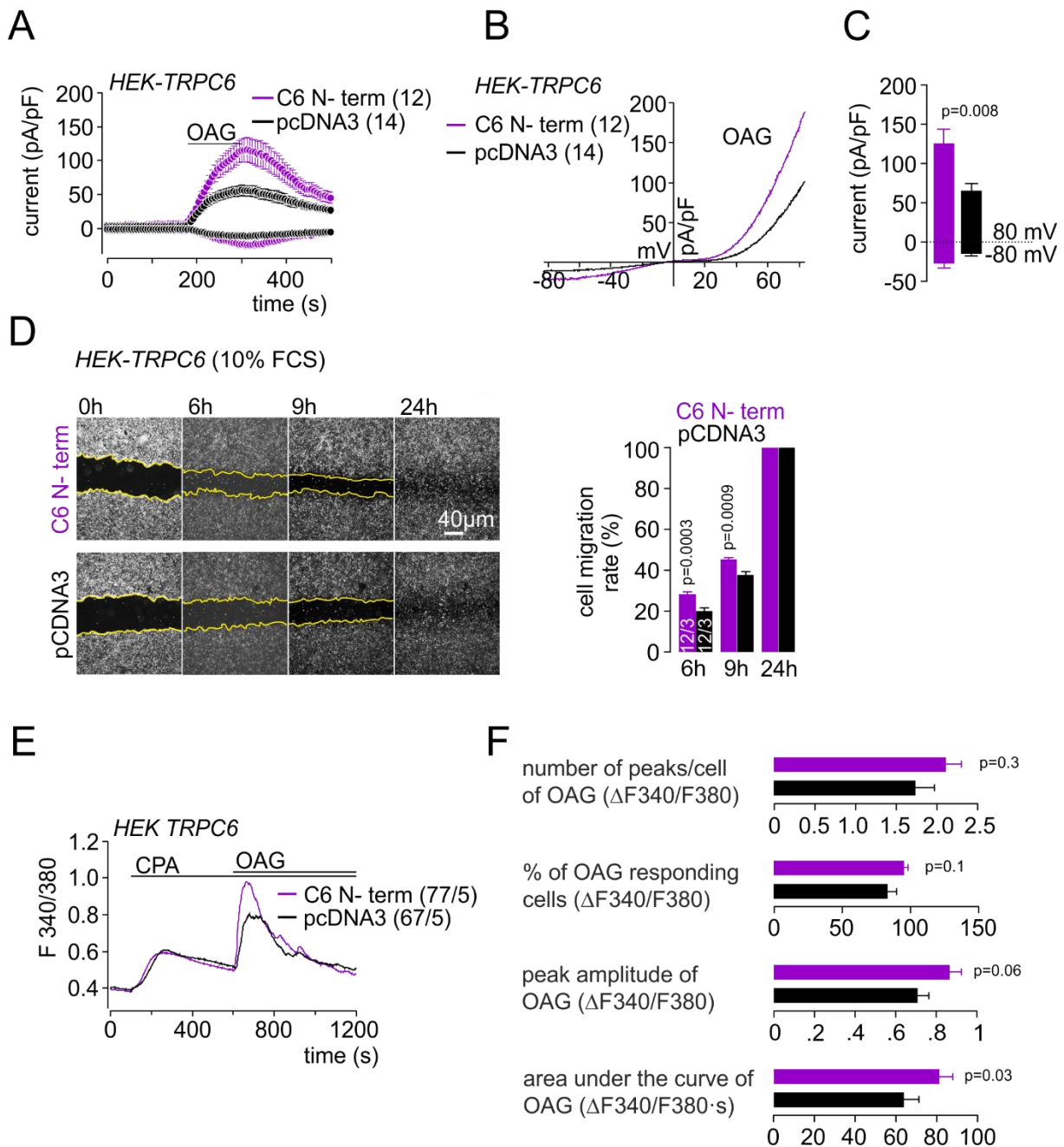


Figure 3-12. Co-expression of the TRPC6 N-terminus (1-249 aa) cDNA in HEK293 cells stably expressing the full length *Trpc6* cDNA frees TRPC6 function from GIT1 inhibition

(A) TRPC6 inward and outward currents at -80 and +80 mV plotted versus time, recorded from HEK-TRPC6 cells transfected with the TRPC6 N-terminus cDNA (purple) or pCDNA3 (empty vector, black) as a control. The TRPC6 N-terminus binds the endogenous GIT1 protein and relieves the TRPC6 channel from inhibition by GIT1 protein. (B) Current-voltage relationship in the presence or absence of TRPC6 N-terminal fragment and upon TRPC6 channel activation with 100 μ M OAG. (C) Bar graphs summarizing current amplitudes at -80 and +80 mV after TRPC6 channel activation by 100 μ M OAG.

(D) Left: Scratch migration assay of HEK-TRPC6 cells in the presence (upper panel) or absence of co-expressed TRPC6 N- terminus (lower panel) (images were taken with the 5x objective) in the presence of 10% fetal calf serum. Empty pCDNA3 vector was transfected as a control. Right: Bar graphs summarizing the percentage of area repopulated by migrating cells over time. **(E)** Mean calcium imaging traces obtained from HEK-TRPC6 cells transfected as indicated. The OAG-induced TRPC6-dependent calcium entry was slightly higher in cells overexpressing the TRPC6 N- terminus cDNA. **(F)** Bar graphs summarizing the number of peaks per OAG responding cells, percentage (%) of OAG responding cells, peak amplitude and area under the curve. Data are shown as mean \pm SEM with n = number of cells/number of dishes. Normality was tested and p values were calculated using Mann–Whitney test.

3.13 GIT1 protein does not affect TRPC6 channel membrane localization

The TRPC6 protein was shown to localize at the plasma membrane of HEK-TRPC6 cells and human platelets (Figure 3-4 B, Figure 3-5 C). GIT1 protein, which binds and modulates TRPC6 channel function was visualized by fluorescent microscopy at the cytoplasmic fraction of the cell (Figure 3-5 B, C). To investigate whether GIT1 protein affects the TRPC6 localization at the plasma membrane, either directly or indirectly, an independent assay was performed, the surface biotinylation assay. In addition, the TRPC6 channel was either activated by OAG or not to study the impact of GIT1 protein on the TRPC6 channel externalization in the presence and absence of OAG. HEK-TRPC6 cells were transfected with *Git1*-IGFP or the IGFP cDNAs as a control, and either treated with the TRPC6 agonist OAG for 2 min or left untreated. Thereafter, cells were incubated with the biotinylation reagent sulfo-NHS-SS-biotin, which is membrane impermeable biotinylates extracellular protein domains. The biotinylated cell-surface proteins were isolated by streptavidin-agarose beads. After washing, biotinylated proteins were eluted by 2X SDS denaturing buffer, separated by SDS-PAGE, which was followed by Western blot. The TRPC6 protein was present in the input, the protein lysate before incubation in the presence of streptavidin beads, as well as in the biotinylated protein fraction, in both, GIT1 or GFP expressing control cells, independent of OAG treatment (Figure 3-13 A). To control the surface biotinylation and that the biotin is not taken up by cells to biotinylate

RESULTS

intracellular protein domains, the Western blot membrane was incubated with antibodies against calnexin, an integral protein of the endoplasmic reticulum, or the α -subunit of the Na^+/K^+ ATPase, a marker for the plasma membrane. In the Western blot, the calnexin was detectable only in the input fraction but not among the biotinylated proteins (Figure 3-13 B). In contrast, the plasma membrane Na^+/K^+ ATPase was present in the input and among the biotinylated proteins (Figure 3-13 C). The results indicate that GIT1 protein does not inhibit the TRPC6 channel function through preventing TRPC6 translocation to the plasma membrane, but rather by a direct effect on the plasma membrane TRPC6 channel. In addition, OAG appears not to have an effect on TRPC6 targeting to the plasma membrane.

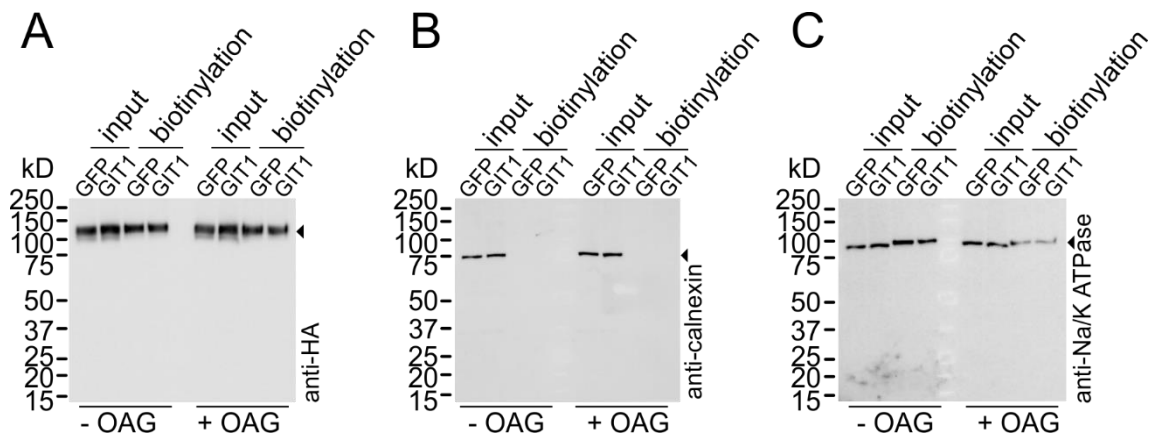


Figure 3-13. GIT1 protein did not alter TRPC6 localization at the plasma membrane

(A) Immunoblot of the HEK-TRPC6 cells transfected either with *Git1*-IGFP cDNA or IGFP as a control. Cell surface biotinylation assay was performed in the absence (-OAG) or presence (+OAG) of 100 μM OAG. Cells were incubated with the biotinylation reagent sulfo-NHS-SS-biotin and biotinylated proteins were retained from the cell lysate by streptavidin-agarose beads. After washing the beads, proteins were eluted by SDS denaturing buffer, separated by SDS-PAGE, blotted to nitrocellulose membrane and the TRPC6 protein was visualized by the anti-HA antibody. The amount of TRPC6 protein on the cell surface shown by Western blot are similar in the presence and absence of GIT1 protein. **(B, C)** Western blot membranes were incubated with antibodies against either calnexin, an integral protein of the endoplasmic reticulum **(B)** or the α - subunit of the Na^+/K^+ ATPase, a plasma membrane marker **(C)** to control the surface biotinylation.

3.14 TRPC6 plays an important role in *in vitro* platelet adhesion

Platelet adhesion occurs generally as the first step following vascular injury. In this process platelets can recruit additional platelets to the site of lesion, which plays a critical role in platelet activation. Under healthy condition, platelets do not adhere to the blood vessels. In case of vessel injury, the exposure of the extracellular matrix activates platelets, a process which induces the release of soluble agonist and the appearance of active forms of adhesive molecules, enabling platelet adhesion. Several ligands are involved in platelet adhesion including proteins in the plasma, such as collagen and fibrinogen (Ruggeri and Mendolicchio, 2007). Collagen and fibrinogen play a role in platelet activation by promoting signaling (Huang et al., 2019), which in turn leads to calcium influx through several ion channels expressed on platelets plasma membrane including TRPC6 and ORAI channels (Braun et al., 2009; Hassock et al., 2002). The function of TRPC6 in human platelets is still not clear and the effect of TRPC6 gene deletion on platelet aggregation and bleeding time are controversial (Ramanathan et al., 2012; Vemana et al., 2015). In my study, the TRPC6 protein was identified in the human platelets in a complex containing different proteins involved in cell adhesion and cytoskeleton organization (Table 3-1). Upon activation, platelets undergo structural changes, which required many adaptor proteins. GIT1 protein, a multidomain adaptor protein, which plays a role in the cell motility and lamellipodia formation, was identified in the platelets (Sato et al., 2008). Moreover, the PLC γ 2 protein, which was identified in the TRPC6 complex, is known to interact with GIT1 (Haendeler et al., 2003) and TRPC6 proteins (Farmer et al., 2019). Upon clustering and activation of the fibrinogen, a signal transduction triggers PLC γ 2 activation and therefore the release of the DAG, which in turn activates TRPC6 channel. Once platelets are stimulated, a signaling cascade through collagen activates PAK2 phosphorylation, which interacts with GIT1-PIX complex (Manser et al., 1998; Zhao et al., 2000) and was shown in this study to form a complex with the TRPC6 protein in the human platelets (Table 3-1). As a result, the ERK1/2 (MAPK), which is a downstream substrate of PAK2 is phosphorylated and involved in further

signaling pathways (Park et al., 2007) (Figure 3-14). Considering this scheme (Figure 3-14), we suggested that TRPC6 protein may involve in the early stages of blood hemostasis such as platelet adhesion, which could be compensated in late stages of hemostasis by other mechanisms. To investigate the role of TRPC6 channel in platelet adhesion, human platelets resuspended in Tyrode's buffer were treated with the TRPC6 agonist OAG, the TRPC6 specific inhibitor SAR7334 or its solvent dimethyl sulfoxide (DMSO) as a control. The treated platelets were transferred immediately to glass coverslips pre-coated either with fibrinogen or collagen. After 15 and 60 min, the corresponding glass coverslips were washed several times to remove non-adherent platelets and then the attached platelets were fixed and permeabilized and finally, actin filaments were stained to count adherent platelets. As shown in (Figure 3-15), adherence of human platelets increased over time in control DMSO platelets (Figure 3-15 A, B). OAG treatment of human platelets results in a significant increase in platelets adhesion to both fibrinogen and collagen after 60 min incubation (Figure 3-15 A, B). Platelets treated with the TRPC6 antagonist (SAR7334) show significantly reduced adhesion compared with the OAG and the control treated cells (Figure 3-15 A, B), indicating a basic activity of the TRPC6 channel in the human platelets contributing to the fibrinogen/collagen adhesion. To support these findings, platelets obtained from wild-type and TRPC6 gene-deficient mice were isolated and adhesion was performed in similar experiments as described above for the human platelets. Platelets collected from eight wild-type males and eight TRPC6 knockout males were plated on glass coverslips pre-coated with fibrinogen. After 15, 30 and 60 min, the coverslips were washed several times, fixed, permeabilized and stained to visualize platelet actin filaments. After quantification of platelets, which adhere at each time point (Figure 3-15 C), platelet adhesion is significantly reduced in TRPC6 deficient cells compared with platelets from the wild-type mice (Figure 3-15 D), which additionally confirms the important role of TRPC6 channel in human and mouse platelet adhesion.

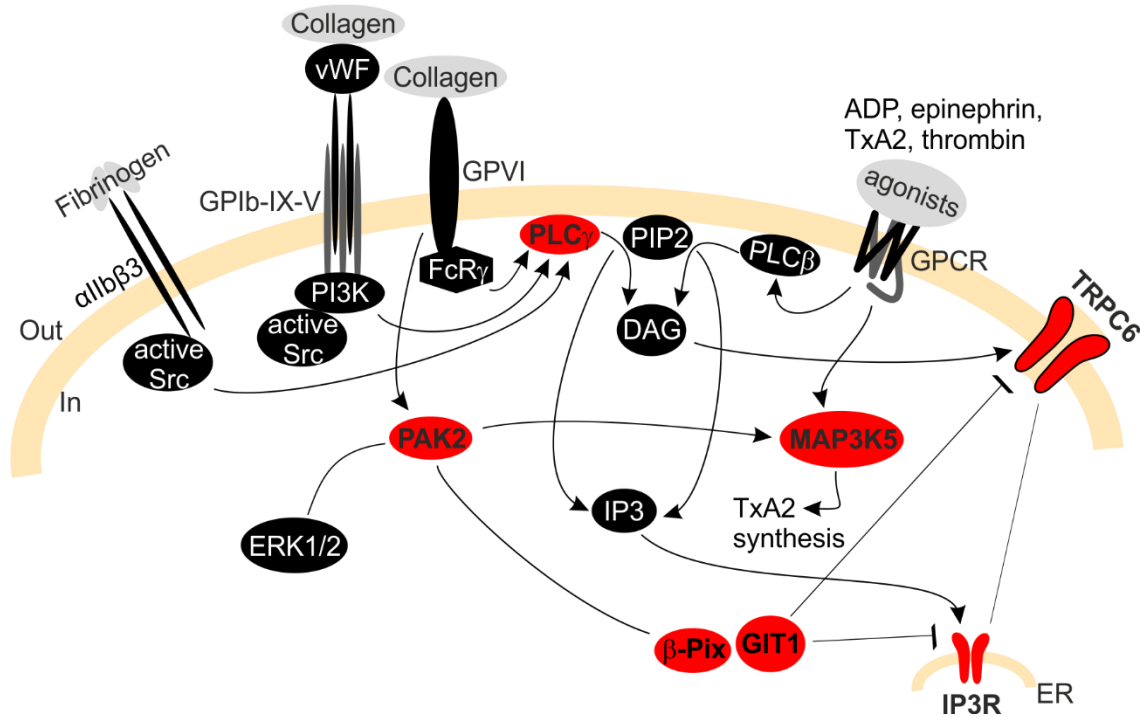


Figure 3-14. Signaling pathway of TRPC6 associated proteins in human platelets

(A) Scheme illustrating platelet activation through the G protein-coupled receptors and glycoprotein receptors (fibrinogen and collagen receptors) and the downstream signaling pathways involving TRPC6 associated proteins like GIT1, IP3Rs, PLC γ , β -Pix, MAP3K5 and PAK2 (highlighted in red). In the platelet adhesion assay (results shown in Figure 3-15) on fibrinogen/collagen coated coverslips, platelets were treated either with 100 μM OAG to activate TRPC6 channel or 20 nM SAR7334 to inhibit the TRPC6 channel.

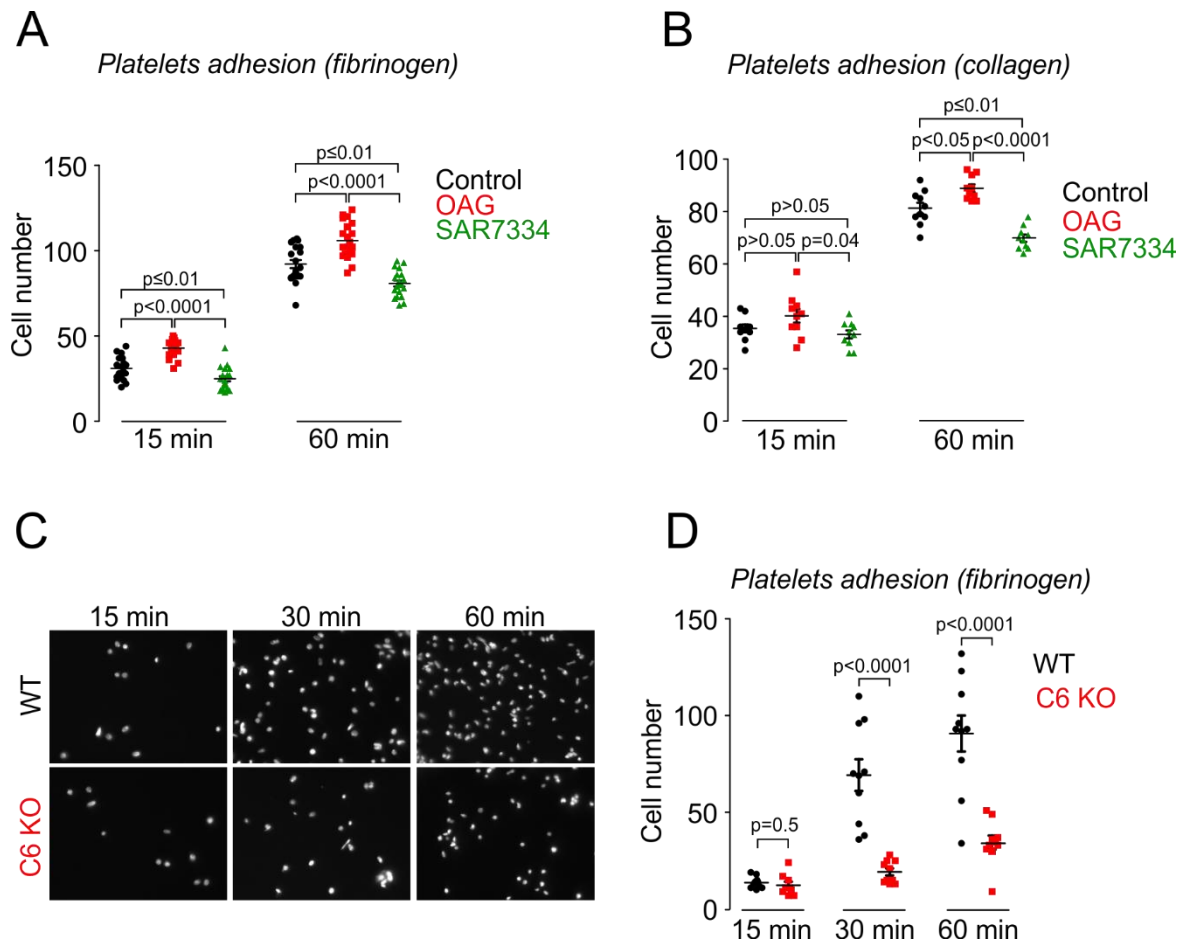


Figure 3-15. The TRPC6 channel contributes to platelet adhesion

(A, B) Scatter plots showing the number of human platelets attached to fibrinogen or collagen. Washed human platelets were treated with DMSO (solvent control, black), OAG (red) or SAR7334 (green) then allow to adhere to fibrinogen (A) or collagen (B) for 15 and 60 min. (C) Example figures illustrating the number of wild-type (WT) and TRPC6 knockout (C6 KO) platelets attached to the fibrinogen coated coverslips after allowing them to adhere for 15, 30 and 60 min. (D) Corresponding to B, the number of adherent mouse platelets was summarized as scatter plot showing platelets from wild-type (black) and TRPC6 knockout mice (red) allowed to attach to 100 µg/mL fibrinogen coated coverslips for 15, 30 and 60 min. TRPC6 gene deletion or pharmacological inhibition of the TRPC6 channel results in reduced number of platelets, which adhere on fibrinogen or collagen coated coverslips, indicating the involvement of TRPC6 in platelet adhesion in human and mice. In each condition and in each time point, two coverslips were used. Ten to fifteen images were taken randomly from each coverslip. Data are shown as mean ± SEM and p values were calculated using one-way ANOVA followed by Bonferroni's multiple comparisons test for B and C and unpaired two-tailed Student's t test for E.

3.15 Collagen and OAG stimulate proteins phosphorylation in human platelets

Platelet receptor activation with GPVI agonists leads to the stimulation of the PAK2 phosphorylation (Vidal et al., 2002), which is downstream Rho GTPases, Rac1 and links to the ERK kinases and GIT1/PIX complex signaling resulting in platelet aggregation and lamellipodia formation (Aslan et al., 2013a). To understand how TRPC6 activation by its agonist OAG results in an increased platelet adhesion, I investigate whether OAG (100 μ M) can stimulate PAK2 and its downstream effectors phosphorylation. Human platelets were treated with collagen or OAG for 5, 10, 15 and 20 min and DMSO treated platelets were used as a control. After treatment, platelet lysate was prepared from each sample. After estimation of the total protein concentration in each condition, 100 μ g of protein lysates were separated by SDS-PAGE, blotted to nitrocellulose membrane and the membrane was incubated with antibodies against the PAK2 and ERK1/2 kinases, both the phosphorylated enzymes, the non-phosphorylated and phosphorylated enzymes. The collagen treatment induced PAK2 phosphorylation compared with the non-treated platelets (Figure 3-16 A, E). The PAK2 phosphorylation after collagen stimulation was not increasing overtime, which suggested that PAK2 phosphorylation at 5 min already reaches saturation (Figure 3-16 A, E). In addition, antibody against the phosphorylated ERK1/2 showed an increase in the ERK1/2 phosphorylation after 5 min collagen treatment, which was further enhanced after 10, 15 min of treatment (Figure 3-16 B, F). In human platelets treated with OAG, the phosphorylated ERK1/2 detected by Western blot using anti-phospho-ERK1/2 antibody, was increased compared with the non-treated platelets and reached almost a maximum level at 5 min, which might explain the absence of any significant increase at further time points 10, 15 or 20 min (Figure 3-16 B, F). However, using an antibody against the phosphorylated fraction of PAK2 after platelets were treated with OAG, the phosphorylation seems to increase over time and reaches a maximum level after 15 min of OAG treatment (Figure 3-16 A, E). Moreover, we

RESULTS

could observe in Western blot that platelets treated with the OAG exhibited more than one band in the PAK2 phosphorylated fraction compared with the non-treated platelets and platelets treated with the collagen. Suggesting that the TRPC6 agonist, OAG could activate platelets by additional pathways in comparison with that of collagen. Taken together, treatment of human platelets with OAG to activate TRPC6 channel leads to platelet activation and a subsequent PAK2 and ERK1/2 phosphorylation in a similar way as collagen does. Furthermore, platelet treatment with OAG and collagen, triggered phosphorylation of the protein kinases PAK2 and ERK1/2, which rapidly occurred and reached saturation levels. In addition, platelet treatment with OAG showed an increase in the amount of protein kinase PAK2 compared with the collagen treated platelets (Figure 3-16 C).

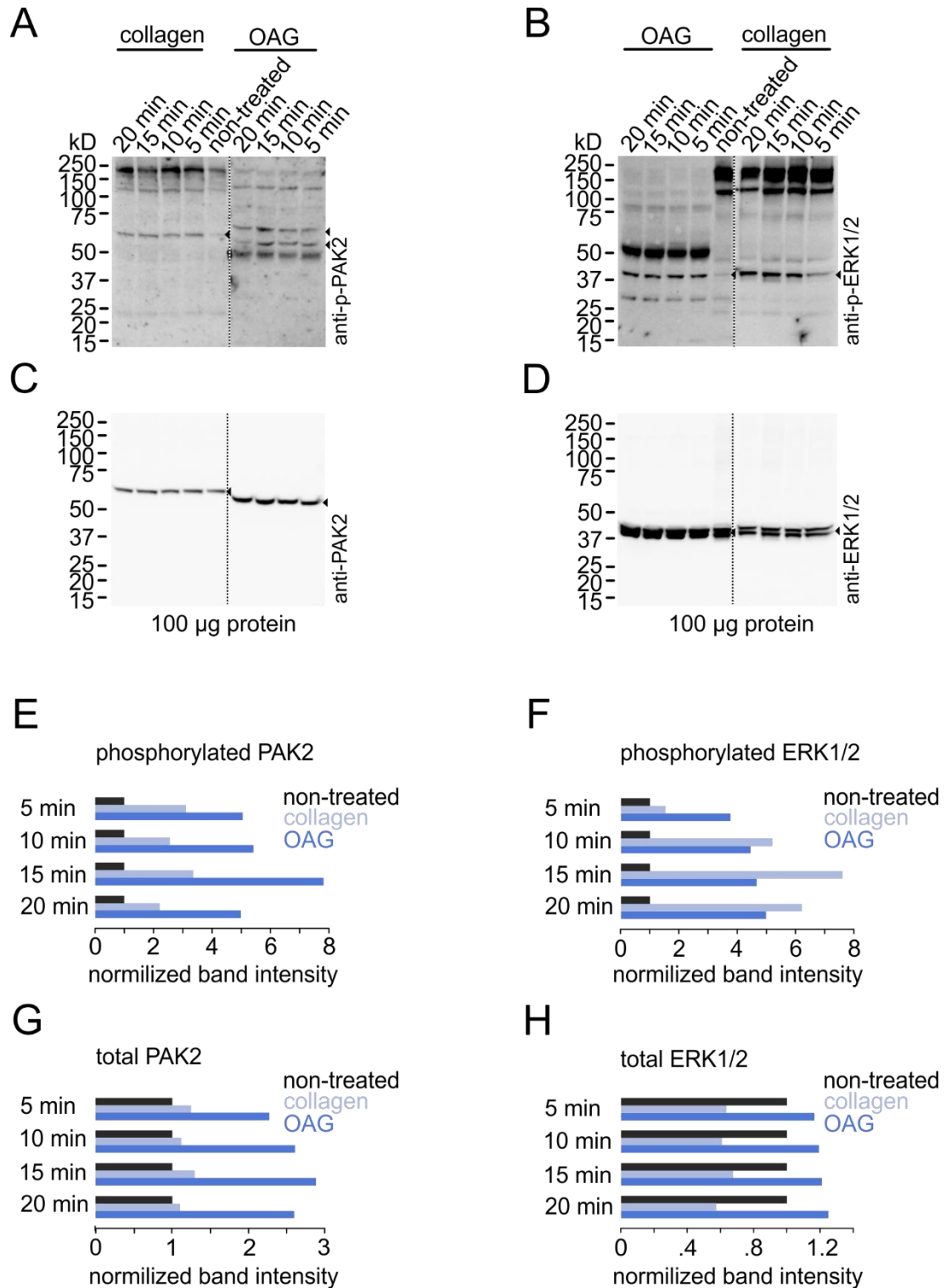


Figure 3-16. Platelet treatment with the collagen or OAG stimulates PAK2 and ERK1/2 phosphorylation

(A, B) Time course of the p21 activated kinases (PAK2) and extracellular signal-regulated kinases (ERK1/2) phosphorylation after platelet stimulation with collagen or TRPC6 agonist, OAG. Human platelets were treated with collagen or OAG for 5, 10, 15 and 20 min and 100 µg protein of human

RESULTS

platelet lysate was used for Western blot analysis. Collagen and OAG treated samples were applied to the gel in **(A)** and **(B)**. After blotting, the membrane was incubated with the anti-p-PAK2 (Ser20) **(A)** and anti-p-ERK1/2 (Thr202/Tyr204) **(B)**. The non-treated platelets were used as a control. **(C, D)** Western blots showing total proteins after stripping the upper blots and re-incubating them with the corresponding antibodies represented by the anti-PAK2 antibody to detect the amount of PAK2 protein **(C)** after treatment with collagen or OAG. Anti-ERK1/2 antibody was used to detect the amount of ERK1/2 protein **(D)** after stimulation of human platelets with OAG or collagen. The TRPC6 activation by OAG stimulates platelet activation and triggers protein kinase PAK2 and ERK1/2 phosphorylation. **(E, F, G, H)** Bar graphs summarizing band intensities of the correspondent Western blots A, B, C and D and showing the phosphorylated PAK2 **(E)**, the phosphorylated ERK1/2 **(F)**, the total PAK2 **(G)** and the total ERK1/2 **(H)** after platelet treatment with collagen or OAG for 5, 10, 15 and 20 min. Band intensities were normalized to the non-treated platelets.

4 Discussion

TRPC6 channel in human platelets

During the last years, strong evidence indicates that transient receptor potential canonical 6 (TRPC6), a non-selective cation channel, contributes to the regulation of intracellular calcium levels. It has been suggested that TRPC6 channel is involved in many cellular processes and alterations in its function can result in different diseases (Guilbert et al., 2008; Kuwahara et al., 2006; Winn et al., 2005). TRPC6 channel has been identified in different tissues and cell types (Nilius and Flockerzi, 2014). In human platelets, TRPC6 protein was identified for the first time almost twenty years ago (Hassock et al., 2002). The TRPC6 protein was found to be highly expressed in the plasma membrane and was activated by thrombin and OAG independently of store operated calcium entry (SOCE). Several studies have been focusing on the role of TRPC6 channel in human platelets. However controversial results were obtained using mice lacking the *Trpc6* gene (Paez Espinosa et al., 2019; Ramanathan et al., 2012). To better understand how many cellular functions are accomplished, several reports and studies are focusing on the protein-protein interactions in the cell „interactome” (Cusick et al., 2005). Thus, in my study the mass spectrometry was used as a sensitive technique to map the TRPC6 protein interactome in the human platelets.

Mass spectrometry was coupled with an antibody-based affinity purification procedure to investigate the TRPC6 protein in primary human platelets and to identify potential TRPC6 associated proteins, which could be involved in modulating the channel's activity *in vitro* and *in vivo*. Using an antibody against the C- terminus of the human TRPC6 protein as well as non-specific immunoglobulins as a control (Figure 3-1), I was able to enrich the TRPC6 protein and its associated proteins after solubilization of the human platelet membrane proteins using digitonin as a detergent (Talvenheimo and Rudnick, 1980). The mild non-ionic detergent

(digitonin) solubilizes membrane proteins without disrupting the interactions between proteins, which make it suitable and extensively used in studying protein interactions. To keep the TRPC6 protein complex intact, a synthesized antigenic peptide was used, which corresponds to the TRPC6 sequence recognized by the specific anti-hTRPC6 antibody 1263 directed against the C-terminus. By adding high concentrations of the competing peptide, the native TRPC6 protein complex bound to the antibody was eluted without disrupting any putative interactions. In mass spectrometry and Western blot analysis, the TRPC6 protein was detectable at around 106 kDa in the fraction enriched using the specific anti-hTRPC6 antibody 1263. As expected, there was no TRPC6 protein detectable in the fraction enriched by the non-specific rabbit immunoglobulins (Figure 3-1 E, F, G). To estimate the molecular weight of the TRPC6 channel complex, a blue native PAGE (BN-PAGE) followed by SDS-PAGE (Wittig et al., 2006) was performed, by which protein complexes were separated under their folded state where they gain their charges from the coomassie staining. In the two-dimensional BN/SDS-PAGE, the TRPC6 channel complex band was mainly concentrated at a molecular weight of around 242 kDa (Figure 3-1 H). Nonetheless, TRPC6 complex band spreading to a much higher molecular weight was detected less abundantly. The TRPC6 protein has a molecular weight of 106 kDa as a monomer, where the functional channel is composed of four monomeric subunits to form a tetrameric channel (Bai et al., 2020; Gaudet, 2007; Tang et al., 2018). It has been shown by (Kol et al., 2013) that TRPV3 could be found as dimers using BN-PAGE to separate protein complexes in their native condition. Similar, we observed that most of the TRPC6 protein detected by BN-PAGE is representing a dimer as previously described for the TRPV3 channel (Kol et al., 2013). Nevertheless, the spreading band detected at higher molecular weight could represent the TRPC6 protein complex including other proteins, which may regulate the channel's function in human platelets.

TRPC6 associating proteins in human platelets

Using mass spectrometry technique to identify protein complexes usually yields a high number of identified proteins, which could bind either specifically or non-specifically. Therefore, I performed many steps and followed several criteria to exclude any potential non-specific binding proteins. First, using the specific anti-hTRPC6 antibody and non-specific immunoglobulins as a control facilitate thereafter the discrimination between the specific and non-specific bindings. Second, taken advantage of the native elution method described previously by (Firer, 2001), the competing peptide was used to reduce the number of non-specific proteins. Third, analyzing mass spectrometric results based on the abundance ratio plot participates in differentiating between the robust specific binding proteins and the non-specific ones. The latter analysis relies on plotting the ratios of at least two independent affinity enrichment experiments. Each ratio represents the abundance of a given protein identified in the fraction enriched by the specific antibody compared with the control non-specific immunoglobulins. Using this approach, I could identify twelve potential TRPC6 associated proteins, which have been detected in two independent experiments and only in the fraction purified using the specific anti-hTRPC6 antibody but not in the control fraction (Figure 3-2 C, Table 3-1). Among these twelve proteins, I could identify the Inositol 1,4,5-trisphosphate receptors (IP3R), Mitogen-activated protein kinase 5 (MAP3K5), ARF GTPase-activating protein (GIT1), Phospholipase C γ 2 (PLC γ 2), Rho guanine nucleotide exchange factor 7 (β -Pix) and Myosin XVIII A (MYO18A) (Figure 3-2 C, Table 3-1). Several of these proteins have been already shown to bind either to the TRPC6 channel or to bind together. For example, TRPC6 proteins have been reported to form a complex with the Inositol 1,4,5-trisphosphate receptors (IP3R) (Boulay et al., 1999). ARF GTPase-activating protein (GIT1) was also shown to bind itself to the Inositol 1,4,5-trisphosphate receptors (IP3R) (Zhang et al., 2009), to the Phospholipase C γ (PLC γ) (Haendeler et al., 2003) and to other proteins like Rho guanine nucleotide exchange factor 7 (β -Pix) and myosin XVIII A (MYO18A) (Hsu et al., 2010; Premont

et al., 2004). These data confirm further the specificity of our affinity purifications. However, TRPC3 and TRPC7, which have been shown to interact with the TRPC6 in different systems (Goel et al., 2002; Hofmann et al., 2002), were not detected. In addition, some other proteins which have been suggested to bind TRPC6 protein were not detected in the human platelets like MxA, Fyn, Na⁺/K⁺ ATPase, Calpain and Caldesmon-1. This could be explained by differences in the procedure used to solubilize and prepare samples. Another reason could be that these proteins are absent in platelets or that their expression level in human platelets are very low. It could well be that the TRPC6 channel does not build any heteromultimers with other TRPC proteins in the human platelets but forms only homomultimeric channels. The most abundant potential associated proteins detected by mass spectrometry were further confirmed by co-immunoprecipitation followed by Western blot analysis (Figure 3-2 D, E, F). In human platelets, TRPC6 interacts with Inositol trisphosphate receptor (IP3Rs) type 1 and 2, indicating that the interaction of TRPC6 and IP3R type 1 in HEK293 cells (Boulay et al., 1999) is not a mere overexpression effect.

GIT1 protein

G-protein-coupled receptor kinase interacting protein 1 (GIT1) was identified by (Premont et al., 1998) and was found to be involved in many cellular processes including receptor trafficking, the assembly of protein complex, interaction with focal adhesion proteins, cell motility, and cell growth (Manabe et al., 2002; Zhao et al., 2000). The G-protein-coupled receptor kinase interacting protein (GIT) family consists of two members, GIT1 and GIT2 proteins. The scaffolding proteins family of GIT were identified as a part of the G-protein-coupled receptor kinases (GRKs), which have been shown to play a critical role in receptor phosphorylation and internalization (Premont et al., 1998). GIT proteins structure is highly conserved across species. For example, GIT1 and GIT2 proteins share high (>85%) sequence identity between human and mouse and chicken (Hoefen and Berk, 2006). The human

sequence of GIT1 and GIT2 share around 65% sequence identity and 85% similarity. GIT1 exists in one version whereas GIT2 can be spliced into at least ten variants, which are tissue-dependently expressed (Premont et al., 2000). Immunoprecipitation assays confirmed that GIT1 and GIT2 proteins can form homo- and heterodimers (Kim et al., 2003). The structural domains of the full length GIT1 protein consists of N- terminal ADP-ribosylation factor GTPase activating protein (ARF-GAP) domain, which was proposed to keep proper membrane trafficking and localization of GIT1 protein (Matafora et al., 2001), three ankyrin (ANK) repeats are mediating protein-protein interactions and a Spa2-homology domain (SHD), which exists only in GIT and some yeast proteins. In addition, GIT1 protein contains a coiled-coil domain with a leucine zipper, predicted to play a role in the homo- and heterodimerization of GIT protein (Paris et al., 2003). A paxillin-binding domain located at the C- terminus of GIT1, by which the binding to the paxillin localizes GIT1 protein to the focal complexes (West et al., 2001). GIT1 is a multidomain protein suggested to serve as a scaffolding protein to gather complex components for different signaling pathways. GIT1 was shown to play an important role in controlling membrane trafficking, cell adhesion, cytoskeleton organization, cell migration and receptor internalization (Hoefen and Berk, 2006).

GIT1 protein is localized at the cytoplasm and circulate between three intracellular compartments: cytoplasmic complexes, focal adhesion and membrane protrusions (Manabe et al., 2002). GIT proteins have a wide distribution in the organism, and this was confirmed and visualized using transgenic mice generated by inserting the β -galactosidase (β -Gal) reporter into either *Git1* or *Git2* gene. High expression level of GIT1 mRNA was observed in the testes, whereas low expression levels were detected in the liver and spleen (Premont et al., 1998). In general, the expression of GIT1 protein in comparison to GIT2, seems to be more cell specific and restricted to certain tissues and it shows higher expression level as well (Schmalzigaug et al., 2007). In platelets, GIT1 protein was detected more abundantly in the human platelets compared with the mouse platelets (Huang et al., 2016). Furthermore, GIT1 protein was shown

to bind integrins $\alpha\text{IIb}\beta\text{3}$ in the platelets. During platelet aggregation, GIT1 protein undergoes Src phosphorylation downstream integrins $\alpha\text{IIb}\beta\text{3}$, which may regulate cytoskeletal reorganization (Sato et al., 2008).

Several studies have investigated GIT1 signaling partners and tried to clarify by which mechanism GIT1 activity is controlled. However, the mechanism regulating GIT1 function is still poorly characterized. So far, GIT1 protein has been shown to bind GIT2 through the leucine zipper in the coiled-coil domain to form heterodimers (Premont et al., 2004). The α/β PIX proteins (p21-activated kinase interacting exchange factors) bind to the SHD domain of GIT1 (Zhao et al., 2000). Through PIX proteins, GIT1 forms a protein complex containing PAK, Rac1 and Cdc42 proteins (Manser et al., 1998; Zhao et al., 2000). In addition, the kinase mitogen-activated protein kinase 1 (MEK1) (Yin et al., 2004) and phospholipase $C\gamma$ (PLC gamma) but not PLC β or PLC δ (Haendeler et al., 2003) interact with GIT1 protein through its SHD domain. It is also believed that paxillin protein at the focal adhesion sites can attach to GIT1 protein via GIT1 paxillin binding domain located at the carboxylic terminus (Zhao et al., 2000). The latter interaction is suggested to play a role in maintaining GIT1 localization at the focal adhesion complexes. Until now, the ankyrin repeat domain of GIT1 appears to mediate the binding to the endosomes.

Furthermore, many protein functions are regulated by phosphorylation (Cohen, 2002). GIT1 is shown to be phosphorylated by Src kinase and focal adhesion kinase (FAK) and the overexpression of these proteins enhances GIT1 protein phosphorylation (Bagrodia et al., 1999). Indeed, GIT1 protein was shown to participate in many cellular processes and any alteration in GIT1 protein function may lead to various disorders and diseases including cancer (Chang et al., 2015). Moreover, GIT1 gene has been suggested to be involved in attention deficit hyperactivity disorder (ADHD) (Won et al., 2011) and was also mentioned to associate with Huntington's disease (HD) (Goehler et al., 2004). However, the role of GIT1 in platelets

biology is still not well defined and there are no known diseases related to GIT1 protein in the platelets.

TRPC6 channel modulation by GIT1 protein

TRPC6 protein has been described to interact with proteins which play an important role in the vesicle trafficking like MxA in HEK293 cells (Lussier et al., 2005) and RhoA (Tian et al., 2010). Along these lines, I could identify GIT1 protein as an interaction partner of the TRPC6 protein and confirm the mass spectrometric results by co-immunoprecipitation followed by Western blot analysis in the human platelets (Figure 3-2 F). Thus, I investigated how GIT1 protein binds and modulates the function of the TRPC6 channel. For this aim, I used a simple system, HEK293 cells stably expressing the *Trpc6* cDNA. Before starting to use this cell line, I confirmed the expression, localization and function of both proteins in this cell line. Using a specific antibody against the mouse sequence of TRPC6 and an anti-GIT1 antibody, TRPC6 and GIT1 proteins were detectable at 106 and 85 kDa, respectively in this cell line (Figure 3-4 A, Figure 3-5 A). In contrast to the TRPC6 protein, which was not detected by Western blot in the non-transfected HEK293 cell lysate (Figure 3-4 A), GIT1 protein band was observed in the non-transfected HEK293 cell lysate, which indicates the endogenous expression of GIT1 protein in HEK293 cells (Figure 3-5 A). To investigate TRPC6 localization, I co-transfected HEK293 cells with *Trpc6* fused to GFP and TMEM16A (Ca²⁺ activated Cl⁻ channel) fused to RFP as a plasma membrane marker. Based on the fluorescent confocal images taken from HEK293 cells, TRPC6 protein was found to colocalize with the TMEM16A (Ca²⁺ activated Cl⁻ channel) mainly at the plasma membrane (Figure 3-4 B). In contrast, confocal images from HEK293 cells expressing *Git1* fused to GFP and TMEM16A fused to RFP cDNAs showed that GIT1 protein does not colocalized with the TMEM16A at the plasma membrane and is mostly localized in the cytoplasm (Figure 3-5 B). The latter finding was further confirmed by immunofluorescence imaging in human platelets stained with the anti-TRPC6 and anti-GIT1

antibodies. In agreement with the live cell imaging results in the heterogeneous system, the TRPC6 protein was mainly located at the plasma membrane whereas GIT1 show a diffuse cytoplasmic localization (Figure 3-5 C).

Diacylglycerol (DAG) or its membrane permeable analogue 1-oleoyl-2-acetyl-sn-glycerol (OAG) were shown to activate TRPC6 channel and the use of DAG lipase inhibitor (RHC80267) resulted in elevation of the TRPC6 activity (Hofmann et al., 1999). The OAG does not activate only TRPC6, but also the closely related members TRPC3/7 can be activated by this compound as well. Nevertheless, OAG is still the most common compound used as an activator to study TRPC3/6/7 channels activity in different cellular systems (Hofmann et al., 1999; Zhang and Trebak, 2014). Here I used OAG as an agonist to investigate the TRPC6 channel activity in HEK293 cells. In addition to its function as an agonist for the TRPC 3/6/7, OAG induces calcium release from intracellular stores (Smani et al., 2008). To exclude any contribution of calcium release in response to OAG, HEK293 cells were first treated in the presence of extracellular calcium by the reversible sarco/endoplasmic reticulum Ca^{2+} ATPase (SERCA) inhibitor; cyclopiazonic acid (CPA), which is believed to reduce the affinity of the SERCA pump for ATP binding (Ma et al., 1999). After stores depletion by cyclopiazonic acid (CPA), I could activate TRPC6 channel by OAG, which induces calcium influx from the extracellular space (Figure 3-4 C). In addition, the whole-cell patch clamp recording in HEK293 cells stably expressing *Trpc6* cDNA, OAG application results in a typical double rectifying TRPC6 current in the current-voltage relationships (IV) (Figure 3-4 D, E). In HEK293 cells stably expressing *Trpc6* cDNA and transfected with *Git1*-IGFP cDNA, a significant reduction in the calcium signal was observed in response to the OAG in comparison with the control IGFP transfected cells (Figure 3-6 A, B). Store depletion by CPA prior to OAG application was slightly reduced in GIT1 transfected cells compared with control cells. This could be in part explained by the inhibitory effect applied by GIT1 protein on the Inositol trisphosphate receptor (IP3R), which leads to decreased IP3-gated calcium release and this might contribute to the

passive calcium release in these cells (Zhang et al., 2009). Consistent with the calcium imaging results, the whole-cell membrane current recordings showed that OAG application developed a current, which reached a maximum level within 150 second and eventually declined slowly over time. Furthermore, OAG-induced TRPC6 currents was significantly inhibited in cells overexpressing *Git1*-IGFP cDNA (Figure 3-6 C, D, E). In sum, these results indicate that GIT1 protein modules the TRPC6 channel function and significantly reduce the OAG-induced TRPC6-dependent calcium entry and current.

It has been admitted that TRPC6 carries a calmodulin/IP3R binding site on its carboxylic terminus (Boulay et al., 1999). Because the IP3R was identified in the mass spectrometry results as a part of the TRPC6 complex to bind to the TRPC6 channel (Boulay et al., 1999) and to GIT1 protein (Zhang et al., 2009), I co-expressed these three proteins to see if the inhibitory effect of GIT1 protein on the TRPC6 channel would depend on the presence of the IP3R. Calcium-imaging recordings in the HEK293 cells show that this is not the case (Figure 3-8).

Migration

GIT1 is a multifunction protein and many findings have pointed that GIT1 protein accelerates cell migration (Totaro et al., 2014) and may thereby involve in cancer progression (Yoo et al., 2012). Therefore, we asked whether GIT1 protein would also play a role in cell migration in the presence of the TRPC6 protein. So far, our results unveil that TRPC6 expressing cells showed a higher migration rate compared with control cells (Figure 3-7 G) suggesting the involvement of TRPC6 protein in the cell migration as previously described by (Bernaldo de Quiros et al., 2013; Jardin et al., 2018). The TRPC6 has been also proposed as a possible gene target to reduce the migratory capacity of some cancer cells (Bernaldo de Quiros et al., 2013). Furthermore, several studies reported that TRPC6-induced cell migration is mediated *via* an increase in the intracellular calcium level combined with activation of the calcineurin-nuclear

factor of activated T-cell (NFAT) pathway, which in turn leads to an increase in the *Trpc6* gene expression level (Chigurupati et al., 2010).

Surprisingly, even though TRPC6 and GIT1 proteins were suggested to accelerate cell migration, GIT1 protein did not increase cell migration when TRPC6 channel was present. In contrast, the overexpression of *Git1*-IGFP cDNA in HEK-TRPC6 cells results in a significant inhibition of the cell migration compared with IGFP control (Figure 3-7 A, B, C, D). Taken together, in this cell system which expresses the TRPC6 channel, GIT1 protein inhibits calcium influx through this channel, which in turn results in a reduction of the cell motility. Thus far, we hypothesized the existence of a fine-tuning effect, which modulates TRPC6 channel function in the presence of GIT1 protein. Moreover, to test whether the observed effect is mainly due to cell migration and not to cell proliferation, HEK-TRPC6 cells were cultured in a serum free media containing 1% of fetal calf serum for twenty-four hours (Figure 3-7 C, D). Under these conditions, the cell proliferation should be sufficiently inhibited, which allow us to observe the scratch closure independently of cell proliferation. Indeed, our data confirmed that GIT1 protein inhibits the cell migration of HEK293 cells stably expressing *Trpc6* cDNA independent of the cell proliferation effect.

Molecular binding domain

One of the common TRPC channels features is their activation or regulation downstream phospholipase C (PLC) pathway (Rohacs, 2013). This activation can be translated into calcium signals which control further cellular functions (Freichel et al., 2005). On the other hand, several studies suggested that the function of many TRPC channels can be modulated by several interacting proteins (Eder et al., 2007). For the TRPC6 channel, many molecular domains on the N- and C- terminal tails of the TRPC6 protein appeared to be potential binding sites for other regulatory proteins (Boulay et al., 1999; Lussier et al., 2005). In order to investigate further the TRPC6 and GIT1 interaction, the molecular domains responsible for this

binding were mapped by conducting *in vitro* pull-down assays. Many reports illustrated that GIT1 interaction with other signaling molecules is mediated through different domains, which consist of an N-terminal ARF-GAP domain, three ankyrin repeats (ANK), a Spa2 homology domain (SHD) and a paxillin-binding domain at the carboxylic terminus (Manabe et al., 2002). Different fragments of GIT1 protein were fused to glutathione S-transferase (GST) (Figure 3-9 A) followed by incubation with the full length of TRPC6 to test the binding ability of GIT1 fragments towards TRPC6 protein. The ankyrin repeat domain was identified as the TRPC6 binding site on GIT1 protein (Figure 3-9 B). Notably, each fragment of GIT1 containing the ankyrin repeat domain bound the TRPC6 protein although with different affinities. The differences in GIT1 fragments length as well as the amino acids sequence heterogeneity could both interfere with TRPC6 binding and therefore cause the different amounts of TRPC6 to be bound. In conclusion, the ankyrin repeat domain of GIT1 protein containing three ankyrin repeats, 130-244 aa is essential for TRPC6 binding (Figure 3-9 B, C).

To better understand how the TRPC6 and GIT1 proteins are associating and forming together a complex, I focused on the potential TRPC6 binding sites, which are located intracellularly. The TRPC6 N- and C- terminals are supposed to provide binding sites for regulatory proteins (Boulay et al., 1999; Lussier et al., 2005; Zhang et al., 2001). Therefore, I tested whether the 1-401 aa of the amino terminus or the 727-930 aa of the carboxyl terminus of TRPC6 protein are essential for GIT1 protein binding by conducting a co-immunoprecipitation assay (Figure 3-10 C, F). While the TRPC6 C- terminus showed no binding to the full length of GIT1 protein, the amino terminus 1-401 aa of TRPC6 was binding to GIT1 protein and vice versa (Figure 3-10 C, F). Furthermore, we speculated that GIT1 protein binds to either one or multiple domains located at the amino terminus of TRPC6 protein, which is composed of an ankyrin repeat domain and a coiled coil domain. Both structures are widely present in many proteins and are suggested to be involved in different biological function such as controlling gene expression and mediating protein-protein interactions (Barbara et al., 2007; Gorina and Pavletich, 1996). The ankyrin repeat domain is a 33 residue, which was first discovered in

yeast and *Drosophila* (Breedon and Nasmyth, 1987) and it consists of two alpha helices connected by loops. The coiled coil domain is a protein structure, which consists usually of repeated, hydrophobic and charged amino acids organized in 2-7 alpha helices (Liu et al., 2006). To decide whether one or both structures of the TRPC6 N- terminus contribute to the TRPC6-GIT1 interaction, two fragments from TRPC6 N- terminus were employed to conduct *in vitro* pull-down assays (Figure 3-11 A, B). In this assay each of the two different fragments of the TRPC6 N- terminus, 1-249 aa and 247-401 aa were incubated with the ankyrin repeat domain of GIT1 protein 130-244 aa. Only the first 249 aa of TRPC6, containing the four ankyrin repeats, are essential for the binding with GIT1 protein (Figure 3-11 C, D).

Inhibition of the endogenous GIT1

The GIT1 protein is endogenously present in cell lysate from HEK293 stably expressing *Trpc6* cDNA, which suggests the possibility of a basic and endogenous inhibitory effect of GIT1 on TRPC6 channel function (Figure 3-5 A). To investigate further this hypothesis, I employed the biochemical finding described above and in (Figure 3-10). Since GIT1 protein is present endogenously in the HEK293 cells stably expressing *Trpc6* cDNA, these cells were transfected with the TRPC6 N- terminus 1-401 aa in order to bind and deplete the endogenous GIT1 protein. Depletion of GIT1 by this process should rescue TRPC6 channel activity. As expected, the overexpression of TRPC6 N- terminus leads to endogenous GIT1 depletion and subsequently rescues TRPC6 channel function as demonstrated by patch clamp recordings (Figure 3-12 A, B, C) and the *in vitro* scratch migration assay (Figure 3-12 D).

Plasma membrane localization of TRPC6 protein

The plasma membrane location of the TRPC6 channel is required to record TRPC6 currents from the plasma membrane. However, it is still unclear by which mechanism the TRPC6 channel is translocated to the plasma membrane. In HEK293 cells overexpressing TRPC6, it

is suggested that TRPC6 is localized to the plasma membrane by an exocytotic mechanism (Cayouette et al., 2004). Several proteins were found to modulate TRPC6 channel function by facilitating its translocation to the plasma membrane (Chaudhuri et al., 2016; Monet et al., 2012). In order to investigate how GIT1 protein suppresses the TRPC6 channel activity, we hypothesized that GIT1 protein either inhibits the TRPC6 channel translocation to the plasma membrane or it acts directly on the channel at the plasma membrane and constrains its function.

Therefore, the expression levels of TRPC6 protein at the plasma membrane were evaluated in the presence and absence of GIT1 protein. However, the TRPC6 fraction located at the plasma membrane in the presence or absence of GIT1 protein was not different, indicating that GIT1 protein is constraining the TRPC6 channel activity by rather a direct binding and inhibition.

Platelet adhesion

Several TRPC channels have been identified in the platelets. TRPC1, 3, 4, 5, 6 proteins are supposed to be expressed in platelets (Brownlow and Sage, 2005; Hassock et al., 2002). The TRPV1 protein (Harper et al., 2009) has been also identified in these non-nucleated cells and suggested to play a role in agonist-induced platelet activation. Several proteomics screenings could identify TRPC6, TRPV2 and TRPM4 specific peptides in protein lysates from human platelets (Lewandrowski et al., 2009). To our knowledge, TRPC6 currents have not been recorded from human platelets. The only currents were recorded from the murine hematopoietic „megakaryocytes”, which are responsible for platelet production (Bunting, 1909). So far, mutations in the TRPC6 channel are linked to a renal disease called focal segmental glomerulosclerosis characterized by a nephrotic syndrome (Reiser et al., 2005; Winn et al., 2005). Patients develop this syndrome have a higher risk of thromboembolic

disorder complication due mainly to the leakage of antithrombin III. It is not known whether the mutant TRPC6 present in the platelets contributes to this phenotype.

Different studies have investigated the function of the TRPC6 in the platelets and its role in the blood hemostasis. One study (Ramanathan et al., 2012) suggested that the role of TRPC6 in regulating murine platelets was not significant in contrast to the latter study conducted by (Paez Espinosa et al., 2019), which proposed that TRPC6 is involved in the regulation of murine platelet function. The different results obtained by these studies could be explained by the differences in the type or intensity of the stimulus used to activate the platelets (Paez Espinosa et al., 2019; Ramanathan et al., 2012). Here, I focused on the TRPC6 protein expression, the identification of binding proteins and the role of the TRPC6 containing complex on platelet function. Platelet activation plays an important role in the blood coagulation process (Heemskerk et al., 2002). In response to vascular damage, platelet adhesion is considered as the first step by which platelets connect to the extracellular matrix with the help of different receptors on their surface. Collagen and fibrinogen have been shown to activate signaling pathways through activation of glycoprotein receptor (GP) VI, which is expressed on the platelet surface (Huang et al., 2019; Mangin et al., 2018). The glycoprotein (GP) VI binds *via* its cytoplasmic tail to the Fc receptor (FcR) γ -chain, which promotes its phosphorylation by the Src family kinases (SFK) Lyn and Fyn upon receptor clustering. The later downstream signaling cascade initiates a PLC γ 2 activation, results in an increase in the intracellular calcium concentrations and thereby activation of integrins and granular secretion (Mangin et al., 2018; Nieswandt and Watson, 2003). In our study, the PLC γ 2 and other proteins like GIT1 were identified as partners of TRPC6 in the human platelets. Since GIT1 protein is involved in cell motility and lamellipodia formation, a platelet adhesion assay was performed on coverslips coated with fibrinogen or collagen. Both fibrinogen and collagen have been shown to signal *via* the glycoprotein (GP) VI cascade, which subsequently stimulates the PLC γ 2 and in turn leads to the generation of diacylglycerol (DAG) resulting in activation of the TRPC6 channel

(Figure 4-1). The number of adherent platelets to the immobilized ligand (fibrinogen/collagen) coated coverslips was increasing over time under control conditions. After platelet treatment with the TRPC6 agonist OAG, the platelet adhesion increases significantly compared with control treated platelets. In contrast, the suppression of TRPC6 channel activity by the TRPC6 antagonist SAR7334 decreases the number of platelets bound to the immobilized fibrinogen/collagen (Figure 3-15 A, B). Since the TRPC6 agonist OAG activates also the closely related TRPC3 and TRPC7 channels, which are described to be expressed in the platelets and their precursor megakaryocyte, respectively (Brownlow and Sage, 2005; Ramanathan and Mannhalter, 2016) it was not possible to exclude totally the contribution of these two OAG-sensitive channels in the observed effect. Therefore, I performed a similar experiment, but this time using murine platelets isolated from mice lacking the *Trpc6* gene. Incubation of the platelets acutely isolated from the wild-type and *Trpc6* knockout mice on the fibrinogen coated coverslips for 15, 30 and 60 min showed similar results to those obtained previously with the human platelets (Figure 3-15 C, D). Deletion of the *Trpc6* gene alters platelet adhesion to fibrinogen *in vitro* and results in a significantly lower number of attached platelets compared with the wild-type cells (Figure 3-15 C, D). Altogether, these data suggest that TRPC6 channel contributes to the early stages of blood hemostasis by modulating the ability of platelets to adhere to the extracellular matrix.

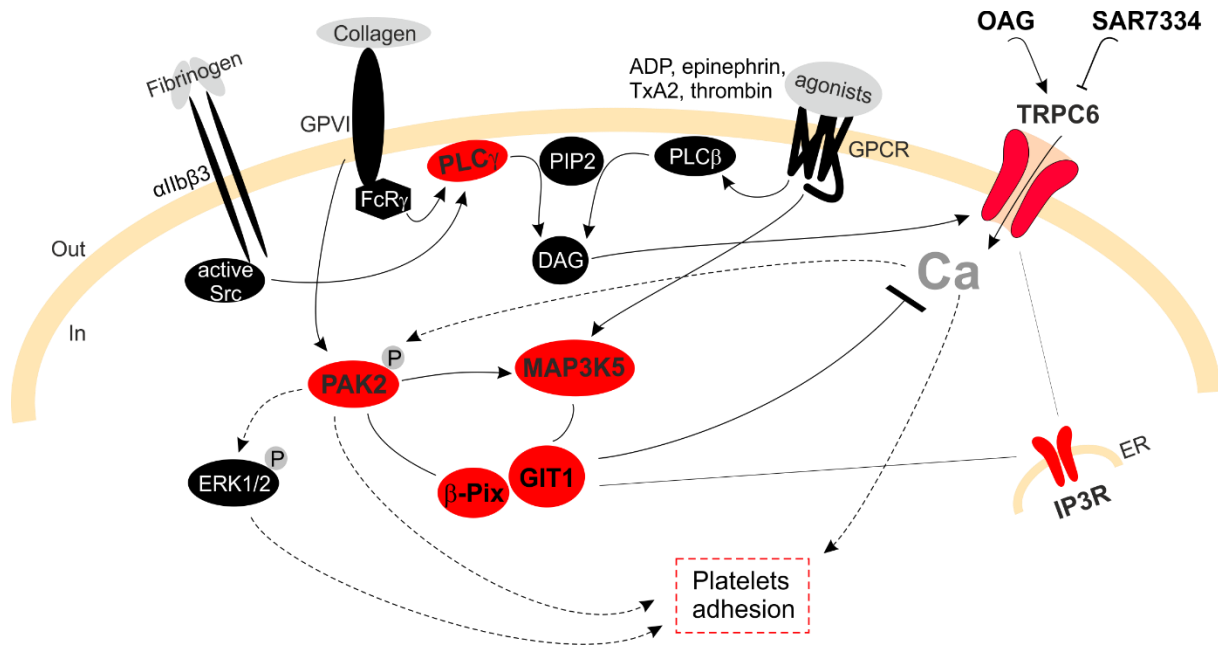


Figure 4-1. Graphical abstract summarizing the TRPC6 associated proteins signaling pathways in the platelet hemostasis

Platelet activation, through collagen and fibrinogen binding to the glycoproteins on the platelets surface, stimulates the hydrolysis of PIP2 by the PLC γ which triggers the release of DAG. The second messenger DAG activates TRPC6 channel resulting in calcium influx in the platelets. Both, platelet adhesion by collagen or fibrinogen, could be enhanced by OAG, the TRPC6 agonist or inhibited by SAR7334, the TRPC6 antagonist applied to the washed platelets. The TRPC6 activation contributes to the phosphorylation of PAK2 and ERK1/2, which together with the intracellular calcium contribute to platelet adhesion. GIT1 protein, which binds β -Pix and modulates IP3Rs, MAP3K5 and PAK2, was identified as a novel TRPC6 channel regulator. GIT1 protein constrains TRPC6 channel activity and therefore may play a role in controlling platelet adhesion. The TRPC6 associated proteins identified by mass spectrometry are highlighted in red.

Platelet activation upon collagen binding by the glycoprotein receptor, which is located on the platelet surface, results in the stimulation of a number of downstream signaling pathways, which activates the phosphorylation of many protein kinases (Vidal et al., 2002). In the human platelets TRPC6-interactome, I identified the p21-activated kinase (PAK2). I investigate the phosphorylation pattern of the PAK2 protein and its downstream substrate MAPK (ERK1/2) kinases upon platelet activation with either OAG or collagen. In Western blot analysis, antibodies against the phosphorylated form of PAK and ERK were used to estimate their levels

of activation, which could also be considered as a readout of platelet activation (Aslan et al., 2013a; Aslan et al., 2013b). Although platelet treatment with both agonists, OAG and collagen, induces phosphorylation of PAK2 and ERK1/2, the phosphorylation kinetics showed differences: Collagen treatment induced PAK2 phosphorylation as a rapid response occurring in less than 5 min (Figure 3-16 A, E) as previously shown by (Aslan et al., 2013a). The phosphorylation of ERK1/2 also increased but reaches saturation only after 15 min of collagen treatment (Figure 3-16 B, F). Different to collagen treatment, OAG treatment triggers slower phosphorylation of PAK2 with a peak after 15 min of stimulation. Furthermore, after OAG treatment, the anti-PAK2 antibody against the phosphorylated fraction recognized additional proteins at 62 and 58 kDa (Figure 3-16 A), which were not visible after collagen treatment. Taken together, these results suggest that both agonists, OAG and collagen, are able to stimulate human platelets and activate the phosphorylation of PAK2 and ERK1/2 protein kinases (Aslan et al., 2013b). However, TRPC6 activation by OAG induces platelet activation and triggers the downstream phosphorylation of PAK2 and ERK1/2 *via* an unknown mechanism, which emerged to be different to that induced by collagen.

5 Conclusion and outlook

By antibody-based affinity enrichment of the TRPC6 containing protein complex followed by quantitative label-free mass spectrometry I identified several proteins to be specifically associated with the TRPC6 protein in human platelets: The G-protein-coupled receptor kinase interacting protein-1 (GIT1) and proteins of the phospholipase C γ , ARHGEFs, MAPK, PAK2 and IP3R pathway. Furthermore, I demonstrated that GIT1 protein, interacts with the TRPC6 channel *via* its ankyrin repeat domain, and constrains its function. My current study provides evidence that the N- terminus of TRPC6 containing the four ankyrin repeats is the molecular domain binding to GIT1 protein and this domain is sufficient to deplete the endogenous GIT1 protein in HEK293 cells.

Since GIT1 protein is one of the major players of cell adhesion, motility and migration, it has been suggested by many studies that GIT1 is promoting cancer progression and metastasis (Chang et al., 2015). Moreover, many evidences have shown that targeting GIT1 by microRNAs could have a beneficial impact on the cancer progression (Chan et al., 2014). Along with these results, the identification of the first 401 aa of the TRPC6 N- terminus, which binds and depletes the endogenous GIT1 protein *in vitro* could be used in further studies as a negative regulator to inhibit cell migration and therefore cancer progression and metastasis, which might have a beneficial impact on the cancer treatment.

As a readout of the platelet activation, the phosphorylation of protein kinases PAK2 and ERK1/2 upon collagen and OAG stimulation was investigated. The TRPC6 channel activation by OAG results in the phosphorylation of both PAK2 and ERK1/2 suggesting the contribution of TRPC6 channel in the platelet activation signaling pathway. Furthermore, the employment of pharmacological agonists and antagonists of the TRPC6 channel may further support our

results and shed light on the molecular mechanism of TRPC6 channel contribution in kinase phosphorylation and platelet activation.

Mutations in the TRPC6 protein are associated with focal segmental glomerulosclerosis, an autosomal dominant form of human kidney disease (Reiser et al., 2005; Winn et al., 2005). It would be very exciting to look at these patients, which present a nephrotic syndrome and have a higher risk of thromboembolic disorders due to the leakage of antithrombin III, whether they have an altered platelets function because of TRPC6 mutation.

In summary, here I provide a novel insight into the role of TRPC6 in the human platelet adhesion process. The results point to the involvement of TRPC6 channel in the early stages of blood hemostasis. Finally, new therapies employing the new discovered TRPC6 modulators (agonist/antagonist) (Bai et al., 2020; Maier et al., 2015) can be used to target TRPC6 channel in the human platelets, which might be beneficial for patients with platelets dysfunction.

6 References

- Aslan, J.E., Baker, S.M., Loren, C.P., Haley, K.M., Itakura, A., Pang, J., Greenberg, D.L., David, L.L., Manser, E., Chernoff, J., *et al.* (2013a). The PAK system links Rho GTPase signaling to thrombin-mediated platelet activation. *Am J Physiol Cell Physiol* 305, C519-528.
- Aslan, J.E., Itakura, A., Haley, K.M., Tormoen, G.W., Loren, C.P., Baker, S.M., Pang, J., Chernoff, J., and McCarty, O.J. (2013b). p21 activated kinase signaling coordinates glycoprotein receptor VI-mediated platelet aggregation, lamellipodia formation, and aggregate stability under shear. *Arterioscler Thromb Vasc Biol* 33, 1544-1551.
- Bagrodia, S., Bailey, D., Lenard, Z., Hart, M., Guan, J.L., Premont, R.T., Taylor, S.J., and Cerione, R.A. (1999). A tyrosine-phosphorylated protein that binds to an important regulatory region on the cool family of p21-activated kinase-binding proteins. *J Biol Chem* 274, 22393-22400.
- Bai, Y., Yu, X., Chen, H., Horne, D., White, R., Wu, X., Lee, P., Gu, Y., Ghimire-Rijal, S., Lin, D.C., *et al.* (2020). Structural basis for pharmacological modulation of the TRPC6 channel. *Elife* 9.
- Barbara, K.E., Willis, K.A., Haley, T.M., Deminoff, S.J., and Santangelo, G.M. (2007). Coiled coil structures and transcription: an analysis of the *S. cerevisiae* coilome. *Mol Genet Genomics* 278, 135-147.
- Bautista, D.M., Siemens, J., Glazer, J.M., Tsuruda, P.R., Basbaum, A.I., Stucky, C.L., Jordt, S.E., and Julius, D. (2007). The menthol receptor TRPM8 is the principal detector of environmental cold. *Nature* 448, 204-208.
- Bernaldo de Quiros, S., Merlo, A., Secades, P., Zambrano, I., de Santa Maria, I.S., Ugidos, N., Jantus-Lewintre, E., Sirera, R., Suarez, C., and Chiara, M.D. (2013). Identification of TRPC6 as a possible candidate target gene within an amplicon at 11q21-q22.2 for migratory capacity in head and neck squamous cell carcinomas. *BMC Cancer* 13, 116.
- Boulay, G., Brown, D.M., Qin, N., Jiang, M., Dietrich, A., Zhu, M.X., Chen, Z., Birnbaumer, M., Mikoshiba, K., and Birnbaumer, L. (1999). Modulation of Ca(2+) entry by polypeptides of the inositol 1,4, 5-trisphosphate receptor (IP3R) that bind transient receptor potential (TRP): evidence for roles of TRP and IP3R in store depletion-activated Ca(2+) entry. *Proc Natl Acad Sci U S A* 96, 14955-14960.
- Boulay, G., Zhu, X., Peyton, M., Jiang, M., Hurst, R., Stefani, E., and Birnbaumer, L. (1997). Cloning and expression of a novel mammalian homolog of *Drosophila* transient receptor potential (Trp) involved in calcium entry secondary to activation of receptors coupled by the Gq class of G protein. *J Biol Chem* 272, 29672-29680.
- Braun, A., Varga-Szabo, D., Kleinschnitz, C., Pleines, I., Bender, M., Austinat, M., Bosl, M., Stoll, G., and Nieswandt, B. (2009). Orai1 (CRACM1) is the platelet SOC channel and essential for pathological thrombus formation. *Blood* 113, 2056-2063.
- Breeden, L., and Nasmyth, K. (1987). Similarity between cell-cycle genes of budding yeast and fission yeast and the Notch gene of *Drosophila*. *Nature* 329, 651-654.

- Brown, S.B., Clarke, M.C., Magowan, L., Sanderson, H., and Savill, J. (2000). Constitutive death of platelets leading to scavenger receptor-mediated phagocytosis. A caspase-independent cell clearance program. *J Biol Chem* 275, 5987-5996.
- Brownlow, S.L., and Sage, S.O. (2005). Transient receptor potential protein subunit assembly and membrane distribution in human platelets. *Thromb Haemost* 94, 839-845.
- Bunting, C.H. (1909). Blood-Platelet and Megalokaryocyte Reactions in the Rabbit. *J Exp Med* 11, 541-552.
- Bye, A.P., Unsworth, A.J., and Gibbins, J.M. (2016). Platelet signaling: a complex interplay between inhibitory and activatory networks. *J Thromb Haemost* 14, 918-930.
- Camacho Londono, J.E., Tian, Q., Hammer, K., Schroder, L., Camacho Londono, J., Reil, J.C., He, T., Oberhofer, M., Mannebach, S., Mathar, I., *et al.* (2015). A background Ca²⁺ entry pathway mediated by TRPC1/TRPC4 is critical for development of pathological cardiac remodelling. *Eur Heart J* 36, 2257-2266.
- Cao, E., Liao, M., Cheng, Y., and Julius, D. (2013). TRPV1 structures in distinct conformations reveal activation mechanisms. *Nature* 504, 113-118.
- Carrillo, C., Hichami, A., Andreoletti, P., Cherkaoui-Malki, M., del Mar Cavia, M., Abdoul-Azize, S., Alonso-Torre, S.R., and Khan, N.A. (2012). Diacylglycerol-containing oleic acid induces increases in [Ca(2+)](i) via TRPC3/6 channels in human T-cells. *Biochim Biophys Acta* 1821, 618-626.
- Caterina, M.J., Schumacher, M.A., Tominaga, M., Rosen, T.A., Levine, J.D., and Julius, D. (1997). The capsaicin receptor: a heat-activated ion channel in the pain pathway. *Nature* 389, 816-824.
- Cayouette, S., Lussier, M.P., Mathieu, E.L., Bousquet, S.M., and Boulay, G. (2004). Exocytotic insertion of TRPC6 channel into the plasma membrane upon Gq protein-coupled receptor activation. *J Biol Chem* 279, 7241-7246.
- Chan, S.H., Huang, W.C., Chang, J.W., Chang, K.J., Kuo, W.H., Wang, M.Y., Lin, K.Y., Uen, Y.H., Hou, M.F., Lin, C.M., *et al.* (2014). MicroRNA-149 targets GIT1 to suppress integrin signaling and breast cancer metastasis. *Oncogene* 33, 4496-4507.
- Chang, J.S., Su, C.Y., Yu, W.H., Lee, W.J., Liu, Y.P., Lai, T.C., Jan, Y.H., Yang, Y.F., Shen, C.N., Shew, J.Y., *et al.* (2015). GIT1 promotes lung cancer cell metastasis through modulating Rac1/Cdc42 activity and is associated with poor prognosis. *Oncotarget* 6, 36278-36291.
- Chaudhuri, P., Rosenbaum, M.A., Sinharoy, P., Damron, D.S., Birnbaumer, L., and Graham, L.M. (2016). Membrane translocation of TRPC6 channels and endothelial migration are regulated by calmodulin and PI3 kinase activation. *Proc Natl Acad Sci U S A* 113, 2110-2115.
- Chen, W., Thielmann, I., Gupta, S., Subramanian, H., Stegner, D., van Kruchten, R., Dietrich, A., Gambaryan, S., Heemskerk, J.W., Hermanns, H.M., *et al.* (2014). Orai1-induced store-operated Ca(2+) entry enhances phospholipase activity and modulates canonical transient receptor potential channel 6 function in murine platelets. *J Thromb Haemost* 12, 528-539.

- Chigurupati, S., Venkataraman, R., Barrera, D., Naganathan, A., Madan, M., Paul, L., Pattisapu, J.V., Kyriazis, G.A., Sugaya, K., Bushnev, S., *et al.* (2010). Receptor channel TRPC6 is a key mediator of Notch-driven glioblastoma growth and invasiveness. *Cancer Res* 70, 418-427.
- Clapham, D.E., Julius, D., Montell, C., and Schultz, G. (2005). International Union of Pharmacology. XLIX. Nomenclature and structure-function relationships of transient receptor potential channels. *Pharmacol Rev* 57, 427-450.
- Clemetson, K.J. (2012). Platelets and primary haemostasis. *Thromb Res* 129, 220-224.
- Cohen, P. (2002). The origins of protein phosphorylation. *Nat Cell Biol* 4, E127-130.
- Coller, B.S. (2011). Historical perspective and future directions in platelet research. *J Thromb Haemost* 9 *Suppl* 1, 374-395.
- Cosens, D.J., and Manning, A. (1969). Abnormal electroretinogram from a *Drosophila* mutant. *Nature* 224, 285-287.
- Coughlin, S.R. (2005). Protease-activated receptors in hemostasis, thrombosis and vascular biology. *J Thromb Haemost* 3, 1800-1814.
- Cusick, M.E., Klitgord, N., Vidal, M., and Hill, D.E. (2005). Interactome: gateway into systems biology. *Hum Mol Genet* 14 *Spec No.* 2, R171-181.
- D'Esposito, M., Strazzullo, M., Cuccurese, M., Spalluto, C., Rocchi, M., D'Urso, M., and Ciccodicola, A. (1998). Identification and assignment of the human transient receptor potential channel 6 gene TRPC6 to chromosome 11q21-->q22. *Cytogenet Cell Genet* 83, 46-47.
- Dietrich, A., and Gudermann, T. (2014). TRPC6: physiological function and pathophysiological relevance. *Handb Exp Pharmacol* 222, 157-188.
- Dietrich, A., Mederos y Schnitzler, M., Emmel, J., Kalwa, H., Hofmann, T., and Gudermann, T. (2003). N-linked protein glycosylation is a major determinant for basal TRPC3 and TRPC6 channel activity. *J Biol Chem* 278, 47842-47852.
- Dietrich, A., Mederos, Y.S.M., Gollasch, M., Gross, V., Storch, U., Dubrovskaja, G., Obst, M., Yildirim, E., Salanova, B., Kalwa, H., *et al.* (2005). Increased vascular smooth muscle contractility in TRPC6^{-/-} mice. *Mol Cell Biol* 25, 6980-6989.
- Eder, P., Schindl, R., Romanin, C., and Groschner, K. (2007). Protein-Protein Interactions in TRPC Channel Complexes. In *TRP Ion Channel Function in Sensory Transduction and Cellular Signaling Cascades*, W.B. Liedtke, and S. Heller, eds. (Boca Raton (FL)).
- Engelke, M., Friedrich, O., Budde, P., Schafer, C., Niemann, U., Zitt, C., Jungling, E., Rocks, O., Luckhoff, A., and Frey, J. (2002). Structural domains required for channel function of the mouse transient receptor potential protein homologue TRP1beta. *FEBS Lett* 523, 193-199.
- Engelmann, B., and Massberg, S. (2013). Thrombosis as an intravascular effector of innate immunity. *Nat Rev Immunol* 13, 34-45.

- Erler, I., Hirnet, D., Wissenbach, U., Flockerzi, V., and Niemeyer, B.A. (2004). Ca²⁺-selective transient receptor potential V channel architecture and function require a specific ankyrin repeat. *J Biol Chem* 279, 34456-34463.
- Farmer, L.K., Rollason, R., Whitcomb, D.J., Ni, L., Goodliff, A., Lay, A.C., Birnbaumer, L., Heesom, K.J., Xu, S.Z., Saleem, M.A., *et al.* (2019). TRPC6 Binds to and Activates Calpain, Independent of Its Channel Activity, and Regulates Podocyte Cytoskeleton, Cell Adhesion, and Motility. *J Am Soc Nephrol* 30, 1910-1924.
- Fecher-Trost, C., Wissenbach, U., Beck, A., Schalkowsky, P., Stoerger, C., Doerr, J., Dembek, A., Simon-Thomas, M., Weber, A., Wollenberg, P., *et al.* (2013a). The in vivo TRPV6 protein starts at a non-AUG triplet, decoded as methionine, upstream of canonical initiation at AUG. *J Biol Chem* 288, 16629-16644.
- Fecher-Trost, C., Wissenbach, U., Beck, A., Schalkowsky, P., Stoerger, C., Doerr, J., Dembek, A., Simon-Thomas, M., Weber, A., Wollenberg, P., *et al.* (2013b). The in vivo TRPV6 protein starts at a non-AUG triplet, decoded as methionine, upstream of canonical initiation at AUG. *J Biol Chem* 288, 16629-16644.
- Finney-Hayward, T.K., Popa, M.O., Bahra, P., Li, S., Poll, C.T., Gosling, M., Nicholson, A.G., Russell, R.E., Kon, O.M., Jarai, G., *et al.* (2010). Expression of transient receptor potential C6 channels in human lung macrophages. *Am J Respir Cell Mol Biol* 43, 296-304.
- Firer, M.A. (2001). Efficient elution of functional proteins in affinity chromatography. *Journal of biochemical and biophysical methods* 49, 433-442.
- Floyd, C.N., and Ferro, A. (2012). The platelet fibrinogen receptor: from megakaryocyte to the mortuary. *JRSM Cardiovasc Dis* 1.
- Foller, M., Kasinathan, R.S., Koka, S., Lang, C., Shumilina, E., Birnbaumer, L., Lang, F., and Huber, S.M. (2008). TRPC6 contributes to the Ca(2+) leak of human erythrocytes. *Cell Physiol Biochem* 21, 183-192.
- Freichel, M., Vennekens, R., Olausson, J., Stolz, S., Philipp, S.E., Weissgerber, P., and Flockerzi, V. (2005). Functional role of TRPC proteins in native systems: implications from knockout and knock-down studies. *J Physiol* 567, 59-66.
- Gaudet, R. (2007). Structural Insights into the Function of TRP Channels. In *TRP Ion Channel Function in Sensory Transduction and Cellular Signaling Cascades*, W.B. Liedtke, and S. Heller, eds. (Boca Raton (FL)).
- Gay, L.J., and Felding-Habermann, B. (2011). Contribution of platelets to tumour metastasis. *Nat Rev Cancer* 11, 123-134.
- Gayle, R.B., 3rd, Maliszewski, C.R., Gimpel, S.D., Schoenborn, M.A., Caspary, R.G., Richards, C., Brasel, K., Price, V., Drosopoulos, J.H., Islam, N., *et al.* (1998). Inhibition of platelet function by recombinant soluble ecto-ADPase/CD39. *J Clin Invest* 101, 1851-1859.
- Gees, M., Colsoul, B., and Nilius, B. (2010). The role of transient receptor potential cation channels in Ca²⁺ signaling. *Cold Spring Harb Perspect Biol* 2, a003962.
- Geraldo, R.B., Sathler, P.C., Lourenco, A.L., Saito, M.S., Cabral, L.M., Rampelotto, P.H., and Castro, H.C. (2014). Platelets: still a therapeutic target for haemostatic disorders. *Int J Mol Sci* 15, 17901-17919.

- Goehler, H., Lalowski, M., Stelzl, U., Waelter, S., Stroedicke, M., Worm, U., Droege, A., Lindenberg, K.S., Knoblich, M., Haenig, C., *et al.* (2004). A protein interaction network links GIT1, an enhancer of huntingtin aggregation, to Huntington's disease. *Mol Cell* 15, 853-865.
- Goel, M., Sinkins, W., Keightley, A., Kinter, M., and Schilling, W.P. (2005). Proteomic analysis of TRPC5- and TRPC6-binding partners reveals interaction with the plasmalemmal Na(+)/K(+)-ATPase. *Pflugers Arch* 451, 87-98.
- Goel, M., Sinkins, W.G., and Schilling, W.P. (2002). Selective association of TRPC channel subunits in rat brain synaptosomes. *J Biol Chem* 277, 48303-48310.
- Golebiewska, E.M., and Poole, A.W. (2015). Platelet secretion: From haemostasis to wound healing and beyond. *Blood Rev* 29, 153-162.
- Gorina, S., and Pavletich, N.P. (1996). Structure of the p53 tumor suppressor bound to the ankyrin and SH3 domains of 53BP2. *Science* 274, 1001-1005.
- Guilbert, A., Dhennin-Duthille, I., Hiani, Y.E., Haren, N., Khorsi, H., Sevestre, H., Ahidouch, A., and Ouadid-Ahidouch, H. (2008). Expression of TRPC6 channels in human epithelial breast cancer cells. *BMC Cancer* 8, 125.
- Haendeler, J., Yin, G., Hojo, Y., Saito, Y., Melaragno, M., Yan, C., Sharma, V.K., Heller, M., Aebersold, R., and Berk, B.C. (2003). GIT1 mediates Src-dependent activation of phospholipase Cgamma by angiotensin II and epidermal growth factor. *J Biol Chem* 278, 49936-49944.
- Hardie, R.C., and Minke, B. (1992). The trp gene is essential for a light-activated Ca²⁺ channel in *Drosophila* photoreceptors. *Neuron* 8, 643-651.
- Harper, A.G., Brownlow, S.L., and Sage, S.O. (2009). A role for TRPV1 in agonist-evoked activation of human platelets. *J Thromb Haemost* 7, 330-338.
- Harper, M.T., Londono, J.E., Quick, K., Londono, J.C., Flockerzi, V., Philipp, S.E., Birnbaumer, L., Freichel, M., and Poole, A.W. (2013). Transient receptor potential channels function as a coincidence signal detector mediating phosphatidylserine exposure. *Sci Signal* 6, ra50.
- Harteneck, C., Klose, C., and Krautwurst, D. (2011). Synthetic modulators of TRP channel activity. *Adv Exp Med Biol* 704, 87-106.
- Hartmann, J., Dragicevic, E., Adelsberger, H., Henning, H.A., Sumser, M., Abramowitz, J., Blum, R., Dietrich, A., Freichel, M., Flockerzi, V., *et al.* (2008). TRPC3 channels are required for synaptic transmission and motor coordination. *Neuron* 59, 392-398.
- Hassock, S.R., Zhu, M.X., Trost, C., Flockerzi, V., and Authi, K.S. (2002). Expression and role of TRPC proteins in human platelets: evidence that TRPC6 forms the store-independent calcium entry channel. *Blood* 100, 2801-2811.
- Heemskerk, J.W., Bevers, E.M., and Lindhout, T. (2002). Platelet activation and blood coagulation. *Thromb Haemost* 88, 186-193.
- Hirnet, D., Olausson, J., Fecher-Trost, C., Boddington, M., Nastainczyk, W., Wissenbach, U., Flockerzi, V., and Freichel, M. (2003). The TRPV6 gene, cDNA and protein. *Cell Calcium* 33, 509-518.

- Hisatsune, C., Kuroda, Y., Nakamura, K., Inoue, T., Nakamura, T., Michikawa, T., Mizutani, A., and Mikoshiba, K. (2004). Regulation of TRPC6 channel activity by tyrosine phosphorylation. *J Biol Chem* 279, 18887-18894.
- Hoefen, R.J., and Berk, B.C. (2006). The multifunctional GIT family of proteins. *J Cell Sci* 119, 1469-1475.
- Hofmann, T., Chubanov, V., Gudermann, T., and Montell, C. (2003). TRPM5 is a voltage-modulated and Ca(2+)-activated monovalent selective cation channel. *Curr Biol* 13, 1153-1158.
- Hofmann, T., Obukhov, A.G., Schaefer, M., Harteneck, C., Gudermann, T., and Schultz, G. (1999). Direct activation of human TRPC6 and TRPC3 channels by diacylglycerol. *Nature* 397, 259-263.
- Hofmann, T., Schaefer, M., Schultz, G., and Gudermann, T. (2002). Subunit composition of mammalian transient receptor potential channels in living cells. *Proc Natl Acad Sci U S A* 99, 7461-7466.
- Hsu, R.M., Tsai, M.H., Hsieh, Y.J., Lyu, P.C., and Yu, J.S. (2010). Identification of MYO18A as a novel interacting partner of the PAK2/betaPIX/GIT1 complex and its potential function in modulating epithelial cell migration. *Mol Biol Cell* 21, 287-301.
- Hsu, Y.J., Hoenderop, J.G., and Bindels, R.J. (2007). TRP channels in kidney disease. *Biochim Biophys Acta* 1772, 928-936.
- Hu, H.Z., Gu, Q., Wang, C., Colton, C.K., Tang, J., Kinoshita-Kawada, M., Lee, L.Y., Wood, J.D., and Zhu, M.X. (2004). 2-aminoethoxydiphenyl borate is a common activator of TRPV1, TRPV2, and TRPV3. *J Biol Chem* 279, 35741-35748.
- Huang, J., Li, X., Shi, X., Zhu, M., Wang, J., Huang, S., Huang, X., Wang, H., Li, L., Deng, H., *et al.* (2019). Platelet integrin alphaIIb beta3: signal transduction, regulation, and its therapeutic targeting. *J Hematol Oncol* 12, 26.
- Huang, Y., Joshi, S., Xiang, B., Kanaho, Y., Li, Z., Bouchard, B.A., Moncman, C.L., and Whiteheart, S.W. (2016). Arf6 controls platelet spreading and clot retraction via integrin alphaIIb beta3 trafficking. *Blood* 127, 1459-1467.
- Huebsch, L.B., and Harker, L.A. (1981). Disorders of platelet function: mechanisms, diagnosis and management. *West J Med* 134, 109-127.
- Inoue, R., Okada, T., Onoue, H., Hara, Y., Shimizu, S., Naitoh, S., Ito, Y., and Mori, Y. (2001). The transient receptor potential protein homologue TRP6 is the essential component of vascular alpha(1)-adrenoceptor-activated Ca(2+)-permeable cation channel. *Circ Res* 88, 325-332.
- Jardin, I., Diez-Bello, R., Lopez, J.J., Redondo, P.C., Salido, G.M., Smani, T., and Rosado, J.A. (2018). TRPC6 Channels Are Required for Proliferation, Migration and Invasion of Breast Cancer Cell Lines by Modulation of Orai1 and Orai3 Surface Exposure. *Cancers (Basel)* 10.
- Jordt, S.E., Bautista, D.M., Chuang, H.H., McKemy, D.D., Zygmunt, P.M., Hogestatt, E.D., Meng, I.D., and Julius, D. (2004). Mustard oils and cannabinoids excite sensory nerve fibres through the TRP channel ANKTM1. *Nature* 427, 260-265.

- Jung, S., Strotmann, R., Schultz, G., and Plant, T.D. (2002). TRPC6 is a candidate channel involved in receptor-stimulated cation currents in A7r5 smooth muscle cells. *Am J Physiol Cell Physiol* 282, C347-359.
- Jurk, K., and Kehrel, B.E. (2005). Platelets: physiology and biochemistry. *Semin Thromb Hemost* 31, 381-392.
- Kim, S., Ko, J., Shin, H., Lee, J.R., Lim, C., Han, J.H., Altrock, W.D., Garner, C.C., Gundelfinger, E.D., Premont, R.T., *et al.* (2003). The GIT family of proteins forms multimers and associates with the presynaptic cytomatrix protein Piccolo. *J Biol Chem* 278, 6291-6300.
- Kol, S., Braun, C., Thiel, G., Doyle, D.A., Sundstrom, M., Gourdon, P., and Nissen, P. (2013). Heterologous expression and purification of an active human TRPV3 ion channel. *FEBS J* 280, 6010-6021.
- Koupenova, M., Kehrel, B.E., Corkrey, H.A., and Freedman, J.E. (2017). Thrombosis and platelets: an update. *Eur Heart J* 38, 785-791.
- Kuwahara, K., Wang, Y., McAnally, J., Richardson, J.A., Bassel-Duby, R., Hill, J.A., and Olson, E.N. (2006). TRPC6 fulfills a calcineurin signaling circuit during pathologic cardiac remodeling. *J Clin Invest* 116, 3114-3126.
- Kwon, Y., Hofmann, T., and Montell, C. (2007). Integration of phosphoinositide- and calmodulin-mediated regulation of TRPC6. *Mol Cell* 25, 491-503.
- Lefrancais, E., Ortiz-Munoz, G., Caudrillier, A., Mallavia, B., Liu, F., Sayah, D.M., Thornton, E.E., Headley, M.B., David, T., Coughlin, S.R., *et al.* (2017). The lung is a site of platelet biogenesis and a reservoir for haematopoietic progenitors. *Nature* 544, 105-109.
- Lessard, C.B., Lussier, M.P., Cayouette, S., Bourque, G., and Boulay, G. (2005). The overexpression of presenilin2 and Alzheimer's-disease-linked presenilin2 variants influences TRPC6-enhanced Ca²⁺ entry into HEK293 cells. *Cell Signal* 17, 437-445.
- Leuner, K., Kazanski, V., Muller, M., Essin, K., Henke, B., Gollasch, M., Harteneck, C., and Muller, W.E. (2007). Hyperforin--a key constituent of St. John's wort specifically activates TRPC6 channels. *FASEB J* 21, 4101-4111.
- Lewandrowski, U., Wortelkamp, S., Lohrig, K., Zahedi, R.P., Wolters, D.A., Walter, U., and Sickmann, A. (2009). Platelet membrane proteomics: a novel repository for functional research. *Blood* 114, e10-19.
- Li, Z., Delaney, M.K., O'Brien, K.A., and Du, X. (2010). Signaling during platelet adhesion and activation. *Arterioscler Thromb Vasc Biol* 30, 2341-2349.
- Liao, M., Cao, E., Julius, D., and Cheng, Y. (2013). Structure of the TRPV1 ion channel determined by electron cryo-microscopy. *Nature* 504, 107-112.
- Lichtenegger, M., Tiapko, O., Svobodova, B., Stockner, T., Glasnov, T.N., Schreibmayer, W., Platzer, D., de la Cruz, G.G., Krenn, S., Schober, R., *et al.* (2018). An optically controlled probe identifies lipid-gating fenestrations within the TRPC3 channel. *Nat Chem Biol* 14, 396-404.
- Lindemann, S., Kramer, B., Seizer, P., and Gawaz, M. (2007). Platelets, inflammation and atherosclerosis. *J Thromb Haemost* 5 Suppl 1, 203-211.

- Liu, C., and Montell, C. (2015). Forcing open TRP channels: Mechanical gating as a unifying activation mechanism. *Biochem Biophys Res Commun* 460, 22-25.
- Liu, J., Zheng, Q., Deng, Y., Cheng, C.S., Kallenbach, N.R., and Lu, M. (2006). A seven-helix coiled coil. *Proc Natl Acad Sci U S A* 103, 15457-15462.
- Lussier, M.P., Cayouette, S., Lepage, P.K., Bernier, C.L., Francoeur, N., St-Hilaire, M., Pinard, M., and Boulay, G. (2005). MxA, a member of the dynamin superfamily, interacts with the ankyrin-like repeat domain of TRPC. *J Biol Chem* 280, 19393-19400.
- Ma, H., Zhong, L., Inesi, G., Fortea, I., Soler, F., and Fernandez-Belda, F. (1999). Overlapping effects of S3 stalk segment mutations on the affinity of Ca²⁺-ATPase (SERCA) for thapsigargin and cyclopiazonic acid. *Biochemistry* 38, 15522-15527.
- Macpherson, L.J., Geierstanger, B.H., Viswanath, V., Bandell, M., Eid, S.R., Hwang, S., and Patapoutian, A. (2005). The pungency of garlic: activation of TRPA1 and TRPV1 in response to allicin. *Curr Biol* 15, 929-934.
- Madej, M.G., and Ziegler, C.M. (2018). Dawning of a new era in TRP channel structural biology by cryo-electron microscopy. *Pflugers Arch* 470, 213-225.
- Mahaut-Smith, M.P. (2012). The unique contribution of ion channels to platelet and megakaryocyte function. *J Thromb Haemost* 10, 1722-1732.
- Maier, T., Follmann, M., Hessler, G., Kleemann, H.W., Hachtel, S., Fuchs, B., Weissmann, N., Linz, W., Schmidt, T., Lohn, M., *et al.* (2015). Discovery and pharmacological characterization of a novel potent inhibitor of diacylglycerol-sensitive TRPC cation channels. *Br J Pharmacol* 172, 3650-3660.
- Manabe, R., Kovalenko, M., Webb, D.J., and Horwitz, A.R. (2002). GIT1 functions in a motile, multi-molecular signaling complex that regulates protrusive activity and cell migration. *J Cell Sci* 115, 1497-1510.
- Mangin, P.H., Onselaer, M.B., Receveur, N., Le Lay, N., Hardy, A.T., Wilson, C., Sanchez, X., Loyau, S., Dupuis, A., Babar, A.K., *et al.* (2018). Immobilized fibrinogen activates human platelets through glycoprotein VI. *Haematologica* 103, 898-907.
- Manser, E., Loo, T.H., Koh, C.G., Zhao, Z.S., Chen, X.Q., Tan, L., Tan, I., Leung, T., and Lim, L. (1998). PAK kinases are directly coupled to the PIX family of nucleotide exchange factors. *Mol Cell* 1, 183-192.
- Matafora, V., Paris, S., Dariozzi, S., and de Curtis, I. (2001). Molecular mechanisms regulating the subcellular localization of p95-APP1 between the endosomal recycling compartment and sites of actin organization at the cell surface. *J Cell Sci* 114, 4509-4520.
- Meseguer, V., Alpizar, Y.A., Luis, E., Tajada, S., Denlinger, B., Fajardo, O., Manenschijn, J.A., Fernandez-Pena, C., Talavera, A., Kichko, T., *et al.* (2014). TRPA1 channels mediate acute neurogenic inflammation and pain produced by bacterial endotoxins. *Nat Commun* 5, 3125.
- Miehe, S., Crause, P., Schmidt, T., Lohn, M., Kleemann, H.W., Licher, T., Dittrich, W., Rutten, H., and Strubing, C. (2012). Inhibition of diacylglycerol-sensitive TRPC channels by synthetic and natural steroids. *PLoS One* 7, e35393.

- Monet, M., Francoeur, N., and Boulay, G. (2012). Involvement of phosphoinositide 3-kinase and PTEN protein in mechanism of activation of TRPC6 protein in vascular smooth muscle cells. *J Biol Chem* 287, 17672-17681.
- Montell, C., and Rubin, G.M. (1989). Molecular characterization of the *Drosophila* trp locus: a putative integral membrane protein required for phototransduction. *Neuron* 2, 1313-1323.
- Mountford, J.K., Petitjean, C., Putra, H.W., McCafferty, J.A., Setiabakti, N.M., Lee, H., Tonnesen, L.L., McFadyen, J.D., Schoenwaelder, S.M., Eckly, A., *et al.* (2015). The class II PI 3-kinase, PI3KC2alpha, links platelet internal membrane structure to shear-dependent adhesive function. *Nat Commun* 6, 6535.
- Muller, C., Morales, P., and Reggio, P.H. (2018). Cannabinoid Ligands Targeting TRP Channels. *Front Mol Neurosci* 11, 487.
- Nieswandt, B., and Watson, S.P. (2003). Platelet-collagen interaction: is GPVI the central receptor? *Blood* 102, 449-461.
- Nilius, B., and Flockerzi, V. (2014). Mammalian transient receptor potential (TRP) cation channels. Preface. *Handb Exp Pharmacol* 223, v - vi.
- Nilius, B., Prenen, J., Droogmans, G., Voets, T., Vennekens, R., Freichel, M., Wissenbach, U., and Flockerzi, V. (2003). Voltage dependence of the Ca²⁺-activated cation channel TRPM4. *J Biol Chem* 278, 30813-30820.
- Nishizuka, Y. (1995). Protein kinase C and lipid signaling for sustained cellular responses. *FASEB J* 9, 484-496.
- Offermanns, S. (2006). Activation of platelet function through G protein-coupled receptors. *Circ Res* 99, 1293-1304.
- Ozaki, Y., Asazuma, N., Suzuki-Inoue, K., and Berndt, M.C. (2005). Platelet GPIb-IX-V-dependent signaling. *J Thromb Haemost* 3, 1745-1751.
- Paez Espinosa, E.V., Lin, O.A., Karim, Z.A., Alshbool, F.Z., and Khasawneh, F.T. (2019). Mouse transient receptor potential channel type 6 selectively regulates agonist-induced platelet function. *Biochem Biophys Res* 20, 100685.
- Paris, S., Longhi, R., Santambrogio, P., and de Curtis, I. (2003). Leucine-zipper-mediated homo- and hetero-dimerization of GIT family p95-ARF GTPase-activating protein, PIX-, paxillin-interacting proteins 1 and 2. *Biochem J* 372, 391-398.
- Park, E.R., Eblen, S.T., and Catling, A.D. (2007). MEK1 activation by PAK: a novel mechanism. *Cell Signal* 19, 1488-1496.
- Pedersen, S.F., Owsianik, G., and Nilius, B. (2005). TRP channels: an overview. *Cell Calcium* 38, 233-252.
- Phelps, C.B., Huang, R.J., Lishko, P.V., Wang, R.R., and Gaudet, R. (2008). Structural analyses of the ankyrin repeat domain of TRPV6 and related TRPV ion channels. *Biochemistry* 47, 2476-2484.
- Philippaert, K., Pironet, A., Mesuere, M., Sones, W., Vermeiren, L., Kerselaers, S., Pinto, S., Segal, A., Antoine, N., Gysemans, C., *et al.* (2017). Steviol glycosides enhance pancreatic beta-cell function and taste sensation by potentiation of TRPM5 channel activity. *Nat Commun* 8, 14733.

- Poenie, M., and Tsien, R. (1986). Fura-2: a powerful new tool for measuring and imaging [Ca²⁺]_i in single cells. *Prog Clin Biol Res* 210, 53-56.
- Premont, R.T., Claing, A., Vitale, N., Freeman, J.L., Pitcher, J.A., Patton, W.A., Moss, J., Vaughan, M., and Lefkowitz, R.J. (1998). beta2-Adrenergic receptor regulation by GIT1, a G protein-coupled receptor kinase-associated ADP ribosylation factor GTPase-activating protein. *Proc Natl Acad Sci U S A* 95, 14082-14087.
- Premont, R.T., Claing, A., Vitale, N., Perry, S.J., and Lefkowitz, R.J. (2000). The GIT family of ADP-ribosylation factor GTPase-activating proteins. Functional diversity of GIT2 through alternative splicing. *J Biol Chem* 275, 22373-22380.
- Premont, R.T., Perry, S.J., Schmalzigaug, R., Roseman, J.T., Xing, Y., and Claing, A. (2004). The GIT/PIX complex: an oligomeric assembly of GIT family ARF GTPase-activating proteins and PIX family Rac1/Cdc42 guanine nucleotide exchange factors. *Cell Signal* 16, 1001-1011.
- Qin, N., Neeper, M.P., Liu, Y., Hutchinson, T.L., Lubin, M.L., and Flores, C.M. (2008). TRPV2 is activated by cannabidiol and mediates CGRP release in cultured rat dorsal root ganglion neurons. *J Neurosci* 28, 6231-6238.
- Ramanathan, G., Gupta, S., Thielmann, I., Pleines, I., Varga-Szabo, D., May, F., Mannhalter, C., Dietrich, A., Nieswandt, B., and Braun, A. (2012). Defective diacylglycerol-induced Ca²⁺ entry but normal agonist-induced activation responses in TRPC6-deficient mouse platelets. *J Thromb Haemost* 10, 419-429.
- Ramanathan, G., and Mannhalter, C. (2016). Increased expression of transient receptor potential canonical 6 (TRPC6) in differentiating human megakaryocytes. *Cell Biol Int* 40, 223-231.
- Reiser, J., Polu, K.R., Moller, C.C., Kenlan, P., Altintas, M.M., Wei, C., Faul, C., Herbert, S., Villegas, I., Avila-Casado, C., *et al.* (2005). TRPC6 is a glomerular slit diaphragm-associated channel required for normal renal function. *Nat Genet* 37, 739-744.
- Riccio, A., Medhurst, A.D., Mattei, C., Kelsell, R.E., Calver, A.R., Randall, A.D., Benham, C.D., and Pangalos, M.N. (2002). mRNA distribution analysis of human TRPC family in CNS and peripheral tissues. *Brain Res Mol Brain Res* 109, 95-104.
- Riehle, M., Buscher, A.K., Gohlke, B.O., Kassmann, M., Kolatsi-Joannou, M., Brasen, J.H., Nagel, M., Becker, J.U., Winyard, P., Hoyer, P.F., *et al.* (2016). TRPC6 G757D Loss-of-Function Mutation Associates with FSGS. *J Am Soc Nephrol* 27, 2771-2783.
- Rohacs, T. (2013). Regulation of transient receptor potential channels by the phospholipase C pathway. *Adv Biol Regul* 53, 341-355.
- Ruggeri, Z.M., and Mendolicchio, G.L. (2007). Adhesion mechanisms in platelet function. *Circ Res* 100, 1673-1685.
- Sadler, J.B., Lamb, C.A., Gould, G.W., and Bryant, N.J. (2016). Iodixanol Gradient Centrifugation to Separate Components of the Low-Density Membrane Fraction from 3T3-L1 Adipocytes. *Cold Spring Harb Protoc* 2016, pdb prot083709.
- Samapati, R., Yang, Y., Yin, J., Stoerger, C., Arenz, C., Dietrich, A., Gudermann, T., Adam, D., Wu, S., Freichel, M., *et al.* (2012). Lung endothelial Ca²⁺ and permeability

- response to platelet-activating factor is mediated by acid sphingomyelinase and transient receptor potential classical 6. *Am J Respir Crit Care Med* 185, 160-170.
- Sato, H., Suzuki-Inoue, K., Inoue, O., and Ozaki, Y. (2008). Regulation of adaptor protein GIT1 in platelets, leading to the interaction between GIT1 and integrin alpha(IIb)beta3. *Biochem Biophys Res Commun* 368, 157-161.
- Schagger, H., and von Jagow, G. (1991). Blue native electrophoresis for isolation of membrane protein complexes in enzymatically active form. *Anal Biochem* 199, 223-231.
- Schindelin, J., Arganda-Carreras, I., Frise, E., Kaynig, V., Longair, M., Pietzsch, T., Preibisch, S., Rueden, C., Saalfeld, S., Schmid, B., *et al.* (2012). Fiji: an open-source platform for biological-image analysis. *Nat Methods* 9, 676-682.
- Schmalzigaug, R., Phee, H., Davidson, C.E., Weiss, A., and Premont, R.T. (2007). Differential expression of the ARF GAP genes GIT1 and GIT2 in mouse tissues. *J Histochem Cytochem* 55, 1039-1048.
- Sell, T.S., Belkacemi, T., Flockerzi, V., and Beck, A. (2014). Protonophore properties of hyperforin are essential for its pharmacological activity. *Sci Rep* 4, 7500.
- Senis, Y.A., Mazharian, A., and Mori, J. (2014). Src family kinases: at the forefront of platelet activation. *Blood* 124, 2013-2024.
- Shi, J., Geshi, N., Takahashi, S., Kiyonaka, S., Ichikawa, J., Hu, Y., Mori, Y., Ito, Y., and Inoue, R. (2013). Molecular determinants for cardiovascular TRPC6 channel regulation by Ca²⁺/calmodulin-dependent kinase II. *J Physiol* 591, 2851-2866.
- Smani, T., Patel, T., and Bolotina, V.M. (2008). Complex regulation of store-operated Ca²⁺ entry pathway by PKC-epsilon in vascular SMCs. *Am J Physiol Cell Physiol* 294, C1499-1508.
- Spassova, M.A., Hewavitharana, T., Xu, W., Soboloff, J., and Gill, D.L. (2006). A common mechanism underlies stretch activation and receptor activation of TRPC6 channels. *Proc Natl Acad Sci U S A* 103, 16586-16591.
- Storch, U., Forst, A.L., Philipp, M., Gudermann, T., and Mederos y Schnitzler, M. (2012). Transient receptor potential channel 1 (TRPC1) reduces calcium permeability in heteromeric channel complexes. *J Biol Chem* 287, 3530-3540.
- Streb, H., Irvine, R.F., Berridge, M.J., and Schulz, I. (1983). Release of Ca²⁺ from a nonmitochondrial intracellular store in pancreatic acinar cells by inositol-1,4,5-trisphosphate. *Nature* 306, 67-69.
- Talvenheimo, J., and Rudnick, G. (1980). Solubilization of the platelet plasma membrane serotonin transporter in an active form. *J Biol Chem* 255, 8606-8611.
- Tang, Q., Guo, W., Zheng, L., Wu, J.X., Liu, M., Zhou, X., Zhang, X., and Chen, L. (2018). Structure of the receptor-activated human TRPC6 and TRPC3 ion channels. *Cell Res* 28, 746-755.
- Tesfai, Y., Brereton, H.M., and Barritt, G.J. (2001). A diacylglycerol-activated Ca²⁺ channel in PC12 cells (an adrenal chromaffin cell line) correlates with expression of the TRP-6 (transient receptor potential) protein. *Biochem J* 358, 717-726.

- Tian, D., Jacobo, S.M., Billing, D., Rozkalne, A., Gage, S.D., Anagnostou, T., Pavenstadt, H., Hsu, H.H., Schlondorff, J., Ramos, A., *et al.* (2010). Antagonistic regulation of actin dynamics and cell motility by TRPC5 and TRPC6 channels. *Sci Signal* 3, ra77.
- Tian, Y., Schreiber, R., and Kunzelmann, K. (2012). Anoctamins are a family of Ca²⁺-activated Cl⁻ channels. *J Cell Sci* 125, 4991-4998.
- Totaro, A., Astro, V., Tonoli, D., and de Curtis, I. (2014). Identification of two tyrosine residues required for the intramolecular mechanism implicated in GIT1 activation. *PLoS One* 9, e93199.
- Tsvilovskyy, V.V., Zholos, A.V., Aberle, T., Philipp, S.E., Dietrich, A., Zhu, M.X., Birnbaumer, L., Freichel, M., and Flockerzi, V. (2009). Deletion of TRPC4 and TRPC6 in mice impairs smooth muscle contraction and intestinal motility in vivo. *Gastroenterology* 137, 1415-1424.
- Varga-Szabo, D., Braun, A., and Nieswandt, B. (2009). Calcium signaling in platelets. *J Thromb Haemost* 7, 1057-1066.
- Vemana, H.P., Karim, Z.A., Conlon, C., and Khasawneh, F.T. (2015). A critical role for the transient receptor potential channel type 6 in human platelet activation. *PLoS One* 10, e0125764.
- Venkatachalam, K., and Montell, C. (2007). TRP channels. *Annu Rev Biochem* 76, 387-417.
- Vidal, C., Geny, B., Melle, J., Jandrot-Perrus, M., and Fontenay-Roupie, M. (2002). Cdc42/Rac1-dependent activation of the p21-activated kinase (PAK) regulates human platelet lamellipodia spreading: implication of the cortical-actin binding protein cortactin. *Blood* 100, 4462-4469.
- Voets, T., Droogmans, G., Wissenbach, U., Janssens, A., Flockerzi, V., and Nilius, B. (2004). The principle of temperature-dependent gating in cold- and heat-sensitive TRP channels. *Nature* 430, 748-754.
- Weissmann, N., Dietrich, A., Fuchs, B., Kalwa, H., Ay, M., Dumitrascu, R., Olschewski, A., Storch, U., Mederos y Schnitzler, M., Ghofrani, H.A., *et al.* (2006). Classical transient receptor potential channel 6 (TRPC6) is essential for hypoxic pulmonary vasoconstriction and alveolar gas exchange. *Proc Natl Acad Sci U S A* 103, 19093-19098.
- Weissmann, N., Sydykov, A., Kalwa, H., Storch, U., Fuchs, B., Mederos y Schnitzler, M., Brandes, R.P., Grimminger, F., Meissner, M., Freichel, M., *et al.* (2012). Activation of TRPC6 channels is essential for lung ischaemia-reperfusion induced oedema in mice. *Nat Commun* 3, 649.
- Welsh, D.G., Morielli, A.D., Nelson, M.T., and Brayden, J.E. (2002). Transient receptor potential channels regulate myogenic tone of resistance arteries. *Circ Res* 90, 248-250.
- Wes, P.D., Chevesich, J., Jeromin, A., Rosenberg, C., Stetten, G., and Montell, C. (1995). TRPC1, a human homolog of a *Drosophila* store-operated channel. *Proc Natl Acad Sci U S A* 92, 9652-9656.

- West, K.A., Zhang, H., Brown, M.C., Nikolopoulos, S.N., Riedy, M.C., Horwitz, A.F., and Turner, C.E. (2001). The LD4 motif of paxillin regulates cell spreading and motility through an interaction with paxillin kinase linker (PKL). *J Cell Biol* 154, 161-176.
- Winn, M.P., Conlon, P.J., Lynn, K.L., Farrington, M.K., Creazzo, T., Hawkins, A.F., Daskalakis, N., Kwan, S.Y., Ebersviller, S., Burchette, J.L., *et al.* (2005). A mutation in the TRPC6 cation channel causes familial focal segmental glomerulosclerosis. *Science* 308, 1801-1804.
- Wissenbach, U., Niemeyer, B.A., Fixemer, T., Schneidewind, A., Trost, C., Cavalié, A., Reus, K., Meese, E., Bonkhoff, H., and Flockerzi, V. (2001). Expression of CaT-like, a novel calcium-selective channel, correlates with the malignancy of prostate cancer. *J Biol Chem* 276, 19461-19468.
- Wittig, I., Braun, H.P., and Schagger, H. (2006). Blue native PAGE. *Nat Protoc* 1, 418-428.
- Won, H., Mah, W., Kim, E., Kim, J.W., Hahm, E.K., Kim, M.H., Cho, S., Kim, J., Jang, H., Cho, S.C., *et al.* (2011). GIT1 is associated with ADHD in humans and ADHD-like behaviors in mice. *Nat Med* 17, 566-572.
- Wu, L.J., Sweet, T.B., and Clapham, D.E. (2010). International Union of Basic and Clinical Pharmacology. LXXVI. Current progress in the mammalian TRP ion channel family. *Pharmacol Rev* 62, 381-404.
- Yin, G., Haendeler, J., Yan, C., and Berk, B.C. (2004). GIT1 functions as a scaffold for MEK1-extracellular signal-regulated kinase 1 and 2 activation by angiotensin II and epidermal growth factor. *Mol Cell Biol* 24, 875-885.
- Yoo, S.M., Antonyak, M.A., and Cerione, R.A. (2012). The adaptor protein and Arf GTPase-activating protein Cat-1/Git-1 is required for cellular transformation. *J Biol Chem* 287, 31462-31470.
- Yu, Y., Fantozzi, I., Remillard, C.V., Landsberg, J.W., Kunichika, N., Platoshyn, O., Tigno, D.D., Thistlethwaite, P.A., Rubin, L.J., and Yuan, J.X. (2004). Enhanced expression of transient receptor potential channels in idiopathic pulmonary arterial hypertension. *Proc Natl Acad Sci U S A* 101, 13861-13866.
- Zhang, L., Ji, T., Wang, Q., Meng, K., Zhang, R., Yang, H., Liao, C., Ma, L., and Jiao, J. (2017). Calcium-Sensing Receptor Stimulation in Cultured Glomerular Podocytes Induces TRPC6-Dependent Calcium Entry and RhoA Activation. *Cell Physiol Biochem* 43, 1777-1789.
- Zhang, S., Hisatsune, C., Matsu-Ura, T., and Mikoshiba, K. (2009). G-protein-coupled receptor kinase-interacting proteins inhibit apoptosis by inositol 1,4,5-triphosphate receptor-mediated Ca²⁺ signal regulation. *J Biol Chem* 284, 29158-29169.
- Zhang, X., Hu, M., Yang, Y., and Xu, H. (2018). Organellar TRP channels. *Nat Struct Mol Biol* 25, 1009-1018.
- Zhang, X., and Trebak, M. (2014). Transient receptor potential canonical 7: a diacylglycerol-activated non-selective cation channel. *Handb Exp Pharmacol* 222, 189-204.
- Zhang, Z., Tang, J., Tikunova, S., Johnson, J.D., Chen, Z., Qin, N., Dietrich, A., Stefani, E., Birnbaumer, L., and Zhu, M.X. (2001). Activation of Trp3 by inositol 1,4,5-

REFERENCES

trisphosphate receptors through displacement of inhibitory calmodulin from a common binding domain. *Proc Natl Acad Sci U S A* 98, 3168-3173.

Zhao, Z.S., Manser, E., Loo, T.H., and Lim, L. (2000). Coupling of PAK-interacting exchange factor PIX to GIT1 promotes focal complex disassembly. *Mol Cell Biol* 20, 6354-6363.

Zhu, X., Chu, P.B., Peyton, M., and Birnbaumer, L. (1995). Molecular cloning of a widely expressed human homologue for the *Drosophila* trp gene. *FEBS Lett* 373, 193-198.

7 Curriculum vitae

"The curriculum vitae was removed from the electronic version of the doctoral thesis for reasons of data protection."

8 Publications

Manuscript in preparation

Bentrcia T, Belkacemi A, Fecher-Trost C, Veit Flockerzi
GIT1 protein modulates TRPC6 channel function in human platelets

Published abstracts

Stoerger, C; Schalkowsky, P; Bentrcia, T; Weissgerber, P; Flockerzi, V
Protein expression profiling of TRPV6 channel proteins in adult mice
Naunyn-Schmiedeberg's Archives of Pharmacology Volume 387, Supplement 1 S94 (2014)
(80th Annual Meeting of the Deutsche Gesellschaft für Experimentelle und Klinische
Pharmakologie und Toxikologie, Hannover, 1-3, April 2014)

Bentrcia T, Flockerzi V
Novel modulator of TRPC6 function in platelets
Naunyn-Schmiedeberg's Archives of Pharmacology Volume 392, Supplement 1 S16 (2019)
(85th Annual Meeting of the Deutsche Gesellschaft für Experimentelle und Klinische
Pharmakologie und Toxikologie, Stuttgart, 25-28, Februar 2019)

Conference abstracts

1. Joint Symposium of the IRTG 1830, September 2-4, 2019, Weiskirchen, Germany
Title of talk: A novel modulator of TRPC6 channel function
2. FASEB Science Research Conference, The Ion Channel Regulation Conference
"Molecules to Disease", July 7-12, 2019, Lisbon, Portugal
Title of poster: A novel modulator of TRPC6 function
3. Fourth German Pharm-Tox Summit-85th Annual Meeting of the German Society for
Experimental and Clinical Pharmacology and Toxicology (DGPT) and 21st Annual Meeting
of the Association of the Clinical Pharmacology (VKliPha), February 25-28, 2019, Stuttgart,
Germany
Title of talk: Novel modulator of TRPC6 function in platelets
4. Trainee Retreat and 5th Colloquium of the IRTG 1830, April 1-3, 2019, Trippstadt,
Germany
Title of talk/poster: Novel modulator of TRPC6 function in platelets
5. Fourth Colloquium of the IRTG 1830, August 13-14, 2018, Nonnweiler, Germany
Title of talk/poster: Novel modulator of TRPC6 function
6. Sixth Joint Symposium of the IRTG 1830, August 28-31, 2017, Annweiler, Germany
Title of poster: TRPC6 function – continuation
7. Fourth Joint Symposium of the IRTG, September 14-16, 2015, Bad Dürkheim, Germany
Title of poster: Identification and characterization of the TRPC6 Protein

8. Network Meeting of the IRTG 1830 and TRAM-MGK, March 16-17, 2015, Kaiserslautern, Germany

Title of talk/poster: Identification and characterization of the TRPV6/TRPC6 proteins

9 Supplementary data

Accession	Description	Coverage exp1 (1263)	Coverage exp1 (rblgG)	Coverage exp2 (1263)	Coverage exp2 (rblgG)
P31946	14-3-3 protein beta/alpha OS=Homo sapiens GN=YWHAB PE=1 SV=3 - [1433B_HUMAN]			40,65	65,85
P62258	14-3-3 protein epsilon OS=Homo sapiens GN=YWHAE PE=1 SV=1 - [1433E_HUMAN]			60,78	70,98
Q04917	14-3-3 protein eta OS=Homo sapiens GN=YWHAH PE=1 SV=4 - [1433F_HUMAN]			46,34	69,92
P61981	14-3-3 protein gamma OS=Homo sapiens GN=YWHAG PE=1 SV=2 - [1433G_HUMAN]	30,77		41,30	68,83
P27348	14-3-3 protein theta OS=Homo sapiens GN=YWHAQ PE=1 SV=1 - [1433T_HUMAN]	9,39		33,06	65,31
P63104	14-3-3 protein zeta/delta OS=Homo sapiens GN=YWHAZ PE=1 SV=1 - [1433Z_HUMAN]	64,08	9,39	54,69	68,98
Q99943	1-acyl-sn-glycerol-3-phosphate acyltransferase alpha OS=Homo sapiens GN=AGPAT1 PE=2 SV=2 - [PLCA_HUMAN]				10,60
P16885	1-phosphatidylinositol 4,5-bisphosphate phosphodiesterase gamma-2 OS=Homo sapiens GN=PLCG2 PE=1 SV=4 - [PLCG2_HUMAN]	12,73		12,81	
Q16698	2,4-dienoyl-CoA reductase, mitochondrial OS=Homo sapiens GN=DECR1 PE=1 SV=1 - [DECR_HUMAN]				22,99
O75832	26S proteasome non-ATPase regulatory subunit 10 OS=Homo sapiens OX=9606 GN=PSMD10 PE=1 SV=1 - [PSD10_HUMAN]				13,72
O00231	26S proteasome non-ATPase regulatory subunit 11 OS=Homo sapiens OX=9606 GN=PSMD11 PE=1 SV=3 - [PSD11_HUMAN]				5,69
Q9UNM6	26S proteasome non-ATPase regulatory subunit 13 OS=Homo sapiens OX=9606 GN=PSMD13 PE=1 SV=2 - [PSD13_HUMAN]				7,71
O00487	26S proteasome non-ATPase regulatory subunit 14 OS=Homo sapiens OX=9606 GN=PSMD14 PE=1 SV=1 - [PSDE_HUMAN]				11,29
Q13200	26S proteasome non-ATPase regulatory subunit 2 OS=Homo sapiens GN=PSMD2 PE=1 SV=3 - [PSMD2_HUMAN]				8,59
Q15008	26S proteasome non-ATPase regulatory subunit 6 OS=Homo sapiens OX=9606 GN=PSMD6 PE=1 SV=1 - [PSMD6_HUMAN]				5,40
P51665	26S proteasome non-ATPase regulatory subunit 7 OS=Homo sapiens GN=PSMD7 PE=1 SV=2 - [PSD7_HUMAN]				5,25
P35998	26S proteasome regulatory subunit 7 OS=Homo sapiens OX=9606 GN=PSMC2 PE=1 SV=3 - [PRS7_HUMAN]				4,39

SUPPLEMENTARY DATA AND INFORMATION

Accession	Description	Coverage exp1 (1263)	Coverage exp1 (rblgG)	Coverage exp2 (1263)	Coverage exp2 (rblgG)
Q02218	2-oxoglutarate dehydrogenase, mitochondrial OS=Homo sapiens OX=9606 GN=OGDH PE=1 SV=3 - [ODO1_HUMAN]				2,54
Q99714	3-hydroxyacyl-CoA dehydrogenase type-2 OS=Homo sapiens GN=HSD17B10 PE=1 SV=3 - [HCD2_HUMAN]				43,30
P10809	60 kDa heat shock protein, mitochondrial OS=Homo sapiens GN=HSPD1 PE=1 SV=2 - [CH60_HUMAN]			3,49	18,50
Q01813	6-phosphofructokinase type C OS=Homo sapiens GN=PFKP PE=1 SV=2 - [K6PP_HUMAN]			8,16	30,23
P17858	6-phosphofructokinase, liver type OS=Homo sapiens GN=PFKL PE=1 SV=6 - [K6PL_HUMAN]				11,03
P52209	6-phosphogluconate dehydrogenase, decarboxylating OS=Homo sapiens GN=PGD PE=1 SV=3 - [6PGD_HUMAN]			12,01	10,77
P11021	78 kDa glucose-regulated protein OS=Homo sapiens GN=HSPA5 PE=1 SV=2 - [GRP78_HUMAN]	12,23		35,32	47,40
O95870	Abhydrolase domain-containing protein 16A OS=Homo sapiens GN=ABHD16A PE=1 SV=3 - [ABHGA_HUMAN]				5,02
Q8IZP0	Abl interactor 1 OS=Homo sapiens GN=ABI1 PE=1 SV=4 - [ABI1_HUMAN]				5,31
P68032	Actin, alpha cardiac muscle 1 OS=Homo sapiens GN=ACTC1 PE=1 SV=1 - [ACTC_HUMAN]				49,60
P60709	Actin, cytoplasmic 1 OS=Homo sapiens GN=ACTB PE=1 SV=1 - [ACTB_HUMAN]	66,13	57,87	68,27	68,27
P63261	Actin, cytoplasmic 2 OS=Homo sapiens GN=ACTG1 PE=1 SV=1 - [ACTG_HUMAN]	66,13		68,27	68,27
P61160	Actin-related protein 2 OS=Homo sapiens GN=ACTR2 PE=1 SV=1 - [ARP2_HUMAN]			21,32	29,44
O15143	Actin-related protein 2/3 complex subunit 1B OS=Homo sapiens GN=ARPC1B PE=1 SV=3 - [ARC1B_HUMAN]			8,33	30,65
O15144	Actin-related protein 2/3 complex subunit 2 OS=Homo sapiens GN=ARPC2 PE=1 SV=1 - [ARPC2_HUMAN]				55,33
O15145	Actin-related protein 2/3 complex subunit 3 OS=Homo sapiens GN=ARPC3 PE=1 SV=3 - [ARPC3_HUMAN]	13,48		23,03	39,89
P59998	Actin-related protein 2/3 complex subunit 4 OS=Homo sapiens GN=ARPC4 PE=1 SV=3 - [ARPC4_HUMAN]				27,98
O15511	Actin-related protein 2/3 complex subunit 5 OS=Homo sapiens GN=ARPC5 PE=1 SV=3 - [ARPC5_HUMAN]				66,89
P61158	Actin-related protein 3 OS=Homo sapiens GN=ACTR3 PE=1 SV=3 - [ARP3_HUMAN]			31,34	53,83
P13798	Acylamino-acid-releasing enzyme OS=Homo sapiens GN=APEH PE=1 SV=4 - [ACPH_HUMAN]				13,11

SUPPLEMENTARY DATA AND INFORMATION

Accession	Description	Coverage exp1 (1263)	Coverage exp1 (rblgG)	Coverage exp2 (1263)	Coverage exp2 (rblgG)
P07741	Adenine phosphoribosyltransferase OS=Homo sapiens OX=9606 GN=APRT PE=1 SV=2 - [APT_HUMAN]				12,78
Q01518	Adenylyl cyclase-associated protein 1 OS=Homo sapiens GN=CAP1 PE=1 SV=5 - [CAP1_HUMAN]	8,84		23,37	54,32
P05141	ADP/ATP translocase 2 OS=Homo sapiens GN=SLC25A5 PE=1 SV=7 - [ADT2_HUMAN]				38,93
P12236	ADP/ATP translocase 3 OS=Homo sapiens GN=SLC25A6 PE=1 SV=4 - [ADT3_HUMAN]			11,41	33,89
P61204	ADP-ribosylation factor 3 OS=Homo sapiens GN=ARF3 PE=1 SV=2 - [ARF3_HUMAN]			19,89	35,91
P18085	ADP-ribosylation factor 4 OS=Homo sapiens GN=ARF4 PE=1 SV=3 - [ARF4_HUMAN]				25,56
Q96BM9	ADP-ribosylation factor-like protein 8A OS=Homo sapiens GN=ARL8A PE=1 SV=1 - [ARL8A_HUMAN]				18,28
Q9NVJ2	ADP-ribosylation factor-like protein 8B OS=Homo sapiens GN=ARL8B PE=1 SV=1 - [ARL8B_HUMAN]				17,20
P43652	Afamin OS=Homo sapiens OX=9606 GN=AFM PE=1 SV=1 - [AFAM_HUMAN]	5,51		7,85	24,21
P49588	Alanine--tRNA ligase, cytoplasmic OS=Homo sapiens GN=AARS PE=1 SV=2 - [SYAC_HUMAN]				5,68
Q8IZ83	Aldehyde dehydrogenase family 16 member A1 OS=Homo sapiens GN=ALDH16A1 PE=1 SV=2 - [A16A1_HUMAN]				8,60
P02763	Alpha-1-acid glycoprotein 1 OS=Homo sapiens GN=ORM1 PE=1 SV=1 - [A1AG1_HUMAN]			25,87	19,90
P19652	Alpha-1-acid glycoprotein 2 OS=Homo sapiens GN=ORM2 PE=1 SV=2 - [A1AG2_HUMAN]				26,37
P01011	Alpha-1-antichymotrypsin OS=Homo sapiens GN=SERPINA3 PE=1 SV=2 - [AACT_HUMAN]	6,86			22,22
P01009	Alpha-1-antitrypsin OS=Homo sapiens GN=SERPINA1 PE=1 SV=3 - [A1AT_HUMAN]	22,97	22,25	37,32	50,72
P04217	Alpha-1B-glycoprotein OS=Homo sapiens GN=A1BG PE=1 SV=4 - [A1BG_HUMAN]			15,96	23,23
P02765	Alpha-2-HS-glycoprotein OS=Homo sapiens GN=AHSG PE=1 SV=1 - [FETUA_HUMAN]			8,45	19,89
P01023	Alpha-2-macroglobulin OS=Homo sapiens GN=A2M PE=1 SV=3 - [A2MG_HUMAN]	33,58	31,82	48,85	62,82
P12814	Alpha-actinin-1 OS=Homo sapiens GN=ACTN1 PE=1 SV=2 - [ACTN1_HUMAN]	36,21	14,69	53,70	73,99
P35609	Alpha-actinin-2 OS=Homo sapiens GN=ACTN2 PE=1 SV=1 - [ACTN2_HUMAN]				19,69
O43707	Alpha-actinin-4 OS=Homo sapiens GN=ACTN4 PE=1 SV=2 - [ACTN4_HUMAN]	12,18		29,97	66,74
P04745	Alpha-amylase 1 OS=Homo sapiens GN=AMY1A PE=1 SV=2 - [AMY1_HUMAN]		16,24		
P61163	Alpha-centractin OS=Homo sapiens GN=ACTR1A PE=1 SV=1 - [ACTZ_HUMAN]			9,57	28,72

SUPPLEMENTARY DATA AND INFORMATION

Accession	Description	Coverage exp1 (1263)	Coverage exp1 (rblgG)	Coverage exp2 (1263)	Coverage exp2 (rblgG)
P06733	Alpha-enolase OS=Homo sapiens GN=ENO1 PE=1 SV=2 - [ENOA_HUMAN]	5,76	14,52	39,63	47,93
P54920	Alpha-soluble NSF attachment protein OS=Homo sapiens GN=NAPA PE=1 SV=3 - [SNAA_HUMAN]				30,51
P27338	Amine oxidase [flavin-containing] B OS=Homo sapiens OX=9606 GN=MAOB PE=1 SV=3 - [AOFB_HUMAN]				5,00
Q01433	AMP deaminase 2 OS=Homo sapiens GN=AMPD2 PE=1 SV=2 - [AMPD2_HUMAN]			3,87	6,83
P05067	Amyloid beta A4 protein OS=Homo sapiens GN=APP PE=1 SV=3 - [A4_HUMAN]				19,74
P01019	Angiotensinogen OS=Homo sapiens GN=AGT PE=1 SV=1 - [ANGT_HUMAN]	5,98			12,16
P07355	Annexin A2 OS=Homo sapiens GN=ANXA2 PE=1 SV=2 - [ANXA2_HUMAN]	7,08	11,80	15,93	
Q4KMQ2	Anoctamin-6 OS=Homo sapiens GN=ANO6 PE=1 SV=2 - [ANO6_HUMAN]				20,44
P01008	Antithrombin-III OS=Homo sapiens GN=SERPINC1 PE=1 SV=1 - [ANT3_HUMAN]			14,22	21,77
Q10567	AP-1 complex subunit beta-1 OS=Homo sapiens GN=AP1B1 PE=1 SV=2 - [AP1B1_HUMAN]				10,43
O43747	AP-1 complex subunit gamma-1 OS=Homo sapiens OX=9606 GN=AP1G1 PE=1 SV=5 - [AP1G1_HUMAN]				8,03
Q9BXS5	AP-1 complex subunit mu-1 OS=Homo sapiens OX=9606 GN=AP1M1 PE=1 SV=3 - [AP1M1_HUMAN]			8,04	26,48
P61966	AP-1 complex subunit sigma-1A OS=Homo sapiens OX=9606 GN=AP1S1 PE=1 SV=1 - [AP1S1_HUMAN]				25,32
O95782	AP-2 complex subunit alpha-1 OS=Homo sapiens OX=9606 GN=AP2A1 PE=1 SV=3 - [AP2A1_HUMAN]	5,94			
P63010	AP-2 complex subunit beta OS=Homo sapiens GN=AP2B1 PE=1 SV=1 - [AP2B1_HUMAN]	2,45		4,70	9,28
P53680	AP-2 complex subunit sigma OS=Homo sapiens OX=9606 GN=AP2S1 PE=1 SV=2 - [AP2S1_HUMAN]				17,61
P02647	Apolipoprotein A-I OS=Homo sapiens GN=APOA1 PE=1 SV=1 - [APOA1_HUMAN]	53,56	28,46	67,42	78,28
P02652	Apolipoprotein A-II OS=Homo sapiens GN=APOA2 PE=1 SV=1 - [APOA2_HUMAN]				11,00
P06727	Apolipoprotein A-IV OS=Homo sapiens GN=APOA4 PE=1 SV=3 - [APOA4_HUMAN]			28,54	54,55
P04114	Apolipoprotein B-100 OS=Homo sapiens GN=APOB PE=1 SV=2 - [APOB_HUMAN]			4,23	22,27
P05090	Apolipoprotein D OS=Homo sapiens GN=APOD PE=1 SV=1 - [APOD_HUMAN]			22,75	34,39
P02649	Apolipoprotein E OS=Homo sapiens GN=APOE PE=1 SV=1 - [APOE_HUMAN]			19,56	45,11

SUPPLEMENTARY DATA AND INFORMATION

Accession	Description	Coverage exp1 (1263)	Coverage exp1 (rblgG)	Coverage exp2 (1263)	Coverage exp2 (rblgG)
O95445	Apolipoprotein M OS=Homo sapiens GN=APOM PE=1 SV=2 - [APOM_HUMAN]				23,94
Q07812	Apoptosis regulator BAX OS=Homo sapiens OX=9606 GN=BAX PE=1 SV=1 - [BAX_HUMAN]				38,02
O95831	Apoptosis-inducing factor 1, mitochondrial OS=Homo sapiens OX=9606 GN=AIFM1 PE=1 SV=1 - [AIFM1_HUMAN]	5,87		3,92	
P18054	Arachidonate 12-lipoxygenase, 12S-type OS=Homo sapiens GN=ALOX12 PE=1 SV=4 - [LOX12_HUMAN]	8,30		13,42	23,68
Q9Y2X7	ARF GTPase-activating protein GIT1 OS=Homo sapiens OX=9606 GN=GIT1 PE=1 SV=2 - [GIT1_HUMAN]	19,71		49,54	
Q14161	ARF GTPase-activating protein GIT2 OS=Homo sapiens GN=GIT2 PE=1 SV=2 - [GIT2_HUMAN]			12,25	
P05089	Arginase-1 OS=Homo sapiens GN=ARG1 PE=1 SV=2 - [ARG1_HUMAN]		5,90	15,84	
Q6DD88	Atlantin-3 OS=Homo sapiens GN=ATL3 PE=1 SV=1 - [ATLA3_HUMAN]				5,36
P25705	ATP synthase subunit alpha, mitochondrial OS=Homo sapiens GN=ATP5A1 PE=1 SV=1 - [ATPA_HUMAN]			25,32	45,57
P24539	ATP synthase subunit b, mitochondrial OS=Homo sapiens GN=ATP5F1 PE=1 SV=2 - [AT5F1_HUMAN]				34,38
P06576	ATP synthase subunit beta, mitochondrial OS=Homo sapiens GN=ATP5B PE=1 SV=3 - [ATPB_HUMAN]	7,18		20,04	64,84
O75947	ATP synthase subunit d, mitochondrial OS=Homo sapiens GN=ATP5H PE=1 SV=3 - [ATP5H_HUMAN]				78,26
P30049	ATP synthase subunit delta, mitochondrial OS=Homo sapiens GN=ATP5D PE=1 SV=2 - [ATPD_HUMAN]				13,69
P56134	ATP synthase subunit f, mitochondrial OS=Homo sapiens GN=ATP5J2 PE=1 SV=3 - [ATPK_HUMAN]				25,53
O75964	ATP synthase subunit g, mitochondrial OS=Homo sapiens GN=ATP5L PE=1 SV=3 - [ATP5L_HUMAN]				32,04
P36542	ATP synthase subunit gamma, mitochondrial OS=Homo sapiens GN=ATP5C1 PE=1 SV=1 - [ATPG_HUMAN]				41,95
P48047	ATP synthase subunit O, mitochondrial OS=Homo sapiens GN=ATP5O PE=1 SV=1 - [ATPO_HUMAN]				49,77
Q9NVI7	ATPase family AAA domain-containing protein 3A OS=Homo sapiens GN=ATAD3A PE=1 SV=2 - [ATD3A_HUMAN]	26,18		39,12	
P53396	ATP-citrate synthase OS=Homo sapiens GN=ACLY PE=1 SV=3 - [ACLY_HUMAN]				8,63
Q16740	ATP-dependent Clp protease proteolytic subunit, mitochondrial OS=Homo sapiens OX=9606 GN=CLPP PE=1 SV=1 - [CLPP_HUMAN]				11,91

SUPPLEMENTARY DATA AND INFORMATION

Accession	Description	Coverage exp1 (1263)	Coverage exp1 (rblgG)	Coverage exp2 (1263)	Coverage exp2 (rblgG)
O75882	Attractin OS=Homo sapiens OX=9606 GN=ATRN PE=1 SV=2 - [ATRN_HUMAN]				3,15
P02730	Band 3 anion transport protein OS=Homo sapiens GN=SLC4A1 PE=1 SV=3 - [B3AT_HUMAN]				2,41
Q9UHQ4	B-cell receptor-associated protein 29 OS=Homo sapiens GN=BCAP29 PE=1 SV=2 - [BAP29_HUMAN]				20,33
P51572	B-cell receptor-associated protein 31 OS=Homo sapiens GN=BCAP31 PE=1 SV=3 - [BAP31_HUMAN]			7,32	46,75
P02749	Beta-2-glycoprotein 1 OS=Homo sapiens GN=APOH PE=1 SV=3 - [APOH_HUMAN]				31,88
P61769	Beta-2-microglobulin OS=Homo sapiens GN=B2M PE=1 SV=1 - [B2MG_HUMAN]				16,81
Q562R1	Beta-actin-like protein 2 OS=Homo sapiens GN=ACTBL2 PE=1 SV=2 - [ACTBL_HUMAN]			30,05	22,07
Q9HBI1	Beta-parvin OS=Homo sapiens GN=PARVB PE=1 SV=1 - [PARVB_HUMAN]	6,04		22,80	38,46
Q13867	Bleomycin hydrolase OS=Homo sapiens GN=BLMH PE=1 SV=1 - [BLMH_HUMAN]				8,57
Q8WY22	BRI3-binding protein OS=Homo sapiens GN=BRI3BP PE=1 SV=1 - [BRI3B_HUMAN]				9,56
Q9UBW5	Bridging integrator 2 OS=Homo sapiens OX=9606 GN=BIN2 PE=1 SV=3 - [BIN2_HUMAN]				27,79
Q7L273	BTB/POZ domain-containing protein KCTD9 OS=Homo sapiens OX=9606 GN=KCTD9 PE=1 SV=1 - [KCTD9_HUMAN]	22,11			
P04003	C4b-binding protein alpha chain OS=Homo sapiens GN=C4BPA PE=1 SV=2 - [C4BPA_HUMAN]	19,10	24,29	19,93	47,74
O75844	CAAX prenyl protease 1 homolog OS=Homo sapiens OX=9606 GN=ZMPSTE24 PE=1 SV=2 - [FACE1_HUMAN]				7,37
Q99653	Calcineurin B homologous protein 1 OS=Homo sapiens OX=9606 GN=CHP1 PE=1 SV=3 - [CHP1_HUMAN]				10,26
Q96BS2	Calcineurin B homologous protein 3 OS=Homo sapiens OX=9606 GN=TESC PE=1 SV=3 - [CHP3_HUMAN]				20,56
P63098	Calcineurin subunit B type 1 OS=Homo sapiens OX=9606 GN=PPP3R1 PE=1 SV=2 - [CANB1_HUMAN]				23,53
Q8NE86	Calcium uniporter protein, mitochondrial OS=Homo sapiens GN=MCU PE=1 SV=1 - [MCU_HUMAN]				24,22
Q14012	Calcium/calmodulin-dependent protein kinase type 1 OS=Homo sapiens OX=9606 GN=CAMK1 PE=1 SV=1 - [KCC1A_HUMAN]				7,30
Q05682	Caldesmon OS=Homo sapiens GN=CALD1 PE=1 SV=3 - [CALD1_HUMAN]				2,40
P62158	Calmodulin OS=Homo sapiens GN=CALM1 PE=1 SV=2 - [CALM_HUMAN]				44,30

SUPPLEMENTARY DATA AND INFORMATION

Accession	Description	Coverage exp1 (1263)	Coverage exp1 (rblgG)	Coverage exp2 (1263)	Coverage exp2 (rblgG)
Q9NZT1	Calmodulin-like protein 5 OS=Homo sapiens GN=CALML5 PE=1 SV=2 - [CALL5_HUMAN]	41,10	25,34	43,15	
P27824	Calnexin OS=Homo sapiens GN=CANX PE=1 SV=2 - [CALX_HUMAN]			20,44	34,97
P04632	Calpain small subunit 1 OS=Homo sapiens GN=CAPNS1 PE=1 SV=1 - [CPNS1_HUMAN]		14,18		37,69
P07384	Calpain-1 catalytic subunit OS=Homo sapiens GN=CAPN1 PE=1 SV=1 - [CAN1_HUMAN]	10,78	13,31	18,63	53,50
Q99439	Calponin-2 OS=Homo sapiens GN=CNN2 PE=1 SV=4 - [CNN2_HUMAN]				12,62
P27797	Calreticulin OS=Homo sapiens GN=CALR PE=1 SV=1 - [CALR_HUMAN]			24,22	48,92
P22694	cAMP-dependent protein kinase catalytic subunit beta OS=Homo sapiens GN=PRKACB PE=1 SV=2 - [KAPCB_HUMAN]				5,13
P10644	cAMP-dependent protein kinase type I-alpha regulatory subunit OS=Homo sapiens OX=9606 GN=PRKAR1A PE=1 SV=1 - [KAP0_HUMAN]				9,19
P00918	Carbonic anhydrase 2 OS=Homo sapiens GN=CA2 PE=1 SV=2 - [CAH2_HUMAN]			10,00	32,69
P22792	Carboxypeptidase N subunit 2 OS=Homo sapiens GN=CPN2 PE=1 SV=3 - [CPN2_HUMAN]	5,14			7,89
P50416	Carnitine O-palmitoyltransferase 1, liver isoform OS=Homo sapiens OX=9606 GN=CPT1A PE=1 SV=2 - [CPT1A_HUMAN]				18,37
Q9NQ75	Cas scaffolding protein family member 4 OS=Homo sapiens GN=CASS4 PE=1 SV=2 - [CASS4_HUMAN]				5,22
P31944	Caspase-14 OS=Homo sapiens GN=CASP14 PE=1 SV=2 - [CASPE_HUMAN]	16,94	16,94	21,90	13,22
P42574	Caspase-3 OS=Homo sapiens GN=CASP3 PE=1 SV=2 - [CASP3_HUMAN]				9,03
P04040	Catalase OS=Homo sapiens GN=CAT PE=1 SV=3 - [CATA_HUMAN]			6,07	30,17
P07339	Cathepsin D OS=Homo sapiens GN=CTSD PE=1 SV=1 - [CATD_HUMAN]	13,11	16,26	12,14	11,17
P20645	Cation-dependent mannose-6-phosphate receptor OS=Homo sapiens GN=M6PR PE=1 SV=1 - [MPRD_HUMAN]				14,44
P48509	CD151 antigen OS=Homo sapiens OX=9606 GN=CD151 PE=1 SV=3 - [CD151_HUMAN]				8,70
O43866	CD5 antigen-like OS=Homo sapiens GN=CD5L PE=1 SV=1 - [CD5L_HUMAN]	26,80	21,61	25,94	13,83
P08962	CD63 antigen OS=Homo sapiens GN=CD63 PE=1 SV=2 - [CD63_HUMAN]				7,56
P21926	CD9 antigen OS=Homo sapiens GN=CD9 PE=1 SV=4 - [CD9_HUMAN]				14,47
Q8N5K1	CDGSH iron-sulfur domain-containing protein 2 OS=Homo sapiens OX=9606 GN=CISD2 PE=1 SV=1 - [CISD2_HUMAN]				37,78

SUPPLEMENTARY DATA AND INFORMATION

Accession	Description	Coverage exp1 (1263)	Coverage exp1 (rblgG)	Coverage exp2 (1263)	Coverage exp2 (rblgG)
O14735	CDP-diacylglycerol--inositol 3-phosphatidyltransferase OS=Homo sapiens GN=CDIPT PE=1 SV=1 - [CDIPT_HUMAN]				15,02
P60953	Cell division control protein 42 homolog OS=Homo sapiens GN=CDC42 PE=1 SV=2 - [CDC42_HUMAN]				19,90
P00450	Ceruloplasmin OS=Homo sapiens GN=CP PE=1 SV=1 - [CERU_HUMAN]	30,99	8,73	17,09	40,28
O76074	cGMP-specific 3',5'-cyclic phosphodiesterase OS=Homo sapiens GN=PDE5A PE=1 SV=2 - [PDE5A_HUMAN]			8,00	24,80
Q96FZ7	Charged multivesicular body protein 6 OS=Homo sapiens GN=CHMP6 PE=1 SV=3 - [CHMP6_HUMAN]				10,45
O00299	Chloride intracellular channel protein 1 OS=Homo sapiens GN=CLIC1 PE=1 SV=4 - [CLIC1_HUMAN]	41,08	12,45	37,76	48,55
Q9Y696	Chloride intracellular channel protein 4 OS=Homo sapiens GN=CLIC4 PE=1 SV=4 - [CLIC4_HUMAN]				11,86
Q8IWA5	Choline transporter-like protein 2 OS=Homo sapiens OX=9606 GN=SLC44A2 PE=1 SV=3 - [CTL2_HUMAN]				3,40
P06276	Cholinesterase OS=Homo sapiens GN=BCHE PE=1 SV=1 - [CHLE_HUMAN]				6,64
O75390	Citrate synthase, mitochondrial OS=Homo sapiens GN=CS PE=1 SV=2 - [CISY_HUMAN]			7,73	
Q96DZ9	CKLF-like MARVEL transmembrane domain-containing protein 5 OS=Homo sapiens OX=9606 GN=CMTM5 PE=1 SV=2 - [CKLF5_HUMAN]				17,49
Q9NX76	CKLF-like MARVEL transmembrane domain-containing protein 6 OS=Homo sapiens GN=CMTM6 PE=1 SV=1 - [CKLF6_HUMAN]				11,48
Q00610	Clathrin heavy chain 1 OS=Homo sapiens GN=CLTC PE=1 SV=5 - [CLH1_HUMAN]			8,96	32,54
P09496	Clathrin light chain A OS=Homo sapiens OX=9606 GN=CLTA PE=1 SV=1 - [CLCA_HUMAN]				6,85
O00501	Claudin-5 OS=Homo sapiens OX=9606 GN=CLDN5 PE=2 SV=1 - [CLD5_HUMAN]				10,55
P10909	Clusterin OS=Homo sapiens GN=CLU PE=1 SV=1 - [CLUS_HUMAN]	6,01		16,26	30,07
Q14019	Coactosin-like protein OS=Homo sapiens GN=COTL1 PE=1 SV=3 - [COTL1_HUMAN]				19,01
P12259	Coagulation factor V OS=Homo sapiens GN=F5 PE=1 SV=4 - [FA5_HUMAN]				12,68
P00488	Coagulation factor XIII A chain OS=Homo sapiens GN=F13A1 PE=1 SV=4 - [F13A_HUMAN]	11,34	3,28	29,64	58,74
P35606	Coatomer subunit beta' OS=Homo sapiens GN=COPB2 PE=1 SV=2 - [COPB2_HUMAN]				17,00
P48444	Coatomer subunit delta OS=Homo sapiens GN=ARCN1 PE=1 SV=1 - [COPD_HUMAN]				9,59

SUPPLEMENTARY DATA AND INFORMATION

Accession	Description	Coverage exp1 (1263)	Coverage exp1 (rblgG)	Coverage exp2 (1263)	Coverage exp2 (rblgG)
O14579	Coatomer subunit epsilon OS=Homo sapiens OX=9606 GN=COPE PE=1 SV=3 - [COPE_HUMAN]				12,99
P61923	Coatomer subunit zeta-1 OS=Homo sapiens OX=9606 GN=COPZ1 PE=1 SV=1 - [COPZ1_HUMAN]				11,86
P23528	Cofilin-1 OS=Homo sapiens GN=CFL1 PE=1 SV=3 - [COF1_HUMAN]	27,11	15,66	18,67	65,66
Q9P000	COMM domain-containing protein 9 OS=Homo sapiens OX=9606 GN=COMMD9 PE=1 SV=2 - [COMD9_HUMAN]				9,60
P02745	Complement C1q subcomponent subunit A OS=Homo sapiens GN=C1QA PE=1 SV=2 - [C1QA_HUMAN]	23,67	35,10		23,67
P02746	Complement C1q subcomponent subunit B OS=Homo sapiens GN=C1QB PE=1 SV=3 - [C1QB_HUMAN]	35,57	36,76	23,32	41,50
P02747	Complement C1q subcomponent subunit C OS=Homo sapiens GN=C1QC PE=1 SV=3 - [C1QC_HUMAN]	28,57	28,57	25,31	36,33
P00736	Complement C1r subcomponent OS=Homo sapiens GN=C1R PE=1 SV=2 - [C1R_HUMAN]	35,32	46,67	22,70	40,00
P09871	Complement C1s subcomponent OS=Homo sapiens GN=C1S PE=1 SV=1 - [C1S_HUMAN]	36,05	44,48	23,11	43,17
P01024	Complement C3 OS=Homo sapiens GN=C3 PE=1 SV=2 - [CO3_HUMAN]	27,60	16,30	36,26	62,30
P0C0L4	Complement C4-A OS=Homo sapiens GN=C4A PE=1 SV=2 - [CO4A_HUMAN]		9,00	8,94	33,31
P0C0L5	Complement C4-B OS=Homo sapiens GN=C4B PE=1 SV=2 - [CO4B_HUMAN]	13,25	9,69	8,94	34,06
P01031	Complement C5 OS=Homo sapiens GN=C5 PE=1 SV=4 - [CO5_HUMAN]				9,67
Q07021	Complement component 1 Q subcomponent-binding protein, mitochondrial OS=Homo sapiens GN=C1QBP PE=1 SV=1 - [C1QBP_HUMAN]			26,95	31,56
P07360	Complement component C8 gamma chain OS=Homo sapiens GN=C8G PE=1 SV=3 - [CO8G_HUMAN]				27,23
P00751	Complement factor B OS=Homo sapiens GN=CFB PE=1 SV=2 - [CFAB_HUMAN]	6,81		8,51	23,30
P08603	Complement factor H OS=Homo sapiens GN=CFH PE=1 SV=4 - [CFAH_HUMAN]	4,96		15,60	50,12
Q6PJW8	Consortin OS=Homo sapiens OX=9606 GN=CNST PE=1 SV=3 - [CNST_HUMAN]				3,59
P61201	COP9 signalosome complex subunit 2 OS=Homo sapiens OX=9606 GN=COPS2 PE=1 SV=1 - [CSN2_HUMAN]				10,61
Q9UNS2	COP9 signalosome complex subunit 3 OS=Homo sapiens OX=9606 GN=COPS3 PE=1 SV=3 - [CSN3_HUMAN]				8,27
Q9BT78	COP9 signalosome complex subunit 4 OS=Homo sapiens GN=COPS4 PE=1 SV=1 - [CSN4_HUMAN]				11,82

SUPPLEMENTARY DATA AND INFORMATION

Accession	Description	Coverage exp1 (1263)	Coverage exp1 (rblgG)	Coverage exp2 (1263)	Coverage exp2 (rblgG)
Q92905	COP9 signalosome complex subunit 5 OS=Homo sapiens OX=9606 GN=COPS5 PE=1 SV=4 - [CSN5_HUMAN]				8,68
Q9UBW8	COP9 signalosome complex subunit 7a OS=Homo sapiens GN=COPS7A PE=1 SV=1 - [CSN7A_HUMAN]				18,18
Q9H9Q2	COP9 signalosome complex subunit 7b OS=Homo sapiens OX=9606 GN=COPS7B PE=1 SV=1 - [CSN7B_HUMAN]				11,74
Q99627	COP9 signalosome complex subunit 8 OS=Homo sapiens OX=9606 GN=COPS8 PE=1 SV=1 - [CSN8_HUMAN]				23,92
O14618	Copper chaperone for superoxide dismutase OS=Homo sapiens OX=9606 GN=CCS PE=1 SV=1 - [CCS_HUMAN]				7,66
Q15517	Corneodesmosin OS=Homo sapiens GN=CDSN PE=1 SV=3 - [CDSN_HUMAN]			7,94	
P22528	Cornifin-B OS=Homo sapiens GN=SPRR1B PE=1 SV=2 - [SPRR1B_HUMAN]		37,08	42,70	42,70
P31146	Coronin-1A OS=Homo sapiens GN=CORO1A PE=1 SV=4 - [COR1A_HUMAN]				8,03
Q9ULV4	Coronin-1C OS=Homo sapiens GN=CORO1C PE=1 SV=1 - [COR1C_HUMAN]			24,68	16,24
Q13617	Cullin-2 OS=Homo sapiens OX=9606 GN=CUL2 PE=1 SV=2 - [CUL2_HUMAN]				6,98
Q86VP6	Cullin-associated NEDD8-dissociated protein 1 OS=Homo sapiens GN=CAND1 PE=1 SV=2 - [CAND1_HUMAN]			1,71	24,47
P01040	Cystatin-A OS=Homo sapiens GN=CSTA PE=1 SV=1 - [CYTA_HUMAN]		48,98	60,20	
P01037	Cystatin-SN OS=Homo sapiens GN=CST1 PE=1 SV=3 - [CYTN_HUMAN]	24,82	24,82		
P21291	Cysteine and glycine-rich protein 1 OS=Homo sapiens GN=CSRP1 PE=1 SV=3 - [CSRP1_HUMAN]				33,16
P49589	Cysteine--tRNA ligase, cytoplasmic OS=Homo sapiens GN=CARS PE=1 SV=3 - [SYCC_HUMAN]				4,68
P31930	Cytochrome b-c1 complex subunit 1, mitochondrial OS=Homo sapiens GN=UQCRC1 PE=1 SV=3 - [QCR1_HUMAN]			5,63	14,79
P22695	Cytochrome b-c1 complex subunit 2, mitochondrial OS=Homo sapiens GN=UQCRC2 PE=1 SV=3 - [QCR2_HUMAN]				17,00
P14927	Cytochrome b-c1 complex subunit 7 OS=Homo sapiens GN=UQCRB PE=1 SV=2 - [QCR7_HUMAN]				20,72
P47985	Cytochrome b-c1 complex subunit Rieske, mitochondrial OS=Homo sapiens OX=9606 GN=UQCRFS1 PE=1 SV=2 - [UCRI_HUMAN]				21,90
P00403	Cytochrome c oxidase subunit 2 OS=Homo sapiens GN=MT-CO2 PE=1 SV=1 - [COX2_HUMAN]	16,30			11,45

SUPPLEMENTARY DATA AND INFORMATION

Accession	Description	Coverage exp1 (1263)	Coverage exp1 (rblgG)	Coverage exp2 (1263)	Coverage exp2 (rblgG)
P13073	Cytochrome c oxidase subunit 4 isoform 1, mitochondrial OS=Homo sapiens GN=COX4I1 PE=1 SV=1 - [COX4I1_HUMAN]				47,93
P20674	Cytochrome c oxidase subunit 5A, mitochondrial OS=Homo sapiens GN=COX5A PE=1 SV=2 - [COX5A_HUMAN]				20,67
P10606	Cytochrome c oxidase subunit 5B, mitochondrial OS=Homo sapiens GN=COX5B PE=1 SV=2 - [COX5B_HUMAN]				18,60
P09669	Cytochrome c oxidase subunit 6C OS=Homo sapiens GN=COX6C PE=1 SV=2 - [COX6C_HUMAN]				20,00
O14548	Cytochrome c oxidase subunit 7A-related protein, mitochondrial OS=Homo sapiens OX=9606 GN=COX7A2L PE=1 SV=2 - [COX7R_HUMAN]				17,54
P08574	Cytochrome c1, heme protein, mitochondrial OS=Homo sapiens GN=CYC1 PE=1 SV=3 - [CY1_HUMAN]				26,15
Q14204	Cytoplasmic dynein 1 heavy chain 1 OS=Homo sapiens GN=DYNC1H1 PE=1 SV=5 - [DYHC1_HUMAN]				10,31
Q7L576	Cytoplasmic FMR1-interacting protein 1 OS=Homo sapiens GN=CYFIP1 PE=1 SV=1 - [CYFIP1_HUMAN]	2,87		2,95	18,36
P47712	Cytosolic phospholipase A2 OS=Homo sapiens GN=PLA2G4A PE=1 SV=2 - [PA24A_HUMAN]				9,75
Q13011	Delta(3,5)-Delta(2,4)-dienoyl-CoA isomerase, mitochondrial OS=Homo sapiens GN=ECH1 PE=1 SV=2 - [ECH1_HUMAN]			9,15	32,62
P13716	Delta-aminolevulinic acid dehydratase OS=Homo sapiens GN=ALAD PE=1 SV=1 - [HEM2_HUMAN]				13,33
Q08495	Dematin OS=Homo sapiens GN=EPB49 PE=1 SV=3 - [DEMA_HUMAN]				7,90
P81605	Dermcidin OS=Homo sapiens GN=DCD PE=1 SV=2 - [DCD_HUMAN]	22,73	22,73	22,73	22,73
Q08554	Desmocollin-1 OS=Homo sapiens GN=DSC1 PE=1 SV=2 - [DSC1_HUMAN]		2,68	2,46	
Q02413	Desmoglein-1 OS=Homo sapiens GN=DSG1 PE=1 SV=2 - [DSG1_HUMAN]	8,58	9,82	14,01	15,54
P15924	Desmoplakin OS=Homo sapiens GN=DSP PE=1 SV=3 - [DESP_HUMAN]	3,73	5,78	12,09	5,33
P60981	Destrin OS=Homo sapiens GN=DSTN PE=1 SV=3 - [DEST_HUMAN]				23,64
Q9NR28	Diablo homolog, mitochondrial OS=Homo sapiens GN=DIABLO PE=1 SV=1 - [DBLOH_HUMAN]				11,30
Q16555	Dihydropyrimidinase-related protein 2 OS=Homo sapiens GN=DPYSL2 PE=1 SV=1 - [DPYL2_HUMAN]				14,16
Q9Y4D1	Disheveled-associated activator of morphogenesis 1 OS=Homo sapiens GN=DAAM1 PE=1 SV=2 - [DAAM1_HUMAN]				2,78

SUPPLEMENTARY DATA AND INFORMATION

Accession	Description	Coverage exp1 (1263)	Coverage exp1 (rblgG)	Coverage exp2 (1263)	Coverage exp2 (rblgG)
Q8IUX4	DNA dC->dU-editing enzyme APOBEC-3F OS=Homo sapiens OX=9606 GN=APOBEC3F PE=1 SV=3 - [ABC3F_HUMAN]			16,62	
O75190	DnaJ homolog subfamily B member 6 OS=Homo sapiens GN=DNAJB6 PE=1 SV=2 - [DNJB6_HUMAN]		7,36		15,34
O60496	Docking protein 2 OS=Homo sapiens GN=DOK2 PE=1 SV=2 - [DOK2_HUMAN]				5,34
P39656	Dolichyl-diphosphooligosaccharide--protein glycosyltransferase 48 kDa subunit OS=Homo sapiens GN=DDOST PE=1 SV=4 - [OST48_HUMAN]			10,09	35,53
P04843	Dolichyl-diphosphooligosaccharide--protein glycosyltransferase subunit 1 OS=Homo sapiens GN=RPN1 PE=1 SV=1 - [RPN1_HUMAN]				19,77
P04844	Dolichyl-diphosphooligosaccharide--protein glycosyltransferase subunit 2 OS=Homo sapiens GN=RPN2 PE=1 SV=3 - [RPN2_HUMAN]				11,09
P61803	Dolichyl-diphosphooligosaccharide--protein glycosyltransferase subunit DAD1 OS=Homo sapiens GN=DAD1 PE=1 SV=3 - [DAD1_HUMAN]				35,40
P46977	Dolichyl-diphosphooligosaccharide--protein glycosyltransferase subunit STT3A OS=Homo sapiens GN=STT3A PE=1 SV=2 - [STT3A_HUMAN]				2,55
Q16643	Drebrin OS=Homo sapiens GN=DBN1 PE=1 SV=4 - [DREB_HUMAN]				4,01
P51452	Dual specificity protein phosphatase 3 OS=Homo sapiens GN=DUSP3 PE=1 SV=1 - [DUS3_HUMAN]				19,46
Q14203	Dynactin subunit 1 OS=Homo sapiens GN=DCTN1 PE=1 SV=3 - [DCTN1_HUMAN]			1,49	3,91
Q13561	Dynactin subunit 2 OS=Homo sapiens GN=DCTN2 PE=1 SV=4 - [DCTN2_HUMAN]				12,22
O75935	Dynactin subunit 3 OS=Homo sapiens GN=DCTN3 PE=1 SV=1 - [DCTN3_HUMAN]				12,90
Q9UJW0	Dynactin subunit 4 OS=Homo sapiens GN=DCTN4 PE=1 SV=1 - [DCTN4_HUMAN]				8,04
Q05193	Dynamamin-1 OS=Homo sapiens GN=DNM1 PE=1 SV=2 - [DYN1_HUMAN]				6,60
O00429	Dynamamin-1-like protein OS=Homo sapiens GN=DNM1L PE=1 SV=2 - [DNM1L_HUMAN]			7,74	38,04
P50570	Dynamamin-2 OS=Homo sapiens GN=DNM2 PE=1 SV=2 - [DYN2_HUMAN]			4,94	3,10
O60313	Dynamamin-like 120 kDa protein, mitochondrial OS=Homo sapiens GN=OPA1 PE=1 SV=3 - [OPA1_HUMAN]				4,48
Q5T447	E3 ubiquitin-protein ligase HECTD3 OS=Homo sapiens GN=HECTD3 PE=1 SV=1 - [HECD3_HUMAN]	5,11			5,92
O95714	E3 ubiquitin-protein ligase HERC2 OS=Homo sapiens GN=HERC2 PE=1 SV=2 - [HERC2_HUMAN]	0,60			

SUPPLEMENTARY DATA AND INFORMATION

Accession	Description	Coverage exp1 (1263)	Coverage exp1 (rblgG)	Coverage exp2 (1263)	Coverage exp2 (rblgG)
Q63HN8	E3 ubiquitin-protein ligase RNF213 OS=Homo sapiens GN=RNF213 PE=1 SV=3 - [RN213_HUMAN]				2,90
P19474	E3 ubiquitin-protein ligase TRIM21 OS=Homo sapiens OX=9606 GN=TRIM21 PE=1 SV=1 - [RO52_HUMAN]	13,47	18,32	22,32	14,95
Q9NZN3	EH domain-containing protein 3 OS=Homo sapiens GN=EHD3 PE=1 SV=2 - [EHD3_HUMAN]			19,44	18,13
P13804	Electron transfer flavoprotein subunit alpha, mitochondrial OS=Homo sapiens OX=9606 GN=ETF A PE=1 SV=1 - [ETF A_HUMAN]				27,93
P38117	Electron transfer flavoprotein subunit beta OS=Homo sapiens OX=9606 GN=ETF B PE=1 SV=3 - [ETF B_HUMAN]				10,98
P26641	Elongation factor 1-gamma OS=Homo sapiens GN=EEF1G PE=1 SV=3 - [EEF1G_HUMAN]				10,07
Q9Y6C2	EMILIN-1 OS=Homo sapiens OX=9606 GN=EMILIN1 PE=1 SV=3 - [EMIL1_HUMAN]			2,76	5,91
O94919	Endonuclease domain-containing 1 protein OS=Homo sapiens OX=9606 GN=ENDOD1 PE=1 SV=2 - [ENDD1_HUMAN]			5,00	14,60
Q9NZ08	Endoplasmic reticulum aminopeptidase 1 OS=Homo sapiens GN=ERAP1 PE=1 SV=3 - [ERAP1_HUMAN]				5,53
P14625	Endoplasmin OS=Homo sapiens GN=HSP90B1 PE=1 SV=1 - [ENPL_HUMAN]	8,97		18,68	51,81
P42892	Endothelin-converting enzyme 1 OS=Homo sapiens OX=9606 GN=ECE1 PE=1 SV=2 - [ECE1_HUMAN]				6,88
P30084	Enoyl-CoA hydratase, mitochondrial OS=Homo sapiens GN=ECHS1 PE=1 SV=4 - [ECHM_HUMAN]				13,45
Q15006	ER membrane protein complex subunit 2 OS=Homo sapiens OX=9606 GN=EMC2 PE=1 SV=1 - [EMC2_HUMAN]				16,50
Q5J8M3	ER membrane protein complex subunit 4 OS=Homo sapiens OX=9606 GN=EMC4 PE=1 SV=2 - [EMC4_HUMAN]				15,30
Q9NPA0	ER membrane protein complex subunit 7 OS=Homo sapiens OX=9606 GN=EMC7 PE=1 SV=1 - [EMC7_HUMAN]				8,26
O43402	ER membrane protein complex subunit 8 OS=Homo sapiens OX=9606 GN=EMC8 PE=1 SV=1 - [EMC8_HUMAN]				10,00
P27105	Erythrocyte band 7 integral membrane protein OS=Homo sapiens GN=STOM PE=1 SV=3 - [STOM_HUMAN]	11,46		37,15	65,63
Q53GQ0	Estradiol 17-beta-dehydrogenase 12 OS=Homo sapiens GN=HSD17B12 PE=1 SV=2 - [DHB12_HUMAN]				14,42
P20042	Eukaryotic translation initiation factor 2 subunit 2 OS=Homo sapiens OX=9606 GN=EIF2S2 PE=1 SV=2 - [IF2B_HUMAN]				8,41

SUPPLEMENTARY DATA AND INFORMATION

Accession	Description	Coverage exp1 (1263)	Coverage exp1 (rblgG)	Coverage exp2 (1263)	Coverage exp2 (rblgG)
P55884	Eukaryotic translation initiation factor 3 subunit B OS=Homo sapiens GN=EIF3B PE=1 SV=3 - [EIF3B_HUMAN]	27,27		3,19	
Q13347	Eukaryotic translation initiation factor 3 subunit I OS=Homo sapiens OX=9606 GN=EIF3I PE=1 SV=1 - [EIF3I_HUMAN]	21,85			6,46
Q9UBQ5	Eukaryotic translation initiation factor 3 subunit K OS=Homo sapiens GN=EIF3K PE=1 SV=1 - [EIF3K_HUMAN]				17,89
O14980	Exportin-1 OS=Homo sapiens GN=XPO1 PE=1 SV=1 - [XPO1_HUMAN]				8,50
P55060	Exportin-2 OS=Homo sapiens GN=CSE1L PE=1 SV=3 - [XPO2_HUMAN]				11,12
Q9UIA9	Exportin-7 OS=Homo sapiens OX=9606 GN=XPO7 PE=1 SV=3 - [XPO7_HUMAN]			3,40	4,78
Q9BSJ8	Extended synaptotagmin-1 OS=Homo sapiens GN=ESYT1 PE=1 SV=1 - [ESYT1_HUMAN]				5,07
A0FGR8	Extended synaptotagmin-2 OS=Homo sapiens OX=9606 GN=ESYT2 PE=1 SV=1 - [ESYT2_HUMAN]				2,39
P52907	F-actin-capping protein subunit alpha-1 OS=Homo sapiens GN=CAPZA1 PE=1 SV=3 - [CAZA1_HUMAN]			33,22	45,80
P47755	F-actin-capping protein subunit alpha-2 OS=Homo sapiens GN=CAPZA2 PE=1 SV=3 - [CAZA2_HUMAN]	8,39		17,13	23,08
P47756	F-actin-capping protein subunit beta OS=Homo sapiens GN=CAPZB PE=1 SV=4 - [CAPZB_HUMAN]			16,25	45,85
P49327	Fatty acid synthase OS=Homo sapiens GN=FASN PE=1 SV=3 - [FAS_HUMAN]				15,65
Q86UX7	Fermitin family homolog 3 OS=Homo sapiens GN=FERMT3 PE=1 SV=1 - [URP2_HUMAN]	21,74	10,19	40,03	58,62
P02794	Ferritin heavy chain OS=Homo sapiens OX=9606 GN=FTH1 PE=1 SV=2 - [FRIH_HUMAN]				36,07
Q9Y613	FH1/FH2 domain-containing protein 1 OS=Homo sapiens GN=FHOD1 PE=1 SV=3 - [FHOD1_HUMAN]				7,73
P02671	Fibrinogen alpha chain OS=Homo sapiens GN=FGA PE=1 SV=2 - [FIBA_HUMAN]	12,01	13,51	29,21	35,91
P02675	Fibrinogen beta chain OS=Homo sapiens GN=FGB PE=1 SV=2 - [FIBB_HUMAN]	37,47	41,55	42,36	65,99
P02679	Fibrinogen gamma chain OS=Homo sapiens GN=FGG PE=1 SV=3 - [FIBG_HUMAN]	27,37	26,71	62,47	63,13
Q86WI1	Fibrocystin-L OS=Homo sapiens GN=PKHD1L1 PE=2 SV=2 - [PKHL1_HUMAN]				7,92
P02751	Fibronectin OS=Homo sapiens GN=FN1 PE=1 SV=4 - [FINC_HUMAN]	5,91	10,48	11,94	35,33
O75636	Ficolin-3 OS=Homo sapiens OX=9606 GN=FCN3 PE=1 SV=2 - [FCN3_HUMAN]				13,38

SUPPLEMENTARY DATA AND INFORMATION

Accession	Description	Coverage exp1 (1263)	Coverage exp1 (rblgG)	Coverage exp2 (1263)	Coverage exp2 (rblgG)
P20930	Filaggrin OS=Homo sapiens GN=FLG PE=1 SV=3 - [FILA_HUMAN]			2,02	1,08
Q5D862	Filaggrin-2 OS=Homo sapiens GN=FLG2 PE=1 SV=1 - [FILA2_HUMAN]	0,96	6,57	5,90	9,49
P21333	Filamin-A OS=Homo sapiens GN=FLNA PE=1 SV=4 - [FLNA_HUMAN]	32,04	22,86	53,34	70,72
Q5T1M5	FK506-binding protein 15 OS=Homo sapiens GN=FKBP15 PE=1 SV=2 - [FKB15_HUMAN]	4,76			
Q13642	Four and a half LIM domains protein 1 OS=Homo sapiens GN=FHL1 PE=1 SV=4 - [FHL1_HUMAN]				7,12
P04075	Fructose-bisphosphate aldolase A OS=Homo sapiens GN=ALDOA PE=1 SV=2 - [ALDOA_HUMAN]	14,56		48,35	58,79
P47929	Galectin-7 OS=Homo sapiens GN=LGALS7 PE=1 SV=2 - [LEG7_HUMAN]		19,85		
Q3ZCW2	Galectin-related protein OS=Homo sapiens OX=9606 GN=LGALS1 PE=1 SV=2 - [LEGL_HUMAN]				17,44
P09104	Gamma-enolase OS=Homo sapiens GN=ENO2 PE=1 SV=3 - [ENOG_HUMAN]				10,83
P06396	Gelsolin OS=Homo sapiens GN=GSN PE=1 SV=1 - [GELS_HUMAN]	19,57	10,87	34,78	54,22
P11413	Glucose-6-phosphate 1-dehydrogenase OS=Homo sapiens GN=G6PD PE=1 SV=4 - [G6PD_HUMAN]				5,05
P06744	Glucose-6-phosphate isomerase OS=Homo sapiens GN=GPI PE=1 SV=4 - [G6PI_HUMAN]			5,56	11,83
P14314	Glucosidase 2 subunit beta OS=Homo sapiens GN=PRKCSH PE=1 SV=2 - [GLU2B_HUMAN]			10,42	26,89
P00367	Glutamate dehydrogenase 1, mitochondrial OS=Homo sapiens GN=GLUD1 PE=1 SV=2 - [DHE3_HUMAN]				7,35
P07203	Glutathione peroxidase 1 OS=Homo sapiens GN=GPX1 PE=1 SV=4 - [GPX1_HUMAN]			9,36	32,51
P78417	Glutathione S-transferase omega-1 OS=Homo sapiens GN=GSTO1 PE=1 SV=2 - [GSTO1_HUMAN]			9,54	36,10
P09211	Glutathione S-transferase P OS=Homo sapiens GN=GSTP1 PE=1 SV=2 - [GSTP1_HUMAN]			42,86	48,10
P04406	Glyceraldehyde-3-phosphate dehydrogenase OS=Homo sapiens GN=GAPDH PE=1 SV=3 - [G3P_HUMAN]	34,03	17,01	45,67	74,93
P43304	Glycerol-3-phosphate dehydrogenase, mitochondrial OS=Homo sapiens GN=GPD2 PE=1 SV=3 - [GPDM_HUMAN]				18,84
P41250	Glycine--tRNA ligase OS=Homo sapiens GN=GARS PE=1 SV=3 - [SYG_HUMAN]			2,84	12,86
P11216	Glycogen phosphorylase, brain form OS=Homo sapiens GN=PYGB PE=1 SV=5 - [PYGB_HUMAN]			5,69	39,62
P06737	Glycogen phosphorylase, liver form OS=Homo sapiens GN=PYGL PE=1 SV=4 - [PYGL_HUMAN]			4,49	27,39

SUPPLEMENTARY DATA AND INFORMATION

Accession	Description	Coverage exp1 (1263)	Coverage exp1 (rblgG)	Coverage exp2 (1263)	Coverage exp2 (rblgG)
P46976	Glycogenin-1 OS=Homo sapiens GN=GYG1 PE=1 SV=4 - [GLYG_HUMAN]				8,00
P36959	GMP reductase 1 OS=Homo sapiens OX=9606 GN=GMPR PE=1 SV=1 - [GMPR1_HUMAN]				36,52
Q9P2T1	GMP reductase 2 OS=Homo sapiens GN=GMPR2 PE=1 SV=1 - [GMPR2_HUMAN]				13,51
Q9H4G4	Golgi-associated plant pathogenesis-related protein 1 OS=Homo sapiens GN=GLIPR2 PE=1 SV=3 - [GAPR1_HUMAN]				16,88
P62993	Growth factor receptor-bound protein 2 OS=Homo sapiens GN=GRB2 PE=1 SV=1 - [GRB2_HUMAN]				11,06
P01111	GTPase NRas OS=Homo sapiens GN=NRAS PE=1 SV=1 - [RASN_HUMAN]				16,93
Q15382	GTP-binding protein Rheb OS=Homo sapiens OX=9606 GN=RHEB PE=1 SV=1 - [RHEB_HUMAN]				20,11
Q9NR31	GTP-binding protein SAR1a OS=Homo sapiens GN=SAR1A PE=1 SV=1 - [SAR1A_HUMAN]			15,66	27,27
Q9Y6B6	GTP-binding protein SAR1b OS=Homo sapiens GN=SAR1B PE=1 SV=1 - [SAR1B_HUMAN]				15,66
P04899	Guanine nucleotide-binding protein G(i) subunit alpha-2 OS=Homo sapiens GN=GNAI2 PE=1 SV=3 - [GNAI2_HUMAN]			14,37	26,76
P62873	Guanine nucleotide-binding protein G(I)/G(S)/G(T) subunit beta-1 OS=Homo sapiens GN=GNB1 PE=1 SV=3 - [GGB1_HUMAN]			9,12	21,47
P50148	Guanine nucleotide-binding protein G(q) subunit alpha OS=Homo sapiens GN=GNAQ PE=1 SV=4 - [GNAQ_HUMAN]			26,18	26,74
Q14344	Guanine nucleotide-binding protein subunit alpha-13 OS=Homo sapiens GN=GNA13 PE=1 SV=2 - [GNA13_HUMAN]				8,22
Q02153	Guanylate cyclase soluble subunit beta-1 OS=Homo sapiens OX=9606 GN=GUCY1B1 PE=1 SV=1 - [GUCY1_HUMAN]				5,33
Q9H0R4	Haloacid dehalogenase-like hydrolase domain-containing protein 2 OS=Homo sapiens GN=HDHD2 PE=1 SV=1 - [HDHD2_HUMAN]				11,20
P00738	Haptoglobin OS=Homo sapiens GN=HP PE=1 SV=1 - [HPT_HUMAN]	37,19	30,05	27,59	47,54
P00739	Haptoglobin-related protein OS=Homo sapiens GN=HPR PE=1 SV=2 - [HPTR_HUMAN]	26,72	23,56		29,02
P08107	Heat shock 70 kDa protein 1A/1B OS=Homo sapiens GN=HSPA1A PE=1 SV=5 - [HSP71_HUMAN]	8,42		12,32	16,38
P34932	Heat shock 70 kDa protein 4 OS=Homo sapiens GN=HSPA4 PE=1 SV=4 - [HSP74_HUMAN]				15,12
P11142	Heat shock cognate 71 kDa protein OS=Homo sapiens GN=HSPA8 PE=1 SV=1 - [HSP7C_HUMAN]	25,23	3,87	34,21	38,39
P04792	Heat shock protein beta-1 OS=Homo sapiens GN=HSPB1 PE=1 SV=2 - [HSPB1_HUMAN]	44,39	36,10	25,37	78,05

SUPPLEMENTARY DATA AND INFORMATION

Accession	Description	Coverage exp1 (1263)	Coverage exp1 (rblgG)	Coverage exp2 (1263)	Coverage exp2 (rblgG)
P07900	Heat shock protein HSP 90-alpha OS=Homo sapiens GN=HSP90AA1 PE=1 SV=5 - [HS90A_HUMAN]	8,88		23,09	45,08
P08238	Heat shock protein HSP 90-beta OS=Homo sapiens GN=HSP90AB1 PE=1 SV=4 - [HS90B_HUMAN]	7,46		18,23	48,20
P69905	Hemoglobin subunit alpha OS=Homo sapiens GN=HBA1 PE=1 SV=2 - [HBA_HUMAN]				31,69
P68871	Hemoglobin subunit beta OS=Homo sapiens GN=HBB PE=1 SV=2 - [HBB_HUMAN]	19,73		45,58	82,31
P02042	Hemoglobin subunit delta OS=Homo sapiens GN=HBD PE=1 SV=2 - [HBD_HUMAN]				82,31
P02790	Hemopexin OS=Homo sapiens GN=HPX PE=1 SV=2 - [HEMO_HUMAN]	8,44		24,46	29,44
Q9Y251	Heparanase OS=Homo sapiens GN=HPSE PE=1 SV=2 - [HPSE_HUMAN]				9,21
P19367	Hexokinase-1 OS=Homo sapiens GN=HK1 PE=1 SV=3 - [HKK1_HUMAN]			6,00	27,92
P04196	Histidine-rich glycoprotein OS=Homo sapiens GN=HRG PE=1 SV=1 - [HRG_HUMAN]		12,38	5,71	16,95
O60814	Histone H2B type 1-K OS=Homo sapiens GN=HIST1H2BK PE=1 SV=3 - [H2B1K_HUMAN]				15,87
P62805	Histone H4 OS=Homo sapiens GN=HIST1H4A PE=1 SV=2 - [H4_HUMAN]				17,48
P05534	HLA class I histocompatibility antigen, A-24 alpha chain OS=Homo sapiens GN=HLA-A PE=1 SV=2 - [1A24_HUMAN]			22,19	
P04439	HLA class I histocompatibility antigen, A-3 alpha chain OS=Homo sapiens GN=HLA-A PE=1 SV=2 - [1A03_HUMAN]			21,92	33,70
P13747	HLA class I histocompatibility antigen, alpha chain E OS=Homo sapiens OX=9606 GN=HLA-E PE=1 SV=3 - [HLAE_HUMAN]				14,25
P30464	HLA class I histocompatibility antigen, B-15 alpha chain OS=Homo sapiens GN=HLA-B PE=1 SV=2 - [1B15_HUMAN]			19,34	
P18464	HLA class I histocompatibility antigen, B-51 alpha chain OS=Homo sapiens GN=HLA-B PE=1 SV=1 - [1B51_HUMAN]			19,34	28,18
Q86YZ3	Hornerin OS=Homo sapiens GN=HRNR PE=1 SV=2 - [HORN_HUMAN]	9,23	19,93	16,67	20,63
P00492	Hypoxanthine-guanine phosphoribosyltransferase OS=Homo sapiens GN=HPRT1 PE=1 SV=2 - [HPRT_HUMAN]				26,61
Q9Y4L1	Hypoxia up-regulated protein 1 OS=Homo sapiens OX=9606 GN=HYOU1 PE=1 SV=1 - [HYOU1_HUMAN]				25,03
P01876	Ig alpha-1 chain C region OS=Homo sapiens GN=IGHA1 PE=1 SV=2 - [IGHA1_HUMAN]	21,25	27,20	19,83	42,49
P01857	Ig gamma-1 chain C region OS=Homo sapiens GN=IGHG1 PE=1 SV=1 - [IGHG1_HUMAN]	34,85	46,06	43,03	50,91

SUPPLEMENTARY DATA AND INFORMATION

Accession	Description	Coverage exp1 (1263)	Coverage exp1 (rblgG)	Coverage exp2 (1263)	Coverage exp2 (rblgG)
P01859	Ig gamma-2 chain C region OS=Homo sapiens GN=IGHG2 PE=1 SV=2 - [IGHG2_HUMAN]	28,22	48,77	28,22	36,50
P01860	Ig gamma-3 chain C region OS=Homo sapiens GN=IGHG3 PE=1 SV=2 - [IGHG3_HUMAN]		25,20	31,03	39,52
P01861	Ig gamma-4 chain C region OS=Homo sapiens GN=IGHG4 PE=1 SV=1 - [IGHG4_HUMAN]	19,88	19,88	34,25	42,51
P06312	Ig kappa chain V-IV region (Fragment) OS=Homo sapiens GN=IGKV4-1 PE=4 SV=1 - [KV401_HUMAN]	17,36	17,36	17,36	35,54
Q9Y6R7	IgGFc-binding protein OS=Homo sapiens GN=FCGBP PE=1 SV=3 - [FCGBP_HUMAN]		0,81		
P0DOX2	Immunoglobulin alpha-2 heavy chain OS=Homo sapiens OX=9606 PE=1 SV=2 - [IGA2_HUMAN]	10,55	17,58		
P01880	Immunoglobulin heavy constant delta OS=Homo sapiens OX=9606 GN=IGHD PE=1 SV=3 - [IGHD_HUMAN]			6,51	8,33
P01871	Immunoglobulin heavy constant mu OS=Homo sapiens OX=9606 GN=IGHM PE=1 SV=4 - [IGHM_HUMAN]	47,90	46,36	33,11	53,64
P01764	Immunoglobulin heavy variable 3-23 OS=Homo sapiens OX=9606 GN=IGHV3-23 PE=1 SV=2 - [HV323_HUMAN]			18,80	
A0A0C4DH42	Immunoglobulin heavy variable 3-66 OS=Homo sapiens OX=9606 GN=IGHV3-66 PE=3 SV=1 - [HV366_HUMAN]	22,41			
P01780	Immunoglobulin heavy variable 3-7 OS=Homo sapiens OX=9606 GN=IGHV3-7 PE=1 SV=2 - [HV307_HUMAN]		26,50	26,50	23,08
A0A0B4J1X5	Immunoglobulin heavy variable 3-74 OS=Homo sapiens OX=9606 GN=IGHV3-74 PE=3 SV=1 - [HV374_HUMAN]	24,79			
P01591	Immunoglobulin J chain OS=Homo sapiens GN=IGJ PE=1 SV=4 - [IGJ_HUMAN]	23,27	21,38		21,38
P01834	Immunoglobulin kappa constant OS=Homo sapiens OX=9606 GN=IGKC PE=1 SV=2 - [IGKC_HUMAN]	93,46	93,46	79,44	80,37
P0DOX7	Immunoglobulin kappa light chain OS=Homo sapiens OX=9606 PE=1 SV=1 - [IGK_HUMAN]	55,14	49,07		53,74
P01599	Immunoglobulin kappa variable 1-17 OS=Homo sapiens OX=9606 GN=IGKV1-17 PE=1 SV=2 - [KV117_HUMAN]				23,08
P01624	Immunoglobulin kappa variable 3-15 OS=Homo sapiens OX=9606 GN=IGKV3-15 PE=1 SV=2 - [KV315_HUMAN]	26,09	26,09		26,09
P01619	Immunoglobulin kappa variable 3-20 OS=Homo sapiens OX=9606 GN=IGKV3-20 PE=1 SV=2 - [KV320_HUMAN]	46,55	46,55	21,55	21,55
A0A0A0MRZ8	Immunoglobulin kappa variable 3D-11 OS=Homo sapiens OX=9606 GN=IGKV3D-11 PE=3 SV=6 - [KVD11_HUMAN]	26,09			26,09

SUPPLEMENTARY DATA AND INFORMATION

Accession	Description	Coverage exp1 (1263)	Coverage exp1 (rblgG)	Coverage exp2 (1263)	Coverage exp2 (rblgG)
P0DOY3	Immunoglobulin lambda constant 3 OS=Homo sapiens OX=9606 GN=IGLC3 PE=1 SV=1 - [IGLC3_HUMAN]		69,81	55,66	81,13
A0A075B6K4	Immunoglobulin lambda variable 3-10 OS=Homo sapiens OX=9606 GN=IGLV3-10 PE=3 SV=2 - [LV310_HUMAN]	27,83	27,83		20,87
A0A075B6K5	Immunoglobulin lambda variable 3-9 OS=Homo sapiens OX=9606 GN=IGLV3-9 PE=3 SV=1 - [LV39_HUMAN]				23,48
A0A0G2J506	Immunoglobulin lambda variable 5-39 OS=Homo sapiens OX=9606 GN=IGLV5-39 PE=3 SV=1 - [LV539_HUMAN]		18,70		13,01
P0DOX8	Immunoglobulin lambda-1 light chain OS=Homo sapiens OX=9606 PE=1 SV=1 - [IGL1_HUMAN]	33,33	28,70	26,39	47,22
Q14974	Importin subunit beta-1 OS=Homo sapiens GN=KPNB1 PE=1 SV=2 - [IMB1_HUMAN]	2,74		2,85	23,63
O00410	Importin-5 OS=Homo sapiens GN=IPO5 PE=1 SV=4 - [IPO5_HUMAN]				9,66
O95373	Importin-7 OS=Homo sapiens GN=IPO7 PE=1 SV=1 - [IPO7_HUMAN]				7,51
Q96P70	Importin-9 OS=Homo sapiens GN=IPO9 PE=1 SV=3 - [IPO9_HUMAN]				2,40
Q14643	Inositol 1,4,5-trisphosphate receptor type 1 OS=Homo sapiens OX=9606 GN=ITPR1 PE=1 SV=3 - [ITPR1_HUMAN]	20,38		23,97	
Q14571	Inositol 1,4,5-trisphosphate receptor type 2 OS=Homo sapiens GN=ITPR2 PE=1 SV=2 - [ITPR2_HUMAN]	15,44		25,55	
P17301	Integrin alpha-2 OS=Homo sapiens GN=ITGA2 PE=1 SV=1 - [ITA2_HUMAN]			1,52	24,47
P23229	Integrin alpha-6 OS=Homo sapiens OX=9606 GN=ITGA6 PE=1 SV=5 - [ITA6_HUMAN]			4,16	26,28
P08514	Integrin alpha-IIb OS=Homo sapiens GN=ITGA2B PE=1 SV=3 - [ITA2B_HUMAN]	30,51	9,72	26,28	46,01
P05556	Integrin beta-1 OS=Homo sapiens OX=9606 GN=ITGB1 PE=1 SV=2 - [ITB1_HUMAN]	5,76		10,53	22,56
P05106	Integrin beta-3 OS=Homo sapiens GN=ITGB3 PE=1 SV=2 - [ITB3_HUMAN]	19,42	4,70	29,44	62,56
Q13418	Integrin-linked protein kinase OS=Homo sapiens GN=ILK PE=1 SV=2 - [ILK_HUMAN]	16,15	5,31	19,91	42,70
P19827	Inter-alpha-trypsin inhibitor heavy chain H1 OS=Homo sapiens GN=ITIH1 PE=1 SV=3 - [ITIH1_HUMAN]	6,04	3,51	11,42	25,47
P19823	Inter-alpha-trypsin inhibitor heavy chain H2 OS=Homo sapiens GN=ITIH2 PE=1 SV=2 - [ITIH2_HUMAN]			6,55	26,00
Q14624	Inter-alpha-trypsin inhibitor heavy chain H4 OS=Homo sapiens GN=ITIH4 PE=1 SV=4 - [ITIH4_HUMAN]	8,82	5,38	4,84	17,31
Q27J81	Inverted formin-2 OS=Homo sapiens GN=INF2 PE=1 SV=2 - [INF2_HUMAN]				6,00

SUPPLEMENTARY DATA AND INFORMATION

Accession	Description	Coverage exp1 (1263)	Coverage exp1 (rblgG)	Coverage exp2 (1263)	Coverage exp2 (rblgG)
Q96CN7	Isochorismatase domain-containing protein 1 OS=Homo sapiens OX=9606 GN=ISOC1 PE=1 SV=3 - [ISOC1_HUMAN]				14,77
P50213	Isocitrate dehydrogenase [NAD] subunit alpha, mitochondrial OS=Homo sapiens OX=9606 GN=IDH3A PE=1 SV=1 - [IDH3A_HUMAN]				9,56
O75874	Isocitrate dehydrogenase [NADP] cytoplasmic OS=Homo sapiens GN=IDH1 PE=1 SV=2 - [IDHC_HUMAN]				6,28
P48735	Isocitrate dehydrogenase [NADP], mitochondrial OS=Homo sapiens GN=IDH2 PE=1 SV=2 - [IDHP_HUMAN]			15,71	16,81
P14923	Junction plakoglobin OS=Homo sapiens GN=JUP PE=1 SV=3 - [PLAK_HUMAN]		8,19	11,54	11,41
Q9Y624	Junctional adhesion molecule A OS=Homo sapiens OX=9606 GN=F11R PE=1 SV=1 - [JAM1_HUMAN]			5,69	22,41
Q9BX67	Junctional adhesion molecule C OS=Homo sapiens OX=9606 GN=JAM3 PE=1 SV=1 - [JAM3_HUMAN]				9,03
P13645	Keratin, type I cytoskeletal 10 OS=Homo sapiens GN=KRT10 PE=1 SV=6 - [K1C10_HUMAN]	59,93	64,04	57,71	65,41
P02533	Keratin, type I cytoskeletal 14 OS=Homo sapiens GN=KRT14 PE=1 SV=4 - [K1C14_HUMAN]	41,53	52,33	59,96	48,94
P08779	Keratin, type I cytoskeletal 16 OS=Homo sapiens GN=KRT16 PE=1 SV=4 - [K1C16_HUMAN]	34,46	49,68	54,55	49,05
Q04695	Keratin, type I cytoskeletal 17 OS=Homo sapiens GN=KRT17 PE=1 SV=2 - [K1C17_HUMAN]	25,93	32,41	52,08	23,84
P35527	Keratin, type I cytoskeletal 9 OS=Homo sapiens GN=KRT9 PE=1 SV=3 - [K1C9_HUMAN]	64,85	62,60	69,18	77,05
P04264	Keratin, type II cytoskeletal 1 OS=Homo sapiens GN=KRT1 PE=1 SV=6 - [K2C1_HUMAN]	62,73	67,55	69,57	71,43
Q7Z794	Keratin, type II cytoskeletal 1b OS=Homo sapiens GN=KRT77 PE=1 SV=3 - [K2C1B_HUMAN]	7,44	16,78	20,07	14,01
P35908	Keratin, type II cytoskeletal 2 epidermal OS=Homo sapiens GN=KRT2 PE=1 SV=2 - [K22E_HUMAN]	73,40	81,85	77,00	71,21
Q01546	Keratin, type II cytoskeletal 2 oral OS=Homo sapiens GN=KRT76 PE=1 SV=2 - [K22O_HUMAN]			13,17	
P13647	Keratin, type II cytoskeletal 5 OS=Homo sapiens GN=KRT5 PE=1 SV=3 - [K2C5_HUMAN]	44,07	45,42	52,71	45,42
P02538	Keratin, type II cytoskeletal 6A OS=Homo sapiens GN=KRT6A PE=1 SV=3 - [K2C6A_HUMAN]	36,52	43,97	57,09	40,07
P04259	Keratin, type II cytoskeletal 6B OS=Homo sapiens GN=KRT6B PE=1 SV=5 - [K2C6B_HUMAN]	34,75	40,60	57,09	33,69
Q8N1N4	Keratin, type II cytoskeletal 78 OS=Homo sapiens GN=KRT78 PE=2 SV=2 - [K2C78_HUMAN]			19,23	6,92
Q5XKE5	Keratin, type II cytoskeletal 79 OS=Homo sapiens GN=KRT79 PE=1 SV=2 - [K2C79_HUMAN]			22,62	
Q6KB66	Keratin, type II cytoskeletal 80 OS=Homo sapiens GN=KRT80 PE=1 SV=2 - [K2C80_HUMAN]			14,38	

SUPPLEMENTARY DATA AND INFORMATION

Accession	Description	Coverage exp1 (1263)	Coverage exp1 (rblgG)	Coverage exp2 (1263)	Coverage exp2 (rblgG)
Q5T749	Keratinocyte proline-rich protein OS=Homo sapiens GN=KPRP PE=1 SV=1 - [KPRP_HUMAN]	8,12	15,89	22,11	23,14
P33176	Kinesin-1 heavy chain OS=Homo sapiens GN=KIF5B PE=1 SV=1 - [KINH_HUMAN]				3,53
O00139	Kinesin-like protein KIF2A OS=Homo sapiens GN=KIF2A PE=1 SV=3 - [KIF2A_HUMAN]				2,83
P01042	Kininogen-1 OS=Homo sapiens GN=KNG1 PE=1 SV=2 - [KNG1_HUMAN]	9,01	11,80		14,91
P02788	Lactotransferrin OS=Homo sapiens GN=LTF PE=1 SV=6 - [TRFL_HUMAN]		10,14		3,80
Q14766	Latent-transforming growth factor beta-binding protein 1 OS=Homo sapiens GN=LTBP1 PE=1 SV=4 - [LTBP1_HUMAN]				17,08
Q9Y608	Leucine-rich repeat flightless-interacting protein 2 OS=Homo sapiens GN=LRRFIP2 PE=1 SV=1 - [LRRF2_HUMAN]				8,04
P30740	Leukocyte elastase inhibitor OS=Homo sapiens GN=SERPINB1 PE=1 SV=1 - [ILEU_HUMAN]			12,93	11,87
Q08722	Leukocyte surface antigen CD47 OS=Homo sapiens OX=9606 GN=CD47 PE=1 SV=1 - [CD47_HUMAN]				5,88
P48059	LIM and senescent cell antigen-like-containing domain protein 1 OS=Homo sapiens GN=LIMS1 PE=1 SV=4 - [LIMS1_HUMAN]	7,08			39,08
P31025	Lipocalin-1 OS=Homo sapiens GN=LCN1 PE=1 SV=1 - [LCN1_HUMAN]		13,64		12,50
P50851	Lipopolysaccharide-responsive and beige-like anchor protein OS=Homo sapiens GN=LRBA PE=1 SV=4 - [LRBA_HUMAN]	1,26		3,91	9,15
P00338	L-lactate dehydrogenase A chain OS=Homo sapiens GN=LDHA PE=1 SV=2 - [LDHA_HUMAN]			24,70	53,61
P07195	L-lactate dehydrogenase B chain OS=Homo sapiens GN=LDHB PE=1 SV=2 - [LDHB_HUMAN]	6,29		35,63	52,40
Q5SQ64	Lymphocyte antigen 6 complex locus protein G6f OS=Homo sapiens OX=9606 GN=LY6G6F PE=1 SV=2 - [LY66F_HUMAN]				16,84
P10619	Lysosomal protective protein OS=Homo sapiens GN=CTSA PE=1 SV=2 - [PPGB_HUMAN]				7,08
P11279	Lysosome-associated membrane glycoprotein 1 OS=Homo sapiens GN=LAMP1 PE=1 SV=3 - [LAMP1_HUMAN]				8,63
P61626	Lysozyme C OS=Homo sapiens GN=LYZ PE=1 SV=1 - [LYSC_HUMAN]	14,19	14,19		18,24
Q9HD23	Magnesium transporter MRS2 homolog, mitochondrial OS=Homo sapiens OX=9606 GN=MRS2 PE=1 SV=1 - [MRS2_HUMAN]			21,90	
Q9H0U3	Magnesium transporter protein 1 OS=Homo sapiens OX=9606 GN=MAGT1 PE=1 SV=1 - [MAGT1_HUMAN]				17,91
Q9H3U5	Major facilitator superfamily domain-containing protein 1 OS=Homo sapiens OX=9606 GN=MFSD1 PE=2 SV=2 - [MFSD1_HUMAN]				4,95

SUPPLEMENTARY DATA AND INFORMATION

Accession	Description	Coverage exp1 (1263)	Coverage exp1 (rblgG)	Coverage exp2 (1263)	Coverage exp2 (rblgG)
P40926	Malate dehydrogenase, mitochondrial OS=Homo sapiens GN=MDH2 PE=1 SV=3 - [MDHM_HUMAN]				20,71
Q14165	Malectin OS=Homo sapiens GN=MLEC PE=1 SV=1 - [MLEC_HUMAN]			8,56	39,73
O00187	Mannan-binding lectin serine protease 2 OS=Homo sapiens GN=MASP2 PE=1 SV=4 - [MASP2_HUMAN]				3,50
P11310	Medium-chain specific acyl-CoA dehydrogenase, mitochondrial OS=Homo sapiens GN=ACADM PE=1 SV=1 - [ACADM_HUMAN]				4,99
O00264	Membrane-associated progesterone receptor component 1 OS=Homo sapiens OX=9606 GN=PGRMC1 PE=1 SV=3 - [PGR1_HUMAN]				46,15
P01033	Metalloproteinase inhibitor 1 OS=Homo sapiens GN=TIMP1 PE=1 SV=1 - [TIMP1_HUMAN]				10,14
Q9UPN3	Microtubule-actin cross-linking factor 1, isoforms 1/2/3/5 OS=Homo sapiens GN=MACF1 PE=1 SV=4 - [MACF1_HUMAN]				4,43
Q15555	Microtubule-associated protein RP/EB family member 2 OS=Homo sapiens GN=MAPRE2 PE=1 SV=1 - [MARE2_HUMAN]			6,12	23,24
Q02978	Mitochondrial 2-oxoglutarate/malate carrier protein OS=Homo sapiens OX=9606 GN=SLC25A11 PE=1 SV=3 - [M2OM_HUMAN]				22,29
Q9Y6C9	Mitochondrial carrier homolog 2 OS=Homo sapiens OX=9606 GN=MTCH2 PE=1 SV=1 - [MTCH2_HUMAN]				17,16
Q9NS69	Mitochondrial import receptor subunit TOM22 homolog OS=Homo sapiens OX=9606 GN=TOMM22 PE=1 SV=3 - [TOM22_HUMAN]				33,80
Q99683	Mitogen-activated protein kinase kinase kinase 5 OS=Homo sapiens GN=MAP3K5 PE=1 SV=1 - [M3K5_HUMAN]	8,37		6,55	
Q9Y3A3	MOB-like protein phocein OS=Homo sapiens OX=9606 GN=MOB4 PE=1 SV=1 - [PHOEN_HUMAN]				19,56
P26038	Moesin OS=Homo sapiens GN=MSN PE=1 SV=3 - [MOES_HUMAN]	4,16		19,58	43,67
O15427	Monocarboxylate transporter 4 OS=Homo sapiens GN=SLC16A3 PE=1 SV=1 - [MOT4_HUMAN]				4,52
Q99685	Monoglyceride lipase OS=Homo sapiens GN=MGLL PE=1 SV=2 - [MGLL_HUMAN]				22,77
P22234	Multifunctional protein ADE2 OS=Homo sapiens GN=PAICS PE=1 SV=3 - [PUR6_HUMAN]				15,29
Q13201	Multimerin-1 OS=Homo sapiens GN=MMRN1 PE=1 SV=3 - [MMRN1_HUMAN]	6,60		12,21	34,28
Q15746	Myosin light chain kinase, smooth muscle OS=Homo sapiens GN=MYLK PE=1 SV=4 - [MYLK_HUMAN]				1,52
P60660	Myosin light polypeptide 6 OS=Homo sapiens GN=MYL6 PE=1 SV=2 - [MYL6_HUMAN]			21,19	62,91

SUPPLEMENTARY DATA AND INFORMATION

Accession	Description	Coverage exp1 (1263)	Coverage exp1 (rblgG)	Coverage exp2 (1263)	Coverage exp2 (rblgG)
Q6WCQ1	Myosin phosphatase Rho-interacting protein OS=Homo sapiens GN=MPRIP PE=1 SV=3 - [MPRIP_HUMAN]	2,83			
P19105	Myosin regulatory light chain 12A OS=Homo sapiens GN=MYL12A PE=1 SV=2 - [ML12A_HUMAN]	39,77		40,35	62,57
P24844	Myosin regulatory light polypeptide 9 OS=Homo sapiens GN=MYL9 PE=1 SV=4 - [MYL9_HUMAN]				50,58
P35749	Myosin-11 OS=Homo sapiens GN=MYH11 PE=1 SV=3 - [MYH11_HUMAN]				8,77
Q7Z406	Myosin-14 OS=Homo sapiens GN=MYH14 PE=1 SV=2 - [MYH14_HUMAN]				5,76
P35579	Myosin-9 OS=Homo sapiens GN=MYH9 PE=1 SV=4 - [MYH9_HUMAN]	20,61	21,12	50,46	64,74
P58546	Myotrophin OS=Homo sapiens GN=MTPN PE=1 SV=2 - [MTPN_HUMAN]				33,90
Q13423	NAD(P) transhydrogenase, mitochondrial OS=Homo sapiens GN=NNT PE=1 SV=3 - [NNTM_HUMAN]				19,34
Q9UI09	NADH dehydrogenase [ubiquinone] 1 alpha subcomplex subunit 12 OS=Homo sapiens OX=9606 GN=NDUFA12 PE=1 SV=1 - [NDUAC_HUMAN]				26,21
Q9P0J0	NADH dehydrogenase [ubiquinone] 1 alpha subcomplex subunit 13 OS=Homo sapiens GN=NDUFA13 PE=1 SV=3 - [NDUAD_HUMAN]				29,86
Q16795	NADH dehydrogenase [ubiquinone] 1 alpha subcomplex subunit 9, mitochondrial OS=Homo sapiens OX=9606 GN=NDUFA9 PE=1 SV=2 - [NDUA9_HUMAN]				9,28
O96000	NADH dehydrogenase [ubiquinone] 1 beta subcomplex subunit 10 OS=Homo sapiens OX=9606 GN=NDUFB10 PE=1 SV=3 - [NDUBA_HUMAN]				12,21
O95168	NADH dehydrogenase [ubiquinone] 1 beta subcomplex subunit 4 OS=Homo sapiens OX=9606 GN=NDUFB4 PE=1 SV=3 - [NDUB4_HUMAN]				21,71
P17568	NADH dehydrogenase [ubiquinone] 1 beta subcomplex subunit 7 OS=Homo sapiens OX=9606 GN=NDUFB7 PE=1 SV=4 - [NDUB7_HUMAN]				18,25
O95169	NADH dehydrogenase [ubiquinone] 1 beta subcomplex subunit 8, mitochondrial OS=Homo sapiens OX=9606 GN=NDUFB8 PE=1 SV=1 - [NDUB8_HUMAN]				22,58
Q9Y6M9	NADH dehydrogenase [ubiquinone] 1 beta subcomplex subunit 9 OS=Homo sapiens GN=NDUFB9 PE=1 SV=3 - [NDUB9_HUMAN]				20,11
O75489	NADH dehydrogenase [ubiquinone] iron-sulfur protein 3, mitochondrial OS=Homo sapiens GN=NDUFS3 PE=1 SV=1 - [NDUS3_HUMAN]				28,79

SUPPLEMENTARY DATA AND INFORMATION

Accession	Description	Coverage exp1 (1263)	Coverage exp1 (rblgG)	Coverage exp2 (1263)	Coverage exp2 (rblgG)
O43181	NADH dehydrogenase [ubiquinone] iron-sulfur protein 4, mitochondrial OS=Homo sapiens OX=9606 GN=NDUFS4 PE=1 SV=1 - [NDUS4_HUMAN]				12,00
O43920	NADH dehydrogenase [ubiquinone] iron-sulfur protein 5 OS=Homo sapiens GN=NDUFS5 PE=1 SV=3 - [NDUS5_HUMAN]				29,25
O75251	NADH dehydrogenase [ubiquinone] iron-sulfur protein 7, mitochondrial OS=Homo sapiens OX=9606 GN=NDUFS7 PE=1 SV=3 - [NDUS7_HUMAN]				8,45
O00217	NADH dehydrogenase [ubiquinone] iron-sulfur protein 8, mitochondrial OS=Homo sapiens OX=9606 GN=NDUFS8 PE=1 SV=1 - [NDUS8_HUMAN]				10,95
Q9UHQ9	NADH-cytochrome b5 reductase 1 OS=Homo sapiens OX=9606 GN=CYB5R1 PE=1 SV=1 - [NB5R1_HUMAN]				19,02
P00387	NADH-cytochrome b5 reductase 3 OS=Homo sapiens GN=CYB5R3 PE=1 SV=3 - [NB5R3_HUMAN]			20,27	37,21
P28331	NADH-ubiquinone oxidoreductase 75 kDa subunit, mitochondrial OS=Homo sapiens GN=NDUFS1 PE=1 SV=3 - [NDUS1_HUMAN]				6,46
Q9Y2A7	Nck-associated protein 1 OS=Homo sapiens GN=NCKAP1 PE=1 SV=1 - [NCKP1_HUMAN]				2,84
Q6ZNJ1	Neurobeachin-like protein 2 OS=Homo sapiens GN=NBEAL2 PE=1 SV=2 - [NBEL2_HUMAN]				3,89
Q14697	Neutral alpha-glucosidase AB OS=Homo sapiens GN=GANAB PE=1 SV=3 - [GANAB_HUMAN]			5,72	37,18
P15531	Nucleoside diphosphate kinase A OS=Homo sapiens GN=NME1 PE=1 SV=1 - [NDKA_HUMAN]				40,79
P22392	Nucleoside diphosphate kinase B OS=Homo sapiens GN=NME2 PE=1 SV=1 - [NDKB_HUMAN]				40,79
P55209	Nucleosome assembly protein 1-like 1 OS=Homo sapiens GN=NAP1L1 PE=1 SV=1 - [NP1L1_HUMAN]			9,97	27,62
P51575	P2X purinoceptor 1 OS=Homo sapiens GN=P2RX1 PE=1 SV=1 - [P2RX1_HUMAN]				6,77
Q96RD7	Pannexin-1 OS=Homo sapiens OX=9606 GN=PANX1 PE=1 SV=4 - [PANX1_HUMAN]				7,28
O00151	PDZ and LIM domain protein 1 OS=Homo sapiens GN=PDLIM1 PE=1 SV=4 - [PDLI1_HUMAN]				7,60
Q9NR12	PDZ and LIM domain protein 7 OS=Homo sapiens GN=PDLIM7 PE=1 SV=1 - [PDLI7_HUMAN]				7,88
P62937	Peptidyl-prolyl cis-trans isomerase A OS=Homo sapiens GN=PPIA PE=1 SV=2 - [PPIA_HUMAN]			17,58	36,97
P23284	Peptidyl-prolyl cis-trans isomerase B OS=Homo sapiens GN=PPIB PE=1 SV=2 - [PPIB_HUMAN]			10,19	16,20
Q06830	Peroxiredoxin-1 OS=Homo sapiens GN=PRDX1 PE=1 SV=1 - [PRDX1_HUMAN]				39,70

SUPPLEMENTARY DATA AND INFORMATION

Accession	Description	Coverage exp1 (1263)	Coverage exp1 (rblgG)	Coverage exp2 (1263)	Coverage exp2 (rblgG)
P32119	Peroxiredoxin-2 OS=Homo sapiens GN=PRDX2 PE=1 SV=5 - [PRDX2_HUMAN]			14,14	14,14
Q13162	Peroxiredoxin-4 OS=Homo sapiens GN=PRDX4 PE=1 SV=1 - [PRDX4_HUMAN]				58,67
P30044	Peroxiredoxin-5, mitochondrial OS=Homo sapiens GN=PRDX5 PE=1 SV=4 - [PRDX5_HUMAN]				15,89
P30041	Peroxiredoxin-6 OS=Homo sapiens GN=PRDX6 PE=1 SV=3 - [PRDX6_HUMAN]			26,34	52,68
P51659	Peroxisomal multifunctional enzyme type 2 OS=Homo sapiens GN=HSD17B4 PE=1 SV=3 - [DHB4_HUMAN]				12,09
Q00325	Phosphate carrier protein, mitochondrial OS=Homo sapiens GN=SLC25A3 PE=1 SV=2 - [MPCP_HUMAN]			5,25	25,69
P30086	Phosphatidylethanolamine-binding protein 1 OS=Homo sapiens GN=PEBP1 PE=1 SV=3 - [PEBP1_HUMAN]				11,76
Q9NTJ5	Phosphatidylinositide phosphatase SAC1 OS=Homo sapiens GN=SACM1L PE=1 SV=2 - [SAC1_HUMAN]				14,48
P48739	Phosphatidylinositol transfer protein beta isoform OS=Homo sapiens GN=PITPNB PE=1 SV=2 - [PIPNB_HUMAN]				8,12
P48426	Phosphatidylinositol-5-phosphate 4-kinase type-2 alpha OS=Homo sapiens GN=PIP4K2A PE=1 SV=2 - [PI42A_HUMAN]				13,79
P00558	Phosphoglycerate kinase 1 OS=Homo sapiens GN=PGK1 PE=1 SV=3 - [PGK1_HUMAN]	10,07		24,94	6,24
P18669	Phosphoglycerate mutase 1 OS=Homo sapiens GN=PGAM1 PE=1 SV=2 - [PGAM1_HUMAN]				23,23
P36969	Phospholipid hydroperoxide glutathione peroxidase, mitochondrial OS=Homo sapiens GN=GPX4 PE=1 SV=3 - [GPX4_HUMAN]				15,74
Q9Y2Q0	Phospholipid-transporting ATPase IA OS=Homo sapiens OX=9606 GN=ATP8A1 PE=1 SV=1 - [AT8A1_HUMAN]				10,05
P53801	Pituitary tumor-transforming gene 1 protein-interacting protein OS=Homo sapiens OX=9606 GN=PTTG1IP PE=1 SV=1 - [PTTG_HUMAN]				13,89
Q13835	Plakophilin-1 OS=Homo sapiens GN=PKP1 PE=1 SV=2 - [PKP1_HUMAN]		4,42	3,08	3,88
P05155	Plasma protease C1 inhibitor OS=Homo sapiens GN=SERPING1 PE=1 SV=2 - [IC1_HUMAN]	4,80		11,60	19,80
P00747	Plasminogen OS=Homo sapiens GN=PLG PE=1 SV=2 - [PLMN_HUMAN]	8,89	5,43	4,32	26,05
Q9HBL7	Plasminogen receptor (KT) OS=Homo sapiens OX=9606 GN=PLGRKT PE=1 SV=1 - [PLRKT_HUMAN]				27,21
P02775	Platelet basic protein OS=Homo sapiens GN=PPBP PE=1 SV=3 - [CXCL7_HUMAN]		33,59		27,34

SUPPLEMENTARY DATA AND INFORMATION

Accession	Description	Coverage exp1 (1263)	Coverage exp1 (rblgG)	Coverage exp2 (1263)	Coverage exp2 (rblgG)
P16284	Platelet endothelial cell adhesion molecule OS=Homo sapiens OX=9606 GN=PECAM1 PE=1 SV=2 - [PECA1_HUMAN]	4,34		14,36	35,23
P02776	Platelet factor 4 OS=Homo sapiens GN=PF4 PE=1 SV=2 - [PLF4_HUMAN]				42,57
P16671	Platelet glycoprotein 4 OS=Homo sapiens GN=CD36 PE=1 SV=2 - [CD36_HUMAN]	6,57		9,96	18,43
P07359	Platelet glycoprotein Ib alpha chain OS=Homo sapiens OX=9606 GN=GP1BA PE=1 SV=2 - [GP1BA_HUMAN]			17,18	19,02
P13224	Platelet glycoprotein Ib beta chain OS=Homo sapiens GN=GP1BB PE=1 SV=1 - [GP1BB_HUMAN]	10,68			19,90
P14770	Platelet glycoprotein IX OS=Homo sapiens GN=GP9 PE=1 SV=3 - [GPIX_HUMAN]				32,20
P40197	Platelet glycoprotein V OS=Homo sapiens GN=GP5 PE=1 SV=1 - [GPV_HUMAN]				37,86
P08567	Pleckstrin OS=Homo sapiens GN=PLEK PE=1 SV=3 - [PLEK_HUMAN]			32,29	39,71
Q15149	Plectin OS=Homo sapiens GN=PLEC PE=1 SV=3 - [PLEC_HUMAN]			0,75	4,55
Q15365	Poly(rC)-binding protein 1 OS=Homo sapiens GN=PCBP1 PE=1 SV=2 - [PCBP1_HUMAN]				16,29
P0CG48	Polyubiquitin-C OS=Homo sapiens GN=UBC PE=1 SV=3 - [UBC_HUMAN]	49,93		32,85	32,85
O60831	PRA1 family protein 2 OS=Homo sapiens OX=9606 GN=PRAF2 PE=1 SV=1 - [PRAF2_HUMAN]				26,40
O75915	PRA1 family protein 3 OS=Homo sapiens GN=ARL6IP5 PE=1 SV=1 - [PRAF3_HUMAN]			15,96	23,40
Q99471	Prefoldin subunit 5 OS=Homo sapiens OX=9606 GN=PFDN5 PE=1 SV=2 - [PFD5_HUMAN]				25,97
Q93008	Probable ubiquitin carboxyl-terminal hydrolase FAF-X OS=Homo sapiens GN=USP9X PE=1 SV=3 - [USP9X_HUMAN]			0,86	0,74
P07737	Profilin-1 OS=Homo sapiens GN=PFN1 PE=1 SV=2 - [PROF1_HUMAN]	21,43	31,43	40,00	69,29
Q8WUM4	Programmed cell death 6-interacting protein OS=Homo sapiens GN=PDCD6IP PE=1 SV=1 - [PDC6I_HUMAN]				3,46
Q9BUL8	Programmed cell death protein 10 OS=Homo sapiens GN=PDCD10 PE=1 SV=1 - [PDC10_HUMAN]				19,81
P35232	Prohibitin OS=Homo sapiens GN=PHB PE=1 SV=1 - [PHB_HUMAN]				29,41
Q99623	Prohibitin-2 OS=Homo sapiens GN=PHB2 PE=1 SV=2 - [PHB2_HUMAN]				28,09
P12273	Prolactin-inducible protein OS=Homo sapiens GN=PIP PE=1 SV=1 - [PIP_HUMAN]	15,07	15,07	17,12	21,23

SUPPLEMENTARY DATA AND INFORMATION

Accession	Description	Coverage exp1 (1263)	Coverage exp1 (rblgG)	Coverage exp2 (1263)	Coverage exp2 (rblgG)
Q9H939	Proline-serine-threonine phosphatase-interacting protein 2 OS=Homo sapiens OX=9606 GN=PSTPIP2 PE=1 SV=4 - [PPIP2_HUMAN]				11,68
P23219	Prostaglandin G/H synthase 1 OS=Homo sapiens GN=PTGS1 PE=1 SV=2 - [PGH1_HUMAN]				15,69
Q06323	Proteasome activator complex subunit 1 OS=Homo sapiens GN=PSME1 PE=1 SV=1 - [PSME1_HUMAN]				44,18
Q9UL46	Proteasome activator complex subunit 2 OS=Homo sapiens GN=PSME2 PE=1 SV=4 - [PSME2_HUMAN]				42,26
P25786	Proteasome subunit alpha type-1 OS=Homo sapiens GN=PSMA1 PE=1 SV=1 - [PSA1_HUMAN]			10,65	38,78
P25787	Proteasome subunit alpha type-2 OS=Homo sapiens GN=PSMA2 PE=1 SV=2 - [PSA2_HUMAN]				45,73
P25788	Proteasome subunit alpha type-3 OS=Homo sapiens GN=PSMA3 PE=1 SV=2 - [PSA3_HUMAN]				30,59
P25789	Proteasome subunit alpha type-4 OS=Homo sapiens GN=PSMA4 PE=1 SV=1 - [PSA4_HUMAN]				32,18
P28066	Proteasome subunit alpha type-5 OS=Homo sapiens GN=PSMA5 PE=1 SV=3 - [PSA5_HUMAN]				46,47
P60900	Proteasome subunit alpha type-6 OS=Homo sapiens GN=PSMA6 PE=1 SV=1 - [PSA6_HUMAN]				42,28
O14818	Proteasome subunit alpha type-7 OS=Homo sapiens GN=PSMA7 PE=1 SV=1 - [PSA7_HUMAN]			16,13	53,23
P20618	Proteasome subunit beta type-1 OS=Homo sapiens GN=PSMB1 PE=1 SV=2 - [PSB1_HUMAN]				34,85
P40306	Proteasome subunit beta type-10 OS=Homo sapiens OX=9606 GN=PSMB10 PE=1 SV=1 - [PSB10_HUMAN]				10,99
P49721	Proteasome subunit beta type-2 OS=Homo sapiens GN=PSMB2 PE=1 SV=1 - [PSB2_HUMAN]				27,86
P49720	Proteasome subunit beta type-3 OS=Homo sapiens GN=PSMB3 PE=1 SV=2 - [PSB3_HUMAN]				19,02
P28070	Proteasome subunit beta type-4 OS=Homo sapiens GN=PSMB4 PE=1 SV=4 - [PSB4_HUMAN]				37,50
P28074	Proteasome subunit beta type-5 OS=Homo sapiens OX=9606 GN=PSMB5 PE=1 SV=3 - [PSB5_HUMAN]				9,51
P28072	Proteasome subunit beta type-6 OS=Homo sapiens GN=PSMB6 PE=1 SV=4 - [PSB6_HUMAN]				12,97
Q99436	Proteasome subunit beta type-7 OS=Homo sapiens OX=9606 GN=PSMB7 PE=1 SV=1 - [PSB7_HUMAN]				21,30
P28062	Proteasome subunit beta type-8 OS=Homo sapiens OX=9606 GN=PSMB8 PE=1 SV=3 - [PSB8_HUMAN]				25,36
P28065	Proteasome subunit beta type-9 OS=Homo sapiens OX=9606 GN=PSMB9 PE=1 SV=2 - [PSB9_HUMAN]				21,00

SUPPLEMENTARY DATA AND INFORMATION

Accession	Description	Coverage exp1 (1263)	Coverage exp1 (rblgG)	Coverage exp2 (1263)	Coverage exp2 (rblgG)
P02760	Protein AMBP OS=Homo sapiens GN=AMBP PE=1 SV=1 - [AMBP_HUMAN]			9,38	30,40
O60610	Protein diaphanous homolog 1 OS=Homo sapiens GN=DIAPH1 PE=1 SV=2 - [DIAP1_HUMAN]			4,17	25,08
P30101	Protein disulfide-isomerase A3 OS=Homo sapiens GN=PDIA3 PE=1 SV=4 - [PDIA3_HUMAN]	7,52		18,22	42,77
P13667	Protein disulfide-isomerase A4 OS=Homo sapiens GN=PDIA4 PE=1 SV=2 - [PDIA4_HUMAN]			9,77	21,71
Q15084	Protein disulfide-isomerase A6 OS=Homo sapiens GN=PDIA6 PE=1 SV=1 - [PDIA6_HUMAN]			12,95	23,86
P07237	Protein disulfide-isomerase OS=Homo sapiens GN=P4HB PE=1 SV=3 - [PDIA1_HUMAN]			11,22	30,12
Q99497	Protein DJ-1 OS=Homo sapiens GN=PARK7 PE=1 SV=2 - [PARK7_HUMAN]				44,44
Q96A26	Protein FAM162A OS=Homo sapiens GN=FAM162A PE=1 SV=2 - [F162A_HUMAN]				22,73
Q13045	Protein flightless-1 homolog OS=Homo sapiens GN=FLII PE=1 SV=2 - [FLII_HUMAN]				2,92
O95866	Protein G6b OS=Homo sapiens GN=G6B PE=1 SV=1 - [G6B_HUMAN]				16,60
Q8N5M9	Protein jagunal homolog 1 OS=Homo sapiens OX=9606 GN=JAGN1 PE=1 SV=1 - [JAGN1_HUMAN]				13,11
Q9UNF0	Protein kinase C and casein kinase substrate in neurons protein 2 OS=Homo sapiens GN=PAC2 PE=1 SV=2 - [PAC2_HUMAN]				10,29
Q96RT1	Protein LAP2 OS=Homo sapiens GN=ERBB2IP PE=1 SV=2 - [LAP2_HUMAN]	2,48			
Q9Y6F6	Protein MRVI1 OS=Homo sapiens OX=9606 GN=MRVI1 PE=1 SV=3 - [MRVI1_HUMAN]			4,76	
O75323	Protein NipSnap homolog 2 OS=Homo sapiens GN=GBAS PE=1 SV=1 - [NIPS2_HUMAN]				8,04
Q9UFN0	Protein NipSnap homolog 3A OS=Homo sapiens GN=NIPSNAP3A PE=1 SV=2 - [NPS3A_HUMAN]				47,37
P35813	Protein phosphatase 1A OS=Homo sapiens GN=PPM1A PE=1 SV=1 - [PPM1A_HUMAN]				5,50
P31151	Protein S100-A7 OS=Homo sapiens GN=S100A7 PE=1 SV=4 - [S10A7_HUMAN]			33,66	
Q92734	Protein TFG OS=Homo sapiens OX=9606 GN=TFG PE=1 SV=2 - [TFG_HUMAN]				11,75
Q15436	Protein transport protein Sec23A OS=Homo sapiens GN=SEC23A PE=1 SV=2 - [SC23A_HUMAN]				5,36
Q70J99	Protein unc-13 homolog D OS=Homo sapiens GN=UNC13D PE=1 SV=1 - [UN13D_HUMAN]	4,68		11,28	32,20
Q9H3U1	Protein unc-45 homolog A OS=Homo sapiens GN=UNC45A PE=1 SV=1 - [UN45A_HUMAN]				12,18
Q08188	Protein-glutamine gamma-glutamyltransferase E OS=Homo sapiens GN=TGM3 PE=1 SV=4 - [TGM3_HUMAN]	4,91	9,09	6,64	

SUPPLEMENTARY DATA AND INFORMATION

Accession	Description	Coverage exp1 (1263)	Coverage exp1 (rblgG)	Coverage exp2 (1263)	Coverage exp2 (rblgG)
Q92954	Proteoglycan 4 OS=Homo sapiens OX=9606 GN=PRG4 PE=1 SV=3 - [PRG4_HUMAN]				1,92
Q04941	Proteolipid protein 2 OS=Homo sapiens GN=PLP2 PE=1 SV=1 - [PLP2_HUMAN]				18,42
P00734	Prothrombin OS=Homo sapiens GN=F2 PE=1 SV=2 - [THRB_HUMAN]			12,22	19,61
P12931	Proto-oncogene tyrosine-protein kinase Src OS=Homo sapiens GN=SRC PE=1 SV=3 - [SRC_HUMAN]			3,36	17,35
P16109	P-selectin OS=Homo sapiens GN=SELP PE=1 SV=3 - [LYAM3_HUMAN]	6,87		11,81	41,20
P00491	Purine nucleoside phosphorylase OS=Homo sapiens GN=PNP PE=1 SV=2 - [PNPH_HUMAN]			23,18	56,75
P55786	Puromycin-sensitive aminopeptidase OS=Homo sapiens GN=NPEPPS PE=1 SV=2 - [PSA_HUMAN]				11,10
Q8IZP2	Putative protein FAM10A4 OS=Homo sapiens GN=ST13P4 PE=5 SV=1 - [ST134_HUMAN]				11,25
P0DMQ5	Putative transmembrane protein INAFM2 OS=Homo sapiens OX=9606 GN=INAFM2 PE=2 SV=1 - [INAM2_HUMAN]	15,69			
P08559	Pyruvate dehydrogenase E1 component subunit alpha, somatic form, mitochondrial OS=Homo sapiens GN=PDHA1 PE=1 SV=3 - [ODPA_HUMAN]				4,62
P14618	Pyruvate kinase isozymes M1/M2 OS=Homo sapiens GN=PKM2 PE=1 SV=4 - [KPYM_HUMAN]	18,08		41,43	66,29
P31150	Rab GDP dissociation inhibitor alpha OS=Homo sapiens GN=GDI1 PE=1 SV=2 - [GDIA_HUMAN]			8,50	23,49
P50395	Rab GDP dissociation inhibitor beta OS=Homo sapiens GN=GDI2 PE=1 SV=2 - [GDIB_HUMAN]				17,08
Q14644	Ras GTPase-activating protein 3 OS=Homo sapiens GN=RASA3 PE=1 SV=3 - [RASA3_HUMAN]				22,18
Q13576	Ras GTPase-activating-like protein IQGAP2 OS=Homo sapiens GN=IQGAP2 PE=1 SV=4 - [IQGA2_HUMAN]			2,41	25,46
Q15404	Ras suppressor protein 1 OS=Homo sapiens GN=RSU1 PE=1 SV=3 - [RSU1_HUMAN]			20,94	55,23
P15153	Ras-related C3 botulinum toxin substrate 2 OS=Homo sapiens GN=RAC2 PE=1 SV=1 - [RAC2_HUMAN]				27,08
P61026	Ras-related protein Rab-10 OS=Homo sapiens GN=RAB10 PE=1 SV=1 - [RAB10_HUMAN]	17,00		26,50	52,00
Q15907	Ras-related protein Rab-11B OS=Homo sapiens GN=RAB11B PE=1 SV=4 - [RB11B_HUMAN]	10,55		20,64	59,17
P51153	Ras-related protein Rab-13 OS=Homo sapiens GN=RAB13 PE=1 SV=1 - [RAB13_HUMAN]				23,15
P61106	Ras-related protein Rab-14 OS=Homo sapiens GN=RAB14 PE=1 SV=4 - [RAB14_HUMAN]				41,40
P62820	Ras-related protein Rab-1A OS=Homo sapiens GN=RAB1A PE=1 SV=3 - [RAB1A_HUMAN]				64,39

SUPPLEMENTARY DATA AND INFORMATION

Accession	Description	Coverage exp1 (1263)	Coverage exp1 (rblgG)	Coverage exp2 (1263)	Coverage exp2 (rblgG)
Q9H0U4	Ras-related protein Rab-1B OS=Homo sapiens GN=RAB1B PE=1 SV=1 - [RAB1B_HUMAN]	45,77		35,32	71,64
O00194	Ras-related protein Rab-27B OS=Homo sapiens GN=RAB27B PE=1 SV=4 - [RB27B_HUMAN]			19,72	56,42
P61019	Ras-related protein Rab-2A OS=Homo sapiens GN=RAB2A PE=1 SV=1 - [RAB2A_HUMAN]				17,92
Q13637	Ras-related protein Rab-32 OS=Homo sapiens GN=RAB32 PE=1 SV=3 - [RAB32_HUMAN]				40,89
Q96AX2	Ras-related protein Rab-37 OS=Homo sapiens GN=RAB37 PE=1 SV=3 - [RAB37_HUMAN]				30,04
P61018	Ras-related protein Rab-4B OS=Homo sapiens GN=RAB4B PE=1 SV=1 - [RAB4B_HUMAN]				18,31
P61020	Ras-related protein Rab-5B OS=Homo sapiens GN=RAB5B PE=1 SV=1 - [RAB5B_HUMAN]				22,33
P51148	Ras-related protein Rab-5C OS=Homo sapiens GN=RAB5C PE=1 SV=2 - [RAB5C_HUMAN]			16,20	54,17
P20340	Ras-related protein Rab-6A OS=Homo sapiens GN=RAB6A PE=1 SV=3 - [RAB6A_HUMAN]				34,62
Q9NRW1	Ras-related protein Rab-6B OS=Homo sapiens GN=RAB6B PE=1 SV=1 - [RAB6B_HUMAN]			10,10	50,00
P51149	Ras-related protein Rab-7a OS=Homo sapiens GN=RAB7A PE=1 SV=1 - [RAB7A_HUMAN]	13,53	13,04	25,12	57,49
P61006	Ras-related protein Rab-8A OS=Homo sapiens GN=RAB8A PE=1 SV=1 - [RAB8A_HUMAN]				30,92
Q92930	Ras-related protein Rab-8B OS=Homo sapiens GN=RAB8B PE=1 SV=2 - [RAB8B_HUMAN]				31,88
P11234	Ras-related protein Ral-B OS=Homo sapiens GN=RALB PE=1 SV=1 - [RALB_HUMAN]				33,98
P62834	Ras-related protein Rap-1A OS=Homo sapiens GN=RAP1A PE=1 SV=1 - [RAP1A_HUMAN]				65,22
P61224	Ras-related protein Rap-1b OS=Homo sapiens GN=RAP1B PE=1 SV=1 - [RAP1B_HUMAN]	51,63	13,59	45,11	79,35
P61225	Ras-related protein Rap-2b OS=Homo sapiens GN=RAP2B PE=1 SV=1 - [RAP2B_HUMAN]				35,52
Q00765	Receptor expression-enhancing protein 5 OS=Homo sapiens GN=REEP5 PE=1 SV=3 - [REEP5_HUMAN]				15,34
Q12913	Receptor-type tyrosine-protein phosphatase eta OS=Homo sapiens GN=PTPRJ PE=1 SV=3 - [PTPRJ_HUMAN]			1,57	20,12
Q9NS28	Regulator of G-protein signaling 18 OS=Homo sapiens OX=9606 GN=RGS18 PE=1 SV=1 - [RGS18_HUMAN]				8,51
Q16799	Reticulon-1 OS=Homo sapiens GN=RTN1 PE=1 SV=1 - [RTN1_HUMAN]				7,47
O75298	Reticulon-2 OS=Homo sapiens OX=9606 GN=RTN2 PE=1 SV=1 - [RTN2_HUMAN]				7,89
O95197	Reticulon-3 OS=Homo sapiens GN=RTN3 PE=1 SV=2 - [RTN3_HUMAN]				2,62

SUPPLEMENTARY DATA AND INFORMATION

Accession	Description	Coverage exp1 (1263)	Coverage exp1 (rblgG)	Coverage exp2 (1263)	Coverage exp2 (rblgG)
Q9NQC3	Reticulon-4 OS=Homo sapiens OX=9606 GN=RTN4 PE=1 SV=2 - [RTN4_HUMAN]				10,91
Q8TC12	Retinol dehydrogenase 11 OS=Homo sapiens OX=9606 GN=RDH11 PE=1 SV=2 - [RDH11_HUMAN]			8,18	31,45
P02753	Retinol-binding protein 4 OS=Homo sapiens GN=RBP4 PE=1 SV=3 - [RET4_HUMAN]				15,92
P52565	Rho GDP-dissociation inhibitor 1 OS=Homo sapiens GN=ARHGDI1A PE=1 SV=3 - [GDIR1_HUMAN]				24,51
P52566	Rho GDP-dissociation inhibitor 2 OS=Homo sapiens GN=ARHGDI1B PE=1 SV=3 - [GDIR2_HUMAN]				33,83
Q8N392	Rho GTPase-activating protein 18 OS=Homo sapiens GN=ARHGAP18 PE=1 SV=3 - [RHG18_HUMAN]				6,18
Q14155	Rho guanine nucleotide exchange factor 7 OS=Homo sapiens GN=ARHGEF7 PE=1 SV=2 - [ARHG7_HUMAN]	12,70		31,63	
O75116	Rho-associated protein kinase 2 OS=Homo sapiens GN=ROCK2 PE=1 SV=4 - [ROCK2_HUMAN]				25,50
P08134	Rho-related GTP-binding protein RhoC OS=Homo sapiens GN=RHO C PE=1 SV=1 - [RHO C_HUMAN]	16,58		12,95	27,98
P84095	Rho-related GTP-binding protein RhoG OS=Homo sapiens GN=RHO G PE=1 SV=1 - [RHO G_HUMAN]				24,61
P13489	Ribonuclease inhibitor OS=Homo sapiens GN=RNH1 PE=1 SV=2 - [RINI_HUMAN]				6,51
Q14BN4	Sarcolemmal membrane-associated protein OS=Homo sapiens GN=SLMAP PE=1 SV=1 - [SLMAP_HUMAN]				5,19
O14983	Sarcoplasmic/endoplasmic reticulum calcium ATPase 1 OS=Homo sapiens GN=ATP2A1 PE=1 SV=1 - [AT2A1_HUMAN]				17,18
P16615	Sarcoplasmic/endoplasmic reticulum calcium ATPase 2 OS=Homo sapiens GN=ATP2A2 PE=1 SV=1 - [AT2A2_HUMAN]			11,61	34,07
Q93084	Sarcoplasmic/endoplasmic reticulum calcium ATPase 3 OS=Homo sapiens GN=ATP2A3 PE=1 SV=2 - [AT2A3_HUMAN]	7,38		14,09	40,17
O60613	Selenoprotein F OS=Homo sapiens OX=9606 GN=SELENOF PE=1 SV=4 - [SEP15_HUMAN]				16,97
P04279	Semenogelin-1 OS=Homo sapiens GN=SEMG1 PE=1 SV=2 - [SEMG1_HUMAN]				7,36
Q9NVA2	Septin-11 OS=Homo sapiens GN=SEPT11 PE=1 SV=3 - [SEP11_HUMAN]			4,66	17,25
Q15019	Septin-2 OS=Homo sapiens OX=9606 GN=SEPT2 PE=1 SV=1 - [SEPT2_HUMAN]			7,76	23,82
Q14141	Septin-6 OS=Homo sapiens GN=SEPT6 PE=1 SV=4 - [SEPT6_HUMAN]			4,61	24,19
Q16181	Septin-7 OS=Homo sapiens GN=SEPT7 PE=1 SV=2 - [SEPT7_HUMAN]				26,54

SUPPLEMENTARY DATA AND INFORMATION

Accession	Description	Coverage exp1 (1263)	Coverage exp1 (rblgG)	Coverage exp2 (1263)	Coverage exp2 (rblgG)
P10124	Serglycin OS=Homo sapiens OX=9606 GN=SRGN PE=1 SV=3 - [SRGN_HUMAN]			17,09	17,09
Q13177	Serine/threonine-protein kinase PAK 2 OS=Homo sapiens OX=9606 GN=PAK2 PE=1 SV=3 - [PAK2_HUMAN]	20,23		9,16	
P30153	Serine/threonine-protein phosphatase 2A 65 kDa regulatory subunit A alpha isoform OS=Homo sapiens GN=PPP2R1A PE=1 SV=4 - [2AAA_HUMAN]				14,43
Q96HS1	Serine/threonine-protein phosphatase PGAM5, mitochondrial OS=Homo sapiens OX=9606 GN=PGAM5 PE=1 SV=2 - [PGAM5_HUMAN]			7,61	
P62136	Serine/threonine-protein phosphatase PP1-alpha catalytic subunit OS=Homo sapiens GN=PPP1CA PE=1 SV=1 - [PP1A_HUMAN]				10,91
P02787	Serotransferrin OS=Homo sapiens GN=TF PE=1 SV=3 - [TRFE_HUMAN]	52,44	36,10	50,57	64,47
Q96P63	Serpin B12 OS=Homo sapiens GN=SERPINB12 PE=1 SV=1 - [SPB12_HUMAN]			8,15	4,20
P29508	Serpin B3 OS=Homo sapiens GN=SERPINB3 PE=1 SV=2 - [SPB3_HUMAN]		20,51	17,69	
P35237	Serpin B6 OS=Homo sapiens GN=SERPINB6 PE=1 SV=3 - [SPB6_HUMAN]				10,11
P02768	Serum albumin OS=Homo sapiens GN=ALB PE=1 SV=2 - [ALBU_HUMAN]	75,37	77,01	78,65	77,83
P35542	Serum amyloid A-4 protein OS=Homo sapiens GN=SAA4 PE=1 SV=2 - [SAA4_HUMAN]				14,62
P02743	Serum amyloid P-component OS=Homo sapiens GN=APCS PE=1 SV=2 - [SAMP_HUMAN]	34,08	19,28	28,70	31,84
O95810	Serum deprivation-response protein OS=Homo sapiens GN=SDPR PE=1 SV=3 - [SDPR_HUMAN]			6,12	32,94
P27169	Serum paraoxonase/arylesterase 1 OS=Homo sapiens GN=PON1 PE=1 SV=3 - [PON1_HUMAN]				23,10
O75368	SH3 domain-binding glutamic acid-rich-like protein OS=Homo sapiens OX=9606 GN=SH3BGR1 PE=1 SV=1 - [SH3L1_HUMAN]				20,18
Q9Y210	Short transient receptor potential channel 6 OS=Homo sapiens OX=9606 GN=TRPC6 PE=1 SV=1 - [TRPC6_HUMAN]	43,07		40,71	
Q9H9B4	Sideroflexin-1 OS=Homo sapiens OX=9606 GN=SFXN1 PE=1 SV=4 - [SFXN1_HUMAN]				6,83
Q9BWM7	Sideroflexin-3 OS=Homo sapiens OX=9606 GN=SFXN3 PE=1 SV=3 - [SFXN3_HUMAN]				11,53
P67812	Signal peptidase complex catalytic subunit SEC11A OS=Homo sapiens GN=SEC11A PE=1 SV=1 - [SC11A_HUMAN]				15,64
Q15005	Signal peptidase complex subunit 2 OS=Homo sapiens GN=SPCS2 PE=1 SV=3 - [SPCS2_HUMAN]				45,58
P61009	Signal peptidase complex subunit 3 OS=Homo sapiens OX=9606 GN=SPCS3 PE=1 SV=1 - [SPCS3_HUMAN]				21,67

SUPPLEMENTARY DATA AND INFORMATION

Accession	Description	Coverage exp1 (1263)	Coverage exp1 (rblgG)	Coverage exp2 (1263)	Coverage exp2 (rblgG)
P40763	Signal transducer and activator of transcription 3 OS=Homo sapiens GN=STAT3 PE=1 SV=2 - [STAT3_HUMAN]				8,83
Q04837	Single-stranded DNA-binding protein, mitochondrial OS=Homo sapiens GN=SSBP1 PE=1 SV=1 - [SSBP_HUMAN]				15,54
Q5T750	Skin-specific protein 32 OS=Homo sapiens GN=XP32 PE=1 SV=1 - [XP32_HUMAN]		11,20	7,20	22,80
P22531	Small proline-rich protein 2E OS=Homo sapiens GN=SPRR2E PE=2 SV=2 - [SPR2E_HUMAN]				43,06
P05023	Sodium/potassium-transporting ATPase subunit alpha-1 OS=Homo sapiens GN=ATP1A1 PE=1 SV=1 - [AT1A1_HUMAN]			2,44	12,02
P11169	Solute carrier family 2, facilitated glucose transporter member 3 OS=Homo sapiens GN=SLC2A3 PE=1 SV=1 - [GTR3_HUMAN]	4,03		12,70	13,91
P30626	Sorcin OS=Homo sapiens GN=SRI PE=1 SV=1 - [SORCN_HUMAN]				9,60
P09486	SPARC OS=Homo sapiens GN=SPARC PE=1 SV=1 - [SPRC_HUMAN]				16,50
P11277	Spectrin beta chain, erythrocyte OS=Homo sapiens GN=SPTB PE=1 SV=5 - [SPTB1_HUMAN]				7,96
P63208	S-phase kinase-associated protein 1 OS=Homo sapiens GN=SKP1 PE=1 SV=2 - [SKP1_HUMAN]				15,34
Q7KZF4	Staphylococcal nuclease domain-containing protein 1 OS=Homo sapiens GN=SND1 PE=1 SV=1 - [SND1_HUMAN]			3,41	17,25
P38646	Stress-70 protein, mitochondrial OS=Homo sapiens GN=HSPA9 PE=1 SV=2 - [GRP75_HUMAN]				4,57
P31948	Stress-induced-phosphoprotein 1 OS=Homo sapiens GN=STIP1 PE=1 SV=1 - [STIP1_HUMAN]				7,55
Q13586	Stromal interaction molecule 1 OS=Homo sapiens GN=STIM1 PE=1 SV=3 - [STIM1_HUMAN]				9,64
P02814	Submaxillary gland androgen-regulated protein 3B OS=Homo sapiens OX=9606 GN=SMR3B PE=1 SV=2 - [SMR3B_HUMAN]			65,82	
P21912	Succinate dehydrogenase [ubiquinone] iron-sulfur subunit, mitochondrial OS=Homo sapiens OX=9606 GN=SDHB PE=1 SV=3 - [SDHB_HUMAN]				16,07
P04179	Superoxide dismutase [Mn], mitochondrial OS=Homo sapiens OX=9606 GN=SOD2 PE=1 SV=3 - [SODM_HUMAN]			12,61	22,97
O00161	Synaptosomal-associated protein 23 OS=Homo sapiens OX=9606 GN=SNAP23 PE=1 SV=1 - [SNP23_HUMAN]				17,06
Q96C24	Synaptotagmin-like protein 4 OS=Homo sapiens OX=9606 GN=SYTL4 PE=1 SV=2 - [SYTL4_HUMAN]				2,53
O75558	Syntaxin-11 OS=Homo sapiens GN=STX11 PE=2 SV=1 - [STX11_HUMAN]			9,41	44,60

SUPPLEMENTARY DATA AND INFORMATION

Accession	Description	Coverage exp1 (1263)	Coverage exp1 (rblgG)	Coverage exp2 (1263)	Coverage exp2 (rblgG)
Q15833	Syntaxin-binding protein 2 OS=Homo sapiens GN=STXBP2 PE=1 SV=2 - [STXB2_HUMAN]				24,45
Q9Y490	Talin-1 OS=Homo sapiens GN=TLN1 PE=1 SV=3 - [TLN1_HUMAN]	40,97	30,66	63,75	75,29
P17987	T-complex protein 1 subunit alpha OS=Homo sapiens GN=TCP1 PE=1 SV=1 - [TCPA_HUMAN]				16,91
P78371	T-complex protein 1 subunit beta OS=Homo sapiens GN=CCT2 PE=1 SV=4 - [TCPB_HUMAN]				15,51
P50991	T-complex protein 1 subunit delta OS=Homo sapiens GN=CCT4 PE=1 SV=4 - [TCPD_HUMAN]			3,90	19,67
P48643	T-complex protein 1 subunit epsilon OS=Homo sapiens OX=9606 GN=CCT5 PE=1 SV=1 - [TCPE_HUMAN]				16,27
Q99832	T-complex protein 1 subunit eta OS=Homo sapiens GN=CCT7 PE=1 SV=2 - [TCPH_HUMAN]				18,42
P49368	T-complex protein 1 subunit gamma OS=Homo sapiens GN=CCT3 PE=1 SV=4 - [TCPG_HUMAN]				19,27
P50990	T-complex protein 1 subunit theta OS=Homo sapiens GN=CCT8 PE=1 SV=4 - [TCPQ_HUMAN]				17,15
P40227	T-complex protein 1 subunit zeta OS=Homo sapiens GN=CCT6A PE=1 SV=3 - [TCPZ_HUMAN]				21,28
Q8NG11	Tetraspanin-14 OS=Homo sapiens OX=9606 GN=TSPAN14 PE=1 SV=1 - [TSN14_HUMAN]				10,37
Q86UF1	Tetraspanin-33 OS=Homo sapiens OX=9606 GN=TSPAN33 PE=1 SV=1 - [TSN33_HUMAN]				12,72
O75954	Tetraspanin-9 OS=Homo sapiens OX=9606 GN=TSPAN9 PE=1 SV=1 - [TSN9_HUMAN]				9,21
P10599	Thioredoxin OS=Homo sapiens GN=TXN PE=1 SV=3 - [THIO_HUMAN]				20,95
P62341	Thioredoxin reductase-like selenoprotein T OS=Homo sapiens OX=9606 GN=SELENOT PE=1 SV=2 - [SELT_HUMAN]				11,79
P30048	Thioredoxin-dependent peroxide reductase, mitochondrial OS=Homo sapiens GN=PRDX3 PE=1 SV=3 - [PRDX3_HUMAN]				21,48
Q9H3N1	Thioredoxin-related transmembrane protein 1 OS=Homo sapiens OX=9606 GN=TMX1 PE=1 SV=1 - [TMX1_HUMAN]				11,07
Q16762	Thiosulfate sulfurtransferase OS=Homo sapiens OX=9606 GN=TST PE=1 SV=4 - [THTR_HUMAN]				12,46
P26639	Threonine--tRNA ligase, cytoplasmic OS=Homo sapiens GN=TARS PE=1 SV=3 - [SYTC_HUMAN]				17,29
P07996	Thrombospondin-1 OS=Homo sapiens GN=THBS1 PE=1 SV=2 - [TSP1_HUMAN]	16,32	20,85	50,68	68,03
P24557	Thromboxane-A synthase OS=Homo sapiens GN=TBXAS1 PE=1 SV=3 - [THAS_HUMAN]			4,32	25,89
Q9UDY2	Tight junction protein ZO-2 OS=Homo sapiens GN=TJP2 PE=1 SV=2 - [ZO2_HUMAN]	1,34		6,47	1,34

SUPPLEMENTARY DATA AND INFORMATION

Accession	Description	Coverage exp1 (1263)	Coverage exp1 (rblgG)	Coverage exp2 (1263)	Coverage exp2 (rblgG)
O43617	Trafficking protein particle complex subunit 3 OS=Homo sapiens GN=TRAPPC3 PE=1 SV=1 - [TPPC3_HUMAN]				25,56
P37837	Transaldolase OS=Homo sapiens GN=TALDO1 PE=1 SV=2 - [TALDO_HUMAN]			8,90	8,90
Q00577	Transcriptional activator protein Pur-alpha OS=Homo sapiens GN=PURA PE=1 SV=2 - [PURA_HUMAN]			5,90	
P01137	Transforming growth factor beta-1 OS=Homo sapiens GN=TGFB1 PE=1 SV=2 - [TGFB1_HUMAN]				25,90
O43294	Transforming growth factor beta-1-induced transcript 1 protein OS=Homo sapiens GN=TGFB1I1 PE=1 SV=2 - [TGFI1_HUMAN]			4,77	8,24
P61586	Transforming protein RhoA OS=Homo sapiens GN=RHOA PE=1 SV=1 - [RHOA_HUMAN]	16,58		12,95	31,09
P37802	Transgelin-2 OS=Homo sapiens GN=TAGLN2 PE=1 SV=3 - [TAGL2_HUMAN]	23,12	13,07	23,12	66,83
Q9H1D0	Transient receptor potential cation channel subfamily V member 6 OS=Homo sapiens OX=9606 GN=TRPV6 PE=1 SV=3 - [TRPV6_HUMAN]	4,05	4,05		
P55072	Transitional endoplasmic reticulum ATPase OS=Homo sapiens GN=VCP PE=1 SV=4 - [TERA_HUMAN]			17,37	59,80
P29401	Transketolase OS=Homo sapiens GN=TKT PE=1 SV=3 - [TKT_HUMAN]				6,26
Q15631	Translin OS=Homo sapiens GN=TSN PE=1 SV=1 - [TSN_HUMAN]				25,44
Q99598	Translin-associated protein X OS=Homo sapiens OX=9606 GN=TSNAX PE=1 SV=1 - [TSNAX_HUMAN]				12,41
P43307	Translocon-associated protein subunit alpha OS=Homo sapiens OX=9606 GN=SSR1 PE=1 SV=3 - [SSRA_HUMAN]				9,09
P51571	Translocon-associated protein subunit delta OS=Homo sapiens GN=SSR4 PE=1 SV=1 - [SSRD_HUMAN]				30,64
Q9BZW5	Transmembrane 6 superfamily member 1 OS=Homo sapiens OX=9606 GN=TM6SF1 PE=1 SV=2 - [TM6S1_HUMAN]				5,95
P49755	Transmembrane emp24 domain-containing protein 10 OS=Homo sapiens GN=TMED10 PE=1 SV=2 - [TMEDA_HUMAN]				33,79
Q15363	Transmembrane emp24 domain-containing protein 2 OS=Homo sapiens GN=TMED2 PE=1 SV=1 - [TMED2_HUMAN]				27,36
Q7Z7H5	Transmembrane emp24 domain-containing protein 4 OS=Homo sapiens GN=TMED4 PE=1 SV=1 - [TMED4_HUMAN]				19,82
Q9Y3A6	Transmembrane emp24 domain-containing protein 5 OS=Homo sapiens OX=9606 GN=TMED5 PE=1 SV=1 - [TMED5_HUMAN]				9,17

SUPPLEMENTARY DATA AND INFORMATION

Accession	Description	Coverage exp1 (1263)	Coverage exp1 (rblgG)	Coverage exp2 (1263)	Coverage exp2 (rblgG)
Q9Y3B3	Transmembrane emp24 domain-containing protein 7 OS=Homo sapiens GN=TMED7 PE=1 SV=2 - [TMED7_HUMAN]				19,20
Q9BVK6	Transmembrane emp24 domain-containing protein 9 OS=Homo sapiens GN=TMED9 PE=1 SV=2 - [TMED9_HUMAN]				20,00
Q9BVC6	Transmembrane protein 109 OS=Homo sapiens GN=TMEM109 PE=1 SV=1 - [TM109_HUMAN]				8,64
O94886	Transmembrane protein 63A OS=Homo sapiens GN=TMEM63A PE=1 SV=3 - [TM63A_HUMAN]				3,84
Q92973	Transportin-1 OS=Homo sapiens GN=TNPO1 PE=1 SV=2 - [TNPO1_HUMAN]				3,23
Q9Y5L0	Transportin-3 OS=Homo sapiens GN=TNPO3 PE=1 SV=3 - [TNPO3_HUMAN]			6,83	
P02766	Transthyretin OS=Homo sapiens GN=TTR PE=1 SV=1 - [TTHY_HUMAN]			38,78	24,49
Q86YW5	Trem-like transcript 1 protein OS=Homo sapiens GN=TREML1 PE=1 SV=2 - [TRML1_HUMAN]				12,54
P40939	Trifunctional enzyme subunit alpha, mitochondrial OS=Homo sapiens GN=HADHA PE=1 SV=2 - [ECHA_HUMAN]			3,15	32,37
P55084	Trifunctional enzyme subunit beta, mitochondrial OS=Homo sapiens GN=HADHB PE=1 SV=3 - [ECHB_HUMAN]				16,67
P60174	Triosephosphate isomerase OS=Homo sapiens GN=TP11 PE=1 SV=3 - [TPIS_HUMAN]	12,24	9,44	26,57	61,19
Q8NG06	Tripartite motif-containing protein 58 OS=Homo sapiens GN=TRIM58 PE=2 SV=2 - [TRI58_HUMAN]	7,61		7,20	
P29144	Tripeptidyl-peptidase 2 OS=Homo sapiens OX=9606 GN=TPP2 PE=1 SV=4 - [TPP2_HUMAN]				26,34
Q9NYL9	Tropomodulin-3 OS=Homo sapiens GN=TMOD3 PE=1 SV=1 - [TMOD3_HUMAN]				27,27
P09493	Tropomyosin alpha-1 chain OS=Homo sapiens GN=TPM1 PE=1 SV=2 - [TPM1_HUMAN]				43,31
P06753	Tropomyosin alpha-3 chain OS=Homo sapiens OX=9606 GN=TPM3 PE=1 SV=2 - [TPM3_HUMAN]			27,37	39,30
P67936	Tropomyosin alpha-4 chain OS=Homo sapiens GN=TPM4 PE=1 SV=3 - [TPM4_HUMAN]	37,90		48,79	64,11
P07951	Tropomyosin beta chain OS=Homo sapiens GN=TPM2 PE=1 SV=1 - [TPM2_HUMAN]				41,20
P07477	Trypsin-1 OS=Homo sapiens GN=PRSS1 PE=1 SV=1 - [TRY1_HUMAN]			7,29	7,29
Q9BQE3	Tubulin alpha-1C chain OS=Homo sapiens GN=TUBA1C PE=1 SV=1 - [TBA1C_HUMAN]		19,60		60,36
P68366	Tubulin alpha-4A chain OS=Homo sapiens GN=TUBA4A PE=1 SV=1 - [TBA4A_HUMAN]	36,83	21,88	47,99	60,49
Q9NY65	Tubulin alpha-8 chain OS=Homo sapiens GN=TUBA8 PE=1 SV=1 - [TBA8_HUMAN]			36,53	36,53

SUPPLEMENTARY DATA AND INFORMATION

Accession	Description	Coverage exp1 (1263)	Coverage exp1 (rblgG)	Coverage exp2 (1263)	Coverage exp2 (rblgG)
P07437	Tubulin beta chain OS=Homo sapiens GN=TUBB PE=1 SV=2 - [TBB5_HUMAN]	30,18	14,86	44,37	72,30
Q9H4B7	Tubulin beta-1 chain OS=Homo sapiens GN=TUBB1 PE=1 SV=1 - [TBB1_HUMAN]	41,24	28,60	60,31	77,61
P68371	Tubulin beta-4B chain OS=Homo sapiens GN=TUBB4B PE=1 SV=1 - [TBB4B_HUMAN]	26,52		44,27	72,13
Q6IBS0	Twinfilin-2 OS=Homo sapiens GN=TWF2 PE=1 SV=2 - [TWF2_HUMAN]				7,74
P45974	Ubiquitin carboxyl-terminal hydrolase 5 OS=Homo sapiens GN=USP5 PE=1 SV=2 - [UBP5_HUMAN]				5,59
P22314	Ubiquitin-like modifier-activating enzyme 1 OS=Homo sapiens GN=UBA1 PE=1 SV=3 - [UBA1_HUMAN]	3,12		4,16	17,30
P41226	Ubiquitin-like modifier-activating enzyme 7 OS=Homo sapiens GN=UBA7 PE=1 SV=2 - [UBA7_HUMAN]				5,63
Q9NYU2	UDP-glucose glycoprotein glucosyltransferase 1 OS=Homo sapiens GN=UGGT1 PE=1 SV=3 - [UGGG1_HUMAN]			1,54	25,98
O60268	Uncharacterized protein KIAA0513 OS=Homo sapiens OX=9606 GN=KIAA0513 PE=1 SV=1 - [K0513_HUMAN]				6,08
Q92614	Unconventional myosin-XVIIa OS=Homo sapiens GN=MYO18A PE=1 SV=3 - [MY18A_HUMAN]	16,50		31,89	
Q16851	UTP--glucose-1-phosphate uridylyltransferase OS=Homo sapiens GN=UGP2 PE=1 SV=5 - [UGPA_HUMAN]				15,55
Q3ZAQ7	Vacuolar ATPase assembly integral membrane protein VMA21 OS=Homo sapiens OX=9606 GN=VMA21 PE=1 SV=1 - [VMA21_HUMAN]				34,65
Q96RL7	Vacuolar protein sorting-associated protein 13A OS=Homo sapiens GN=VPS13A PE=1 SV=2 - [VP13A_HUMAN]				0,57
Q9UBQ0	Vacuolar protein sorting-associated protein 29 OS=Homo sapiens GN=VPS29 PE=1 SV=1 - [VPS29_HUMAN]				12,64
Q96QK1	Vacuolar protein sorting-associated protein 35 OS=Homo sapiens GN=VPS35 PE=1 SV=2 - [VPS35_HUMAN]				19,97
P50552	Vasodilator-stimulated phosphoprotein OS=Homo sapiens GN=VASP PE=1 SV=3 - [VASP_HUMAN]				18,42
P49748	Very long-chain specific acyl-CoA dehydrogenase, mitochondrial OS=Homo sapiens GN=ACADVL PE=1 SV=1 - [ACADV_HUMAN]				3,21
Q9BV40	Vesicle-associated membrane protein 8 OS=Homo sapiens GN=VAMP8 PE=1 SV=1 - [VAMP8_HUMAN]				18,00
Q9P0L0	Vesicle-associated membrane protein-associated protein A OS=Homo sapiens OX=9606 GN=VAPA PE=1 SV=3 - [VAPA_HUMAN]				12,05
P08670	Vimentin OS=Homo sapiens GN=VIM PE=1 SV=4 - [VIME_HUMAN]				7,94

SUPPLEMENTARY DATA AND INFORMATION

Accession	Description	Coverage exp1 (1263)	Coverage exp1 (rblgG)	Coverage exp2 (1263)	Coverage exp2 (rblgG)
P18206	Vinculin OS=Homo sapiens GN=VCL PE=1 SV=4 - [VINC_HUMAN]	44,89	23,54	54,67	70,37
P02774	Vitamin D-binding protein OS=Homo sapiens GN=GC PE=1 SV=1 - [VTDB_HUMAN]			5,91	22,78
P07225	Vitamin K-dependent protein S OS=Homo sapiens GN=PROS1 PE=1 SV=1 - [PROS_HUMAN]				2,37
P04004	Vitronectin OS=Homo sapiens GN=VTN PE=1 SV=1 - [VTNC_HUMAN]	11,92	9,00	12,55	18,83
P21796	Voltage-dependent anion-selective channel protein 1 OS=Homo sapiens GN=VDAC1 PE=1 SV=2 - [VDAC1_HUMAN]			10,25	38,52
P45880	Voltage-dependent anion-selective channel protein 2 OS=Homo sapiens GN=VDAC2 PE=1 SV=2 - [VDAC2_HUMAN]			8,84	41,16
Q9Y277	Voltage-dependent anion-selective channel protein 3 OS=Homo sapiens GN=VDAC3 PE=1 SV=1 - [VDAC3_HUMAN]			14,13	49,82
P04275	von Willebrand factor OS=Homo sapiens GN=VWF PE=1 SV=4 - [VWF_HUMAN]			3,59	25,31
Q93050	V-type proton ATPase 116 kDa subunit a isoform 1 OS=Homo sapiens GN=ATP6V0A1 PE=1 SV=3 - [VPP1_HUMAN]				3,82
P38606	V-type proton ATPase catalytic subunit A OS=Homo sapiens GN=ATP6V1A PE=1 SV=2 - [VATA_HUMAN]				12,16
P21281	V-type proton ATPase subunit B, brain isoform OS=Homo sapiens GN=ATP6V1B2 PE=1 SV=3 - [VATB2_HUMAN]				6,26
P36543	V-type proton ATPase subunit E 1 OS=Homo sapiens GN=ATP6V1E1 PE=1 SV=1 - [VATE1_HUMAN]				19,91
O75348	V-type proton ATPase subunit G 1 OS=Homo sapiens GN=ATP6V1G1 PE=1 SV=3 - [VATG1_HUMAN]				28,81
Q2M389	WASH complex subunit 7 OS=Homo sapiens GN=KIAA1033 PE=1 SV=2 - [WASH7_HUMAN]			7,25	
Q12768	WASH complex subunit strumpellin OS=Homo sapiens GN=KIAA0196 PE=1 SV=1 - [STRUM_HUMAN]			19,33	
O75083	WD repeat-containing protein 1 OS=Homo sapiens GN=WDR1 PE=1 SV=4 - [WDR1_HUMAN]			16,34	20,96
Q9NQW7	Xaa-Pro aminopeptidase 1 OS=Homo sapiens GN=XPNPEP1 PE=1 SV=3 - [XPP1_HUMAN]				4,49
O43149	Zinc finger ZZ-type and EF-hand domain-containing protein 1 OS=Homo sapiens GN=ZZEF1 PE=1 SV=6 - [ZZEF1_HUMAN]			1,82	
P25311	Zinc-alpha-2-glycoprotein OS=Homo sapiens GN=AZGP1 PE=1 SV=2 - [ZA2G_HUMAN]		9,40	26,17	
Q15942	Zyxin OS=Homo sapiens GN=ZYX PE=1 SV=1 - [ZYX_HUMAN]				10,14

